Deciphering the molecular mechanisms underlying the interaction of *Bacillus velezensis* strain B26 with the model plant *Brachypodium distachyon*

Meha Sharma

Department of Plant Science
McGill University, Montreal,
Canada

November 2022

A thesis submitted to McGill University in partial fulfillment of the requirements of the degree of Doctor of Philosophy

This thesis is dedicated to my beloved mother, Sangeeta Sharma

TABLE OF CONTENT

LIST OF FIGURES

Chapter 3

Chapter 4

Chapter 5

Supplementary Figures

Chapter 3

Chapter 4

LIST OF TABLES

Chapter 3

Chapter 4

Chapter 5

Supplementary Tables

Chapter 4

Chapter 5

LIST OF ABBREVIATIONS

4CL	4 coumarate CoA ligase
ABA	Abscisic acid
ACC	1-aminocyclopropane 1-carboxylate
ACO	1-aminocyclopropane-1-carboxylate oxidase
CE	Control Exudates
CFU	Colony Forming Unit
Cq	Cycle quantification
CR	Control Roots
CT	Computed Tomography
Ct	Cycle threshold
DEGs	Differentially Expressed Genes
DNA	Deoxyribonucleic acid
DPI	Days Post Inoculation
EDTA	Ethylenediamine tetraacetic acid
EPS	Exopolysaccharide
FP	Fraction Partitioned
FT	Flowering Locus T
GAs	Gibberellins

GC-MS	Gas Chromatography-Mass Spectrometry
GO	Gene Ontology
GSP	Gene Specific Primer
GST	Glutathione S-transferase
HCl	Hydrochloric acid
IAA	Indole-3-acetic acid
IBA	Indole Butyric Acid
ICDH	Isocitrate dehydrogenase
IE	Inoculated Exudates
IPA	Indole -3-Propionic Acid
IR	Inoculated Roots
ISR	Induced systemic resistance
KEGG	Kyoto Encyclopedia of Genes and Genomes
LB	Lysogeny Broth
LC-MS	Liquid Chromatography Mass Spectrometry
Mbp	Mega base pair
NADP	Nicotinamide adenine dinucleotide phosphate
NCBI	National Centre for Biotechnology Information
NGS	Next Generation Sequencing
OA	Organic Acid
OD	Optical Density
PCR	Polymerase Chain Reaction
PE	Paired end

PEG	Polyethylene Glycol
PGPR	Plant growth promoting rhizobacteria
PR	Pathogenesis related
qRT-PCR	Real-Time Quantitative Reverse Transcription Polymerase Chain Reaction
QS	Quorum Sensing
RCR	Relative Chemotactic Response
RFI	Relative Fold Increase
RNA	Ribonucleic acid
RT	Reverse Transcriptase
SAUR	Small auxin up-regulated RNA
SIM	Selected Ion Monitoring
TCA	tricarboxylic acid
UPLC	Ultra Performance Liquid Chromatography
VRN	Vernalization

ABSTRACT

Host-associated plant growth-promoting rhizobacteria (PGPR) influence plant health. The metabolites secreted from root exudates are used by PGPR as food and energy source. Most of the root exudates act as a chemoattractant and help bacteria to colonize the surface of plant roots by inducing chemotactic responses in rhizospheric bacteria. Organic acids from the tricarboxylic acid (TCA) cycle, released by roots play an important role in the recruitment of PGPR. In the present study, we investigated the role of *Brachypodium distachyon* root exudates and organic acids on recruiting *Bacillus velezensis* strain B26. GC-MS analysis of root exudates of B26 inoculated *B.distachyon* accession Bd21-3 revealed the highest levels of fumaric and succinic acid production than control root exudates. On contrary, inoculated roots were rich in malic and citric acid. The strongest chemotactic responses were induced by malic, succinic, citric, and fumaric acids. Genes encoding the enzymes malate dehydrogenase (MDH) and citrate synthase (CS) for the production of malate and citrate respectively, from TCA cycle were significantly upregulated in inoculated roots. Intriguingly, maximum biofilm induction was observed by citric acid. Transcript abundance of biofilm encoding genes was higher by succinic and citric acid. These organic acids helped in successful recruitment and colonization of *B. velezensis.* However, it is not clear whether genotypic variations in the host organism influence the PGPR with adaptive consequences for the host. To verify this, we screened four *B. distachyon* genotypes with varied flowering stages for their ability to be colonized by *B. velezensis*. Plants were inoculated with strain B26 and various phenological traits were recorded including Plant height, no. of leaves, no. of awns, no. of tillers, fresh root and shoot weight. All accessions differentially responded to B26 inoculation in terms of phenotypic expression. However, Bd21-3 was the most responsive of all and Bd30-1 did not respond significantly to B26 inoculation. These two contrasting accessions were selected for

further analysis. Following inoculation with B26, phenotypic data showed an increase in the number of awns which led us to investigate expression of *Brachypodium* flowering genes. We characterized the expression patterns of *B. distachyon* flowering genes *FT1*, *FT2*, *VRN1* and *VRN2* in response to *B.velezensis* inoculation and found that strain B26 modulates the transcript abundance of flowering genes. CT-scanning was used to estimate the root volume of inoculated plants, and increased root volume suggested that B26 is responsible for altering the root architecture. Moreover, the transcript abundance of the auxin and gibberellin biosynthesis genes changed in the inoculated roots. This shows that B26 altered the homeostasis of plant hormones as well. Accession Bd21-3 was further analyzed using a transcriptomics approach. Differential gene expression studies were conducted between control and inoculated roots of Bd21-3. We observed that B26 colonization caused differential expression of a diverse set of genes in inoculated roots. These included various signal transduction, ion transport, nutrient uptake and phytohormone biosynthesis transcripts. Taken together, this study identified the molecular basis of a) plant-PGPR interaction b) biofilm formation c) plant growth promotion d) the priming ability of PGPR.

RÉSUMÉ

Les rhizobactéries associées à la croissance des plantes (PGPR) influencent la santé des plantes. Les métabolites secrétés par les exsudats de racines sont utilisés par les PGPR comme source de nutrition et d'énergie. La plupart des exsudats de racines agissent comme chimioattractant et aident les bactéries à coloniser la surface des racines de plantes en induisant des réponses chimiotactiques chez les bactéries rhizobiennes. Les acides organiques produites par le cycle de Krebs relâchés par les racines jouent un rôle important dans le recrutement des PGPR. Dans cette étude nous investiguons le rôle d'exsudats de racines et des acides organiques du *Brachypodium* dans le recrutement du *Bacillus velezensis* souche B26. Une analyse CPG-SM des exsudats de racines de *Brachypodium distachyon* accession Bd21-3 inoculé avec le B26 a révélé des niveaux plus élevés de production d'acide fumarique et succinique que chez les exsudats de racines du groupe témoin. Contrairement aux exsudats de racines, les racines inoculées étaient riches en acides malique et citrique. Les gènes encodant les enzymes malate déshydrogénase et citrate synthase du cycle de Krebs, qui synthétisent le malate et citrate respectivement, étaient significativement surexprimées dans les racines inoculées. Intéressement, le niveau d'induction de biofilm était le plus élevé avec l'acide citrique. L'abondance de transcrits de gènes associées aux biofilms étaient plus élevée avec les acides succinique et citrique. Ces acides organiques ont aidé dans le recrutement et la colonisation du B26. Cependant, il n'est pas clair si les variations génotypiques dans l'organisme hôte influencent les PGPR avec des conséquences adaptatives pour l'hôte. Pour vérifier cela, nous avons comparé quatre génotypes de *B. distachyon* avec des étapes de floraison différentes pour leur capacité à être colonisés par le *B. velezensis*. Les plantes ont été inoculés avec la souche B26 et différents traits phénologiques ont été notés, incluant la hauteur des plantes, le nombre de feuilles, nombre de barbes, nombre de talles, et poids des racines et pousses fraîches. Toutes les

accessions ont montré des différences en expression phénotypique face à l'inoculation avec le B26. Cependant, le Bd21-3 était le plus sensible de tous et la différence chez le Bd30-1 n'était pas significative. Ces deux accessions contrastantes ont été choisies pour de l'analyse supplémentaire. Après l'inoculation avec le B26, les données phénotypiques ont montré une augmentation dans le nombre de barbes, ce qui nous a mené à investiguer l'expression des gènes de floraison du *Brachypodium*. Nous avons caractérisé les motifs d'expression des gènes de floraison du *B. distachyon FT1*, *FT2*, *VRN1* et *VRN2* en réponse à l'inoculation avec le *B. velezensis* et avons trouvé que la souche B26 module l'abondance de transcrits des gènes de floraison. La tomodensitométrie a été utilisée pour estimer le volume des racines des plantes inoculées et une augmentation dans le volume des racines a suggéré que le B26 était responsable pour l'altération de l'architecture des racines. De plus, l'abondance des transcrits des gènes de biosynthèse d'auxines et gibbérellines a changé dans les racines inoculées. Ceci montre que le B26 modifie l'homéostasie des hormones des plantes aussi. L'accession Bd21-3 a été analysée davantage avec une approche transcriptomique. Des études d'expression génique différentielle ont été menées entre les racines témoin et inoculées de Bd21-3. On a observé que la colonisation par le B26 a causé l'expression différentielle d'un ensemble de gènes varié chez les racines inoculées. Ceux-ci ont inclus des transcrits divers de transduction de signal, transport d'ions, consommation de nutriments et biosynthèse de phytohormones. Pris l'ensemble, cette étude a identifié la base moléculaire de a) l'interaction plante-PGPR, b) la formation de biofilm c) la promotion de la croissance des plantes d) la capacité d'amorçage du PGPR.

ACKNOWLEDGEMENTS

I would like to start by thanking my family: my parents, my twin brother, and my sister-in-law without their constant support this journey would not have been possible. I am so grateful to my parents, especially my mother who sacrificed a ton so that I can achieve my goals. I thank Almighty for guiding me at each step and giving me such a supportive family.

A mountain of gratitude goes to my supervisor Dr. Suha Jabaji. She is the right combination of tough and kind and has a remarkable ability to encourage me. I am very thankful to her for providing me this opportunity and supporting me throughout. Her confidence in me and my performance inspired me to constantly perform better. She helped me brainstorm research problems and gave me advice on how to approach them.

I would like to extend my thanks to my committee members Dr. Jean-Benoit Charron and Dr. Jeff Xia for their valuable comments and input in my research. Special thanks to Dr. Jean-Benoit Charron for providing *Brachypodium* seeds and advised me on growing plants. He was always willing to assist me, and I am thankful for this.

I would like to acknowledge the wonderful people of Department of Plant Science whom I have interacted with over years, Guy Rimmer, Serghei Dernovici and Sarah Ann for providing me access to research facilities in the greenhouse and phytorium. A special thanks to Dr. Youssef Chebli for helping in conducting microscopy experiments. I am thankful to Erin Minnett and Susan Gregus for their assistance in administration-related matters.

I am also grateful to NSERC-Discovery Program awarded to Dr. Suha Jabaji and Department of Plant Science for providing me the financial support throughout my graduate studies.

This endeavour would not have been possible without the help of “Funlab” current and ex-members: Dina Saleh, Nathan Liang, Ines Ben Rejeb, Ximena Florez, Mohannad Mahmoud, Mohammad Jamil Kaddoura and Clara Yohana Maia. Members of “Funlab” were very supportive and interactive to work with. My gratitude to them knows no bounds. My special thanks to Nathan Liang for translating my abstract into French and being a great friend in and outside the lab. Words cannot express my appreciation to Mamta Rani who is a valued colleague and a dear friend. In the beginning of my degree, she helped me to get acclimatize in the lab and introduced me to the lab protocols.

Finally, my unending thanks go to my friends Irfan Iqbal, Karuna Kapoor and Diljot Kaur who are like family to me. Their unwavering love and support helped me feel at home in Montreal. I would also like to appreciate my friend Harjeevan Kaur, who has supported my journey since undergrad. A big shout out to all my friends for being my unpaid, personal therapists.

PREFACE AND CONTRIBUTIONS

The following thesis was prepared according to the "Guidelines Concerning Thesis Preparation" of McGill University. This thesis contains three chapters (Chapters 3-5) representing three separate research manuscripts: Chapter 3 is published in *Frontiers in Microbiology,* Chapter 4 is published to *Scientific Reports*, and Chapter 5 is published in *Genomics.* Below are the contributions of each author to the thesis and a general description of the thesis topics.

Contributions of Authors

Meha Sharma (MS) was the primary researcher for each chapter. She designed the experiments as well as conducted and planned all the experimental procedures and analyses with the guidance of Dr. Suha Jabaji (SJ), Department of Plant Science, Macdonald Campus of McGill University. Dr. S. Jabaji provided supervision, guidance, and funding for all chapters.

The first manuscript (Chapter 3) is co-authored by Dina Saleh (DS), Dr. Jean Benoit Charron (JBC), and SJ. DS helped to generate organic acid primers and helped in chemotaxis and biofilm assays. The manuscript was written by MS and edited by SJ and JBC. Funds were provided by NSERC-Discovery (RGPIN-2016-04805). We thank Dr. Youssef Chebli, for assistance in Scanning Electron Microscopy at Multi-Scale Imaging Facility at McGill University, Macdonald Campus.

The second manuscript (Chapter 4) is co-authored by Mamta Rani (MR), JBC and SJ. The study was conceptualized and designed by MS and SJ. Acquisition of data for the study: MS., and partly MR. Analysis of data for the work: M.S. Interpretation of data for the work: MS and SJ Manuscript revision and approval: MS, JBC and SJ. We greatly acknowledge the financial support, through a

Discovery grant (RGPIN-2016-04805) to SJ, which was provided by the Natural Sciences and Engineering Research Council of Canada. We thank JBC for providing wild-type *Brachypodium distachyon* seeds which were originally sourced from Dr. David F. Garvin, USDA. We also thank Dr. DP Woods, UC Davis, for providing overexpressing flowering transgenic lines.

The third manuscript (Chapter 5) is co-authored by SJ. Conceptualization and design of the study: MS and SJ. Acquisition of data for the study: MS, and SJ. Analysis of data for the work: MS. Interpretation of data for the work: MS and SJ. Manuscript revision and approval: MS and SJ. We thank Dr. Youssef Chebli, for assistance in Scanning Electron Microscopy at Multi-Scale Imaging Facility at McGill University, Macdonald Campus.

Contribution to Knowledge

The chapters of this thesis represent a significant contribution to the knowledge of the molecular mechanisms behind PGPR and plant interactions.

Chapter 3

The results of this research represent the first report on:

1. the effect of PGPR on TCA cycle genes in plants.
2. the molecular basis behind the induction of chemotaxis and biofilm formation by *B.velezensis* in presence of root exudates and individual organic acid.

Chapter 4

1. Strain B26 modulates the transcription of flowering genes. According to our knowledge, this is the first report that rhizobacteria can induce flowering genes in *B. distachyon* roots.
2. Our results support the evidence that plant genotype is detrimental to PGPRs' action mode.

3. Our study offers novel information about the long-term effects of a PGPR on plant development, advancing the knowledge of these relevant biological interactions.

Chapter 5

1. Transcriptomic data generated in this study improves our knowledge of plant-PGPR interaction and can serve as a model resource for poorly characterized plant and bacterial species.
2. Our study has established that PGPR stimulates plant growth by modulating the hormone signalling pathway and priming the plants to fight off diseases.
3. This study is the first to investigate *Brachypodium* roots' transcriptome during interaction with a PGPR under stress-free conditions.

Chapter 1. Introduction

A developing plant interacts with a complex community of diverse microbes that influence plant growth and development. Depending on how these microbes affect plant growth, they can be divided into groups that are beneficial, detrimental, and neutral (Dobbelaere *et al.*, 2003, Yin *et al.*, 2021). Plant-microbe interaction can occur at various regions in plants e.g., phyllosphere (on the aerial parts of plant), endosphere (inside plant tissues) and rhizosphere (in the soil closer to plant roots). Based on the region of plant colonization, microbes can be epiphytes (on the surface of plants), endophytes (inside the plant tissues) and rhizopsheric (in the rhizosphere) (Bringel and Couée, 2015, Oburger and Schmidt, 2016). However, the rhizospheric microbes have the greatest impact on plant health. Rhizospheric bacteria that promote plant growth and tolerance to various stresses are known as plant growth-promoting rhizobacteria (PGPR). They stimulate plant growth in various ways: a) increasing nutrient acquisition including phosphorous, iron and fixed nitrogen (Van Loon, 2007, Hodge *et al.*, 2009) b) eliciting induced systemic resistance (ISR) and priming of plant immune system (Van Loon *et al.*, 1998, Pieterse *et al.*, 2014) c) suppressing diseases and alleviation of abiotic stresses (Yang *et al.*, 2009, Goswami and Suresh, 2020) d) producing phytohormones e.g., auxin, cytokinin, gibberellins and ethylene. With the use of PGPR inoculation, many crops have seen improvements in key phenological traits such as root and shoot weights, yield, and seed germination rate(Yasmin *et al.*, 2007, Gagné-Bourque *et al.*, 2015, Agake *et al.*, 2022). In exchange, plant roots secrete bioactive compounds in form of amino acids, organic acids, sugars, and secondary metabolites (Zhang *et al.*, 2014). These organic compounds secreted by roots are known as root exudates which help in the recruitment and adaptation of PGPRs. Numerous studies have proved that the composition of root exudates varies according to plant species and genotype (Rudrappa *et al.*, 2008, Peiffer *et al.*, 2013, Bulgarelli *et al.*, 2015, Mahoney

et al., 2017). Bacteria is attracted to plant roots by a process called chemotaxis, which results in colonisation and later formation of biofilm. These are the first two crucial steps of bacterial contact with plant roots.

PGPRs have been commercially utilized for biofertilization (Vessey, 2003, Somers *et al.*, 2004), phytostimulation (Lugtenberg and Bloemberg, 2002) and as biocontrol against various plant diseases(Chandler *et al.*, 2008). The use of beneficial microbes in agriculture can be traced throughout history. The first commercial biological plant growth-promoting product having Rhizobium sp. was patented in 1896 (Nobbe and Hiltner, 1896). Decades of research have demonstrated that bacterial species such as *Pseudomonas*, *Azospirillum*, *Burkholderia*, *Acetobacter*, and *Bacillus* are excellent growth stimulating agents (Sudhakar *et al.*, 2000, Mehnaz and Lazarovits, 2006, Pii *et al.*, 2015, Kashyap *et al.*, 2019). These studies demonstrate that utilizing beneficial microbes in place of chemical-based fertilizers and pesticides is becoming more popular in the agricultural sector. These microbial products work as potential tools for promoting plant growth and disease control that are non-toxic, sustainable, and safe to environment.

Bacillus sp. is well known for stimulating plant growth by increasing nutrient availability, synthesizing plant hormones, and producing volatiles (Mena-Violante and Olalde-Portugal, 2007, Calvo *et al.*, 2010, Park *et al.*, 2017, Samaras *et al.*, 2022). Endospores produced by *Bacillus* sp. can withstand high temperatures and dehydration, streamlining the formulation of commercial products (Akinrinlola *et al.*, 2018). *Bacillus velezensis* (formerly known as *B. methylotropicus)* strain B26 affects the complete life cycle of the model plant *Brachypodium distachyon* by accelerating its growth and shortening its vegetative period (Gagné-Bourque et al. 2015). *Brachypodium* has proven to be particularly useful for comparative genomics and as a functional

model for various traits in grasses(Brkljacic *et al.*, 2011). *B. velezensis* strain B26 provides resistance against drought stress in *Brachypodium* by upregulating the expression of drought-responsive genes, modulation in the DNA methylation process (Gagné-Bourque *et al.*, 2015) and substantial increase in certain metabolic osmolytes (Gagné-Bourque *et al.*, 2016). However, limited knowledge is available on the molecular mechanisms of how the bacteria adapt, colonize, and exert beneficial effects on plants. The advancement in omics technologies will enable us to understand the genome, transcriptome, and proteome of both microbes and plants during the interaction. The knowledge gaps between the plant and PGPR's close relationship as well as the underlying mechanisms each partner uses to interact successfully would be filled by these techniques.

Therefore, the overarching goal of this thesis is to study the molecular mechanisms behind the interaction of PGPR and plant roots. The following objectives were investigated to achieve this goal:

Objective 1: To understand how root exudates and organic acids affect chemotactic responses, biofilm formation in *B.velezensis* strain B26 and expression of organic acid genes from TCA cycle in *Brachypodium*

Hypothesis: Plant root exudates help the recruitment of beneficial bacteria and in turn bacteria improves root exudate composition.

Objective 2: To investigate the response of B26 inoculation on different *B.distachyon* genotypes and whether growth promotion by B26 is associated with phytohormone homoeostasis

Hypothesis: Genetic diversity among accessions of *B.distachyon* can influence the colonization of *B. velezensis* strain B26.

Objective 3: To investigate changes in *Brachypodium* transcriptome due to B26 and identify the molecular basis of plant-microbe interaction, plant growth promotion and ion transport, defense and stress responsiveness

Hypothesis: Colonized plants by *B. velezensis* will reveal significant changes in expression of genes important for colonization and adaptation

Chapter 2. Review of Literature

2.1 *Brachypodium distachyon* as monocot model plant

Brachypodium distachyon from the Poaceae family is a wild annual grass that originated from the Mediterranean and the Middle Eastern regions (Draper *et al.*, 2001). It has been established as a model plant species for functional genomics in grasses and cereal crops (Brkljacic *et al.*, 2011). Rice is considered a model plant for monocots with available sequenced genome and substantial genetic resources. But the major challenge lies in the large size of the plant, long generation time and demanding growth requirements (Brkljacic *et al.*, 2011). However, *Brachypodium* is now established as an ideal model to study monocots because of the following characteristics: (i) it is phylogenetically more closer to wheat, barley than rice (Bevan *et al.*, 2010); (ii) the genome size is about 300 Mbp which is smallest among diploid grasses (International Brachypodium Initiative2010). (iii) It has a basic chromosome number of n = 5 (Hasterok *et al.*, 2004). (iv) It has a small stature (20 cm) and is a self-pollinated grass with short generation time (8-12 weeks) (Draper *et al.*, 2001). (v) The fully sequenced genome of various *Brachypodium distachyon* accessions is available online. Additionally, *Brachypodium* possesses high transformation efficiency due to which various *Agrobacterium tumefaciens*-mediated transformation methods have been deployed successfully (Păcurar *et al.*, 2008, Vain *et al.*, 2008). Large number of mutant lines have been generated by using T-DNA mutagenesis (Bragg *et al.*, 2012b) and can be accessed through various publicly available online databases (https://jgi.doe.gov/our-science/science-programs/plant-genomics/brachypodium).

Due to the availability of large genetic resources, *Brachypodium* has been used for understanding the concepts of flowering time regulation, drought response, cell wall composition, transcription factors and disease resistance in cereals and forages (Brkljacic *et al.*, 2011).

Moreover, it has been also established as a model to study biotic stresses such as fungal and bacterial infections (Opanowicz *et al.*, 2008). The effect of plant growth-promoting rhizobacteria (PGPR) on the growth and development of *Brachypodium* has been recently reported (Gagné-Bourque et al. 2015).

2.2 Plant Growth Promoting Rhizobacteria (PGPR) as a naturally beneficial organism to plants

PGPR are soil-derived inhabitants that thrive in rhizosphere, colonize plant roots, and exert beneficial effects on the plants. Inoculation of seeds, tubers and roots with plant growth stimulant bacteria was used to be called as "bacterization" in mid of 19th century. The term PGPR was first introduced by Kloepper and Schroth in 1978 as the soil bacteria that colonize the roots of plants in rhizosphere and enhance plant growth. Rhizosphere is plant-root interface which is inhabited by microbes and influenced by the chemicals released from plant roots. These chemicals are known as root exudates which are rich in carbohydrates, organic acids, amino acids, vitamins and some secondary metabolites(Badri and Vivanco, 2009, Vives-Peris *et al.*, 2020). The composition of root exudates changes depending upon the plant genotype, plant development stage and environment in which plant is growing (Chaparro *et al.*, 2013, Pascale *et al.*, 2020). Root exudates can act as chemoattractant or chemorepellent for microbes present in rhizosphere. Moreover, these organic compounds are the primary source of nutrients for rhizospheric microbes. Based on the interactions with plant roots, PGPR can be separated into two categories extracellular PGPR (ePGPR) which exist free-living outside plant cell, in the rhizosphere e.g., *Agrobacterium*, *Azotobacter*, *Azospirillum*, *Bacillus*, *Burkholderia*, *Erwinia* and *Flavobacterium*, etc (Prithiviraj *et al.*, 2003) and intracellular PGPR (iPGPR) which exist inside the plant root cells e.g., *Azorhizobium*, *Bradyrhizobium*, and *Rhizobium* etc. (Vessey, 2003, Gray and Smith, 2005). An ideal PGRP should have ability to compete with other microbes and successfully colonize plant

roots as compared to others, this ability is known as rhizosphere competence (Ahmad and Baker, 1987).

2.3 Initial dialogues during Plant root-PGPR interaction

Successful root colonization by PGPR determines the fate of PGPR as a plant growth promoter. Therefore, root colonization is the foremost and most crucial step for PGPR action. First, chemotaxis and later biofilm formation are the two most crucial steps for root colonization by PGPR.

2.3.1 Chemotaxis

Chemotaxis is defined as the ability of bacteria to direct their movement in gradients of attractants and repellents (Bünning, 1989). Chemotaxis enables bacteria to find better carbon and nitrogen sources as well as more suitable environmental conditions. A stimulant interacts with its cognate chemoreceptor, located on the surface of bacteria, causing bacterial chemotaxis. Once the stimulant has interacted with the chemoreceptor, autophosphorylation of the histidine kinase CheA occurs which further phosphorylates the response regulator CheY. Consequently, the modified CheY in turn interacts with the flagellar motor to control cell swimming and finally facilitate chemotaxis (Hazelbauer, 2012, Walukiewicz *et al.*, 2014). It has been proved that root exudates play a dialogue role between plant roots and rhizospheric microbes for efficient recruitment of PGPR. (Bais *et al.*, 2004, Sun *et al.*, 2012, Beauregard, 2015). These root exudates act as a stimulant that interacts with the bacterial chemoreceptors. For example, *Bacillus velezensis* SQR9 gets chemotactically attracted towards cucumber root exudates and promotes plant growth (Zhang *et al.*, 2014). In another study, root exudates of banana enhanced root colonization and pathogen suppression abilities of *Bacillus amyloliquefaciens* NJN-6 (Yuan *et al.*, 2018).

2.3.2 Biofilm formation

Once the bacteria reach the plant roots through chemotaxis, they grow and reproduce which ultimately leads to biofilm formation on the roots. Biofilms are the bacterial aggregates adhered to biotic or abiotic surfaces by a matrix composed of extracellular polymeric substances (EPS) in the case of *Bacillus* and protein TasA (Ramey *et al.*, 2004, Branda *et al.*, 2006, Flemming and Wingender, 2010). Biofilm helps in a stable and long-term colonization of roots. It also helps bacteria to survive under stressful conditions. During biofilm formation, bacteria communicate with each other, and detect their population by identifying specific molecules secreted by one bacterial species, this process is called Quorum sensing (QS) (Fuqua *et al.*, 1994). There are multiple examples of biofilm forming PGPR in the literature that are significantly more effective in colonization than any other planktonic PGPR(Timmusk *et al.*, 2005, Alaa, 2018, Ansari *et al.*, 2021). Biofilm formation is also influenced by root exudates of host plants. For example, Organic acids from root exudates of banana help root colonization of PGPR strain *Bacillus amyloliquefaciens* NJN-6 through chemotaxis and biofilm formation (Yuan *et al.*, 2015). Citric acid from root exudates of cucumber induced biofilm formation in *Bacillus amyloliquefaciens* SQR9(Zhang *et al.*, 2014).(Allard-Massicotte *et al.*, 2016) studied the colonization of *Bacillus subtills* in *Arabidopsis thaliana.* They found that bacteria first swim towards plant roots through chemotaxis later within a few hours motile cells of bacteria differentiate to biofilm producing cells by losing flagella which leads to long-term colonization. In nutshell, both chemotaxis and biofilm are required by PGPR for efficient colonization.

2.4 Mode of PGPR action

Numerous studies on PGPR conducted in 1980s concluded that rhizobacteria have the ability to beneficially alter the microbial composition of rhizosphere (Kloepper and Schroth, 1981a,

Kloepper and Schroth, 1981b). PGPR stimulate plant growth actively by nitrogen fixation, production of phytohormones, siderophores and promoting plant nutrient availability(Glick *et al.*, 1999, Ortíz-Castro *et al.*, 2009). Another mode of action is indirectly by protecting the plants from diseases through production of antibiotics (Weller, 1988), HCN(Stutz *et al.*, 1986) and antifungal metabolites (Bhattacharyya and Jha, 2012). They also induce defense mechanisms in plants upon pathogen attack which is termed as induced systemic resistance (ISR) (Van Peer *et al.*, 1991, Lugtenberg and Kamilova, 2009).

2.4.1 Direct mechanism

2.4.1.1 Nitrogen fixation: Biofertilizers are rhizobacteria that facilitate nutrient uptake and make it easier for a plant to absorb. Some microbes have ability to convert atmospheric nitrogen to ammonia which is readily utilized by plants. This process is known as biological nitrogen fixation (BNF) (Kim and Rees, 1994, Hoffman *et al.*, 2009). Nitrogen-fixing microbes are divided into two types a) symbiotic bacteria which fix nitrogen by forming symbiotic relationships with leguminous e.g., Rhizobia and non-leguminous e.g., Frankia (Ahemad and Khan, 2012, Nana and Alemneh, 2015) b) non-symbiotic bacteria which are free-living, associative and endophytic colonizers such as *Azospirillum*, *Azotobacter* and *Gluconoacetobacter* etc (Bhattacharyya and Jha, 2012).

2.4.1.2 Phosphorous solubilization: After nitrogen, phosphorus (P), which is abundant in the soil in both organic and inorganic forms, is another crucial mineral for plant growth. Plants cannot absorb this available P which is in an insoluble form. To absorb phosphorus, it should be in the soluble form either as monobasic or dibasic ions(Bhattacharyya and Jha, 2012). One solution is to frequently add phosphatic fertilizers to fields to avoid P deficiency and hence plant development. Another more sustainable and eco-friendly way is to use microbes that can solubilize phosphorus,

known as phosphate solubilizing microorganisms (PSM) (Kucey *et al.*, 1989). PSM inhabiting rhizosphere are phosphate solubilizing bacteria (PSB) which increases the availability of the phosphorus to the plant roots (Youssef and Eissa, 2014). Some examples of effective phosphate solubilizing bacteria include *Bacillus, Azotobacter, Pseudomonas, Burkholderia, Enterobacter, Xanthomonas,* and *Flavobacterium* (Elhaissoufi *et al.*, 2020)

2.4.1.3 Siderophore production: Plants require iron, but it is relatively insoluble in soil. Some strategies are required for plant iron uptake. Under iron-limiting conditions, plants and microbes secrete siderophores, low molecular weight compounds that chelate the ferric ion and provide the host access to it (Bar-Ness *et al.*, 1991, von Wirén *et al.*, 2000). Many studies have concluded the beneficial role of microbial siderophores in plant development.(Jin *et al.*, 2006, Rajkumar *et al.*, 2010, Shameer and Prasad, 2018). For example, Mung bean plants growing under iron-limiting conditions when inoculated with siderophore producing *Pseudomonas* strain GRP3 showed reduced deficiency symptoms as compared to uninoculated plants (Sharma *et al.*, 2003)

2.4.1.4 Phytohormone production: Aside from nutrients, PGPR plays an important role in plant growth promotion by producing phytohormones. PGPR produce Indole-3-acetic acid (IAA), cytokinin and gibberellin which ultimately influence the hormonal balance of plant (Kloepper *et al.*, 2007). Among all phytohormones, auxin is widely produced by PGPR and well studied over the years. The most prominent effect of bacterial IAA is the development of longer roots with an increased number of root hairs which leads to more nutrient uptake and in turn plant release more root exudates that help the recruitment of bacteria (Lambrecht *et al.*, 2000, Sukul *et al.*, 2021). However, IAA produced by PGPR also influence the endogenous pool of plant IAA and hence alters the plant development process. If an optimal level of endogenous auxin pool is maintained

in the plant, the auxin from PGPR may completely inhibit or suppress the plant growth or vice-versa (Gamalero and Glick, 2011). For example, *Dioscorea rotundata* L. when inoculated with *Bacillus subtilis*, an IAA-producing bacteria, produced more roots as compared to non-inoculated plants (Swain *et al.*, 2007). Another phytohormone produced by PGPR is cytokinin which influences cell division and seed germination (Gamalero *et al.*, 2009). Cytokinin is produced by PGPR such as *Azotobacter*, *Rhizobium, Bacillus* and *Paenibacillus*. (Nieto and Frankenberger Jr, 1989, Timmusk *et al.*, 1999, García de Salamone *et al.*, 2001). *Pseudomonas putida*, secretes Gibberellin and is proven to improve soybean under saline and drought conditions (Kang *et al.*, 2014). Few PGPR produces enzyme 1-aminocyclopropane 1-carboxylate (ACC) deaminase, which cleaves the immediate precursor of phytohormone ethylene in plants. During abiotic stress ACC deaminase activity of PGPR results in a decrease in ethylene concentration, facilitating plant growth(Glick *et al.*, 1998, Zahir *et al.*, 2008).

2.4.2 Indirect Method

2.4.2.1 Production of antibiotics: PGPR (Beattie, 2007) defines biocontrol agents as bacteria that reduce the incidence or severity of plant diseases, whereas antagonists are bacteria that exhibit antagonistic activity toward a pathogen. The production of one or more antibiotics is one of the main methods employed by PGPR to combat the harmful effects of phytopathogens. The antibiotics producing PGPRs against plant pathogens have been proposed as an alternative to chemical pesticides in crops. PGPR produces antibiotics such as 2,4-diacetyl phloroglucinol, phenazine-1-carboxylic acid, phenazine-1-carboxamide, butyrolactones, pyoluteorin, pyrrolnitrin, oomycinA, and kanosamine etc(Fernando *et al.*, 2005). *Bacillus* spp. produces various antibiotic lipopeptides e.g., surfactin, iturin and fengycin etc (Hashem *et al.*, 2019). These lipopeptides are useful against pathogenic and antibiotic-resistant bacteria and help plants to survive. *Bacillus*

amyloliquefaciens has been proved as a potent biocontrol against phytopathogens like *Fusarium oxysporum* and *Fusarium ayenaceum* etc (Salazar *et al.*, 2017).

2.4.2.2 Induced systemic resistance (ISR): ISR is a process in which PGPR alleviate the harmful effects of pathogenic bacteria, fungi and virus by activating the plant resistance mechanism (Van Loon *et al.*, 1998, Lugtenberg and Kamilova, 2009). ISR was first studied in carnation plants infected with the pathogenic fungi *Fusarium oxysporum* f. sp. *Dianthi*. Infected carnation plants were inoculated with *Pesudomonas fluorescens* strain WCS417r and inoculated plants showed resistance against the pathogen as compared to non-inoculated plants(Van Peer and Schippers, 1992). This study also concluded that PGPR can prime plants to combat pathogenic attacks faster by inducing plant defense mechanisms. ISR activates the jasmonate and ethylene signalling within the plant, a major plant defense signalling pathway against various pathogens(Verhagen *et al.*, 2004).

2.5 'Omics' to study plant-PGPR interaction

Understanding the complex rhizosphere signalling during plant-PGPR interaction is a topic of extensive research. Most of the studies on plant bacterial interaction are related to phytopathogens, their diversity and metabolite potential, various areas of endophytism which are poorly understood i.e., plant – PGPR interactions, interactions among different PGPRs of the same plant and colonization strategies (Suryanarayanan, 2013). Modern techniques such as whole genome sequencing, comparative genomics, transcriptomics, proteomics etc. are helpful approaches that would fill the gaps in knowledge not only on the intimate relationship between the plant and PGPR but also on the underlying mechanisms that each partner employs leading to a successful interaction. Taken together, the study of plant-PGPR employing high-throughput techniques such

as whole genome sequencing, transcriptomics and metabolomics of both bacteria and plants are necessary.

2.5.1 Whole Genome analysis of PGPR

The whole genome sequencing of the first bacterial genome *Haemophilus influenzae* (Fleischmann *et al.*, 1995) paved the way for bacterial genome studies which were later employed to study PGPR genome. *Bacillus subtilis* was the first Gram positive bacterial species sequenced among soil living bacterium(Kunst *et al.*, 1997, Wipat and Harwood, 1999). Different species of *Pseudomonas fluorescens* were sequenced mostly initially and well-studied (Paulsen *et al.*, 2005, Silby *et al.*, 2009). Currently, Next Generation Sequencing (NGS) has been used to examine the genomes of various PGPRs e.g., *Paenibacillus* (Kim *et al.*, 2010, Eastman *et al.*, 2014), *Burkholderia* spp. (Ormeño-Orrillo *et al.*, 2012), *Enterobacter* spp.(Singh *et al.*, 2017, Abdullahi *et al.*, 2021) and *Serratia marcescens* (Matteoli et al., 2018) etc. To fully comprehend how every part of bacterial cell functions, however, knowledge of the whole genome is necessary. Genomes of PGPR encompass plenty of information which will unlock the mysteries behind the growth and interaction of an organism within the plants (Chaudhry *et al.*, 2017). They encode genes that are required for their endophytic lifestyle and plant beneficial properties (Hardoim *et al.*, 2015). Whole genome analysis of PGPR has provided a tool to examine the genetic features that influence the various bioactivities such as antibiotic resistance, plant growth promotion, metabolite production and colonizing preferences (Kaul *et al.*, 2016a). Moreover, annotation of the genome is necessary for the discovery of various biochemical pathways involved in plant PGPR interaction. Knowing the complete sequence of a genome is, however, only the first step towards understanding how all the components of a bacterial cell work together.

2.5.2 Transcriptome analysis through RNA sequencing

Understanding how bacteria interact with plant roots in the rhizosphere is becoming more accessible due to the development of NGS technology and the availability of various bacterial and plant genomes. To characterize the predicted gene in the genome, gene expression profiling is a powerful approach. Transcriptome analysis through RNA sequencing is a high throughput technique for gene expression analysis of thousands of genes in parallel experiments (Metzker, 2010). RNA sequencing involves the study of transcriptome based on the sequencing of mRNA from a sample. It enables genome-scale coverage, measurement of absolute differential gene expression and understanding post-transcriptional regulatory events such as alternative splicing (Fu *et al.*, 2009, Kalam *et al.*, 2017) etc. RNA sequencing has been applied to study various plant-pathogen interactions (Wang *et al.*, 2017, Slavokhotova *et al.*, 2021), plant-PGPR interaction during stress(Chauhan *et al.*, 2019) however studies related to plant-PGPR interaction under stress free conditions are few and rare. These studies reveal that PGPR differentially alters the hosts' transcriptome. A few examples include, RNA-seq transcriptional analysis of PGPR *Delftia acidovorans* RAY209 during interaction with canola and soybean roots revealed that bacteria exhibited a core regulatory and plant-host specific response to root colonization (Suchan *et al.*, 2020). A detailed transcriptomic analysis of cucumber roots in response to PGPR *Bacillus subtilis* Mbi600 revealed that plant growth promotion and biocontrol ability is due to the upregulation of genes related to both processes (Samaras *et al.*, 2022).

2.5.3 Dual RNA sequencing:

Dual RNA-seq involves simultaneous RNA sequencing of both eukaryotic plant and prokaryotic microbe, it is considered as a very powerful, economical, sensitive and species-independent platform for understandings genes involved in host–bacteria interactions (Westermann *et al.*,

2012). It simultaneously captures the expressed genes of both the host and microbe (Marsh *et al.*, 2017). There are various advantages of using dual RNA sequencing (i) It provides powerful insight into novel interaction dynamics by capturing the changes in gene expression in one organism due to another (Baddal *et al.*, 2015). (ii) It enables the temporal determination of responses and changes in the cellular networks in both organisms. This has been applied to various bacteria-host interactions. For example, dual RNA-Seq of wheat roots colonized by the bacterial endophyte *Azospirillum brasilense*, helped in the identification of genes for the up-regulation of nutrient acquisition and cell cycle genes (Camilios-Neto *et al.*, 2014a). Dual RNA sequencing of the beneficial root endophyte, *Colletotrichum tofieldiae* and its pathogenic relative *C. incanum* along with their host *Arabidopsis* helped to identify the fungal adaptations to the endophytic lifestyle at the level of both gene repertoire and gene regulation within a single fungal genus (Hacquard *et al.*, 2016). Another dual RNA seq study on a plant host and its pathogen was performed to evaluate interactions in a grass-fungal system and they identified important fungal genes responsible for the shift of the fungus from a symbiont to a pathogen (Eaton *et al.*, 2011). The typical patterns of gene expression alterations observed in plant-PGPR transcriptomic investigations are summarised below:

a. Nutrient uptake genes: One of the direct mechanisms via which PGPR promote plant growth is through helping plant in nutrient uptake including nitrogen, phosphorus and sugars. Nitrate ammonia and sugar transporters were differentially expressed in the transcriptome of rice inoculated with *A. brasilense* and *H. seropedicae* (Thomas *et al.*, 2019, Wiggins *et al.*, 2022). Transcriptome analysis of cucumber roots inoculated with *Bacillus subtilis* revealed the upregulation of potassium transporter genes (Samaras *et al.*, 2022).

b. **Phytohormone signalling genes:** Plant phytohormone including auxin, gibberellins, cytokinin and ethylene are majorly produced by PGPRs as well. Differential regulation of several transcripts encoding auxin-responsive proteins (e.g., SAUR genes, Aux/IAA genes, GH3 genes), gibberellin-regulated proteins were differentially expressed in cereals inoculated with PGPR (Rekha *et al.*, 2018b, Shinjo *et al.*, 2020, Wiggins *et al.*, 2022). Ethylene in plants is produced by ACC oxidase which converts 1-aminocyclopropane-1-carboxylic acid (ACC) to ethylene. Barely roots when inoculated with PGPR *Paenibacillus* sp. and *Erwinia gerundensis* showed reduced expression of gene encoding ACC hence less ethylene production and more plant growth (Li *et al.*, 2021).

c. Defense and stress responsiveness genes: Whenever any bacteria (harmful or beneficial) enter the host plant, it alters the defense mechanism in plants. The expression of defense-related genes e.g., pathogenesis-related (PR) proteins, chitinases, thionins etc. is either increased (during pathogen attack) or decreased (during PGPR interaction). For example, the expression of PR protein was reduced when rice roots were inoculated with diazotrophic endophyte *Herbaspirillum seropedicae* (Brusamarello-Santos *et al.*, 2019). While PR proteins were upregulated when rice plants were infected with pathogenic fungus *Magnaporthe oryzae* (Kawahara *et al.*, 2012).

d) Plant metabolic pathway genes: Crosstalk between plant and PGPR influence various plant metabolic pathways including glycolysis and tricarboxylic acid (TCA) cycle. The major organic acids intermediates of TCA cycle are citric acid, succinic acid, fumaric acid, malic acid, and oxaloacetate. These organic acids are part of the plant root exudates which act as signals to recruit PGPRs. Rhizobacteria affects the transcripts encoding for enzymes of TCA cycle e.g., transcripts encoding for malate synthase and succinyl-CoA ligase in rice roots were altered by *Bacillus subtilis* strain RR4 (Rekha *et al.*, 2018b). Genes encoding succinate dehydrogenase and malate

synthase were upregulated in *Lycopersicon esculentum* by PGPRs *Pseudomonas aeruginosa* and *Burkholderia gladioli* (Khanna *et al.*, 2019).

All these studies reveal that RNA sequencing provides a deep understanding of plant-PGPR interaction at a given growth stage of plant or bacteria and the complex network that regulates root-rhizosphere signalling.

2.6 *Bacillus velezensis* strain B26 as a PGPR

The present study is conducted with *Bacillus velezensis* strain B26. It is a gram positive rod shape bacteria which forms tough endospores (Errington, 2003). This strain was firstly isolated from leaf blades and seeds of the bioenergy crop switchgrass (*Panicum virgatum L.*) by (Gagne-Bourgue *et al.*, 2013b). Its genome was sequenced by (Jeukens *et al.*, 2015a). It exerts beneficial effects on plants due to its ability to efficiently colonize plant roots (Gagné-Bourque et al. 2015). B26 has the following characteristics:

2.6.1 Biofertilizer and Bio stimulant

B26 promotes root development by the production of phytohormones such as indole acetic acid (IAA), Gibberellic acid and cytokinin which in turn improves plant nutrient absorption (Gagné-Bourque et al 2015). It has the ability to solubilize soil phosphorous thus it helps in nutrient acquisition (Gagne-Bourgue *et al.*, 2013a). B26 increased accelerated growth rate, and increased root and shoot weights in inoculated *Brachypodium* plants as compared to control plants(Gagné-Bourque *et al.*, 2015). It helped in improvement of timothy growth under drought stress through the modification of osmolyte accumulation in roots and shoots (Gagné-Bourque et al 2016).

2.6.2 Biocontrol

Its culture filtrate contains several well-characterized lipopeptide toxins and it has the potential to act as bio-inoculant for the enhancement of biomass of grasses (Gagné-Bourque et al 2013). It produces various antimicrobials compounds e.g., bacillomyin D, iturin D and E and surfactin C13, C14 and C15; and volatile compounds which directly or indirectly promote plant growth (Gagné-Bourque et al 2013). However, the intricate molecular relationship and the underpinning mechanisms responsible for the above results is not well understood.

2.7 CONNECTING TEXT

Chapter 2 outlined the extensive literature on basic characteristics of PGPR, their mode of action, and methodologies for studying plant-PGPR interaction.

Chapter 3 examines how PGPR is recruited to plant roots and in turn how plants respond to PGPR inoculation. Our focus is on identifying the effect of *Brachypodium* root exudates and individual organic acids on chemotaxis and biofilm formation of *B. velezensis* strain B26. Combination of molecular and microscopic approaches is beneficial to identify the biofilm formation by B26 on the roots of *Brachypodium distachyon*. Additionally, we investigate the impact of B26 inoculation on organic acid-encoding genes of the TCA cycle in *Brachypodium*.

The following chapter is published in Frontiers in Microbiology.

Chapter 3. A Crosstalk Between *Brachypodium* Root Exudates, Organic Acids and *Bacillus velezensis* B26, a Growth Promoting Bacterium

Meha Sharma, Dina Saleh, Jean-Benoit Charron and Suha Jabaji*

Department of Plant Science, Faculty of Agricultural and Environmental Sciences, McGill University, Canada, Montreal, Quebec, Canada

*** Correspondence:** S. Jabaji; Department of Plant Science, McGill University, 21,111 Lakeshore Rd., Ste-Anne-de-Bellevue, Quebec, Canada, H9X 3V9.

Reproduced from:

Sharma, M., Saleh, D., Charron, J.-B. and Jabaji, S. (2020) A crosstalk between Brachypodium root exudates, organic acids, and Bacillus velezensis B26, a growth promoting bacterium. *Frontiers in Microbiology*, **11**, 575578.

Minor modifications were made to follow the McGill University thesis guidelines

3.1 Abstract

Plant growth-promoting rhizobacteria (PGPR) are associated with plant roots and use organic compounds that are secreted from root exudates as food and energy source. Root exudates can chemoattract and help bacteria to colonize the surface of plant roots by inducing chemotactic responses of rhizospheric bacteria. In this study, we show that root colonization of *Brachypodium distachyon* by *Bacillus velezensis* strain B26 depends on several factors. These include root exudates, organic acids, and their biosynthetic genes, chemotaxis, biofilm formation and the induction of biofilm encoding genes. Analysis of root exudates by GC-MS identified five intermediates of the TCA cycle; malic, fumaric, citric, succinic, oxaloacetic acids, and were subsequently evaluated. The strongest chemotactic responses were induced by malic, succinic, citric, and fumaric acids. In comparison, the biofilm formation was induced by all organic acids with maximal induction by citric acid. Relative to the control, the individual organic acids, succinic and citric acids activated the *epsD* gene related to EPS biofilm, and also the genes encoding membrane protein (*yqXM*) and hydrophobin component (*bslA*) of the biofilm of strain B26. Whereas *epsA* and *epsB* genes were highly induced genes by succinic acid. Similarly, concentrated exudates released from inoculated roots after 48 h post-inoculation also induced all biofilm-associated genes. The addition of strain B26 to wild type and overexpressing mutant *icdh* line led to a slight induction but not biologically significant. Thus, B26 has no effect on the expression of the *ICDH* gene, both in the wild type and mutant backgrounds. Our results indicate that root exudates and individual organic acids play an important role in selective recruitment and colonization of PGPR and inducing biofilm. The current study increases the understanding of molecular mechanisms behind biofilm induction by organic acids.

Keywords: TCA cycle, biofilm, root exudate component, *Brachypodium distachyon*, chemotaxis, GC-MS.

3.2 Introduction

Plant-growth promoting rhizobacteria (PGPR) are soil and rhizosphere-derived inhabitants that colonize plant roots and positively influence plant growth and augment immunity (Benizri *et al.*, 2001, Gaiero *et al.*, 2013). It is apparent that effective colonization of the root system is essential for the exertion of beneficial effects of PGPR (Hardoim *et al.*, 2008, Lareen *et al.*, 2016). One of the plant's determinants affecting microbial communities in the rhizosphere is root exudates (Badri and Vivanco, 2009). Abundant amounts of photosynthates of low and high molecular weight compounds are secreted as root exudates into the rhizosphere. Root exudation includes organic acids, enzymes, phenolics, sugar and carbohydrates (mucilage) and proteins (Hawes *et al.*, 2000, Bais *et al.*, 2004). In the rhizosphere, these complex organic compounds may serve as chemoattractants or chemorepellents for plant-beneficial microbes (Badri and Vivanco, 2009, Liu *et al.*, 2017). Therefore, understanding the role of organic acids in root exudates in influencing the PGPR community structure and function is of paramount importance for plant development.

Organic acids are generated from intermediates of the tricarboxylic acid cycle (TCA) and are exuded into the rhizosphere (Zhang and Fernie, 2018). These intermediates are synthesized by various enzymes viz; citrate from Citrate synthase (CS), fumarate from Succinate dehydrogenase (SDH), malate from Malate dehydrogenase (MDH), Fumarate hydratase (FH), succinate from Succinyl-CoA synthetase, and 2-Oxoglutarate from NADP-dependent Isocitrate dehydrogenase (ICDH)(Araujo *et al.*, 2012). Organic acids are an essential driver of bacterial activity in the rhizosphere (Eilers *et al.*, 2010). It is believed that root exudates take on a dialogue role between plants and rhizospheric microbes in the efficient recruitment of rhizospheric microbes (Bais *et al.*, 2004, Sun *et al.*, 2012). Several reports have documented the regulatory role of organic acids in plant-microbe interactions (Kamilova *et al.*, 2006, Adeleke *et al.*, 2017). Others demonstrated that

specific organic acids released from plant roots can attract and recruit specifically single species of bacteria in the rhizosphere. For example, motility and chemotactic response of *Pseudomonas fluorescens* WCS365 towards tomato (*Solanum lycoperscum* L.) roots were induced by malic and citric acids (de Weert *et al.*, 2002). Citric and malic acids secreted from *Arabidopsis thaliana* roots and watermelon (*Citrullus vulgaris* L.) roots attracted and enhanced root binding of *Bacillus subtilis* FB17 biofilm (Rudrappa *et al.*, 2008), and also recruited *Paenibacillus* SQR-21 in the rhizosphere (Ling *et al.*, 2011). However, the effect of PGPR on the expression of TCA cycle genes is still unknown. The first two elements of bacterial interaction with plant roots are the attraction of bacteria towards plant roots through chemotaxis (Gaworzewska and Carlile, 1982), leading to colonization and biofilm formation. Biofilm formation on the roots is indicative of successful plant-PGPR colonization. The biofilm matrix of endospore-forming *Bacillus* species is composed of exopolysaccharides (EPS), amyloid-like fibers, and the coat protein, biofilm-surface layer protein (BslA) which is composed of hydrophobin component (Branda *et al.*, 2004, Branda *et al.*, 2006, Cairns *et al.*, 2014). EPS formation is controlled by 15-gene *epsA-O* operon (Branda *et al.*, 2004). Among the *eps* operons, gene *epsA* and *epsB* are the membrane component of tyrosine kinase, which forms EPS (Elsholz *et al.*, 2014). At the same time synthesis of fibers is controlled by three gene *tapA-sipW-tasA* operon. However, for the delivery of the biofilm matrix component protein (TasA), another gene *yqxM,* is required (Lemon *et al.*, 2008). Although several studies have explored plant-microbe interactions, few explored how root exudates regulate biofilm-associated genes.

It is well documented that *Bacillus* spp. stimulate plant growth by increasing nutrient availability through the synthesis of phytohormones, or suppressing plant diseases (Chauhan *et al.*, 2019). Previously, we demonstrated that *B. velezensis* B26, previuosly known as *B.*

methylotrophicus strain B26, internally colonized the model plant *Brachypodium distachyon* and accelerated its growth by the production of phytohormones, volatiles and various antimicrobial compounds (Gagne-Bourgue *et al.*, 2013a, Gagné-Bourque *et al.*, 2015). Furthermore, exposure of inoculated *Brachypodium* and timothy grass to extended drought conditions improved their tolerance to drought stress by increasing the accumulation of either acquired or inducible osmolytes associated with drought protection compared to non-inoculated plants (Gagné-Bourque *et al.*, 2015, Gagné-Bourque *et al.*, 2016).

However, the role of *Brachypodium* root exudates and the interaction of root colonization with strain B26 are yet to be established. In the present study, the objectives were to determine whether exogenously-added organic acids and GC-MS identified organic acids released from roots of B26-colonized *Brachypodium* could **i**) promote the expression of *Brachypodium* genes encoding the respective organic acids in the TCA cycle; **ii**) induce chemotactic responses of strain B26; **iii**) promote the biofilm formation of B26 by activating the expression of biofilm-associated genes, and that **iv**) strain B26 could alter the expression of *Brachypodium* mutant lines overexpressing organic acid genes relative to the colonized wild type. This study is useful to understand the role of root exudates in plant-PGPR interactions.

3.3 Materials and Methods

3.3.1 Bacterial Strain and Culture Conditions

Bacillus velezensis strain B26 (GenBank Accession number LGAT00000000) formally known as *B. methylotrophicus*strain B26 (Gagne-Bourgue *et al.*, 2013a, Jeukens *et al.*, 2015a), was originally isolated from leaf blades and seeds of the bioenergy crop switchgrass (*Panicum virgatum L.*). The strain B26 was stored in Lysogeny Broth (LB) (BDH chemical Ltd, Mississauga, ON, Canada)

supplemented with 20% glycerol at -80 ºC and recovered on LB at 28 ±1.0 ºC on a rotatory shaker at 120 rpm overnight. Following appropriate dilution in LB broth, 10^8 CFU.mL^{-1} (OD_{600} of 1.0) were used in all experiments unless otherwise stated.

3.3.2 Plant Material and Growth Conditions

Seeds of *Brachypodium* wild type Bd21-3 and T-DNA mutant lines **(Table 3.1)** with overexpression or loss of function were sourced from the DOE Joint Genome Institute, CA (https://jgi.doe.gov/our-science/science-programs/plant-genomics/brachypodium/brachypodium-t-dna-collection/). Seeds of *B. distachyon* wild type accession Bd21-3 were soaked overnight in sterile distilled water at room temperature, after which the lemma was removed. The seeds were sterilized in 70% ethanol for 30 s, 1.3% sodium hypochlorite for 4 min, and then rinsed three times with sterile distilled water (Vain *et al.*, 2008). For stratification and vernalization, sterile seeds were placed between two sterile filter papers moistened with sterile distilled water in a Petri dish incubated at 4 ºC in the dark for 15 days.

Multiplication of *Brachypodium* mutant lines was performed following the protocol of DOE Joint Genome Institute, CA (http://1ofdmq2n8tc36m6i46scovo2e-wpengine.netdna-ssl.com/wp-content/uploads/2015/05/T-DNA-genotyping.pdf). Briefly mutant seeds were sown in pots (6.35 × 6.35 × 7.62 cm) containing G2 Agro Mix® (Plant Products Co. Ltd) and were watered to field capacity. Pots were wrapped with cling film and aluminium foil to preserve the moisture and block any source of light and were left undisturbed to allow vernalization at 4 ºC in the dark. A week later, pots were placed in a growth chamber set under the following conditions: 16 h photoperiod, 150 µmoles .m^2. s^{-1} of light intensity, and day/night temperature of 25°C / 23°C.

3.3.3 Genotyping of T-DNA Mutants

Multiplex PCR was performed using Gene Specific Primers (GSP) and T3 T-DNA left border primer**.** PCR-based genotyping was carried out on T-DNA mutant lines **(Table 3.2)** to screen for homozygous plants. Primer sets were designed based on gene sequences retrieved from Phytozome Bd21-3 v1.1 genome (Phytozome v12.1, https://phytozome.jgi.doe.gov/pz/portal.html). Primer 3 web tool (version 4.0.0) was used to design gene specific primers (GSP) from at least 500 bases on either side of the putative insertion site in the gene (**Table 3.2**). Genotyping of all mutant lines was performed following the protocol of DOE Joint Genome Institute, CA (http://1ofdmq2n8tc36m6i46scovo2e-wpengine.netdna-ssl.com/wp-content/uploads/2015/05/T-DNA-genotyping.pdf). Seeds of homozygous mutant lines JJ19999 overexpressing *Isocitrate dehydrogenase* (*icdh*) were retained for downstream applications. Genotyping of the remaining T-DNA-mutant lines did not yield homozygous lines even after two generations.

3.3.4 Root Exudate Collection

Experiment 1. Semi-hydroponics system (**Supplementary Figure 3.1**) was developed for the collection of root exudates using Magenta GA-7 tissue culture boxes (7.62 x 7.62 x 10.2 cm) (Sigma-Aldrich, US). Pre-germinated seeds of wild type Bd21-3 (5 seeds/box) were transferred to Magenta boxes filled with an inert substrate consisting of a mixture of 1.7- 2.5 mm sterile glass beads of low alkali (Ceroglass, USA) up to 2 cm in height. Beads were saturated with ¼ strength Hoagland's solution (pH 6.0, buffered with 2 mM MES (2-[N-morpholino] ethanesulfonic acid). Glass beads supported good root mass (**Supplementary Figure 3.1**). A total of 12 magenta boxes were used in this experiment, and each box represents an experimental unit. Boxes were transferred

to a growth cabinet (Conviron, Canada) with light intensity of 150 µmoles. $m^2.s^{-1}$ 16 h light and 8 h dark at day/night temperatures of 25°C /23°C. After 40 days of growth, six boxes were inoculated with 500 µl of B26 (OD_{600} of 1) inoculum suspended in phosphate buffer (1M, pH 7) and six control boxes received 500 µL of phosphate buffer alone. All boxes were incubated in a controlled growth cabinet under the previously described conditions. After 48 h, inoculated and control *Brachypodium* seedlings from every two experimental units were pooled (total of 10 seedlings) to make 3 biological replicates per treatment. Prior to exudate collection, roots of intact plants from each replicate were rinsed off once in 20 mL of ultra-pure water for 2 h to remove cell debris and nutrient solution. The root system was placed in a 150 mL glass beaker so that the roots were fully immersed in 20 mL of ultra-pure water with gentle agitation for 24 h under the same growth chamber conditions (**Supplementary Figure 3.1).** The solution (20 mL) was filter-sterilized using 0.22 µm filter, freeze-dried, concentrated at 50x in ultra-pure sterile water and stored at -20 °C for downstream applications. Portions of the inoculated and control roots were processed prior and after root exudate collection for the visualization of B26 biofilm using scanning electron microscopy. The presence of B26 on and inside roots prior and after root exudate collection was confirmed by PCR. The remaining of the roots of each treatment were immersed in liquid nitrogen and stored at -80°C for mass spectrophotometric analysis and gene transcription of organic acids.

Experiment 2: To explore the possible role of plant-derived organic acid genes in chemotactic response and colonization of *Brachypodium* by strain B26, comparative transcript expression was measured between roots of wild type Bd21-3 and homozygous *Isocitrate dehydrogenase (icdh)* T-DNA mutant line. (**Table 3.1**; https://jgi.doe.gov/our-science/science-programs/plant-genomics/brachypodium/brachypodium-t-dna-collection/). Pregerminated seeds of wild type Bd21-3 and *icdh* mutant were grown in semi-hydroponic Magenta boxes. Each Magenta box had

5 seeds of wild type or *icdh* mutant and were grown under controlled conditions as described above. Three Magenta boxes represented biological replicates for wild type and mutant lines. Following 40 days of growth, both wild type and mutant lines were inoculated with strain B26. Roots were harvested 48 h post-inoculation, immersed in liquid nitrogen for downstream gene expression studies.

3.3.5 Organic Acid Analysis Using GC-MS

Sample Preparation: All chemicals were of analytical grade and were purchased from Sigma-Aldrich (Oakville, Ontario, Canada). Freeze-dried root samples (30 mg) were pulverized into powder and lyophilized. Root exudates (116 µL) were transferred to 2 mL Eppendorf microtubes containing 200 µL of 80% methanol. There were three replicates for each treatment. For GC-MS analyses, the samples were sent to Rosalind and Morris Goodman Cancer Research Centre, McGill University, Quebec, Canada. Ceramic beads (32.8 mm) were added to the samples and processed in a homogenizer (Analytikjena SpeedMill Plus) for three times, 45 s each, followed by centrifugation at 4°C for 10 min at 1500 rpm. The supernatants were transferred to 1.5 mL Eppendorf tubes containing 1 µL of 800 ng.µL^{-1} of Myristic-d27 in pyridine and placed in a CentriVap vacuum centrifuge at 4 °C for overnight drying. Myristic-d27 is an internal standard used for retention time-locking.

Sample Derivatization: Samples were derivatized by adding 30 µL of MOX (10 mg Methoxyamine: HCl per 1 ml anhydrous pyridine) to each sample. This methoximation converts unstable keto groups to stable methoxyamines. Samples were later derivatized with MTBSTFA(N-tert-butyldimethylsilyl-N-methyltrifluoroacetamide) to form the more volatile TBDMS (tert-butyldimethylsilyl) derivatives.

GC-MS Data Acquisition: GC-MS analyses were performed using Agilent 5975C mass selective detector coupled to a 7890A gas chromatograph (Agilent Technologies, Santa Clara, CA, USA) with 7693 autosampler and a DB-5MS DG capillary column (30 m plus 10 m Duraguard®) with a diameter of 0.25 mm, film thickness of 0.25 µm (Agilent J &W, Santa Clara, CA, USA) as described by Mamer et al. (2012). The GC-MS was run in electron ionization mode (70 eV) and Selected Ion Monitoring (SIM) mode. Data acquisition was done in Scan and SIM modes using MassHunter (Agilent) software. The spectra obtained were compared against the NIST (National Institute of Standards) database. The root samples had large amounts of malic and citric acids, and were diluted 1:40 before being run again in Scan mode. While root exudates did not require dilution. Data were represented as normalized area which is the area of peak divided by amount of sample in mg (roots) or µL (root exudates).

3.3.6 Chemotaxis Assays

Organic acids including malic, citric, fumaric, and succinic produced by plants act as chemotactic agents to recruit beneficial bacteria to the rhizosphere (Tan *et al.*, 2013), and could provide nutrients for microbial community in the rhizosphere, and act as chemo-attractants representing the initial step for microbial recruitment and colonization process (Sasse *et al.*, 2018). The chemotactic response of strain B26 to organic acids was established using one quantitative method and two qualitative methods.

3.3.6.1 Method 1- Quantitative Chemotaxis Assay

A modified capillary chemotaxis assay was used to quantify the chemotaxis of B26 in response to different organic acids(Mazumder *et al.*, 1999). The chemotactic system consisted of three components; a disposable 200 µL pipette tip as the chamber, a 251/8-gauge needle and 1 mL

syringe as chemotaxis capillary. The syringe was filled with 500 µL of one of the following filter sterilized organic acids: malic, citric, fumaric, succinic and oxalic acids prepared at concentrations of 10, 25, and 50 µmol.L^{-1}. Syringes with 500 µL sterile distilled water served as control for each of the chemoattractant. The needle–syringe capillary system was tightly inserted into the pipette tip containing 150 µL of bacterial suspension (OD_{600} = 1.0). Syringes were left undisturbed for 30 min, and the liquid inside the syringes was collected, serially diluted and plated on Petri-plates containing LBA medium. The plates were incubated overnight at 28 °C. Following 24 h incubation bacterial colonies were counted as the average colony-forming units (CFU) obtained from 5 replicate-plates. The relative chemotactic response (RCR) was calculated, which represents the ratio of the CFU in response to the chemoattractant at a certain concentration to that of the control (sterile water). An RCR ratio > 2 is considered significant.

3.3.6.2 Method 2-Drop Assay

The drop assay (Yuan *et al.*, 2015) was performed to trigger a chemotactic response by B26 bacterial cells. Briefly, B26 was grown in 50 mL of LB media with agitation at 160 rpm at 28 ºC. Pelleted cells were resuspended in 12 mL of sterile chemotaxis buffer (100 mM potassium phosphate [pH 7] with 20 µM EDTA) to which a 4 mL of 1% (v/v) of hydroxypropylcellulose solution was added. The cell suspension was placed in a 60 mm diameter petri plate to which a 10 µL drop of 50 mM of each organic acid (succinic, fumaric, citric, oxalic, malic) or 50 x of concentrated root exudates collected from inoculated and control roots were added to the centre of each Petri plate. Rings of turbidity that appeared in the next 30 min were recorded as an indication of the chemotactic response.

3.3.6.3 Method 3- Chemotactic Response of Strain B26 to Attractants in Carbon-Free Medium

This test was performed using the protocol of Kadouri *et al.* (2003). B26 was grown in LB as previously described. However, the cells were resuspended in potassium phosphate buffer (0.06 M, pH 6.8). Chemotaxis medium consisted of potassium phosphate buffer (pH 6.8), and 0.3% agar. 20 µL of above prepared B26 suspension was placed in the centre of a 60 mm Petri plate containing chemotaxis media. Based on the capillary chemotaxis assay results, malic acid was selected as the attractant. Filter paper discs soaked in 50 µM concentration of malic acid were placed near the border of the plate equidistant from discs soaked in water as controls. The movement of bacterial cells towards malic acid was observed 24 h and 48 h post-inoculation. The experiment was replicated five times.

3.3.7 Biofilm Quantification and Associated Traits

3.3.7.1 Biofilm quantification assay

To determine the effects of the root exudates and organic acids (OAs) on biofilm formation by strain B26, the biofilm assay was performed in 96-well microtiter plate as described by Yuan *et al.* (2015) with modification. B26 cells (OD_{600} of 1.0) were prepared as previously described. The bacterial suspension was pelleted by centrifugation at 8000 rpm for 10 min, washed twice with ½ MSgg medium (Branda *et al.*, 2001), and resuspended in the same volume (5 mL) as the culture medium. To each well, 200 µL of ½ MSgg medium along with 10µL of the above prepared bacterial suspension was added. Concentrated root exudates (50 x) or OAs were added to wells to obtain a final concentration of 10 µM, 25 µM, and 50 µM. The negative control consisted of culture medium alone. There were 6 replicates for each treatment. The plates were incubated for 24 h and 48 h at 37 ^{0}C without shaking. Following incubation, the non-adherent cells were removed

by washing with sterile distilled water, and the remaining adherent cells were stained with 200 µL of 0.1% solution of crystal violet. Plates were left undisturbed at room temperature for 30 min to allow proper staining of the biofilm cells. After 30 min, the excess crystal violet was removed by washing three times with distilled water, and plates were left to dry overnight. The crystal violet stain attached to the wells was later diluted by adding 200 µL of 4:1 (v:v) ethanol and acetone. Fifteen minutes later, solubilized crystal violet was transferred to a new microtiter plate and biofilm mass was quantified using a Synergy HT plate reader (Bio-TEK, Vermont, USA) at OD_{570}.

3.3.7.2 Exopolysaccharides (EPS) quantification assay

EPS form the extracellular matrix of biofilm. To quantify EPS production by B26, the procedure of Krithiga and Jayachitra (2014) was adopted. Strain B26 was grown in 50 mL of sterile LB culture medium and incubated on a shaker incubator (120 rpm) at 28 ºC for five days. Following incubation, the bacterial cells were centrifuged at 10000 rpm for 20 min at 4 ºC. The resulting supernatant was filter sterilized using a 0.45 µm filter (Millipore filter, Ireland) to which 600 mL of previously chilled ethanol was added. The mixture was left overnight, undisturbed in the fridge to allow the precipitation of EPS. The supernatant was removed using a vacuum pump (Bio-Rad), and the EPS layer was collected by centrifugation, and its dry weight was recorded. The experiment was performed with six replications.

3.3.7.3 Alginate quantification Assay

There is direct evidence that alginate functions to maintain cellular hydration, a function that has long been assumed and predicted but not demonstrated (Chang *et al.*, 2007). To determine the amount of alginate produced by B26 under normal and hydric stress conditions, strain B26 was

grown on LB and 5%; -0.47MPA, PEG-amended LB broth, respectively. The isolation of alginate from the culture supernatant was performed according to the method of Knutson and Jeanes (1968). Cell-free supernatant was collected after centrifugation at 10000 rpm for 10 min. Alginate quantification was performed by measuring the uronic acid content from a standard curve of alginic acid of brown algae (Sigma Aldrich, USA), ranging from 10 to 1000 $\mu g.mL^{-1}$ (May and Chakrabarty, 1994). Absorbance at A_{530} was indicative of a positive uronic acid test. The concentration of alginate production was measured in $\mu g.mL^{-1}$ by comparing it with a standard curve. The experiment was performed with six replications for each treatment.

3.3.7.4 Hydrophobicity Assay

Microbial adhesion to hydrocarbons (MATH) assay was performed using the classical method of Rosenberg (2006). The bacterial suspension in LB was centrifuged at 8000 rpm for 10 min and the pellet was resuspended in phosphate magnesium buffer (pH 7.4). Three hundred µL of hydrocarbon, n-hexadecane (Alfa Aesar, United States) was added to the bacterial suspension, incubated for 10 min at 30 ºC, vortexed, and left undisturbed to allow for phase separation. The adherence of bacteria to the hydrocarbon was retrieved, and cell density absorbance was measured at 600 nm. The adhesion of bacteria to the hydrocarbon phase, *FPc* was calculated using the established formula(Zoueki *et al.*, 2010) *FPC= (1-Af /A0) x100* where *Af* is the final absorbance after the addition of the hydrocarbon, *A0* is the original absorbance of bacterial cells before the addition of hydrocarbon. The experiment was performed with six biological replications.

3.3.7.5 Swimming and Swarming Motility Assay

Swimming and swarming motility assays were performed in LB Petri plates containing 0.3% (Swim plate) and 0.5% (Swarm plate) agar, respectively (Be'er and Harshey, 2011). Swarming

motility but not swimming was tested in the presence of malic, citric, fumaric, succinic, and oxalic acids. Petri plates with LB and 0.5% agar were fortified with 10 μM of each organic acid. Each plate was inoculated with 3 μL of strain B26 (OD_{600} of 1) in the centre and incubated for 24 h and 48 h at 28 ºC to determine the diameter of bacterial movement (mm). Assay plates were performed in six replicates.

3.3.8 Scanning Electron Microscopy for Biofilm Formation on Glass slide and Root Surface

3.3.8.1 Biofilm Formation in vitro

B26 was grown in LB medium as previously described. For imaging, 1 mL of the bacterial culture was placed on L-polylysine treated glass coverslips. Coverslips were incubated at 37 ºC for 48 h and were washed in 0.1M phosphate buffer (pH 7.2). Biofilm formed on the coverslips was fixed overnight at 4 ºC in 4% formaldehyde solution (v/v) buffered with 0.1M phosphate buffer (pH 7.2). Slides containing the biofilm-forming bacterium were dehydrated in an increasing series of ethanol (30-100%) with the last step repeated three times. This was followed by critical point drying of the slides using Leica EM-CPD300. The dried biofilm containing slides were coated with 4 nm of gold-palladium (Leica EM-ACE200) and examined using a Hitachi TM-1000 operating at 15 kV.

3.3.8.2 Biofilm Formation on Root Surface

A portion of the inoculated and control *Brachypodium* roots that were subjected before and after the root exudate collection experiment were fixed overnight in 100% methanol following the procedure of (Neinhuis and Edelmann, 1996). Samples were subjected to constant slow shaking at room temperature, followed by three washes of 100% ethanol, four hours each. Tissues were

subjected to critical point drying (Leica EM-ACE200), and later coated with 4 nm gold-palladium and observed with a Hitachi TM-1000 operating at 15 kV. The sample preparation and image acquisition were performed at the McGill University Multi-Scale Imaging Facility, Sainte-Anne-de-Bellevue, Québec, Canada.

3.3.9 Gene Expression Analysis

3.3.9.1 Expression Analysis of Organic Acid Genes in Wild Type Brachypodium Roots

To validate the observed trends of organic acids in root exudates and roots of *Brachypodium* wild type accession line Bd21-3, we examined the expression of genes encoding the respective organic acids in the TCA cycle (**Table 3.2**). Total RNA was extracted from flash-frozen pulverized 100 mg of root tissues 48 h post-inoculation with strain B26 and their respective controls using Spectrum^{TM} Plant Total RNA Kit (Sigma, Aldrich, US) following the manufacturer's protocols. RNA quality was confirmed on a denaturing formaldehyde agarose gel (1.2%) and quantified using a NanoDrop ND-100 spectrophotometer (Thermo Fisher Scientific). RNA (500 ng) was reverse-transcribed using One Script RT ABM kit (Vancouver, Canada) following the manufacturer's protocols. Reverse transcription PCR assays were performed on 3 biological replicates and two technical replicates. Primer sets (**Table 3.2**) were designed based on sequences retrieved from Phytozome Bd21-3 v1.1 genome (Phytozome v12.1, https://phytozome.jgi.doe.gov/pz/portal.html). Primers were designed online from IDT website using Primer Quest Tool (https://www.idtdna.com/PrimerQuest/Home/Index). qRT-PCR conditions were optimized for each primer set and putative products were confirmed by sequencing. PCR amplification was performed in 10 µL reaction containing 1 x SYBR Green master mix (Bio-Rad,US), 200 nM of each primer, and 100 ng of cDNA template. The PCR

thermal cycling parameters were, initial denaturation 95°C for 30 s followed by 40 cycles of 95°C for 15 s, annealing/extension 60°C for 30 s, along with dissociation curve at the end in Stratagene Mx3000 (Stratagene, Cedar Creek, USA). Transcript abundance was measured by using comparative threshold cycle (CT) method ($2^{-\Delta\Delta CT}$) (Livak and Schmittgen, 2001). Target genes were normalized over the housekeeping genes *ACTIN2*. BestKeeper tool (https://www.gene-quantification.de/bestkeeper.html) was used to compare housekeeping genes *ACTIN2* and *UBC18*. *ACTIN2* had the lowest coefficient variation as compared to UBC18.

3.3.9.2 Gene Expression Analysis of T-DNA Mutant Lines

The relative transcript abundance of *ICDH* in *icdh* mutant line was compared with inoculated wild type Bd21-3 accession line. RNA isolation from roots, cDNA synthesis, and qRT-PCR reactions were carried out as described in the above section. Primer sets were designed for T-DNA mutant line JJ19999 based on sequences retrieved from Phytozome Bd21-3 v1.1 genome. (Phytozome v12.1, https://phytozome.jgi.doe.gov/pz/portal.html), and were checked for specificity to amplify only their target gene (**Table 3.2).** *ACTIN2* was used for normalization of relative transcript abundance levels.

3.3.9.3 Expression Analysis of Biofilm Associated genes

The expression of biofilm-associated genes (*epsA, epsB, epsD, yqxM, bslA)* in response to various organic acids and root exudates were estimated by qRT-PCR. Cells of B26, obtained from the biofilm experiment, were induced in ½ MSgg medium amended with 25 µM concentration of each of the organic acids and 50x concentrated exudates released from inoculated and non-inoculated root after 24 h and 48 h as previously described in the biofilm quantification assay. Non-adherent

cells were removed, and RNA was isolated only from adherent cells using NucleoSpin® RNA isolation kit (Macherey-Nagel, Germany) based on the manufacturer's protocol. Primer sets were designed from B26 genome and sequence information is present in (**Table 3.2)**. cDNA synthesis and qRT-PCR conditions were the same as described in the previous section. *RecA* was used as housekeeping gene to normalize data. Data were analysed by $2^{-\Delta\Delta CT}$ method (Livak and Schmittgen, 2001).

3.3.10 Statistical Analysis

Data of all experiments were analysed using IBM Statistics SPSS Version 24(SPSS Inc., Chicago, IL). Comparison of mean was performed by Independent student t-test for comparison between control and inoculated samples. For analysis of more than two treatments as in the case of biofilm quantification and gene expression, data were analysed by univariate analysis using the Tukey's test ($P \leq 0.05$) to determine the statistical significance of the treatments compared to their controls.

3.4 Results

3.4.1 Chemotactic Response of Strain B26 to Organic Acids

The chemotaxis capillary assay revealed that strain B26 was attracted to a variety of organic acids and that B26 cell migration was positively linked to organic acid concentrations (**Table 3.3**). Significant ($P < 0.05$) higher numbers of cells were induced by fumaric and citric acids at concentration of 25 $\mu mol.L^{-1}$, followed by 10 $\mu mol.L^{-1}$ of oxalic acid and 50 $\mu mol.L^{-1}$ of malic acid. The chemotactic response of B26 to oxalic acid at concentrations higher than 10 $\mu mol.L^{-1}$, and citric acid at concentrations of 10 $\mu mol.L^{-1}$ and 50 $\mu mol.L^{-1}$ were similar to those in sterile water (control), and did not induce a chemotactic response (**Table 3.3**). RCR, the ratio of cell

number attracted to organic acids relative to control was significantly ($P \leq 0.05$) high with malic acid (17.6) at 50 µmol.L^{-1}, and citric acid (7.5) at 25 µmol.L^{-1}. This indicates that significant induction of chemotactic response with increasing concentrations of malic acid (**Table 3.3**).

3.4.2 Motility and Chemotaxis-associated Traits of *Bacillus velezensis* Strain B26 Were Triggered by Selected Organic Acids

All tested OAs (succinic, oxalic, citric, malic, and fumaric acids), and concentrated root exudates initiated a chemotactic response on B26 cells compared to the bacteria alone and buffer solution (**Figure 3.1A).** All organic acids, except oxalic acid induced relatively large rings of turbidity. Compared to organic acids, root exudates collected from inoculated (IE) and non-inoculated (CE) *Brachypodium* plants triggered an intense chemotactic response within 30 min with dense turbidity pattern, indicating that root exudates actively recruit cells of B26 (**Figure 3.1A**). Based on the high RCR ratio of malic acid with increasing concentrations (**Table 3.3**), the motility of strain B26 to malic acid as an attractant was illustrated in (**Figure 3.1B)**. The motility cells in the form of a turbid band of B26 cells were visible at 24 h and expanded in the direction of the malic acid, after 48 h (**Figure 3.1B)** as compared to discs imbibed with water (control).

3.4.3 Biofilm Associated Traits

Biofilm associated traits of strain B26 including quantification of EPS, alginate, hydrophobicity and swarming motility were determined. As shown in (**Table 3.4)**, the production of EPS by B26 was 868 µg.mL^{-1}. The production of alginate with hydric stress treatment led to an increase of (18%) compared to media without PEG. The percent hydrophobicity of B26 (69%) was quantified as the fraction of bacteria adhered to the hydrocarbon phase.

To investigate whether strain B26 has the ability of swimming and swarming, B26 was grown on 'Swim plates' fortified with 0.3% and Swarm plates fortified with 0.5% agar. After 48 h of incubation, an extensive and significant ($P \leq 0.05$) increase in the diameter of the swimming zone travelled by bacteria in the Swim plate was observed (**Table 3.4**). The diameter of swarm significantly increased exhibiting the Bull's eye swarming phenotype in plates fortified with malic acid at 24 h (**Figure 3.1C, Table 3.4).** Compared to the control, other organic acids did not affect swarming motility. After 48 h, there were no differences between the control and the swarming patterns of B26 in plates fortified with organic acids.

3.4.4 Exogenously-Added Organic Acids and Root Exudates Enhanced Biofilm Formation in Strain B26

The biofilm formation of strain B26 in response to organic acids and root exudates was measured using a quantitative microtiter plate assay at 24 h and 48 h incubation. Irrespective of the type of organic acid, concentration and time of incubation, the biofilm production of B26 significantly ($P \leq 0.05$) increased after 24 and 48 as compared to the control **(Table 3.5)**. The relative fold increase (RFI) values of biofilm formation of B26 cells to culture media in response to organic acids at 24h ranged from 2.4 for citric acid (25 and 50 µM concentrations) to 3.8 for fumaric acid (10 µM concentration). Whereas the RFI values of biofilm formation at 48 h incubation ranged from 3 for succinic acid (10 µM concentration) to 9.2 for citric acid (50 µM concentration). The effect of *Brachypodium* exudates collected from non-inoculated and inoculated roots on biofilm formation significantly increased relative to the control after incubating the microtiter plates for 24 h and 48h. The RFI values of both treatments relative to the control at 24 h was 5.8 and 7.7, and at 48 h RFI values were 5.7 and 7.7, respectively. However, induction of biofilm formation in response to root exudates sampled from inoculated and non-inoculated roots was similar **(Table 3.5).**

3.4.5 Strain B26 Forms Biofilm on Abiotic Surfaces and *Brachypodium* root Surfaces

Bacterial cells of B26 were visualized for biofilm formation on glass coverslips and root surfaces of *Brachypodium.* Formation and adherence of B26 biofilm was observed on glass slides (**Figure 3.2A**). On *Brachypodium* roots aggregates of B26 rod-shaped cells were encased in a network of mucilage surrounding the roots before and after root exudate collection (**Figures 3.2 C, D**). No such network was observed in control non-inoculated *Brachypodium* roots (**Figure 3.2B).** Additionally, the presence of strain B26 was confirmed on roots prior and after root exudate collection using specific primer set for B26 (Forward Primer 5'CAAGTGCCGTTCAAATAG3', Reverse Primer 5' CTCTAGGATTGTCAGAGG 3') (**Supplementary Figure 3.2**).

3.4.6 Strain B26 Modulated The Levels of Organic Acids in Root Exudates and Roots of *B. distachyon*

A qualitative GC-MS analysis of organic acids in the TCA cycle was performed on roots and root exudates of *Brachypodium* along with their respective controls. Chemical compounds were identified by peak data on the chromatogram **(Supplementary Figure 3.3).** Peak areas observed as the quantifier ions of the TCA cycle metabolites were for succinic, fumaric, oxaloacetic, malic, 2-ketoglutaric, aconitic, citric, isocitric, pyruvic and lactic acids. Organic acids in root exudates were measured in terms of relative peak area. mL^{-1}, while organic acids in *Brachypodium* roots were measured by relative peak area.mg^{-1}. A significant ($P \leq 0.05$) increase was observed in oxaloacetic, malic, fumaric, citric, succinic and 2-ketoglutaric acids in root exudates from B26 inoculated *Brachypodium* roots (IE), compared to root exudates (CE) of the control (**Figure 3.3**). The relative peak area of fumaric acid in exudates of inoculated roots (IE) was the highest among all the organic acids. In contrast, in the case of roots, the maximum peak area was observed in the

malic and citric acids irrespective of treatment or control, indicating the highest production of these two organic acids in roots. However, only fumaric acid significantly increased in inoculated roots (IR) as compared to control roots (CR), while the remaining organic acids in inoculated roots (IR) had similar levels as their respective controls (**Figure 3.3**).

3.4.7 Strain B26 Triggered the Regulation of Organic Acid Genes Encoding the TCA Cycle

To validate the observed trends of organic acids in roots, we examined transcript abundance of the following organic acid genes [*Citrate synthase* (*CS*), *Isocitrate dehydrogenase* (*ICDH*), *Succinyl-CoA synthetase*, *Succinate dehydrogenase* (*SDH*), *Fumarate hydratase* (*FH*) and *Malate dehydrogenase* (*MDH*)] in tissues of inoculated and control roots by qRT-PCR. A significant upregulation in transcripts abundance of *CS* and *MDH* by 3-fold ($P = 0.005$) and 4-fold ($P = 0.002$), respectively were observed in tissue of the inoculated roots (I) (**Figure 3.3**). However, a slight increase ($P \geq 0.05$) in transcript abundance of *FH* (1.7-fold), *ICDH* (1.2-fold) and *Succinyl-CoA synthetase* (1.5-fold) was observed in inoculated roots. On the other hand, transcripts of *Succinate dehydrogenase* (*SDH*) were downregulated in inoculated roots relative to the control (**Figure 3.3**).

3.4.8 Gene Expression Analysis of *icdh* Mutant lines

Multiplex PCR of T-DNA mutants for genes *Succinate dehydrogenase*, *Malate dehydrogenase* and *Citrate synthase* produced heterozygous bands even after two generations. Only lines of mutant NADP-dependent *Isocitrate dehydrogenase (icdh)* produced single homozygous bands of 600 bp compared to the wild type accession line Bd21-3 with a band size of 500 bp, indicating the absence of an insert (**Figure 3.4A**). Hence, only homozygous T-DNA *icdh* lines were retained for expression analysis. As expected, the transcript abundance of gene *ICDH* in non-inoculated mutant *icdh* line was significantly ($P = 0.001$; 2.6-fold) higher than in WtB- (**Figure 3.4B**). In response

to B26 inoculation, a 4.1-fold (P = 0.045) in the mutant *icdh*B+ compared to the WtB- was observed, (**Figure 3.4B).** There was no difference in transcript abundance of *ICDH* between wtB- and wtB+. Nevertheless, a slight increase (1.6-fold), although not statistically significant, in transcript abundance of *icdhB*+ relative to *icdhB*- was observed.

3.4.9 Organic Acids Induced Significant Changes in Biofilm Formation Through Activation of Genes Related to Biofilm and Genes Related to Hydrophobin in Strain B26

Transcript abundance of biofilm genes related to EPS formation; *epsA, epsB, epsD*; the gene *yqxM* encoding for membrane protein and *bslA* which encodes the hydrophobin component of the biofilm, were induced by specific organic acids. Organic acids caused a differential response of genes related to EPS formation at 24 h compared to the control (**Figure 3.5A**). The genes, *epsA,* and *epsB* were significantly upregulated by succinic acid, with a fold increase of 2.1 (P = 0.012), and 17.9 (P = 0.001), respectively, when compared to the control and other organic acids. Fumaric and malic acids significantly increased the transcription of *epsB* with 6.5-fold increase (P = 0.033) and 6.4-fold increase (P = 0.036), respectively. *epsD* was also upregulated by succinic and citric acids (1.8-fold, P = 0.004), and fumaric acid (1.5-fold; P = 0.04 when compared to the control. However, there was no difference in transcript abundance of *epsD* by malic when compared to the control. Genes *yqxM* and *bslA* in strain B26 were significantly induced by citric and succinic acids compared to other organic acids and control at 24 h. On the other hand, after 48 h of biofilm induction, transcript abundance of all the genes was almost similar in every treatment relative to the control. In contrast, succinic acid induced a 9.1-fold increase (P = 0.001) in transcript abundance of *epsB* (**Figure 3.5A**).

3.4.10 *Brachypodium* Root Exudates Differentially and Temporally Stimulated Biofilm Related Genes

The impact of root exudates on biofilm genes was also measured after 24 h and 48 h post-inoculation. At 24 h post-inoculation, transcript abundance of biofilm and extracellular matrix production genes were not significantly altered compared to control, except for *epsA* ($P = 0.002$); and the self-assembly hydrophobin encoding gene *bslA* ($P = 0.04$) that coats the biofilm, (**Figure 3.5B)**. While at 48 h post-inoculation, genes encoding the EPS biofilm formation and *yqxM* encoding gene for membrane protein, were significantly and temporally transcribed in response to exudates of inoculated roots. The highest fold increase was observed in *epsA* and *epsB* (3.2-fold) followed by *epsD* (2.6-fold) compared to exudates of non-inoculated roots and control **(Figure 3.5B)**. Interestingly, significant downregulation of *bslA* was observed relative to the control at 48h post-inoculation.

3.5 Discussion

We previously reported on the successful colonization of *Brachypodium distachyon* Bd21 by the plant growth-promoting bacterium (PGPR), *B. velezensis* strain B26. Strain B26 effectively increased root and shoot weights, and accelerated growth rate and seed yield when plants were grown in a potting mix (Gagné-Bourque *et al.*, 2015). In this study, we focused on the relation between *B. velezensis* strain B26 growth, chemotaxis, biofilm formation, and the role of *Brachypodium* root exudates in promoting colonization.

It is now recognized that successful colonization by PGPR and endophytes involves the initiation of cross-talk of signal molecules that originate from root exudates (de Weert *et al.*, 2002, Badri and Vivanco, 2009, Cao *et al.*, 2011, Feng *et al.*, 2018) and elicit a chemotactic response by bacterial endophytes (Yaryura et al., 2008; Yuan et al., 2015). Root exudates include diverse

groups of metabolites ranging from simple organic anions to complex polymer mucilages (Jones, 1998) and are considered a triggering factor for bacterial chemotaxis. Some of the components may serve as positive attractants leading to the recruitment and colonization of beneficial bacteria or as negative attractants to repel pathogens and parasitic plants (Badri and Vivanco, 2009, Liu *et al.*, 2017, Feng *et al.*, 2018). Simple organic anions including lactate, oxalate, succinate, fumarate, malate and citrate being the primary anion components of root exudates, some of which are vital signals to specifically induce directed motility and chemotactic response of beneficial soil bacteria (Rudrappa *et al.*, 2008, Canarini *et al.*, 2019).

Therefore, a semi-hydroponic system for the collection of roots exudates from intact *Brachypodium* root system grown under sterile conditions was developed using glass beads as an inert substrate to support root growth. This system facilitated the collection of sterile root exudates and the metabolite profiling of organic anions from intact root systems. The use of inert substrates such as glass beads or sand instead of soil or clay that strongly absorbs a variety of metabolites may affect exudation and metabolite profiles. Notably, root exudation studies of *Brachyodium* grown under sterile hydroponic systems resulted in similar metabolite profiles of exudates in sand or glass beads (Kawasaki *et al.*, 2016, Sasse *et al.*, 2019). The most common organic acids released from *Brachypodium* roots were malate, citrate, succinic, fumarate, and oxalate (Kawasaki *et al.*, 2016). In this study, roots and root exudates of *Brachypodium* had similar composition of organic acids. However, fumarate and succinate were the most abundant organic acids followed by malate, citrate and isocitrate released from exudates of *Brachypodium* at 48 h post-inoculation with strain B26 compared to those released from control root exudates. Root excretions of selective and significant amounts of fumarate and succinate followed by malate and citrate may indicate that these organic acids act as chemoattractants for strain B26 and may play an important role in root

colonization of *Brachypodium* (Badri and Vivanco, 2009). In parallel, we also validated the observed trends of organic acids in roots by examining the transcription abundance of genes encoding the respective organic acids in TCA cycle. Malate and citrate are intermediate metabolites of the TCA cycle, and their accumulation in root cells may result in their transcription and synthesis. As expected, a significant upregulation of genes encoding *MDH* and *CS* was observed in inoculated roots. In contrast, B26 did not trigger a significant transcript induction of *ICDH* in inoculated roots (I) relative to the control (C). Accordingly, B26 inoculation of *icdh* mutant line had no effect on *icdhB*+ and the wild type.

Given the unequal distribution of solutes, including organic acids in roots and root exudates, we did not attempt to correlate the internal concentrations to root exudation of organic acids with the assumption that higher internal concentration would lead to higher root exudation is misleading (Mariano *et al.*, 2005). Certain components of root exudates, including organic acids (e.g., fumarate, citrate, malate, and succinate) can positively trigger the induction of genes involved in the matrix and biofilm formation (Rudrappa *et al.*, 2008, Zhang *et al.*, 2014, Yuan *et al.*, 2015). In this study, the establishment that fumarate, succinate, malate and citrate were the most abundant organic acids in root exudates of inoculated *Brachypodium* roots, prompted us to study the transcription of genes encoding the components of the extracellular matrix of the biofilm, *epsA,B,D; yqxM* involved in biofilm matrix formation (Branda *et al.*, 2006) and *bslA* for self-assembling the hydrophobin that coats the biofilm (Zhang *et al.*, 2015). Succinic acid distinctly and temporally triggered the upregulation of *epsA ,epsB* genes encoding biofilm. While citric acid upregulated *yqxM* that is required for biofilm formation, and *bslA.* Fumaric acid and malic acid induced *epsB*. Similarly, *Brachypodium* root exudates also positively influenced the biofilm formation gene *epsA* in strain B26. These findings agree with Zhang *et al.* (2015). They showed

that root exudates and individual organic acid viz., fumaric, citric, malic, and succinic acids can trigger the differential induction of several biofilms and matrix formation genes of *Bacillus amyloliquefaciens* SQR9 in maize roots. Our findings suggest that selective organic acids and root exudates of *Brachypodium* are involved in biofilm induction.

The down regulation of the *bslA* gene at 48 h but not at 24 h in response to root exudates may well be due to the age of biofilm cells. The arrested growth of *Bacillus* biofilm after 50 h of incubation terminated the synthesis of biofilm matrix components (i.e., exopolysaccharides and the hydrophobin protein BslA) (Bartolini *et al.*, 2019). The reduction of *bslA* gene expression by root exudates after 48 h of incubation, may be to the onset of biofilm cells' age. The secreted protein, BslA is an essential component of biofilm surface repellence of *B. subtilis* biofilms. Once the surface repellence is lost, the biofilm starts disrupting (Kobayashi and Iwano, 2012).

For successful root colonization, chemotaxis and biofilm formation are the two most crucial activities performed by PGPR (Van de Broek *et al.*, 1998, Zhang *et al.*, 2014, Bhattacharyya *et al.*, 2017). Bacterial motility has an essential role in biofilm formation (Houry *et al.*, 2010, Allard-Massicotte *et al.*, 2016). In our study, the chemotactic response towards concentrated root exudates of *Brachypodium*, and a variety of individual organic acids that are involved in the TCA cycle played a functional role as signalling molecules, and initiated a chemotactic response using the quantitative capillary assay. A strong chemotactic response of B26 was observed particularly toward malic acid, followed by citric acid, succinic acid, and fumaric acid. Equally, under conditions of carbon-free medium, the motility of strain B26 had almost doubled in the presence of malic acid. These findings indicate that malic acid sustained bacterial growth in the absence of any other external compounds and reinforced the notion that organic acids in root exudates, and individual organic acids, can initiate a chemotactic response in strain B26

leading to biofilm formation. All organic acids, except oxalic acid, were capable of inducing a strong chemotactic response. These results agree with recent studies showing organic acids released from the roots of banana and tomato help the colonization *of Bacillus amyloliquefaciens* NJN-6 and *B*. *amyloliquefaciens* T-5, respectively (Tan *et al.*, 2013, Yuan *et al.*, 2015). Consistent with our results, the above studies also showed that oxalic acid did not induce a strong chemotactic response of their bacteria. Moreover, concentrated *Brachypodium* root exudates initiated strong chemotactic response. However, we cannot ignore that signalling compounds other than organic acids, including sugar, amino acids, and phenolic compounds are important components of the plant root exudates and could also serve as signals (Badri and Vivanco, 2009). In summary, the ability of B26 cells to move towards *Brachypodium* roots in response to carbon-containing compounds and proliferate is an essential trait that enables strain B26 to be competitive in the rhizosphere.

The enhancement of biofilm formation in response to root exudates was previously reported in *Bacillus velezensis* strain S3-1 in maize (Jin *et al.*, 2019), *Bacillus velezensis* strain FZB42 in tomato (Al-Ali *et al.*, 2018), *B. subtilis* in *Arabidopsis* and tomato (Rudrappa *et al.*, 2008, Chen *et al.*, 2012) and *Bacillus amyloliquefaciens* NJN-6 in banana root exudates (Yuan *et al.*, 2015). To further confirm that root exudates and exogenously-added organic acids affect biofilm formation of strain B26, quantitative microtiter assay showed that citric acid and oxalic acid promoted maximum biofilm formation after 48 h compared to the control, and most importantly, *Brachypodium* root exudate stimulated biofilm formation of strain B26. Similar results were reported where citric acid stimulated biofilm formation by *Bacillus amyloliquefaciens* SQR9 (Zhang *et al.*, 2014) and oxalic acid induced biofilm formation by *Bacillus velezensis* Strain S3-1 (Jin *et al.*, 2019).

Bacterial biofilms are congregations of bacterial cells within a matrix composed of EPS, alginates, and some proteins that contribute to the adherence of root systems (Davey and O'toole, 2000, Czaczyk and Myszka, 2007). Plant growth-promoting bacteria can take advantage of nutrients from root exudates to reproduce and facilitate the biofilm formation. The adhesion of bacteria to a solid surface in the form of biofilm is influenced by various traits viz; bacterial cell surface hydrophobicity; EPS production, and swarming ability (Nagórska *et al.*, 2010, Al-Ali *et al.*, 2018). PGPR most effectively mitigate the impact of abiotic stresses on plants through the production of polysaccharides and biofilm. Interestingly, our strain B26 exhibited all of the biofilm mentioned-associated traits. The bacterial polysaccharide and alginate play a vital role in maintaining the biofilm architecture and providing stress tolerance to plants(Halverson, 2009). Direct evidence points to the function of alginate in maintaining cellular hydration and biofilm formation under desiccation conditions (Chang *et al.*, 2007). Our study showed evidence that when strain B26 is under hydric stress, alginate production is substantially increased by 18%. These results may implicate the role of alginate in desiccation tolerance of B26 (Gagné-Bourque *et al.*, 2015). Previously, we reported that inoculation of *Brachypodium* and timothy grass with B26 affected the whole growth cycle of the plants, by accelerating the growth rates, lessening drought stress after 8 weeks, and improving plant growth through the osmolyte accumulation in roots and shoots (Gagné-Bourque *et al.*, 2015, Gagné-Bourque *et al.*, 2016). The notion that alginate also contributes to maintaining a hydrated microenvironment protecting B26 residents from desiccation and facilitating biofilm formation under stressful conditions may well be entertained and requires further testing.

Inoculation of *Brachypodium* roots with strain B26 allowed us to visualize the biofilm formation on roots prior and after collection of root exudates and compare it to that developed on

the abiotic surface (glass slides). As expected, different structures of the matrix were detected on the abiotic and biotic surfaces. A mesh-like form adhered to inoculated *Brachypodium* roots before and after root exudate collection. Hence, rinsing the roots in ultrapure water did not affect the biofilm formation on inoculated roots and is required for cell fixation and colonization of plant tissues (Gagné-Bourque *et al.*, 2015, Posada *et al.*, 2018). This matrix was absent in control roots. The biofilm has advantages to bacterial cells because it gives them protection from predators, provides a physical barrier against the diffusion of unwanted molecules and helps them retain nutrients (Bogino *et al.*, 2013). Similar types of biofilm matrix were formed by *Bacillus subtilis* EA-CB0575 in tomato and banana roots (Posada *et al.*, 2018).

3.6 Conclusion

In conclusion, our results indicate that colonized roots by PGPR improve the composition of root exudate and facilitate the chemotaxis and biofilm formation. We hypothesize that the biofilm induction by OAs is due to the upregulation of various biofilm-associated genes. Moreover, chemotaxis and biofilm formation results indicate that the strain B26 is primed for the endophytic lifestyle by organic acid and root exudates. These findings increased our understanding of molecular mechanisms behind the role of organic acid and root exudates in recruiting PGPR. Our results imply that *strain B26* is involved in modulating the organic acids of the TCA cycle. The increase in the transcription of TCA cycle intermediates in inoculated *Brachypodium* roots indicates the role of B26 in improving root exudate composition. This is the first report describing the effect of PGPR on TCA cycle genes in plants. Yet our current knowledge on the quantitative composition of organic acids and other compounds excreted by *Brachypodium* roots is still fragmented, and these further merit studies.

3.7 Author Contribution

Conception and design of the study: MS and SJ. Acquisition of data for the study: MS, and partly DS. Analysis of data for the work: MS. Interpretation of data for the work: MS and SJ. Manuscript revision and approval: MS, DS, JBC and SJ.

3.8 Acknowledgements

We greatly acknowledge Dr Youssef Chebli (Multiscale Imaging Facility Manager, Macdonald Campus) for assistance with SEM. Financial support, through a Discovery grant (RGPIN-2016-04805) to S. Jabaji, was provided by the Natural Sciences and Engineering Research Council of Canada.

3.9 Conflict of Interest Statement

The authors declare that the research was conducted in the absence of any commercial or financial relationships that could be construed as a potential conflict of interest.

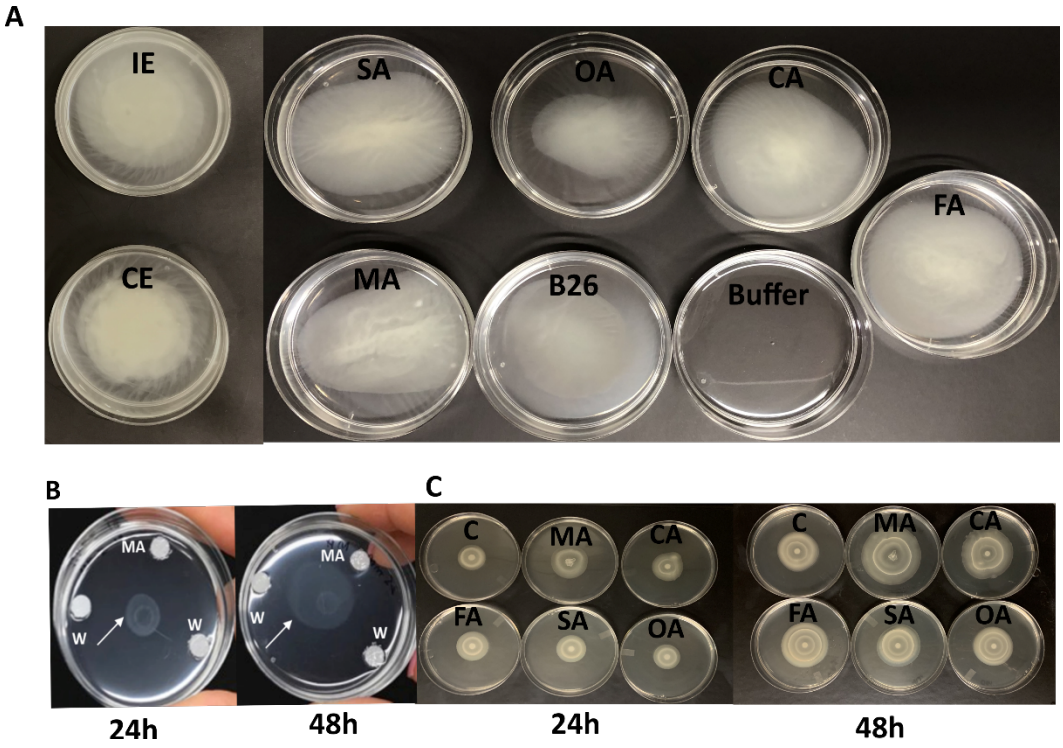

Figure 3.1 (A) Chemotactic response of Bacillus velezensis B26 towards different organic acids, inoculated (IE), and non-inoculated concentrated root exudates (CE) of Bd21-3. (B) Chemotactic responses of B26 towards malic acid (MA) after 24 h and 48 h. (C) Bull's eye type swarming pattern made by B26 on 0.5% agar fortified with organic acids after 24h and 48 h. MA, malic acid, CA, citric acid; FA, fumaric acid, SA, succinic acid, OA, oxalic acid; C, water.

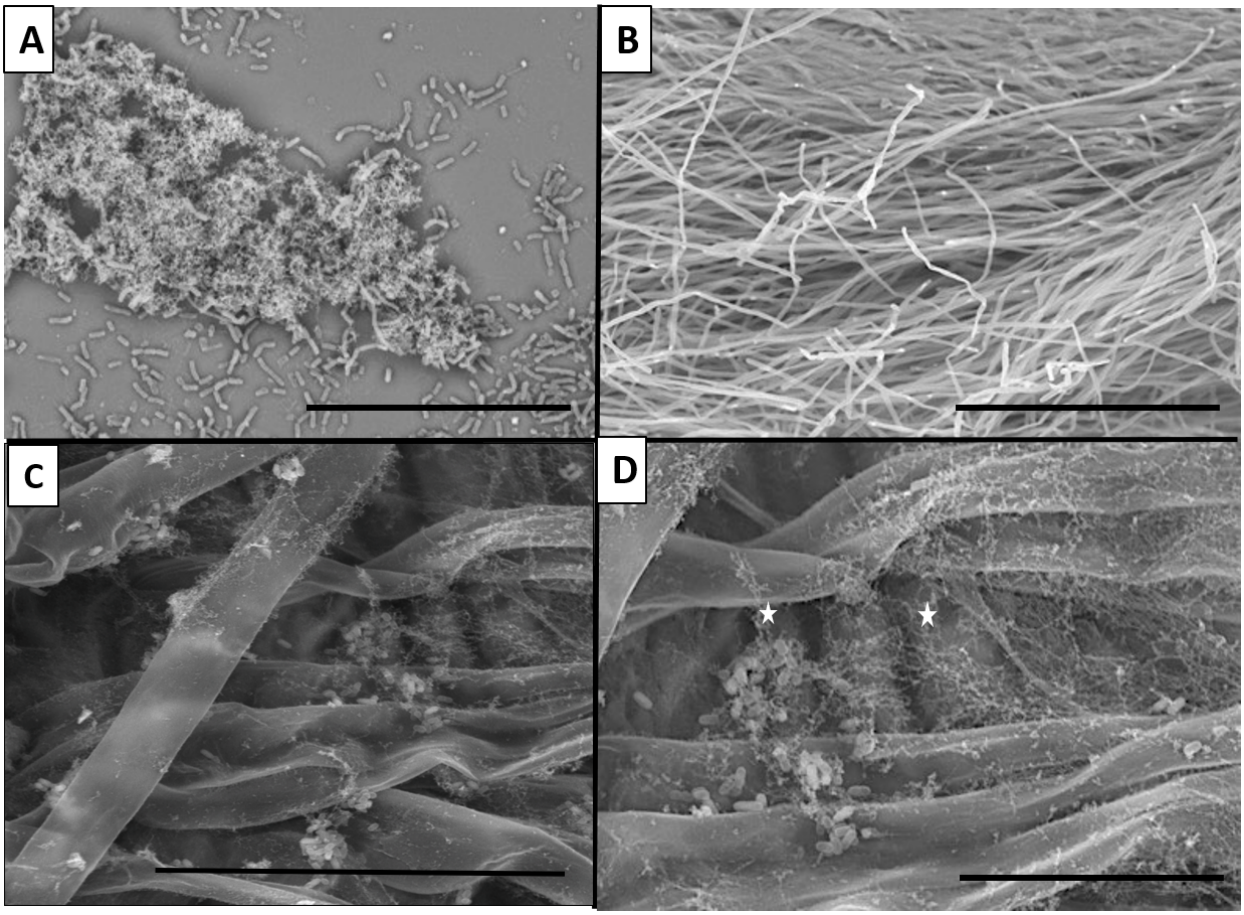

Figure 3.2 Scanning electron microscopy (SEM) micrographs of (A) Biofilm formation by B26 on glass surface (Bar = 30µm). (B) Control *Brachypodium distachyon* Bd21-3 roots (Bar = 300 µm). (C) Biofilm formation by B26 on the surface of roots prior to root exudate collection of Bd21-3 (Bar =50µm). (D) Magnified view of biofilm formed by B26 on Bd21-3 roots after root exudate collection (Bar = 20 µm).

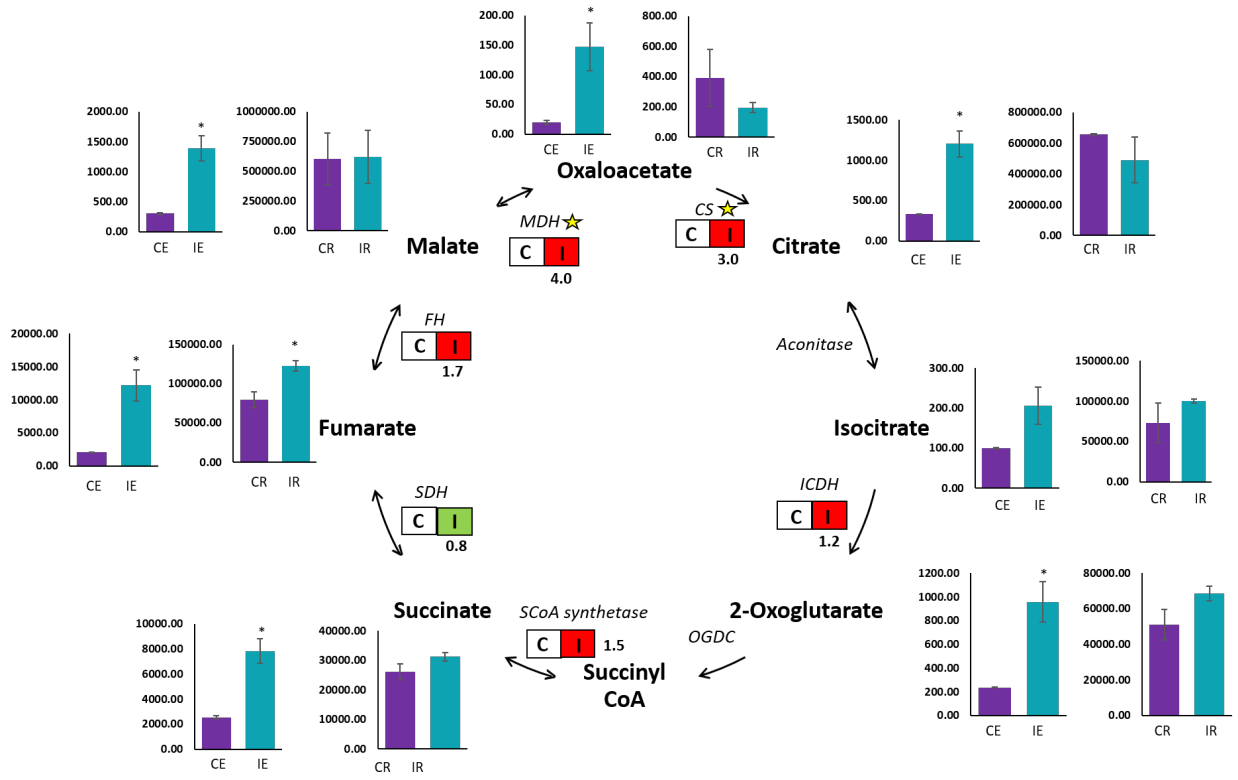

Figure 3.3 GC-MS and transcript analysis of TCA cycle genes in Bd21-3 roots inoculated with B26 for 48 h. Bar graphs represent the GC-MS results of control roots (CR), inoculated roots (IR), control root exudates (CE), and inoculated root exudates (IE). Significant changes are shown by an asterisk according to Independent t-Test ($P \leq 0.05$). Transcription of encoding genes of the TCA cycle are shown by boxes with non-inoculated roots (C) and inoculated roots (I). Red illustrates an increase in relative transcript abundance in response to B26, and green represents a decrease in expression. Fold change in transcript abundance is indicated below each box. Yellow stars represent significant differences ($P \leq 0.05$) between control and treatment. CS, Citrate synthase; ICDH, Isocitrate dehydrogenase; SCoA synthetase, Succinyl CoA synthetase; SDH, Succinate dehydrogenase; FH, Fumarate hydratase; MDH, Malate dehydrogenase.

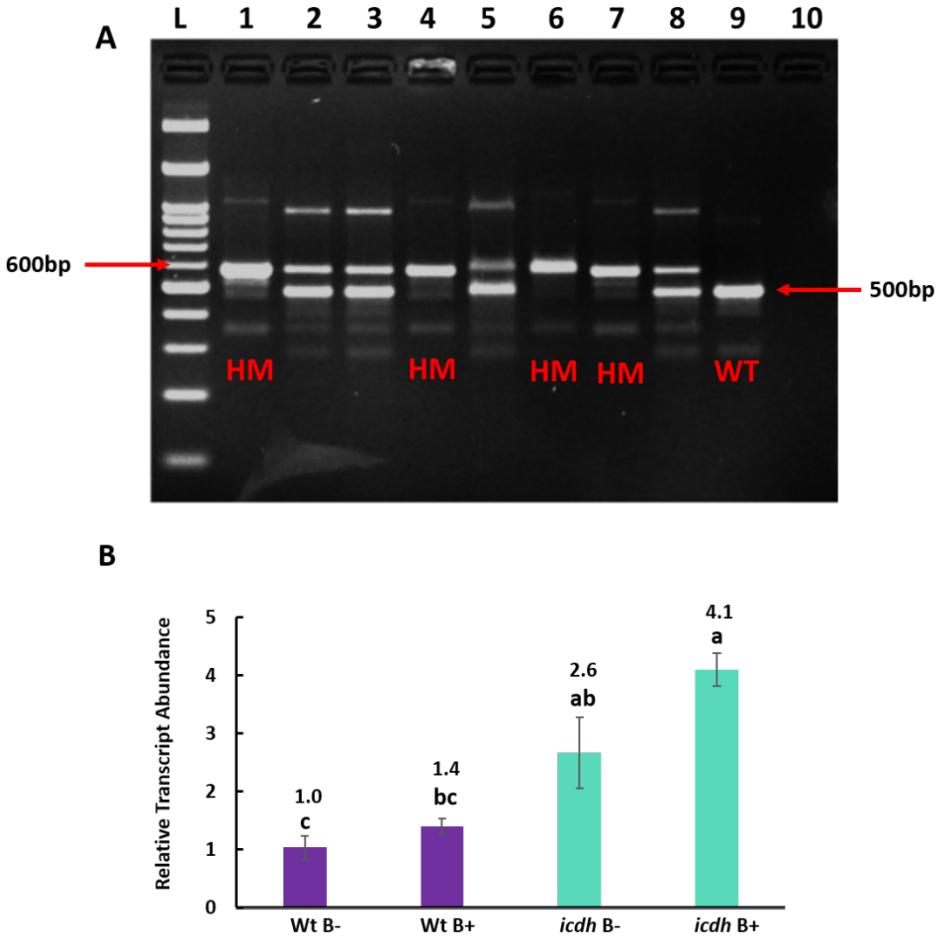

Figure 3.4 (A) Genotyping of homozygous (HM) *Isocitrate dehydrogenase* (*icdh*) mutants of Bd21-3. L: 100 bp ladder, lanes 1-8: DNA from different *Isocitrate dehydrogenase* of Bd21-3 T-DNA line JJ19999, lane 9: Wild Type Bd21-3(WT), lane 10: Negative Control. (B) Relative transcript abundance of gene *ICDH* in non-inoculated wild type Bd21-3 roots (WtB-); inoculated wild type Bd21-3 roots and (WtB+); selected homozygous mutant (*icdh B-)* and inoculated mutant (*icdh B*+). Numbers above bar graphs represent significant fold change relative to the control (wtB-). Means with same letters are not significant, while means with different letters are significant according to Tukey's test ($p \leq 0.05$).

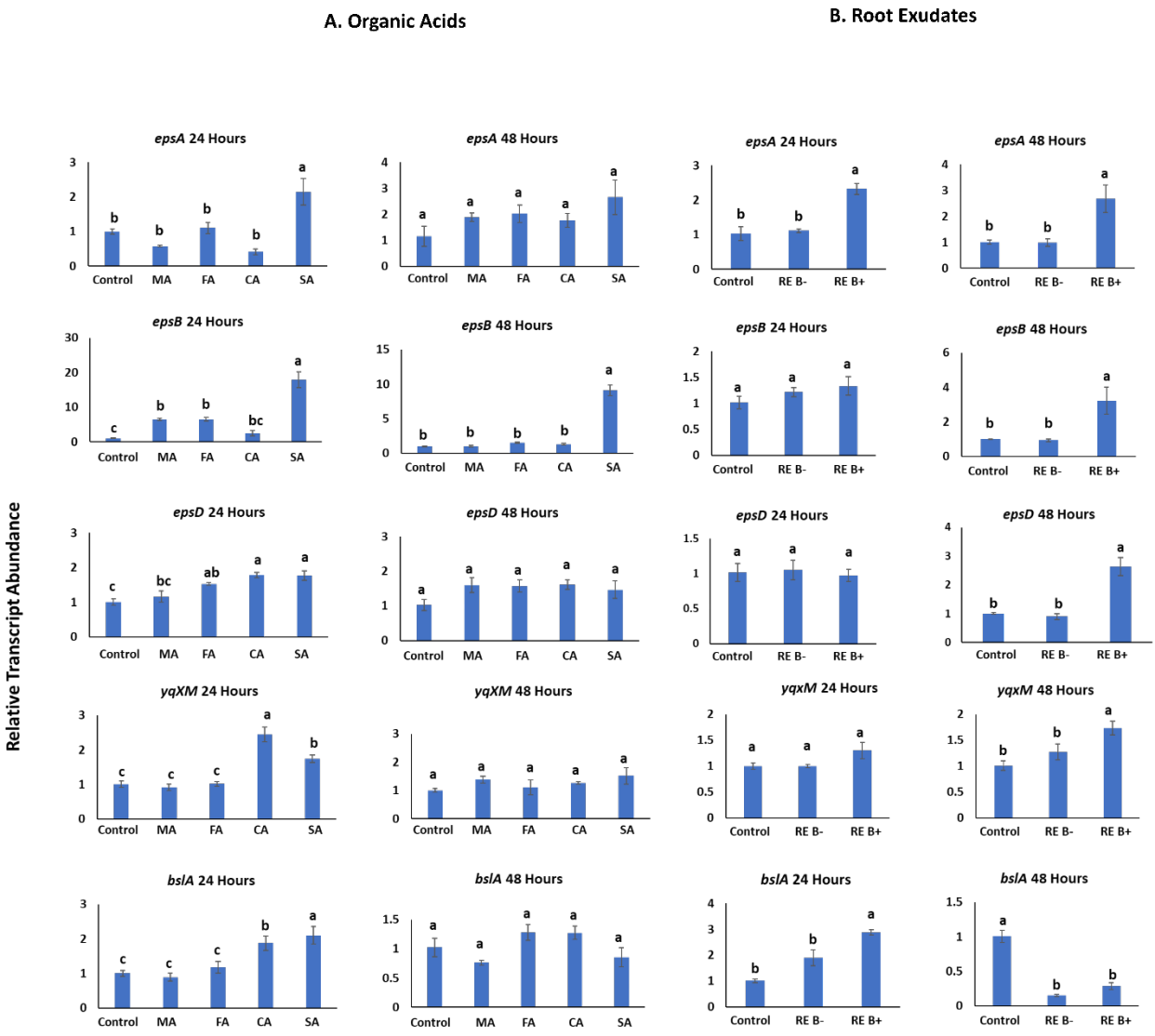

Figure 3.5 Transcript abundance of biofilm-related genes in induced B26 biofilm after 24 h and 48 h of induction with (A) various organic acids. MA, malic acid, FA, fumaric acid, CA, citric acid, SA, succinic acid. (B) with exudates from non-inoculated (RE B-) and inoculated roots (RE B+) and control (without root exudates). Letters (a,b,c) above the bar graphs represent means with significance according to Tukey's test ($P \leq 0.05$).

Table 3.1 Organic acid T-DNA mutant lines of *Brachypodium*

Gene	T-DNA line	Gene Tagged	Construct	Insert Class	No. of homozygous mutants identified	Type of Mutation	Reference
Malate Dehydrogenase	JJ27103	Bradi3g12460	pJJ2LBA	Exon	NA	Overexpression due to activation tagging	(Hsia *et al.*, 2017)
Succinate Dehydrogenase	JJ11635,JJ11665,JJ11645,JJ11605, JJ11687, JJ11687,JJ11574,JJ11675,JJ11621	Bradi3g13980	pJJ2LBA	5' UTR	NA	Overexpression due to activation tagging	(Hsia *et al.*, 2017)
Citrate Synthase	JJ2510	Bradi3g08910	pJJ2LB	Exon	NA	Loss of function due to Insertional mutation	(Bragg *et al.,* 2012)
Isocitrate Dehydrogenase	JJ19999	Bradi2g45420	pJJ2LBA	Near*	4	Overexpression due to activation tagging$	(Hsia *et al.*, 2017)

* Near means within 1000 bp of the 3' or 5' end of the gene

$ Activation tagging construct is designed to increase the transcription of nearby genes

Table 3.2 List of Primers used in this study

Gene of interest	Primer Name	Sequence (5'→3')	Annealing Temperature (°C)	Product Size (bp)	Source
Primers for insertion mutation detection					
Citrate synthase	CS-IN-F	CTGAGGCATTACACCCCTGT	56	427	BdiBd21-3.3G0119500.1
	CS-IN-R	TTCAGCAGTGAGAAGCCAGA			
Malate dehydrogenase	MD-IN-F	AAAAATGGGGCAGATCATCA	56	443	BdiBd21-3.3G0165100.1
	MD-IN-R	CATTGCAGGGTCGGTTACTT			
Succinate Dehydrogenase	SD-IN-F	TGTCTTTCATGCGATTCAGC	56	480	BdiBd21-3.3G0184500.1
	SD-IN-R	CACCTGGAAGGAGGAATGAA			
Isocitrate Dehydrogenase	ID-IN-F	ACTAATGGCGGATCTGA	56	496	BdiBd21-3.2G0578900.1
	ID-IN-R	GGTTCCCGGTGTTTGATTTA			
Hygromycin	Hyg-F	ATGAAAAAGCCTGAACTCACCGCGAC	58	950	Vogel Lab
	Hyg-R	CTATTTCTTTGCCCTCGGACGAGTGC			
T-DNA Left Border Primer	T3 TDNA LB	AGCTGTTTCCTGTGTGAAATTG	56	120	Vogel lab
	R9 TDNA LB	GATAAGCTGTCAAACATGAGAATTCAG	56	120	Vogel lab
qRT-PCR primers for Organic acid genes					
Citrate synthase	CS-Q-F	CTCCCGTCCTTCCTTCAAATAA	55	226	BdiBd21-3.3G0119500.1
	CS-Q-R	GATATCTAGAACCCGAGCAAGTC			
Malate dehydrogenase	RT-MD-F	TGCCAAGTGCTGTCCTAATG	55	171	BdiBd21-3.3G0165100.1
	RT-MD-R	AGCACTTCAGCCACAAAGGT			
Succinate Dehydrogenase	SD-Q-F	CACGTCTTAGAAACCGCTGTA	60	112	BdiBd21-3.3G0184500.1
	SD-Q-R	CCCATGACTTCGCCCTTATT			
Isocitrate Dehydrogenase	ID-Q-F	TACCCGTCATTTCCGTGTTC	60	92	BdiBd21-3.2G0578900.1
	ID-Q-R	TGTGTGCAAGTCCTCTTGTC			
Fumarase Hydratase	FH-Q-F	GGTGAACTTAGCCTACCAGAAA	60	108	BdiBd21-3.1G0851300.1
	FH-Q-R	ACCCATAACCTGAGCACAAA			
Succinyl coA Synthetase Alpha subunit	LSC1-F	GGATCCTCAGACAGAAGGTATTG	60	131	BdiBd21-3.1G0308500.1
	LSC1-R	GTGCAGTAAGTCCAGCTATGAA			
Succinyl coA Synthetase Beta subunit	LSC2-F	GGAGGAACCAGCATTGAAGA	60	119	BdiBd21-3.3G0651500.1
	LSC2-R	GCCAGACCATCAACAACTTTAC			
Ubiquitin	UBC18-F	GGAGGCACCTCAGGTCATTT	60	193	(Hong *et al.*, 2008)
	UBC18-R	ATAGCGGTCATTGTCTTGCG			
Actin	BdACTIN2-F	GTCGTTGCTCCTCCTGAAAG	55	188	(Derbyshire and Byrne, 2013)
	BdACTIN2-R	ATCCACATCTGCTGGAAGGT			
Primers for Biofilm associated genes					

epsA	epsA-F	GCTGCGAAATATGGTCATGG	60	141	B26 Genome
	epsA-R	AGCGTCTGCTTCACTTTCTC			
epsB	epsB-F	CGCTCTATTCTCGTCACTTCTT	60	140	B26 Genome
	epsB-R	GTCTCGTGTATCGTCGGTTT			
epsD	epsD-F	GACAACGGCTACGACATGAT	60	102	B26 Genome
	epsD-R	GTACAGCACCTTTGTCCCTT			
yqxM	yqxM-F	ATTTTTACGGCTTTCGTTCATT	60	269	(Xu *et al.*, 2013)
	yqxM-R	GTCCGCTCTTTTCCCTTATTCT			
bslA	bslA-F	CTGTCATGGCAAGTTTATTCGG	60	140	B26 Genome
	bslA-R	CTGGCTGGCACCTGTATATT			
RecA	recA-F	AAAAAACAAAGTCGCTCCTCCG	60	109	(Xu *et al.*, 2013)
	recA-R	CGATATCCAGTTCAGTTCCAAG			

Table 3.3 Chemotaxis of a B26 towards different organic acids

Chemoattractant	Chemoattractant concentration (µmol.L^{-1})	CFU.mL^{-1}*	RCR
Malic Acid	Control	0.36 ± 0.02 ^{c}	
	10	4.31 ± 0.26 ^{b}	11.87
	25	5.10 ± 0.44 ^{b}	14.07
	50	6.37 ± 0.26 ^{a}	17.59
Citric Acid	Control	1.05 ± 0.41 ^{b}	
	10	2.22 ± 0.37 ^{bc}	2.11
	25	7.86 ± 0.22 ^{a}	7.45
	50	0.64 ± 0.11 ^{b}	0.62
Fumaric Acid	Control	5.12 ± 0.65 ^{c}	
	10	0.55 ± 0.05 ^{b}	0.11
	25	13.56 ± 0.37 ^{a}	2.65
	50	0.51 ± 0.06 ^{b}	0.1
Succinic Acid	Control	0.36 ± 0.022 ^{c}	
	10	1.21 ± 0.14 ^{b}	3.31
	25	0.94 ± 0.06 ^{b}	2.61
	50	2.16 ± 0.22 ^{a}	5.95
Oxalic Acid	Control	2.76 ± 1.35 ^{b}	
	10	7.35 ± 0.52 ^{a}	2.65
	25	3.29 ± 0.39 ^{b}	1.18
	50	3.15 ± 0.23 ^{b}	1.14

*CFU numbers in columns represent the means of CFU $\times 10^3$ ± standard error of the mean $\times 10^3$ of 4 replicates. Means of specific chemoattractant with different letters within a column differ significantly according to the Tukey's test ($P \leq 0.05$).

RCR, relative chemotactic ratio is calculated based on the ratio of the colony-forming units (CFU $\times 10^3$) in response to the chemoattractant to the CFU $\times 10^3$ of the control (sterile water). An RCR ratio > 2 is considered significant.

Table 3.4 Biofilm-associated traits and swarming and swimming motility of B26

Biofilm Characteristics[#]		Swimming motility (zone diameter mm)[$]			Swarming motility (Swarm diameter mm)*	
		Treatment[#]	24 h	48 h	24 h	48 h
Hydrophobicity (%)	69	Control	10.7±0.3[b]	30.54±1.5[a]	25.3 ± 0.3 [b]	40.0 ± 2.8 [a]
EPS (μg.mL^{-1})	868.3± 22.0	Malic Acid	NA	NA	31.0 ± 2.0 [a]	48.3 ± 3.3 [a]
LB +Alginate (μg.mL^{-1})	375.2±17.9 [a]	Citric Acid	NA	NA	28.0 ± 1.1 [b]	43.3 ± 4.4 [a]
5%PEG +Alginate (μg.mL^{-1})	456.0±24.0 [b]	Fumaric Acid	NA	NA	27.6 ± 1.4 [b]	39.0 ± 2.0 [a]
		Succinic Acid	NA	NA	24.6 ± 0.8 [b]	36.6 ± 3.3 [a]
		Oxalic Acid	NA	NA	24.0 ± 1.1 [b]	38.6 ± 3.1 [a]

[#] Hydrophobicity, EPS, Exopolysaccharide, alginate, swimming and swarming motility represent the average of six replicates.
[$] Means within rows with different superscript letters are significant according to Independent t-Test ($P \leq 0.05$). NA, not applicable
[*] Means within columns with different superscript letters are significant according to according to Tukey's test ($p \leq 0.05$)

Table 3.5 Effect of different concentrations of organic acids and concentrated root exudate of *Brachypodium* accession Bd21-3 on biofilm formation of *Bacillus velezensis* B26 in 1/2 MSgg medium

Treatment*	Concentration	Biofilm formation (OD_{570}, 24 h)	RFI(OD_{570},24h)	Biofilm formation (OD570, 48 h)	RFI (OD570, 48 h)
Malic Acid	Media $	0.14 ± 0.01 [b]	-	0.16 ± 0.01 [b]	-
	10uM	0.50 ± 0.01 [a]	3.6	0.55 ± 0.04 [a]	3.4
	25uM	0.46 ± 0.02 [a]	3.3	0.53 ± 0.02 [a]	3.3
	50uM	0.46 ± 0.01[a]	3.3	0.54 ± 0.02 [a]	3.4
Citric Acid	Media	0.14 ± 0.01 [b]	-	0.16 ± 0.01 [b]	-
	10uM	0.42 ± 0.01 [a]	3	0.56 ± 0.01 [a]	3.5
	25uM	0.34 ± 0.01 [a]	2.4	1.16 ± 0.14 [a]	7.3
	50uM	0.33 ± 0.02 [a]	2.4	1.47 ± 0.20 [a]	9.2
Fumaric Acid	Media	0.14 ± 0.01 [b]	-	0.16 ± 0.01 [b]	-
	10uM	0.53± 0.01 [a]	3.8	0.55 ±0.02 [a]	3.4
	25uM	0.51 ± 0.03 [a]	3.6	0.52 ± 0.01 [a]	3.3
	50uM	0.45 ± 0.02 [a]	3.2	0.51 ± 0.01 [a]	3.2
Oxalic Acid	Media	0.14 ± 0.01 [b]	-	0.16 ± 0.01 [b]	-
	10uM	0.38 ± 0.01 [a]	2.7	0.49 ±0.02 [a]	3.1
	25uM	0.39 ± 0.02 [a]	2.8	0.97 ± 0.07 [a]	6.1
	50uM	0.37 ± 0.01 [a]	2.6	1.22 ± 0.09 [a]	7.6
Succinic Acid	Media	0.14 ± 0.01 [b]	-	0.16 ± 0.01 [b]	-
	10uM	0.41 ± 0.02 [a]	2.9	0.48 ± 0.03 [a]	3
	25uM	0.38 ± 0.04 [a]	2.7	0.52 ± 0.03 [a]	3.3
	50uM	0.41 ± 0.02 [a]	2.9	0.54 ±0.04 [a]	3.4
Root Exudate	Media	0.14 ± 0.01 [b]	-	0.16 ± 0.01 [b]	-
	Root Exudates B-	0.81±0.04 [a]	5.8	0.91 ± 0.06 [a]	5.7

Root Exudates B+	1.08±0.07 [a]	7.7	1.23 ± 0.05 [a]	7.7

*, Numbers represent the mean of 5 replicates ± standard error of the mean. Superscript letters within a column represent significance according to Tukey's test ($P \leq 0.05$).

[$], ½ MSgg is the medium specific for biofilm growth of *Bacillus*; Root exudates B-, Non-inoculated roots; Root exudates B+, Inoculated with B26; RFI: Relative Fold Increase, RFI is ratio of the treatment to media.

3.10 CONNECTING TEXT

In chapter 3, we found that *Brachypodium* root exudates, citric acid and malic acid-induced biofilm formation in B26 by upregulation of various biofilm-associated genes. Transcription of genes encoding *citrate synthase* and *malate dehydrogenase* were also upregulated in inoculated roots. This indicates the role of malic acid and citric acid in recruitment of B26.

Chapter 4 focuses on studying the potential use of four diverse *B. distachyon* genotypes to study PGPR-grass interactions throughout the whole growth cycle of the genotypes. Selection of best genotype was done on the basis of phenotypic performance. We identified the molecular basis behind this increase by looking into the expression of flowering pathway genes of *Brachypodium*. Intriguingly, phenotypic and CT-scanning data suggested an increase in root weight and root mass in inoculated roots. This promoted us to identify and quantify the phytohormone levels of inoculated roots using LC-MS and molecular approaches.

The following chapter is published in Scientific Reports.

Chapter 4. *Bacillus velezensis* strain B26 modulates the inflorescence and root architecture of *Brachypodium distachyon* via hormone homeostasis

Meha Sharma[1], Jean -Benoit Charron[1], Mamta Rani[1] and Suha Jabaji[1*]

[1]Department of Plant Science, Macdonald Campus of McGill University, 21,111 Lakeshore Rd., Ste-Anne de Bellevue, H9X 3V9, Quebec, Canada

*Corresponding author
S. Jabaji, Department of Plant Science, Macdonald Campus of McGill University, 21,111 Lakeshore Rd., Ste-Anne de Bellevue, H9X 3V9, Quebec, Canada

Reproduced from:
Sharma, M., Charron, J.-B., Rani, M. and Jabaji, S. (2022) *Bacillus velezensis* strain B26 modulates the inflorescence and root architecture of *Brachypodium distachyon* via hormone homeostasis. *Scientific reports*, **12**, 1-12.

Minor modifications were made to follow the McGill University thesis guidelines

4.1 Abstract

Plant growth-promoting rhizobacteria (PGPR) influence plant health. However, the genotypic variations in host organisms affect their response to PGPR. To understand the genotypic effect, we screened four diverse *B. distachyon* genotypes at varying growth stages for their ability to be colonized by *B. velezensis* strain B26. We reasoned that B26 may have an impact on the phenological growth stages of *B. distachyon* genotypes. Phenotypic data suggested the role of B26 in increasing the number of awns and root weight in wild type genotypes and overexpressing transgenic lines. Thus, we characterized the expression patterns of flowering pathway genes in inoculated plants and found that strain B26 modulates the transcript abundance of flowering genes. An increased root volume of inoculated plants was estimated by CT-scanning which suggests the role of B26 in altering the root architecture. B26 also modulated plant hormone homeostasis. A differential response was observed in the transcript abundance of auxin and gibberellins biosynthesis genes in inoculated roots. Our results reveal that *B. distachyon* plant genotype is an essential determinant of whether a PGPR provides benefit or harm to the host and shed new insight into the involvement of *B. velezensis* in the expression of flowering genes.

4.2 Introduction

Bacillus species are one type of rhizobacteria that can boost plant growth through the induction of antibiosis, facilitating nutrient availability through the synthesis of phytohormones, and competitive omission (Tiwari *et al.*, 2019). Such interactions help in endurance and adaptation of both host and PGPR in any stress environment (De Zelicourt *et al.*, 2013). We previously demonstrated that *Bacillus velezensis* strain B26, is a growth-promoting bacterium of timothy grass and the model plant *Brachypodium distachyon*, which enhanced the growth and accelerated

flowering time through the production of hormones, volatiles and various antimicrobial compounds (Gagne-Bourgue *et al.*, 2013a, Gagne-Bourque *et al.*, 2015). We also showed that strain B26 improves the growth of these grasses under extended drought conditions by modulating the expression of drought-responsive genes in *B. distachyon,* and also by the modification of osmolytes in roots and shoots of timothy grass (Gagne-Bourque *et al.*, 2015). Successful colonization of *B. distachyon* roots by strain B26 is based on the composition of roots exudates (the type of organic acid and their biosynthetic genes), chemotaxis and the induction of biofilm and their encoding genes(Sharma *et al.,* 2020).

It is well established that plant genotype can impact the degree of plant growth-promotion of some PGPR (Bodenhausen *et al.*, 2014). The effects of inoculation of 20 rice cultivars of genetically distinct groups with *Azospirillum* sp. provided varied results in terms of the number of tillers(Sasaki *et al.*, 2010). Also, different accessions of *Arabidopsis* displayed different microbial communities, indicating that plant host genetic factors shape the associated microbiota (Bodenhausen *et al.*, 2014, Haney *et al.*, 2015). The genotypes of the model grass *B. distachyon* has an important role in defining the plant host responses to PGPR(Do Amaral *et al.*, 2016). However, it is unclear whether the host's genotypic variations affect the microbiome in such a way that leads to adaptive consequences to the host. The study of Do Amaral *et al.* (2016) and others only described the short-term growth responses on plants(Pillay and Nowak, 1997)

B. distachyon is closely related to cultivated monocotyledons such as rice, wheat, and maize, and is a model plant to study plant-microbe interactions and stress tolerance (Gagne-Bourgue *et al.*, 2013a, Shi *et al.*, 2015, Saleh *et al.*, 2020). Due to ease in genetic transformation, *B.distachyon* is ideal for generating transgenic lines (Bragg *et al.*, 2012a). Various transgenic lines

have been generated in the background of *B.distachyon* accession line Bd21-3 with loss and gain of function of a target gene (Thole *et al.*, 2012, An *et al.*, 2016). Moreover, *B. distachyon* accessions exhibit variation in various phenotypic traits (Tyler *et al.*, 2014).

The reproductive success of many plants hinges on flowering(Ream *et al.*, 2014). Flowering responds to environmental cues such as long exposure to cold temperatures (i.e., vernalization) and photoperiods (i.e., variation in day length). The regulation of the flowering process in *B. distachyon* is controlled by several key genes, which include *VERNALIZATION 1* (*VRN1*), *VRN2* and *FLOWERING LOCUS FT1* (*FT1*) (Lv *et al.*, 2014, Ream *et al.*, 2014, Woods *et al.*, 2016).The expression of these genes is affected by temperature and photoperiods (Schwartz *et al.*, 2010). It was demonstrated that the over-expression of *FT1* accelerates flowering in *B. distachyon* and wheat (Shimada *et al.*, 2009, Ream *et al.*, 2014). However, the flowering pathways are not limited to the shoot apical meristem where flowers are originated, but it depends on shoot-root communication (Bouché *et al.*, 2016, Adeyemo *et al.*, 2019). For example, the majority of flowering genes in *Arabidopsis* and *Cassava* are variably expressed when plants are exposed to photoperiod that induces flowering (Bouché *et al.*, 2016, Adeyemo *et al.*, 2019).These studies provide a new understanding on the involvement of the root in the flowering process. Signalling molecules from roots including phytohormones modulate shoot growth and root architecture (Notaguchi and Okamoto, 2015). Additionally, the plant growth stimulation by beneficial rhizobacteria has been associated with the biosynthesis of plant growth regulators produced by rhizobacteria including auxins, gibberellins, cytokinins and ABA (Egamberdieva *et al.*, 2017). These microbial signals alter the plant hormone levels. Previously, we reported on the beneficial traits mediated by phytohormones produced by *B. velezesnis* strain B26 (Gagne-Bourgue *et al.*, 2013a) causing increased fitness of plant resulting in 121% more spikelets in inoculated *B.*

distachyon than the respective control (Gagne-Bourge *et al.,* 2015). Despite significant advances in plant-rhizobacteria interactions, regulation of plant flowering genes in response to rhizobacteria is scarce (Lu *et al.*, 2018).

Here, we aim to (i) study the potential use of *B. distachyon* genotypes for studies of PGPR-grass interactions throughout the whole growth cycle of the genotypes. (ii) characterize the responses of expression patterns of selected flowering genes to *B. velezensis* inoculation in *Brachypodium* wild accessions and (iii) understand whether strain B26 could alter the expression of *Brachypodium* transgenic lines overexpressing flowering genes relative to the colonized wild type (iv) understand whether growth promotion by strain B26 is differentially associated with phytohormone homoeostasis and transcript abundance. We screened four diverse genotypes of *Brachypodium* for their ability to be colonized by *B.velezensis.* We reasoned that *B. velezensis* may have an impact on the inflorescence and root architecture of *B. distachyon* genotypes

4.3 Materials and Methods

4.3.1 Bacterial Strain, Growth, and Inoculum Preparation

The Plant Growth Promoting Rhizobacteria (PGPR) viz., *Bacillus velezensis* strain B26 (Jeukens *et al.*, 2015b), formally known as *B. subtilis* (Gagne-Bourgue *et al.*, 2013a) was used in this study. The strain B26 was stored in 20% glycerol stocks in Lysogeny Broth (LB) (BDH chemical Ltd, Mississauga, ON, Canada) at -80 ^{0}C. Revival of strain B26 was done on LB at 28 ±1.0 ^{0}C on a rotatory shaker at 120 rpm until an OD_{600} of 1.0 (10^{6} CFU mL^{-1}) was reached. Cells of strain B26 were centrifuged, washed, and suspended in a volume of phosphate buffer (1M, pH 7) and used as inoculum for all experiments.

4.3.2 Plant Material and growth conditions of wild type and transgenic lines

Four *Brachypodium distachyon* accessions were selected based on their origins, vernalization requirements and flowering time. Selected accessions were Bd21, Bd21-3, Bd18-1 and Bd30-1 **(Supplementary Table 4.1).** Wild type seeds were provided by Dr Jean-Benoit Charron, Macdonlad Campus, McGill University, Canada which were originally sourced from Dr David F. Garvin(Vogel *et al.*, 2006, Garvin *et al.*, 2008), U.S Department of Agriculture (USDA)-Agriculture Research Service (ARS).

4.3.2.1 Growth conditions of wild-type B.distachyon accessions: Seeds were sterilized following the methodology of Vain *et al.* (2008). Stratification and vernalization of seeds were done by placing them between two moist filter papers in a Petri dish and incubating them at 4 ^{0}C in the dark. The number of days for seed incubation was decided according to the vernalization requirement of wild type accessions **(Supplementary Table 4.1).** After vernalization, seeds were sown in pots (6.35×6.35×7.62 cm) containing G2 Agro Mix® (Fafard et Frères Ltd, Saint-Remi, QC, Canada). Four sterile seeds were planted in each pot and pots were arranged in a Randomized Complete Block Design (RCBD). Pots were transferred to a growth cabinet (Conviron, Winnipeg, MB, Canada) with the light intensity of 150 μmoles $m^2.s^{-1}$, 16 hours light and 8 hours dark at day/night temperatures of 25°C /23°C. Every two weeks, plants were fertilized with 2g/litre of N-P-K Fertilizer 20-20-20 (Plant Products Co. Ltd, Laval, QC, Canada).

4.3.2.2 Growth conditions of transgenic lines: Transgenic lines *UBI: FT1* and *UBI: VRN1* were used along with wild type Bd21-3. *UBI:FT1* encodes a phosphatidylethanolamine binding protein known as florigen that travels from leaves to the shoot apical meristem to induce flowering (Ream *et al.*, 2014).While *UBI:VRN1* encodes for floral homeotic MADS-box transcription factor. Seeds of transgenic lines overexpressing flowering genes were kindly provided by Dr Daniel P Woods,

University of California-Davis, U.S. Seeds were imported with approved import permit P-2019-01394 from Canada Food Inspection Agency (CFIA). Seeds were sterilized as previously described for wild accession lines. Transgenic lines did not require vernalization, while the wild type was vernalized for three weeks at 4 ^{0}C in the dark. Four sterile seeds were planted in each pot and pots were arranged in a Randomized Complete Block Design (RCBD). Plants were grown in a controlled growth chamber with a higher light intensity of 300 μmoles $m^2.s^{-1}$, 20 hours light and 4 hours dark at day/night temperatures of 21°C /18°C as recommended (Woods *et al.*, 2019).

4.3.3 Genotyping of Transgenic lines

To confirm the homozygosity of transgenic lines, PCR-based genotyping was carried out. DNA was extracted from young leaves of transgenic plants following the modified CTAB method. cDNA specific forward primer and pANIC vector AcV5 tag reverse primer were used to detect transgene **(Table 4.1).** Wild type Bd21-3 was used as control. The presence and absence of amplification confirmed the transgene. Single-band amplification was considered a homozygous plant containing transgene. Only homozygous plants were used.

4.3.4 B26 Inoculation and Assessment of Plant Growth Parameters of Wild type Accessions and Transgenic Lines

Experiment 1: To examine the differential response of *B. distachyon* to B26 inoculation, wild accession lines were inoculated with strain B26 at defined phenological growth stages using BBCH numerical scale (Hong *et al.*, 2011). Twenty-one days old plants (BBCH 23) were inoculated with 10 mL of B26 cells suspended in phosphate buffer (10^6 $CFUmL^{-1}$), while control plants received 10 mL of phosphate buffer per pot. Plants were harvested after 14- and 28-days post-inoculation (dpi) at defined phenological (BBCH 61) and (BBCH73) growth stages, respectively, and various

phenotypic parameters were recorded. Five pots were harvested at each harvesting time point by carefully removing the substrate and washing the roots carefully. Growth parameters including Plant height, number of leaves, awns, tillers, fresh root and shoot weight were recorded. At each harvesting stage leaf and root samples were collected and stored at -80°C for downstream applications. The experiment was repeated twice.

Experiment 2. To determine the effect of inoculation on *B. distachyon* flowering, overexpressing transgenic lines were observed for plant growth parameters. 14-days old (BBCH 13) transgenic lines and wild type Bd21-3 were inoculated with 10 mL of B26 inoculum as described in the previous section. Data was recorded after 14 dpi (BBCH53), 28 dpi (BBCH69) and 42 dpi (BBCH87). At each harvesting time point, data of 5 pots per accession were recorded for plant height, number of leaves, awns, tillers, awn weight, fresh root and shoot weight. At each harvesting stage leaf and root samples were collected and stored at -80°C for downstream applications.

Experiment 3: To compare the total root volume between control and inoculated plants, macro CT-Scanning was done. A Semi-hydroponics system was developed for scanning of roots using Magenta GA-7 tissue culture boxes that were filled with sterile glass low alkali beads (Ceroglass, USA) saturated with Hoagland's solution as fully described in Sharma *et al.,* (2020). Pre-germinated seeds of wild type Bd21-3, transgenic lines *UBI:FT1* and *UBI:VRN1* (6 seeds/box) were transferred to Magenta boxes where each box is an experimental unit. Boxes were incubated in a controlled growth cabinet (Conviron, Canada) with light intensity of 300 μmoles m^2/s,16 hours light and 8 hours dark at day/night temperatures of 21°C /18°C. After 14 days of growth, three boxes of each line received B26 inoculum (500 μL OD_{600} of 1) suspended in phosphate buffer (1M, pH), and three control boxes received 500μL of phosphate buffer alone. All boxes were incubated in a controlled growth cabinet. A total of 6 Magenta boxes were used per line.

4.3.5 B26 Quantification in Root and Leaves of Selected Wild Type *B. distachyon* Accessions

Quantification of B26 DNA copy number was performed in roots and leaves of Bd21-3 and Bd30-1 at 14, and 28 dpi using qPCR. Genomic DNA was extracted from 1 g of powdered tissue using the modified CTAB method. DNA from the pure culture of B26 was also extracted from a single B26 colony using the boiling method (Woodman, 2008). For detection purposes, conventional PCR was done using B26 strain-specific primers in inoculated leaves and roots of selected accessions. B26 bacterial DNA served as a positive control in PCR. Cloning and qPCR reactions were performed as described in Gagne-Bourque *et al.,* (2015). To calculate the quantity of bacterial DNA in inoculated roots and leaves, Cq (Cycle quantification) values of plant DNA were correlated with Cq values in the standard curve. Moreover, for reliability of the designed method, correlation coefficient and the amplification efficiency were calculated from the formula $X_o = E_{AMP}^{(b-Cq)} = 10^{(Cq-b)/m))}$, where X_o = initial reaction copies, E_{AMP} = Exponential amplification, b = y-intercept of the standard curve (log_{10} of copies), m= slope of standard curve.

4.3.6 Phytohormone Analysis

To determine the effect of inoculation on phytohormones, endogenous levels of plant phytohormones including auxin, cytokinin, gibberellins and abscisic acid was measured using the modified protocol of Li *et al.,* (2017). Inoculated and control roots of Bd21-3, transgenic lines; *UBI:FT1* and *UBI:VRN1* from Experiment 2 were subjected to phytohormone analysis after 28dpi. Root samples were crushed in liquid nitrogen. Samples were sent in triplicates to The Metabolomics Innovation Centre, UVic-Genome BC Proteomics Centre, Victoria, BC, Canada. Briefly, 100 mg of each sample was precisely weighed into a 2-mL safe-lock Eppendorf tube. 4 µL of 5% formic acid in water per mg of raw tissue and two 4-mm stainless steel balls were added.

The sample was homogenized at a shaking frequency of 30 Hz on a MM 4000 mixer mill for 1 min three times. Methanol, at 16 µL per mg raw tissue was then added. The sample was homogenized again for 1 min three times, followed by sonication in an ice-water bath for 5 min and centrifugal clarification at 21,000 g and 10 ºC for 10 min. The clear supernatant was collected for the analysis of auxins, cytokinin, gibberellins and abscisic acid. Phytohormones were analysed with UPLC- multiple-reaction monitoring (MRM) mass spectrometry on an Agilent 1290 UHPLC coupled to an Agilent 6495B QQQ mass spectrometer equipped with an ESI source which was operated in the negative-ion mode. LC separation was carried out on a C18 UPLC column (2.1 x 150 mm, 1.8 µm). Concentrations of the detected compounds in the sample solutions were calculated by interpolating the constructed linear-regression calibration curve with the measured analyte-to-internal standard peak area ratios.

4.3.7 CT-Scanning of Wild type Bd21-3 and transgenic lines

The total root volume of inoculated and non-inoculated wild accession Bd21-3, transgenic lines *UBI:FT1* and *UBI:VRN1* grown in magenta boxes were compared by performing macro CT-scanning at 28 dpi. The root systems were scanned using macro-CT scanning with the Canon CT Aquilion Prime SP at the CT Scanning Laboratory for Agricultural and Environmental Research, Macdonald Campus of McGill University, Sainte-Anne-de-Bellevue, Quebec, Canada. Each magenta box served as one replicate with six plants per experimental treatment. Each box was in a standing up position at the time of CT scanning, and the lower part of each box was CT scanned individually. The main CT scanning settings were tube voltage, 80 kV; tube current, 50 mA; voxel dimensions, 0.188 x 0.188 x 0.5 mm^3 (X x Y x Z, with Z the axis of the CT scanner couch). Given the presence of glass beads (between which roots grew), root amount (instead of root system architecture) was studied and estimated from the CT scanning data, more particularly from the

histogram of CT numbers. A CT number (CTN) is an indirect measure of density; a macro-CT scanner is calibrated so that air CTN = –1000, water CTN = 0, CTN for glass beads appeared to be around +2000. Because of edge effects, the non-flat surface of the growth medium and the variable filling with glass beads, root amount was estimated within two volumes, a "larger volume V" and a "smaller volume V". Size of volumes (in voxels): larger volume V, 100 x 300 x 100 (53016 mm^3); smaller volume V, 100 x 150 x 80 (21206 mm^3). For comparison purposes, two ranges of CT numbers were used in root amount estimation with the smaller volume V (to define so-called pseudo-root voxels): [–700, +300] and [–800, +400]. Only the range [–700, +300] was used with the largest volume.

4.3.8 RNA extraction, cDNA synthesis and qRT-PCR analysis

4.3.8.1 Transcript abundance of Flowering genes in selected B. distachyon wild type and transgenic lines:

In response to B26 inoculation, we decided to choose the best phenotypic performer in terms of growth parameters (Bd21-3) and the least phenotypic performer (Bd30-1). We examined the gene expression of *Brachypodium* flowering pathway genes viz., *FT1*, *FT2*, *VRN1* and *VRN2* in leaves of Bd21-3 and Bd30-1 from Experiment 1 at 14 dpi and 28 dpi. To study the genotypic response of B26 on *B. distachyon* transgenic lines, transcript abundance of *FT1* and *VRN1* was measured in control and inoculated transgenic lines; *UBI: FT1* and *UBI: VRN1* along with wild type Bd21-3 roots and leaves from Experiment 2 at 28dpi. Briefly, total RNA was extracted from flash-frozen pulverized 100 mg of inoculated and control tissues using Spectrum™ Plant Total RNA Kit (Sigma Aldrich, US) following the manufacturer's protocols. One Script RT ABM kit (Vancouver, Canada) was used for reverse-transcription of RNA (500 ng) following the manufacturer's

protocols. PCR assays were performed on three biological replicates and two technical replicates. Primer details are present in (**Table 4.1)**. The conditions for qRT-PCR were adjusted for each primer set. PCR amplification was performed in a 10µL reaction following the protocol of Sharma *et al*. (2020)[5]. The $2^{-\Delta\Delta CT}$ method(Livak and Schmittgen, 2001) was applied to normalize the target gene over the housekeeping genes *UBC18*. Bestkeeper tool was used to compare housekeeping genes *UBC18* and *ACTIN2*. *UBC18* had the lowest coefficient variation as compared to *ACTIN2* so *UBC18* was chosen for the normalization.

4.3.8.2 Transcript abundance of genes encoding phytohormones in Bd21-3:

The effect of B26 inoculation on the phytohormone production by *B.distachyon* roots was quantified using qRT-PCR. Transcript abundance of auxin and gibberellins biosynthesis genes was measured only in roots of Bd21-3 from Experiment 2 at 28 dpi. Primer sets (**Table 4.1**) were designed based on gene sequences retrieved from Phytozome Bd21-3 v1.1 genome (Phytozome v12.1, https://phytozome.jgi.doe.gov/pz/portal.htmL. Primers were designed online from IDT website using Primer Quest Tool (https://www.idtdna.com/PrimerQuest/Home/Index). To confirm the specificity of Primers, sequences were checked for hairpins and hetero-dimer formations using the Oligoanalyzer tool (http://www.idtdna.com/calc/analyzer) and submitted to Nucleotide Blast at NCBI (http://www.ncbi.nlm.nih.gov/) and were custom synthesized by Integrated DNA Technologies (IDT, Iowa, USA). One hundred milligrams of tissue was subjected to RNA extraction. cDNA preparation and qRT-PCR were performed as described in the previous section.

4.3.9 Statistical Analysis

Data of all experiments were analysed using IBM Statistics SPSS Version 24(SPSS Inc., Chicago, IL). Comparison of means was performed by independent student t-test for comparison between

control and inoculated samples. Tukey's test was performed to compare the means of multiple treatments. We considered a $p < 0.05$ acceptable for statistical significance. Experiments 1 and 2 were performed using 5 replicates for each control and inoculated pots. To prevent contamination of treatments, two growth chambers were used for control and inoculated plants. To study the confounding effect of growth chambers, the experiments were repeated twice by exchanging the growth chambers of treatment with control plants.

4.4 Results

4.4.1 Bacterial Inoculation Elicited Varied Growth Response of B. *distachyon* Accessions

A differential response was observed in Bd21, Bd21-3, Bd18-1 and Bd30-1 in response to B26 colonization **(Figure 4.1a)**. At 14 days post inoculation (dpi), a significant increase of 150% in the number of awns and 250% increase in the shoot weight of inoculated accession Bd21 compared to non-inoculated control was observed (**Figure 4.1b, Supplementary Table 4.2**). The plant height and number of leaves of inoculated Bd18-1 increased by 34% and 78%, respectively compared to the control. At 28 dpi, Bd21-3 showed a significant increase in all growth parameters compared to the control **(Figure 4.1c)**. While Bd30-1 at 28dpi, did not show a significant response to B26 inoculation as indicated by the growth parameters (**Figure 4.1c**). However, there was no difference in flowering time of inoculated and non-inoculated plants. Control and inoculated accessions flowered at the same time but an increase in the number of awns was observed.

4.4.2 *B. distachyon* Accessions Sustained Populations of Strain B26 in Root and Shoot tissues

Quantification was done in roots and shoots of *B. distachyon* accession Bd21-3 that responded well to B26 inoculation in terms of growth parameters, and accession Bd30-1 that showed similar

growth responses to B26 as the control after 14 dpi and 28 dpi **(Table 4.2)**. Strain B26 had similar sustaining endophytic populations in roots and shoots in both genotypes. In the case of Bd21-3, more copies were found in roots at 28dpi as compared to shoots **(Table 4.2).** On the contrary, Bd30-1 had more copies in shoots at 14dpi. However, more B26 gene copies were found in tissues of Bd21-3 as compared to Bd30-1.

4.4.3 Differential Expression Patterns of Selected Flowering genes in inoculated *B.distachyon* genotypes

The expression analysis of flowering genes: *FT1, FT2, VRN1* and *VRN2* in leaves in response to B26 inoculation of Bd21-3 and Bd30-1 is depicted in **(Figure 4.2)**. Significantly higher expression levels ($p < 0.05$) of *FT1* (6.70-fold); *FT2* (12.1-fold); and *VRN1* (7.6-fold) transcripts were detected in inoculated Bd21-3 compared to the control at 28 dpi **(Figure 4.2a)**. The expression of *VRN2* in response to B26 was similar to the control. Inoculation of B26 in genotype Bd30-1, showed a significant up-regulation in *FT1* transcript abundance (4.8-fold) at 28dpi. **(Figure 4.2b)**. In contrast, to Bd21-3, a substantial increase (21.8-fold) in *VRN2* transcript levels in inoculated Bd30-1 was detected at 28 dpi.

4.4.4 Strain B26 Improves Root and Shoot weights of transgenic lines

Detection of transgene in *UBI: FT1* and *UBI: VRN1* was done by PCR. cDNA specific forward primer and pANIC vector AcV5 tag reverse primer were used to detect transgene in transgenic lines**.** PCR with *VRN1-F* /*FT1-F* and AcV5 tag yielded an expected band size of approximately 260bp and 500bp, respectively which confirmed the presence of transgene **(Supplementary Figure 4.1a, b)**. No amplification was observed in wild type Bd21-3 as there is no transgene

present. A wide differential growth response among the transgenic lines compared to the wild type genotype Bd21-3 was observed **(Figure 4.3a**). At 28 dpi, the root and shoot weights of transgenic line *UBI: FT1* significantly increased by 132% and 162%, respectively in response B26 **(Supplementary Table 4.3)**. Growth parameters such as the number of awns, root and awn weight of the wild type genotype Bd21-3 increased significantly by 34%, 52% and 43%, respectively **(Figure 4.3b, Supplementary Table 4.3).** No significant difference was observed between inoculated and control *UBI: FT1* at 14 dpi except for root weight.

4.4.5 Strain B26 Modifies Root Volume of Wild type and transgenic lines

B26 inoculation had a positive effect on the root volumes as estimated by macro CT-scanning. An increase of 3.56, 1.67 and 1.90 times, respectively in the root volume of wild type Bd21-3, transgenic lines *UBI:FT1* and *UBI:VRN1* inoculated roots as compared to control roots (**Table 4.3).**

4.4.6 Transcript Abundance of Flowering genes in Roots and Leaves of Inoculated Transgenic Lines

A 28 dpi, the phenotypic observations of flowering transgenic lines **(Figure 4.3 a, b)** showed the effect of inoculation is more noticeable in roots and awns of transgenics. This prompted us to study the expression of flowering genes in both roots and shoots of transgenic lines at this growth stage. Each transgenic line was compared with the wild type separately. A significant upregulation in transcripts of *FT1* gene (17,981-fold) was observed in inoculated roots of *UBI:FT1* relative to non-inoculated wild type. Strain B26 did not induce *FT1* nor *VRN1* genes in shoot tissues of inoculated transgenic plants. However, transcripts levels of *VRN1* gene were down-regulated in both roots and shoots of *UBI: FT1* and *UBI: VRN1* compared to the inoculated wild type (**Figure 4.4**).

4.4.7 B26 Affects Phytohormone Homeostasis

4.4.7.1 Quantification of the endogenous level of phytohormones

To complement earlier observations of the growth promotion of inoculated wild type Bd21-3 and transgenic lines, we measured the endogenous levels of phytohormones. Indole acetic acid (IAA), indole butyric acid (IBA) and indole -3-propionic acid (IPA), abscisic acid (ABA), kinetin and zeatin(cytokinin), gibberellins A_1, A_3, A_4 and A_7, were measured in roots of control and inoculated plants. Irrespective of the treatment, gibberellins (GA) were the most abundantly detected phytohormones. The phytohormone homeostasis in Bd21-3 was significantly affected by B26. Growth promotion of the wild type Bd21-3 by strain B26 is significantly (p <0.05) associated with increases in GA_4 (2-fold). While the amount of GA_7, and IAA were significantly less by 4.8 and 2.3-fold, respectively as compared to control roots **(Figure 4.5)**. In case of *UBI:FT1*, GA_1 was significantly higher in inoculated roots than control. However, the concentration of other phytohormones was detected less in inoculated *UBI:FT1* roots as compared to control roots. In contrast, levels of GA_1, GA_7 and IAA were 2.75, 1.59 and 1.89 times respectively higher significantly in inoculated roots of *UBI: VRN1* when compared to control roots. However, Kinetin, Zeatin and GA_3 were below the detection level.

4.4.7.2 Transcript abundance of genes related to Phytohormones in Bd21-3

A significant upregulation in transcripts of genes related to auxin biosynthesis was observed in wild type Bd21-3 only. *Anthranilate synthase alpha subunit 1(ASA1)* which catalyses the rate-limiting step of tryptophan biosynthesis (Niyogi and Fink, 1992) and Indole-3-acetic acid inducing gene (*IAA18)* were significantly up-regulated by 2.3 and 4.9-fold , respectively in inoculated roots as compared to control roots **(Figure 4.6)**. A significant downregulation was observed in transcript abundance of *GA20ox1* which encodes gibberellin 20-oxidase enzyme that is involved in the later

steps of the gibberellins (GA) biosynthesis pathway(Rieu *et al.*, 2008) Interestingly, DELLA proteins, a key negative regulator of GA signalling (Yoshida *et al.*, 2014) was significantly up-regulated by 3.8-fold in inoculated roots as compared to control roots **(Figure 4.6).**

4.5 Discussion

The data presented here indicate that *B. distachyon* is a useful model to study PGPR-plant association and could serve as a model for rice and wheat. A central finding in this study is that plant genotype is a crucial determinant of whether rhizobacteria inoculation promotes plant or not growth. The four genotypes behaved differently throughout the whole life cycle of the plants for each growth parameter and showed statistically positive or negative responses for one or more of the parameters tested. Such response is exemplified in genotype Bd21 and Bd21-3 by which induction of flowering was accelerated in response to B26. These results are not uncommon among plant accessions since naturally occurring resistance is common in studies of plant-microbe interactions. *B. distachyon* genotypes demonstrated significant and varied responses to infection by pathogenic insects and fungi (Sandoya and de Oliveira Buanafina, 2014). Moreover, several *B. distachyon* genotypes differed in their ability to associate with two diazotrophic strains and several genotypes responded negatively to the strains (Do Amaral *et al.*, 2016). Also, wild accessions of *Arabidopsis thaliana* showed reduced growth in response to *Pseudomonas fluorescence* (Haney *et al.*, 2015). Of interest, genotype Bd30-1 which performed less favourably among the other 3 accessions, had sustained B26 populations in roots and shoots, but was insufficient to induce growth promotion in accession Bd30-1. This suggests that a different mechanism is implicated, and this requires further analysis.

Molecular studies on the regulation of flowering genes (*FT1*, *FT2, VRN1* and *VRN2)* in response to environmental cues have been intensively studied in *Arabidopsi*s, cereals (Kim *et al.*, 2009,

Amasino and Michaels, 2010), and *B. distachyon* (Ream *et al.*, 2014). However, molecular studies on the regulation of flowering genes in response to rhizobacteria are scarce (Poupin *et al.*, 2013, Lu *et al.*, 2018). Flowering in *B. distachyon* is mostly regulated by three key genes viz., *VERNALIZATION1* (*VRN1*), *VRN2*, and *FLOWERING LOCUS T* (*FT*). *VRN1*, *VRN2* and *FT* form a regulatory loop in wheat and barley (Dennis and Peacock, 2009, Distelfeld *et al.*, 2009, Greenup *et al.*, 2009). We focused on studying transcript levels of flowering genes in Bd21-3 a genotype known as rapid flowering and Bd30-1 a genotype known to show intermediate flowering. The inoculation of genotype Bd21-3 with strain B26, induced an abundance of *FT1* transcript levels in shoots and it was not a limiting factor in the upregulation of *VRN1*. Our results are in agreement with the elevated expression patterns of *FT1* and *VRN*1 in the rapid flowering *B. distachyon* accessions(Ream *et al.*, 2014). Intriguingly, this trend supports the proposed model for wheat and barley during cold exposure (Dubcovsky *et al.*, 2006, Sasani *et al.*, 2009). However, *VRN2* acts as a repressor of flowering and was expressed at lower levels in spring accession of wheat and barley (Woods *et al.*, 2016). In *B. distachyon, VRN2* was also expressed at lower levels in the spring accession Bd21-3 (Schwartz *et al.*, 2010). The current study supports this evidence since *VRN2* was down-regulated in Bd21-3 accession line. In the case of the intermediate flowering accession line, Bd30-1, the expression of *VRN2* was remarkably high compared to Bd21-3. Similar results were obtained by Ream *et al.* (2014) in which Bd2-3 had more amounts of *BdVRN2* and less amount of *BdFT1*, suggesting that *VRN2* may play a role as a flowering repressor. Both Bd2-3 and Bd30-1 belongs to the Intermediate rapid flowering class.

To fully understand the role of B26 inoculation on flowering genes, we tested overexpressing flowering transgenic lines *UBI: FT1* and *UBI: VRN1*. Phenotypic data suggested an increase in awn and root weights in inoculated transgenic plants. This triggered us to investigate flowering

genes in roots in response to B26. Numerous flowering genes are identified in roots but were solely studied in the shoots. Bouché *et al.* (2016) reported that flowering genes in the roots of *Arabidopsis* are differentially expressed during flowering and concluded that roots may be involved in flowering by sending systemic signals or may participate actively in the regulation of flowering genes. However, the causal relationship was not very well established. In our study, the increase in expression of *FT1* in inoculated roots of *UBI: FT1* positively correlates with root weight. These transgenes are expressed under the control of maize ubiquitin constitutive promoter (Ream *et al.*, 2014) which upregulates the flowering gene expression, irrespective of bacterial treatment. Hence the increase in the transcript of *FT1* in inoculated roots of *UBI: FT1* is solely due to B26 inoculation. These results indicate that strain B26 modulates the transcription of flowering genes. This is the first report, according to our knowledge, that rhizobacteria can induce flowering genes in *B. distachyon* roots.

Non-symbiotic rhizobacteria contribute beneficial traits to colonized plants through bioactive compounds including, phytohormones (Patel and Saraf, 2017). These phytohormones influence the physiological processes of plants at very low levels (Kudoyarova *et al.*, 2019). Indeed, many studies demonstrated that rhizobacteria is associated with phytohormone concentrations and involved in homeostasis such as IAA, gibberellins, and IBA (Dodd *et al.*, 2010). In our study, the endogenous phytohormones concentrations in the roots were modified by strain B26. Surprisingly, the concentrations of IAA and GA_7 in inoculated Bd21-3 were lower than the control, but the transcripts of IAA were moderately up-regulated. This might be interpreted that strain B26 positively affected plant growth via metabolizing these phytohormones in the soil, a widespread trait among soil bacteria (Arshad and Frankenberger Jr, 1997). This plant hormonal homeostasis may rise from microbial consumption and production of hormones or fluctuations in plant

hormones in planta (Dodd *et al.*, 2010). Thus, plant-associated microbes can modulate plant metabolism by altering the plant hormone levels. Indeed, improved root growth of inoculated transgenic line *UBI: FT1* is attributed to GA_1 production and in *UBI: VRN1* to GA_7 and IAA. There is considerable evidence that gibberellins in grasses influence flower initiation (Mutasa-Göttgens and Hedden, 2009) Given that B26 affected endogenous amounts of phytohormones, the question then arises whether B26 effects on wild and transgenic lines resulted in larger root volume. We examined the roots of wild type and transgenic lines by Macro CT scanning that were inoculated with B26 and compared them to the control. Consistent with the induction of phytohormones in inoculated wild and transgenic lines, B26 had a positive effect on root volume of all accession lines. These results are congruent with preceding data and provide additional evidence of phytohormone modulation in *Brachypodium* roots by B26.

In summary, this report offers novel information about the long-term effects of a PGPR on plant development, advancing the knowledge on these relevant biological interactions. Our study shed new light on the involvement of strain B26 by influencing the flowering process in the roots. Key causal relationships cannot be established since we know little about the expression role of flowering genes in the *Brachypodium* roots and how they are connected to above-ground tissues. We also conclude that plant genotypes are critical to a successful interaction with PGPR.

4.6 Acknowledgements

We greatly acknowledge the financial support, through a Discovery grant (RGPIN-2016-04805) to S. Jabaji, which was provided by the Natural Sciences and Engineering Research Council of Canada. We thank Dr JB Charron for providing wild type *Brachypodium distachyon* seeds which

were originally sourced from Dr. David F. Garvin, USDA. We also thank Dr. DP Woods, UC Davis, for providing overexpressing flowering transgenic lines.

4.7 Author Contributions

Conception and design of the study: MS and SJ. Acquisition of data for the study: MS, and partly MR. Analysis of data for the work: MS. Interpretation of data for the work: MS and SJ. Manuscript revision and approval: MS, JBC and SJ.

4.8 Conflict of Interest Statement

The authors declare that the research was conducted in the absence of any commercial or financial relationships that could be construed as a potential conflict of interest.

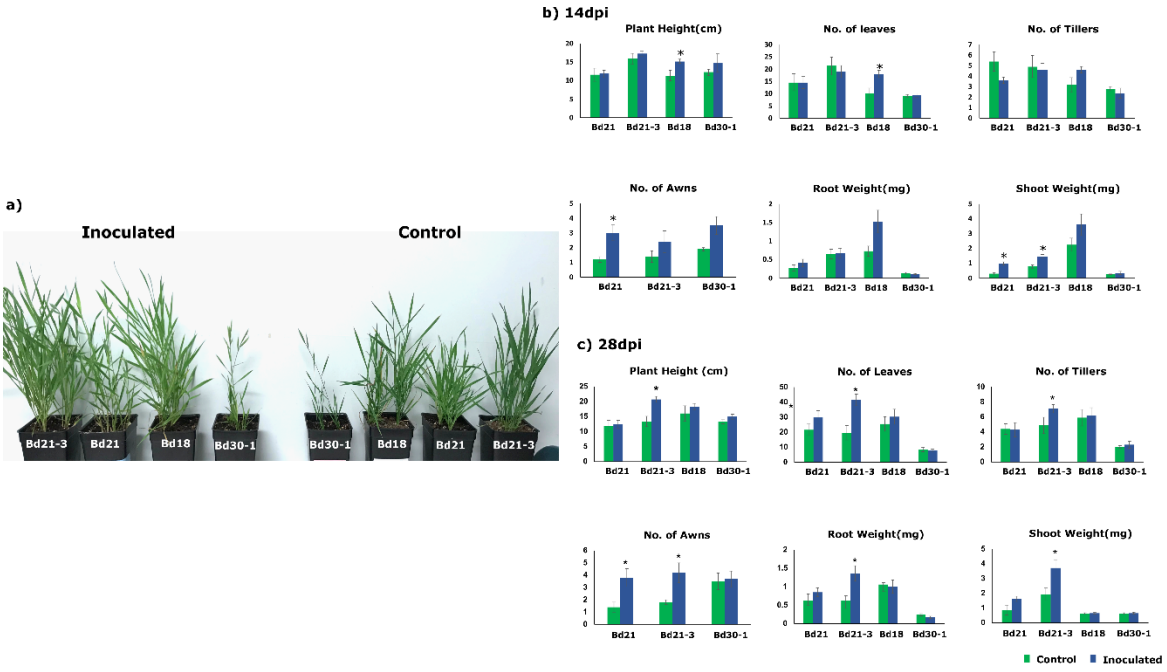

Figure 4.1 a) *Brachypodium* accession lines displaying growth response at 28 days post-inoculation (dpi). The left panel of figure 1a) shows accession lines (Bd21-3, Bd21, Bd18-1 and Bd30-1) inoculated with *Bacillus velezensis* strain B26. The right panel shows control accession lines b) Growth response parameters (Plant height, No. of leaves, No. of tillers, No, of awns, Root weight and shoot weight) of wild type *B.distachyon* genotypes in response to B26 inoculation at 14 days post-inoculation (dpi) c) at 28 dpi. Bars represent the mean of five biological replicates. t-test was used to determine statistical differences between inoculated and non-inoculated plants. * indicates significance according to Independent Student t-test ($p < 0.05$). Note: Bd18-1 did not flower at 14 and 28dpi.

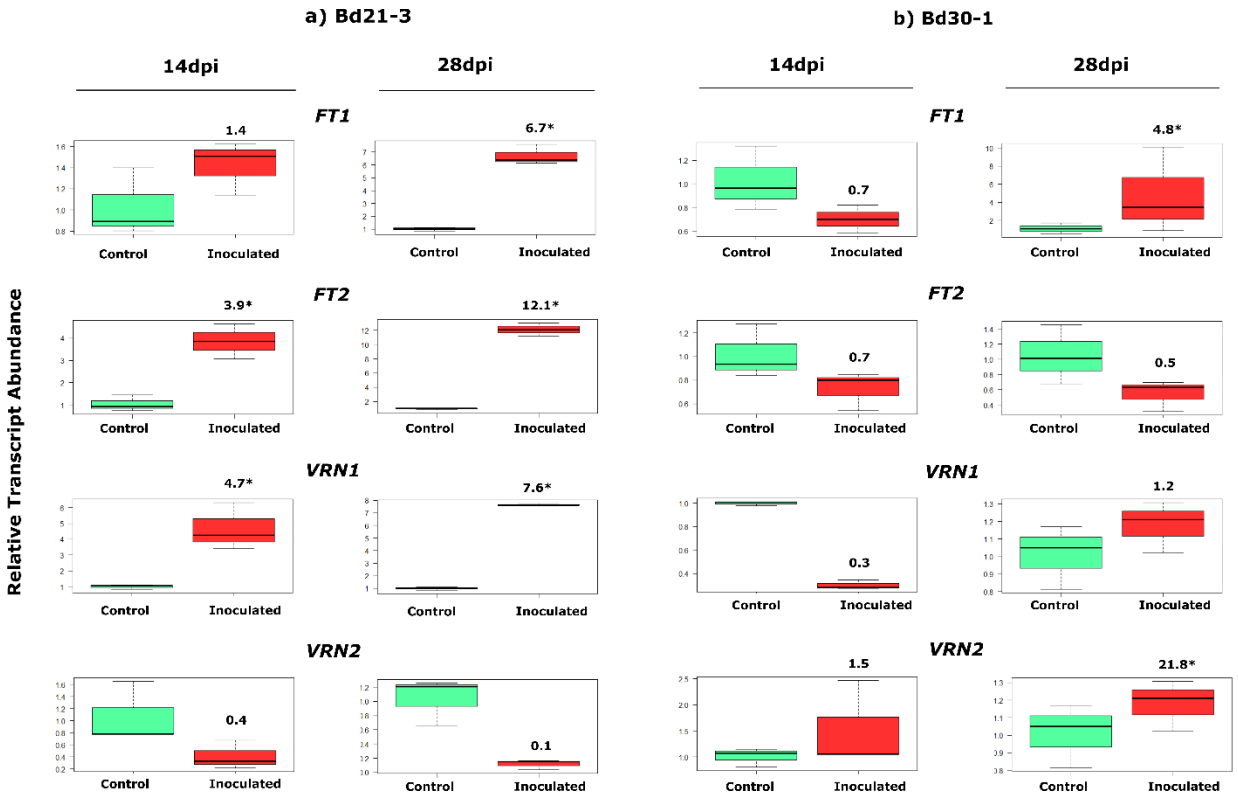

Figure 4.2 A comparison of relative transcript abundance of flowering genes (*FT1, FT2, VRN1* and *VRN2*) in shoots of control and inoculated a) Bd21-3 (rapid flowering line) and b) Bd30-1(intermediate flowering line) at 14 and 28dpi. Numbers above the box plot represent fold change. * indicates significance according to Independent Student t-test ($p < 0.05$).

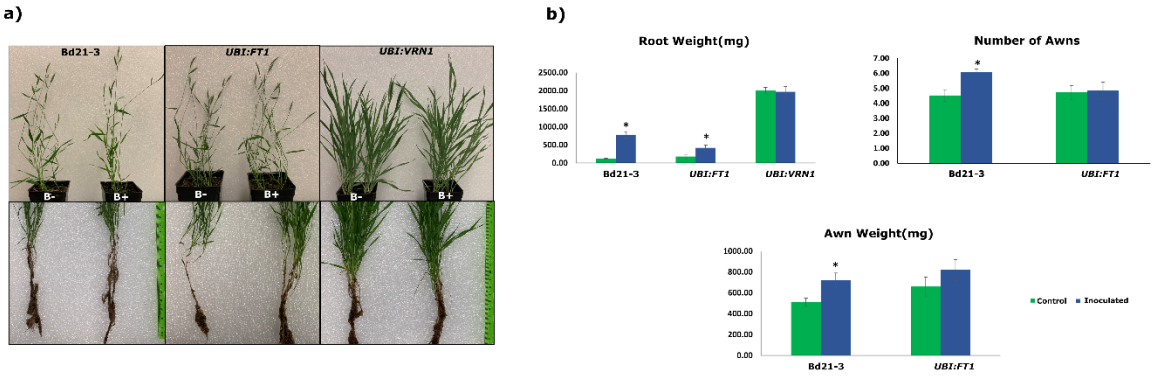

Figure 4. 3 a) Comparison of shoot (upper panel) and root (lower panel) phenotypes at 28 dpi between inoculated (B+) *Brachypodium* wild type Bd21-3 and transgenic lines *UBI:FT1*, *UBI:VRN1* and their respective controls (B-). b) Comparison of growth parameters of inoculated Bd21-3 and transgenic lines with non-inoculated control plants. Standard errors are displayed for each bar graph. Independent Student t-test was used to determine statistical differences. * indicates significance ($p < 0.05$). Each bar represents the mean of 5 replicates.

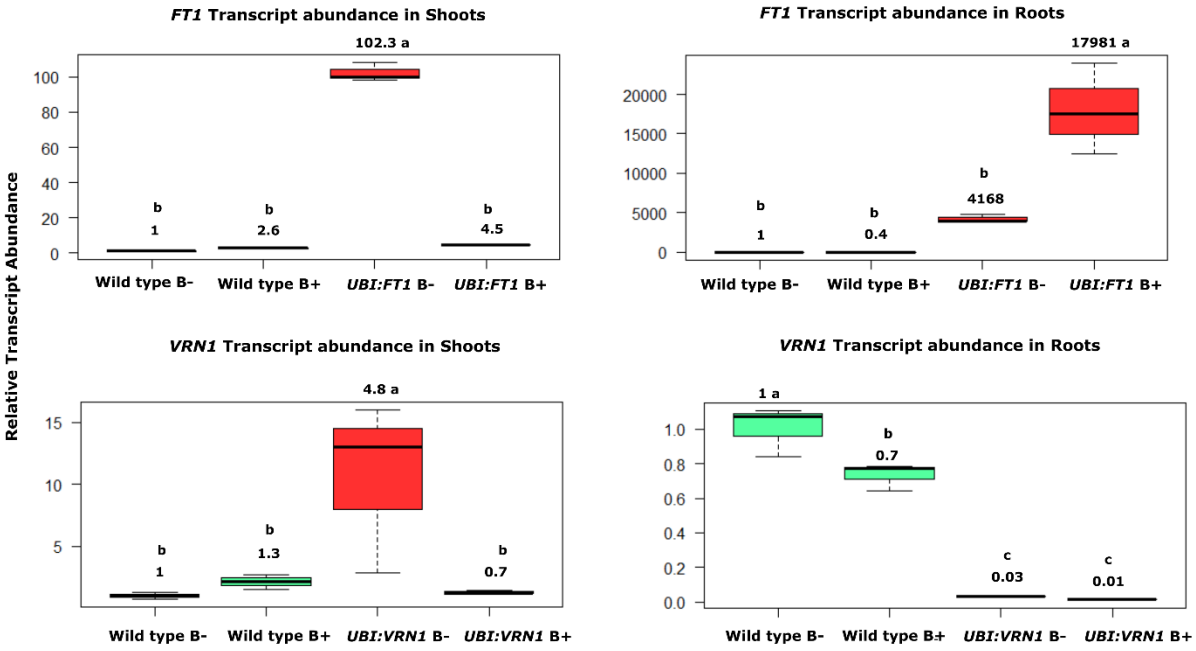

Figure. 4 Comparison of relative transcript abundance of flowering genes in shoots and roots of inoculated (B+) and control (B-) wild type Bd21-3 and transgenic lines *UBI:FT1*, *UBI:VRN1* at 28 dpi. Numbers above the box plots represent fold change. Different alphabet above each box represent significance according to Tukey's test ($p < 0.05$)

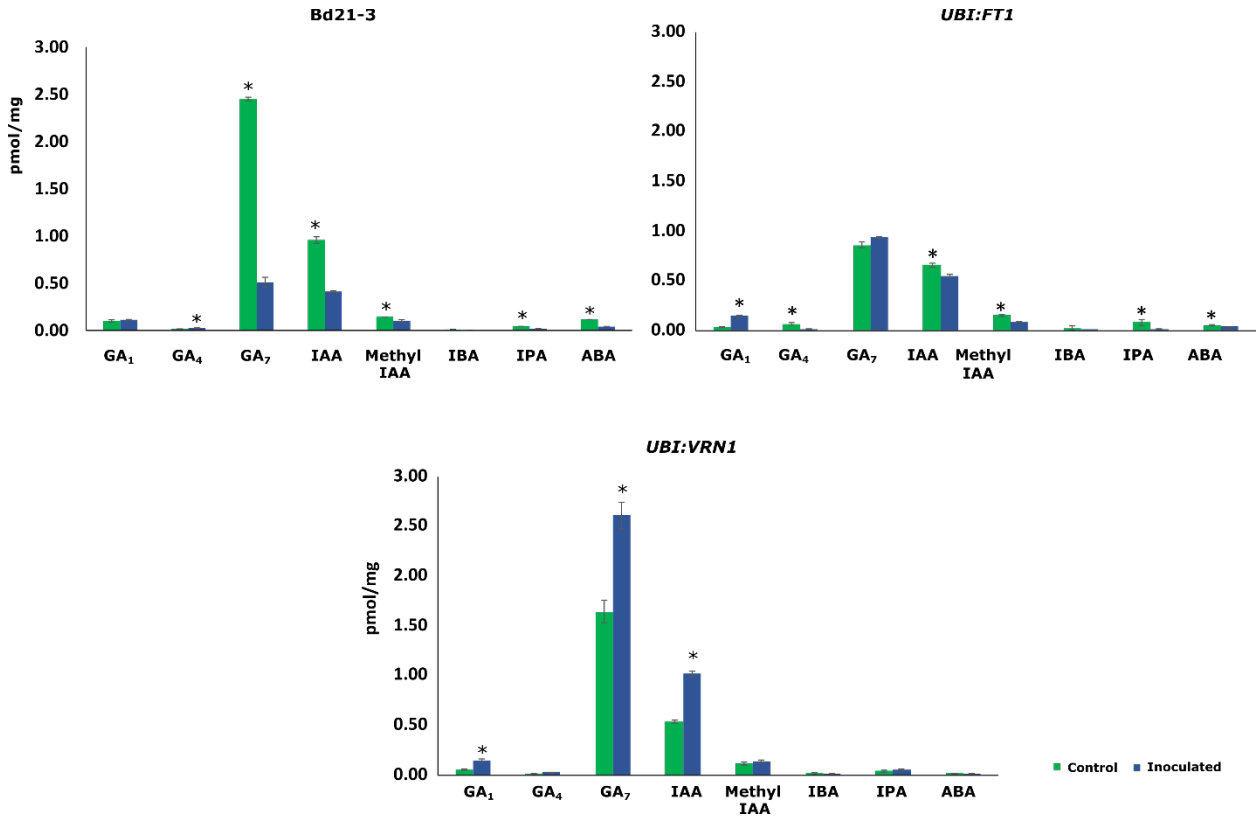

Figure 4. 5 Quantification of phytohormones concentrations (pmol/mg) in inoculated (B+) and control (B-) of wild type Bd21-3 and transgenic lines *UBI:FT1*, *UBI:VRN1*. Bars represent the mean of three biological replicates. GA, gibberellic acid (GA_1,GA_4 GA_7), IAA, indoleacetic acid, IBA, indole butyric acid (IBA), IPA (indole -3-propionic acid).

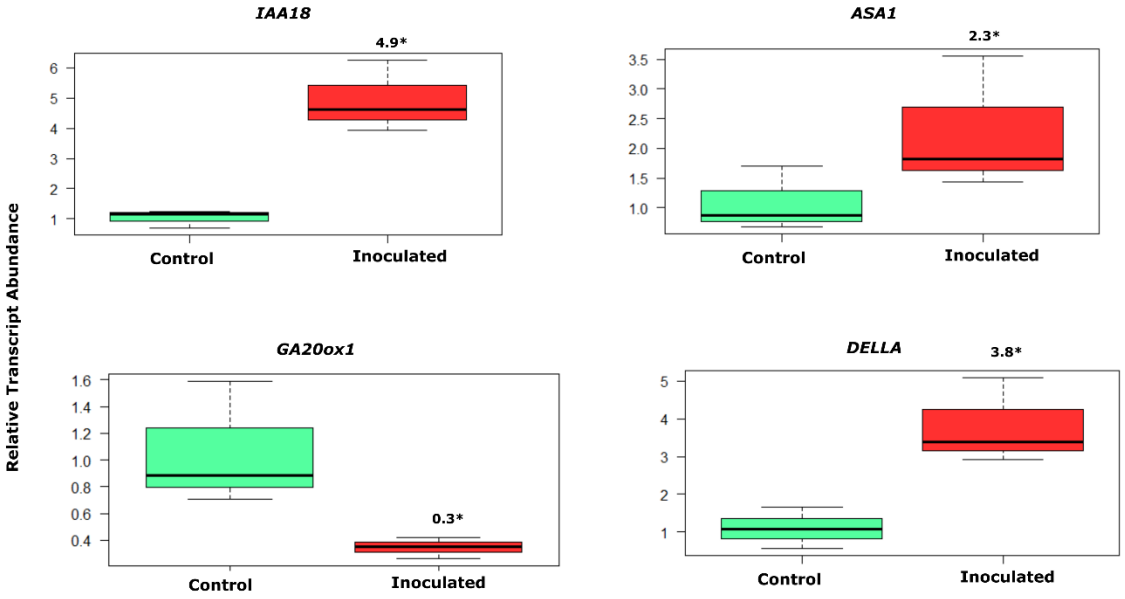

Figure 4. 6 Relative transcript abundance of genes encoding biosynthesis of auxin and gibberellins in roots of control and inoculated Bd21-3 at 28 dpi. Numbers above the box plots represent fold change. Independent Student t-test was used to determine the statistical differences between inoculated and control roots. * indicates significance ($p < 0.05$).

Table 4.1 List of primers used in this study

Gene of interest	Primer Name	Primer Sequence (5'to 3')	Product Size (bp)	Reference
Primers for B26 Quantification				
B26 Quantification	B26-F B26-R	CAAGTGCCGTTCAAATAG CTCTAGGATTGTCAGAGG	565	(Gagne-Bourque *et al*., 2015)
Primer for transgene detection				
pANIC vector AcV5 tag	BdAcV5-R	agaccagccgctcgcatctttccaag	100	(Ream *et al.,* 2014)
qRT-PCR Primers for Flowering Genes				
FT1	BdFT1-F BdFT1-R	TTCGGGAACAGGAACGTGTCCAAC AGCATCTGGGTCTACCATCACGAG	100	(Ream *et al.,* 2014)
FT2	BdFT2-F BdFT2-R	AGTACTTGCACTGGCTGGTCAC CCGAGCTGCTGGAATAGAAGGAAC	115	
VRN1	BdVRN1_F BdVRN1_R	GCTCTGCAGAAGGAACTTGTGG CTAGTTTGCGGGTGTGTTTGCTC	140	
VRN2	BdVRN2_F BdVRN2_R	ATGCATGAGAGAGAGGCGAAGG TCGTAGCGGATCTGCTTCTCGTAG	150	
Ubiquitin	UBC18-F UBC18-R	GGAGGCACCTCAGGTCATTT ATAGCGGTCATTGTCTTGCG	100	(Sandoya and de Oliveira Buanafina, 2014)
qRT-PCR Primers for genes related to Phytohormones				
Anthranilate synthase alpha subunit1(ASA1)	ASA1-F ASA1-R	GCTCCAAGCCACAACACTAT CCGCCTTATTCTCGCATTCT	139bp	BdiBd21-3.1G0905900.1
Auxin responsive protein (IAA18)	IAA18-F IAA18-R	AAGCCGTCACCTCAATCATC TTCACGAACACGCCCTTT	119bp	BdiBd21-3.2G0073500.1
Gibberellin 20-oxidase	GA20ox1-F GA20ox1-R	AAGTCGCTGGCTTTCTTCC CCACGTGAAATCCGGGTAAA	105bp	BdiBd21-3.1G0010900.1
DELLA PROTEIN	DELLA-F DELLA-R	CGTCAACTCAGTCTTCGAGAT TGAGCCAGAGTTGTGGTTAG	136bp	BdiBd21-3.1G0148400.1

Table 4.2 Determined Cq values and gene copy number of B26 leaf and root samples of Bd21-3 and Bd30-1 inoculated with B26

Accession	dpi	Average Cq[$] values		Gene copies/g of sample		Log_{10}	
		Shoot	Root	Shoot	Root	Shoot	Root
Bd21-3	**14dpi**	32.8±0.6[b]	32.8±0.6[b]	855754	1003888	5.9	5.9
	28dpi	32.7±0.5[b]	30.2±1.2[a]	903143	5227176	5.9	6.7
Bd30-1	**14dpi**	32.5±0.8[b]	34.8±1.2[a]	1124891	274849	6	5.3
	28dpi	33.7±1.1[b]	34.9±1.4[a]	539400	259528	5.7	5.3
	42dpi	33.3±0.7[b]	34.9±0.9[a]	631073	238371	5.8	5.3

$ Cq values -quantification cycle (Cq)
a,b letter to represent the significant difference. Means with same letters are not significant, while means with different letters are significant within column according to Independent Student t-Test ($p < 0.05$).

Table 4.3 Estimated root volume of *B.distachyon* wild type and transgenic lines from CT-Scanning data

Accessions	Control (mm^3)	Inoculated(mm^3)	Difference
Bd21-3	425.7	1517.5	1091.8
UBI:FT1	881.2	1480.2	599
UBI:VRN1	637	1213	576

4.9 CONNECTING TEXT

In chapters 3 and 4, we have proved how plant roots are recruiting *B. velezensis* towards itself and how *B. velezensis* impacted the phenotypic traits *Brachypodium*.

Chapter 5 focuses on the identification of molecular mechanism behind the interaction of *B. velezensis* and *Brachypodium* by investigating the transcriptome of inoculated and control *Brachypodium* roots. The main focus is given to identify molecular mechanisms behind nutrient uptake, defence responsiveness, phytohormone homeostasis and ion transport in *Brachypodium* roots colonized by *B. velezensis.*

The following chapter is published in Genomics

Chapter 5. Transcriptional landscape of *Brachypodium distachyon* roots during interaction with *Bacillus velezensis* strain B26

Meha Sharma[1]* and Suha Jabaji[1]*

[1]Department of Plant Science, Macdonald Campus of McGill University, 21,111 Lakeshore Rd., Ste-Anne de Bellevue, H9X 3V9, Quebec, Canada

*Corresponding authors

M.Sharma, S. Jabaji, Department of Plant Science, Macdonald Campus of McGill University, 21,111 Lakeshore Rd., Ste-Anne de Bellevue, H9X 3V9, Quebec, Canada
Email: **meha.sharma@mail.mcgill.ca**
S. Jabaji, Department of Plant Science, Macdonald Campus of McGill University, 21,111 Lakeshore Rd., Ste-Anne de Bellevue, H9X 3V9, Quebec, Canada

Reproduced from:
Sharma M, Jabaji S. (2023) Transcriptional landscape of *Brachypodium distachyon* roots during interaction with *Bacillus velezensis* strain B26. *Genomics.***15**:110583.

Minor modifications were made to follow the McGill University thesis guidelines

5.1 Abstract

Plant growth promoting rhizobacteria (PGPR) communicate with plants through roots. The molecular mechanism by which plants and PGPR respond to each other is not very well known. In the current study, we did RNA sequence analysis of *Brachypodium distachyon* Bd21-3 roots inoculated with PGPR, *Bacillus velezensis* strain B26. From our list of differentially expressed genes, we concentrated on transcripts that have a high possibility of participating in plant-PGPR interaction. Transcripts associated to the hormone signalling pathway were differentially expressed. We identified the upregulation of various transcripts linked to ion transporters. Reduction in expression of defense signalling genes indicated that B26 suppresses the plant defense mechanisms to begin successful interaction with roots. Transcripts associated with lignin branch of the phenylpropanoid pathway were upregulated as well, leading to more accumulation of lignin in the cell wall which enhances mechanical strength of plants. Overall, this study is an excellent resource for investigating associations between plant-PGPR interactions.

5.2 Introduction

The symbiotic interactions between plants and PGPR result in several benefits to plants. Plants secrete some chemo-attractants that help in recruiting PGPR towards it (Haichar *et al.*, 2008, Liu *et al.*, 2017). Additionally, PGPRs also produce compounds that influence growth and development concurrently. Although this interaction seems effortless, the beneficial relationship is actually highly complex. Once successful colonization establishes, rhizobacteria start feeding on carbohydrates and amino acids produced by the plant. However, PGPR stimulates plant growth through various direct i.e., producing phytohormones (Indole-3-acetic acid, cytokinin,

gibberellin), enhancing nutrient acquisition and indirect ways i.e., acting as biocontrol agents, providing stress tolerance.

Several species of *Bacillus* have been reported as PGPR in various plant species e.g., rice (Liu *et al.*, 2017), tomato (Batista *et al.*, 2021), wheat(Sood *et al.*, 2020), canola(Valetti *et al.*, 2018) *Arabidopsis*(Asari *et al.*, 2017), timothy(Gagné-Bourque *et al.*, 2016), *Brachypodium distachyon* (Gagné-Bourque *et al.*, 2015) and many more. It has been speculated that *Bacillus* species may boost nutrient uptake through the generation of phytohormones, the solubilization of soil nutrients, and the stimulation of the root development (Calvo, 2013, Vacheron *et al.*, 2013). We previously reported that *Bacillus velezensis* strain B26, a non-pathogenic PGPR, can be considered a potential candidate to improve agricultural productivity through the synthesis of phytohormones, secondary metabolites, competitive omission in the rhizosphere, and facilitating nutrient availability (Gagné-Bourque *et al.*, 2015, Sharma *et al.*, 2022). Both *Brachypodium distachyon* accession Bd21-3 and strain B26 are useful as a model to study plant-PGPR interaction since both of them are easy to cultivate and have their genome sequenced (Brkljacic *et al.*, 2011, Jeukens *et al.*, 2015a). Our previous reports demonstrate that strain B26 helped inoculated *B.distachyon* and timothy to mitigate drought stress (Gagné-Bourque *et al.*, 2015, Gagné-Bourque *et al.*, 2016). This microbe-mediated induction of abiotic stress response is termed Induced Systemic Tolerance (IST) (Yang *et al.*, 2009, Ngumbi and Kloepper, 2016). Additionally, root colonization by PGPR leads to induced systemic resistance (ISR) through the activation of different defense-related pathways, which are effective against a broad range of diseases (Bakker *et al.*, 2003, Cartieaux *et al.*, 2008, Bukhat *et al.*, 2020).

To better understand B26 and *B.distachyon* interaction, we tried to identify signals released from the host and perceived by bacteria. Root exudates secreted by *B.distachyon* roots influenced the chemotaxis and biofilm formation ability which lead to the successful colonization of strain B26 in *B.distachyon* roots(Sharma *et al.*, 2020). Our previous phenotypic data of different *B.distachyon* genotypes inoculated with B26 demonstrated the genotype-specific effect of B26 in the growth promotion (Sharma *et al.*, 2022). These observations provide a valuable framework for understanding the plant-PGPR interaction. However, to further understand the molecular and regulatory pathways of *B.distachyon* affected by B26 further investigation was still required. Next-generation sequencing techniques such as whole genome sequencing, comparative genomics, transcriptomics, and proteomics are helpful approaches that would fill the gaps not only in understanding the intimate relationship between the plant-PGPR but also in the underlying mechanisms that each partner employs leading to a successful interaction (Knief, 2014, Kaul *et al.*, 2016b). Plant-PGPR interactions can be studied through transcriptome analysis which helps in capturing momentary changes in plant during the interaction. There is substantial literature on transcriptional changes in the plant during plant-pathogen interaction (Kawahara *et al.*, 2012, Kong *et al.*, 2015, Chittem *et al.*, 2020, Zhang *et al.*, 2022) and plant-PGPR interaction during the stress (Shanmugam and Kanoujia, 2011, Chauhan *et al.*, 2019, Zhang *et al.*, 2020). Most of the studies on plant-PGPR interactions are related to microbial diversity and their metabolite potential, but there are various areas which are still poorly understood (Suryanarayanan, 2013, Kong and Liu, 2022).

In this study, we carried out RNA sequencing of *B.distachyon* roots inoculated with *Bacillus velezensis* strain B26 cells under sterile conditions without any stress. The objective of this study is to investigate changes in *B.distachyon* transcriptome due to strain B26 and identify the molecular

basis of a) plant-microbe interaction b) plant growth promotion and ion transport c) defense and stress responsiveness.

5.3 Material and Methods

5.3.1 Bacterial Strain, Growth, and Inoculum Preparation

Bacillus velezensis strain B26 was used in this study. The strain B26 was frozen in 20% glycerol stocks in Lysogeny Broth (LB) (BDH chemical Ltd, Mississauga, ON, Canada) at -80°C. The bacterial strain was cultured in LB at 28°C with shaking at 120 revolutions per minute (rpm) until an OD_{600} of 1.0 (10^6 Colony Forming Unit/ml) was reached. Bacterial culture was centrifuged, resulting pellet was washed and suspended in an equal volume of phosphate buffer (1 Molar, pH 7) which was then used as inoculum for plants.

5.3.2 Plant material, Bacterial Inoculation and Sample Collection

Brachypodium distachyon accession Bd21-3 was used. Seeds of Bd21-3 were soaked overnight in sterile distilled water at room temperature. The lemma was removed, and seeds were surface sterilized. Seeds were soaked in 70% ethanol for 30 seconds and gently shaken in 1.3% sodium hypochlorite for 4 minutes and then rinsed three times with sterile distilled water (Vain *et al.*, 2008). Sterile seeds were placed between two sterile filter papers saturated with distilled water in a petri dish incubated at 4°C in the dark for 7 days. Semi-hydroponics system using Magenta GA-7 tissue culture boxes was used to grow plants. Each box was filled with sterile glass low alkali beads (Ceroglass, USA) saturated with Hoagland's solution as described in Sharma *et al.* (2020). Six germinated seeds were transferred to each box and were incubated in a controlled growth

cabinet (Conviron, Canada) with light intensity of 150 µmoles m^2/s,16 hours light and 8 hours dark at day/night temperatures of 21°C /18°C. B26 inoculation was done after 14 days of growth. Each box received 500 µL (OD_{600} of 1) B26 inoculum suspended in phosphate buffer (1 Molar, pH 7), and the control box received 500 µL of phosphate buffer alone. Five replicates were used for each treatment and control. All boxes were incubated in a controlled growth cabinet. After 28 days post inoculation (dpi), whole roots were retrieved. Roots were washed in sterilized deionized water and frozen at -80°C for RNA extraction.

5.3.3 RNA extraction and sequencing

Total RNA from roots was extracted from flash-frozen pulverized 100 mg of inoculated and control samples using Spectrum™ Plant Total RNA Kit (Sigma Aldrich, US) following the manufacturer's protocols. Total RNA from pure culture bacteria was isolated using NucleoSpin® RNA isolation kit (Macherey-Nagel, Germany) based on the manufacturer's protocol. Five RNA biological replicates for each treatment and control were sent for library preparation and sequencing at IDSeq Inc, (Sacramento, California). Isolated RNA sample quality was assessed by High Sensitivity RNA Tapestation (Agilent Technologies Inc., California, USA) and quantified by Qubit 2.0 RNA HS assay (ThermoFisher, Massachusetts, USA). Ribosomal RNA depletion removal was performed with QIAseq® FastSelect rRNA plant kit combined with QIAseq 5s/16s/23S kit (Qiagen, Hilden, Germany) per manufacturer's instructions. All library construction was done according to the NEBNext® UltraTM II Directional RNA Library Prep Kit for Illumina® (New England BioLabs Inc., Massachusetts, USA). Final libraries quantity was assessed by Qubit 2.0 (ThermoFisher, Massachusetts, USA) and quality was assessed by TapeStation D1000 ScreenTape (Agilent Technologies Inc., California, USA). Final library size was about 430 base pairs (bp) with an insert size of about 300 bp. Illumina® 8-nt dual-indices

were used. Equimolar pooling of libraries was performed based on QC values and sequenced on an Illumina® Novaseq s4 (Illumina, California, USA) with a read length configuration of 150 bp for 67 million Paired-End (PE) reads per sample (33.5 million in each direction).

5.3.4 Reference-based Transcriptome analysis

5.3.4.1. Quality check, trimming and mapping

To check the quality of raw reads FastQC 0.11.9 (Andrews, 2010) was performed before trimming and after trimming. The output of FastQC is a control statistic and a judgment on each metric (pass, warn and fail). Raw reads were subjected to Trimmomatic software version 0.40 (Bolger *et al.*, 2014) to remove adapters, poly-N homopolymers and low-quality bases using a minimum read length of 50 bp and phred score of 33. Reference-based transcriptome assembly approach was used. Firstly, trimmed reads of both control and inoculated roots were mapped to annotated *B.distachyon* Bd21-3 v1.2 genome (https://phytozome-next.jgi.doe.gov/info/BdistachyonBd21_3_v1_2) downloaded from Phytozome 13 using splice-aware alignment tool STAR 2.7.9a with default settings (Dobin *et al.*, 2013). An overview of the analysis is provided in **Figure 5.1.**

5.3.4.2 Differential gene Expression:

Strand-specific read counting was performed on mapped sorted BAM files using featureCounts from subread package 2.0.3 (Liao *et al.*, 2014). The DESeq2 package version 1.34.0 was used for normalization and differential analysis of count data (Love *et al.*, 2014). *DESeq* function was used for differential expression analysis and $\log_2$ fold change calculation between control and inoculated roots using negative binomial distribution. *lfcShrink* function with *apeglm*

shrinkage estimator was used for fold change shrinkage(Zhu *et al.*, 2019). Genes with corrected p-value or p-adjust ≤ 0.05 and $|\log_2$ (fold change)| ≥1.5 were considered significant.

5.3.4.3. Gene Ontology(GO), Metabolic Pathway Analysis:

GO enrichment analysis was carried out with GOSeq 1.44.0 to detect enriched gene ontology terms in differentially expressed genes (DEGs) in control and inoculated roots, using a false discovery rate (FDR) ≤ 0.05 (Young *et al.*, 2010). A fully annotated Bd21-3 v1.2 gene list was downloaded from Phytozome 13. For pathway enrichment analysis, significant DEGs were analyzed by the Kyoto Encyclopedia of Genes and Genomes (KEGG) Orthology Based Annotation System (KOBAS) program (Bu *et al.*, 2021). Enriched pathways with FDR ≤ 0.05 were considered significant. The iTAK database (http://itak.feilab.net/cgi-bin/itak/online_itak.cgi) was used for Transcription Factors analysis of DEGs (Zheng *et al.*, 2016). FASTA sequences of DEGs were used as input of iTAK. The metabolic pathway analysis of the DEGs was carried out by the MapMan software V3.6.0RC1 (Thimm *et al.*, 2004). DEGs were given as input in the experiment folder. Pathway analysis was done for biotic stress.

5.3.5 Validation of RNA sequencing using qRT-PCR

To validate the results of RNA sequencing, qRT-PCR was performed. The same samples used for RNA sequencing were subjected to qRT-PCR validation using three replicates for each control and treatment group. RNA of 500 nanogram (ng) concentration was reverse-transcribed using Affinity Script qPCR cDNA Synthesis Kit (Agilent, USA), following the manufacturer's

protocols. Specific primers for the selected genes were designed using the OligoAnalyzer tool from IDT. Primer sequences are listed in **Supplementary Table 5.1.** qRT-PCR conditions were optimized for each primer set. PCR amplification was performed in 10 µL reaction containing 1X SYBR Green master mix (Bio-Rad,USA) 200 nanomoles (nM) of each primer, 100 ng of cDNA template. The PCR thermal cycling parameters were initial denaturation 95°C for 30 seconds followed by 40 cycles of 95°C for 15 seconds, annealing/extension 60°C for 30 seconds, along with dissociation curve at the end in Stratagene Mx3000 (Stratagene, Cedar Creek, USA). Transcript abundance was measured by using the comparative threshold cycle (CT) method ($2^{-\Delta\Delta Ct}$) (Livak and Schmittgen, 2001). Target gene was normalized over the housekeeping genes ACTIN2. Bestkeeper tool (https://www.gene-quantification.de/bestkeeper.html) was used to compare housekeeping genes ACTIN2 (Derbyshire and Byrne, 2013) and UBC18 (Hong *et al.*, 2008). ACTIN2 had the lowest coefficient variation as compared to UBC18. Comparison of mean was performed by independent student t-test between control and inoculated samples using IBM Statistics SPSS Version 24 (SPSS Inc., Chicago, IL).

5.3.6 Root Cell wall thickness measurement

5.3.6.1. Sample preparation and microscopic observations

After 28 dpi, control and inoculated roots were fixed in 100% methanol. Resin infiltration was performed using freshly prepared spurr resin in three steps with increasing resin concentration up to 100% with the last step repeated three times. Resin polymerization was done at 65°C for 24 h. The polymerized resin blocks were sectioned with a Leica Ultracut UCT (Leica microsystems). 5µm thick sections were hand cut with glass knife and immediately transferred into water on the glass slide and then allowed to dry on a slide warming plate for few minutes. Sections were stained in 0.1% toluidine blue and washed with ethanol and distilled water. The stained sections were

observed with a Zeiss Axio Imager Z1 microscope (Zeiss, Germany) equipped with a 40X EC Plan NeoFluar, NA0.75 objective and an AxioCam MR R3 (Zeiss). Sample preparation for microscopical observations and light microscopy imaging was performed at the McGill University ECP3- Multi-Scale Imaging Facility, Sainte-Anne-de-Bellevue, Quebec, Canada.

5.3.6.2. Cell wall thickness measurement

FIJI software (Schindelin *et al.*, 2012) was used to measure the thickness of xylem cell walls. Three sections of control and inoculated samples were measured. For each section five xylem vessels were measured at three random spots. The measurements of the thickness of the walls were performed by drawing perpendicular lines stretching from the plasma membrane of one cell to the plasma membrane of the adjacent cell using segmented tracing in FIJI.

5.4 Results

5.4.1 Transcriptome sequencing and read mapping onto *B.distachyon* genome

Transcriptome sequencing of control and inoculated roots produced 41.4 - 71.1 million reads of 150bp in length. Raw reads were trimmed to remove adaptor sequences and low-quality reads using the trimmomatic tool. It generated around 26.7- 46.5 million clean reads (**Supplementary Table 5.2**) of a minimum Phred quality score 33. Clean reads were mapped to *B.distachyon* Bd21-3 v1.2 genome. Around 74.88% - 79.64% of clean reads were uniquely mapped to the *B.distachyon* genome.

5.4.2 B26 colonization induced Differential Expression of a wide array of genes in Bd21-3 roots

The gene expression count matrix was generated by counting the number of uniquely mapped reads per sample onto known gene loci. A minimal pre-filtration was done to remove genes with no reads. A total of 27809 genes with non-zero total read count were identified. The volcano plot gives an overall distribution of all the DEGs (**Figure 5.2a**). Among these DEGs, 426 genes were significantly upregulated, and 357 genes were significantly downregulated in inoculated roots compared to control roots by setting False discovery rate (FDR) or adjusted p-value ≤ 0.05 and |log2 (fold change)| ≥ 1.5 (**Supplementary Table 5.3**). Heatmap analysis of significant 783 DEGs depicted significant clusters of DEGs between control and inoculated roots (**Figure 5.2b**). Some genes were activated only in inoculated roots as compared to control roots and vice-versa. Due to a similar expression profile, a high degree of correlation was observed between the biological replicates of control and inoculated samples.

To analyze the enriched functional Gene Ontology (GO) terms in response to B26 inoculation, GOSeq tool was used. The majority of the DEGs were significantly represented in the three main GO categories: Biological Process (BP), Cell Component (CC) and Molecular Function (MF). GO enrichment analysis was done on 783 DEGs using GOSeq tool. GO terms with FDR ≤ 0.05 were considered significantly enriched by DEGs. Among up-regulated transcripts, 10 GO terms were enriched significantly whereas 12 GO terms were enriched among significantly down-regulated transcripts (**Table 5.1, Figure 5.3 a, b**). Upregulated transcripts were enriched in various categories such as transmembrane transport, protein phosphorylation, protein tyrosine kinase and protein kinase (**Figure 5.3a**). In the case of downregulated DEGs, they were enriched in categories related involving response to auxin, serine-type endopeptidase inhibitor activity, β-fructofuranosidase, protein tyrosine kinase etc. (**Table 5.1**, **Figure 5.3b**). FASTA sequences of all

DEGs were used for KEGG pathway annotation in KOBAS web server. KEGG pathways for upregulated and downregulated transcripts were identified separately. For upregulated DEGs, a total of 17 significant KEGG pathway categories were identified with FDR ≤ 0.05 (**Table 5.2**). Transcripts corresponding to the biosynthesis of brassinosteroid (KEGG id: bdi00905), secondary metabolites (KEGG id: bdi01110), phenylpropanoid (KEGG id: bdi00940), flavonoid (KEGG id: bdi00941) and amino acid (KEGG id: bdi01230) etc. were overrepresented. While in the case of downregulated DEGs, six significant KEGG pathway categories were identified. The KEGG categories correspond to steroid biosynthesis (KEGG id: bdi00100), hormone signal transduction (KEGG id: bdi04075) and starch and sucrose metabolism (KEGG id: bdi00500) were overrepresented (**Table 5.2**).

5.4.3 B26 strongly impacted functional profiling in Bd21-3 roots

To analyze the enriched functional Gene Ontology (GO) terms in response to B26 inoculation, GOSeq tool was used. The majority of the DEGs were significantly represented in the three main GO categories: Biological Process (BP), Cell Component (CC) and Molecular Function (MF). GO enrichment analysis was done on 783 DEGs using GOSeq tool. GO terms with FDR ≤ 0.05 were considered significantly enriched by DEGs. Among up-regulated transcripts, 10 GO terms were enriched significantly whereas 12 GO terms were enriched among significantly down-regulated transcripts (**Table 5.1, Figure 5.3 a, b**). Upregulated transcripts were enriched in various categories such as transmembrane transport, protein phosphorylation, protein tyrosine kinase and protein kinase (**Figure 5.3a**). In the case of downregulated DEGs, they were enriched in categories related involving response to auxin, serine-type endopeptidase inhibitor activity, β-fructofuranosidase, protein tyrosine kinase etc. (**Table 5.1**, **Figure 5.3b**). FASTA sequences of all DEGs were used for KEGG pathway annotation in KOBAS web server. KEGG pathways for

upregulated and downregulated transcripts were identified separately. For upregulated DEGs, a total of 17 significant KEGG pathway categories were identified with FDR ≤ 0.05 (**Table 5.2**). Transcripts corresponding to the biosynthesis of brassinosteroid (KEGG id: bdi00905), secondary metabolites (KEGG id: bdi01110), phenylpropanoid (KEGG id: bdi00940), flavonoid (KEGG id: bdi00941) and amino acid (KEGG id: bdi01230) etc. were overrepresented. While in the case of downregulated DEGs, six significant KEGG pathway categories were identified. The KEGG categories correspond to steroid biosynthesis (KEGG id: bdi00100), hormone signal transduction (KEGG id: bdi04075) and starch and sucrose metabolism (KEGG id: bdi00500) were overrepresented (**Table 5.2**).

5.4.4 Transcription factors affected due to B26 colonization

DEGs were subjected to transcription factor analysis using iTAK online tool which is suitable for transcriptome factor prediction and functional classification. A total of 23 Transcription Factor (TF) families were differentially expressed in the inoculated Bd21-3 roots which include 39 upregulated transcripts and 23 downregulated transcripts (**Table 5.3**). Among the upregulated TFs, most of them belonged to the NAC family (10) and MYB (my elob lastosis) family (5). However, most downregulated TFs belonged to the Heat Shock Factors (5) and GARP-G2 (Golden2, ARR-B and Psr1) (4) like TFs. Few transcriptional regulators were identified related to Auxin/Indole-3-Acetic Acid and SNF2 (Sucrose Non-Fermentable).

5.4.5 Effect of B26 inoculation on *Brachypodium* Signal Transduction and Phytohormone Biosynthesis

Transcripts associated with plant signal transduction were upregulated in inoculated roots. Genes related to GTP binding proteins and ADP-ribosylation were upregulated **(Supplementary Table 5.3)**. While transcripts associated with phytohormone signal transduction were differentially

expressed. Transcripts related to SAUR (Small auxin-up RNA) family proteins (involved in auxin biosynthesis) were downregulated while auxin-responsive protein IAA (BdiBd21-3.2G0254800) was upregulated in response to inoculation. In case of ethylene biosynthesis, transcripts such as ethylene insensitive proteins (BdiBd21-3.3G0620300), ethylene-responsive transcription factor 1 (ERF1) (BdiBd21-3.1G0007900) and 1-aminocyclopropane-1-carboxylate oxidase (ACO) (BdiBd21-3.2G0449700) were downregulated.

5.4.6 *B.distachyon* interaction with B26 affected genes involved in Nutrient uptake and ion transport

Differential gene expression analyses revealed differentially expressed *B.distachyon* transcripts associated with nutrient uptake and ion transport in inoculated roots in response to B26 colonization. Transcripts related to high-affinity nitrate transport, ammonium, sulfate and sugar transport were upregulated. Transcripts of glutamate receptor, which triggers calcium signal cascades, were upregulated. Aspartate aminotransferase (BdiBd21-3.2G0719800) involved in nitrogen metabolism was upregulated. Inorganic phosphate transporter (BdiBd21-3.5G0033500) was found to be downregulated. Transcripts of aquaporin transporter were differentially expressed as well (**Supplementary Table 5.3**).

5.4.7 Defense and Stress Response Mechanisms genes impacted by B26

B.distachyon transcripts associated with plant defense and stress responses were differentially expressed in inoculated roots. Transcripts encoding the leucine-rich repeat receptor kinase were mostly upregulated (**Supplementary Table 5.3**). Pathogenesis-related (PR) proteins like β-1,3 glucanases, chitinases, peroxidases, phenylpropanoids and flavonoids play an important role in the process of pathogenesis. Transcripts BdiBd21-3.3G0344300 and BdiBd21-3.3G0344500 related

to chitinases were downregulated. β-1,3-glucanase (BdiBd21-3.2G0246100) was upregulated upon B26 inoculation. Transcripts of 4-coumarate-CoA ligase (4CL) (BdiBd21-3.3G0074600), cinnamyl alcohol dehydrogenase (CAD) (BdiBd21-3.3G0084500) and ferulic acid-5-hydroxylase (F5H) involved in phenylpropanoid pathway were upregulated. Laccase (BdiBd21-3.2G0704400) which catalyzes the second step of lignin biosynthesis was upregulated. Transcripts related to flavonoid biosynthesis were upregulated. Glucosyl/Glucuronosyl transferases (BdiBd21-3.2G0627900) and flavonoid 3' monooxygenase (BdiBd21-3.4G0238700) catalyze a series of steps in flavonoid biosynthesis were upregulated. Furthermore, increased expressions of transcripts encoding endoglucanases were found which can help to degrade the cell wall of pathogens. Transcripts involved in jasmonic acid biosynthesis were differentially expressed. Allene oxide cyclase (BdiBd21-3.5G0138400) was upregulated while lipoxygenase (BdiBd21-3.1G0126600) was downregulated.

5.4.8 MapMan Analysis

To compare the metabolic and regulatory pathways, MapMan was used on DEGs. PGPR colonization comes under biotic stress so DEGs were mapped in biotic stress-responsive pathways in MapMan. Around 153 DEGs were mapped in biotic stress-responsive pathways. The majority of displayed DEGs belonged to hormone signalling, cell-wall related processes, abiotic stress, heat shock proteins, transcription factors and secondary metabolites **(Figure 5.4**).

5.4.9 Validation of RNA sequencing through qRT-PCR

For validation of RNA sequencing results, a few upregulated and downregulated genes were randomly selected for qRT-PCR analysis. Relative transcript abundance for transcript encoding

i.e., disease resistance protein RPM1 (BdiBd21-3.4G0038600), peroxidase (BdiBd21-3.1G0537900), antifungal (BdiBd21-3.1G0165501), leucine-rich repeat N-terminal domain (BdiBd21-3.5G0359200) and protein tyrosine kinase (BdiBd21-3.3G0148900) were 1.2, 4.5, 3.2 and 5.3-fold more in inoculated roots as compared to control roots **(Figure 5.5)**. A consistent trend was observed in the expression of these genes determined by RT-qPCR and RNA sequencing which indicates that the RNA sequencing results are reliable.

5.4.10 Secondary cell wall strengthening by B26

Our microscopy images of control and inoculated samples revealed differences in cell wall thickness **(Figure 5.6a, b)**. We measured the xylem secondary cell wall thickness. The average thickness of the control sample was 6.80 ± 0.7 µm while cell wall thickness in inoculated roots was 12.69 ± 1.74 µm, with a significant increase of almost 2-fold as compared to the control **(Figure 5.6c)**.

5.5 Discussion

PGPR interacts with plant roots and alters the root architecture. In our previous studies, we reported that strain B26 increased the root weight and root volume (Gagné-Bourque *et al.*, 2015, Sharma *et al.*, 2022) of colonized *B.distachyon*. Strain B26 also improved the composition of root exudates including organic acids secreted by *B.distachyon* roots (Sharma *et al.*, 2020). The current study was conducted to deeply understand the molecular mechanisms behind the *B.distachyon* roots-PGPR interaction. The results presented in this study demonstrate that B26 inoculation strongly impacted the transcriptome of *B.distachyon*. Interestingly, strain B26 regulated the

expression of genes associated with plant phytohormones, stress tolerance, defense, and nutrient transport etc.

5.5.1 Response of *Brachypodium* roots to B26 colonization

5.5.1.1 Plant phytohormone signalling

It is well documented that rhizospheric bacteria promote plant growth and productivity by influencing the plant's hormonal status (Vacheron *et al.*, 2013, Kudoyarova *et al.*, 2019, Grover *et al.*, 2021). Currently, in our study, transcripts associated with phytohormones were differentially expressed. For example, auxin biosynthesis via tryptophan-dependent pathway and auxin-responsive IAA transcripts were upregulated **(Supplementary Table 5.4)**. Similar results were observed when tobacco roots were inoculated with PGPR *Paenibacillus polymyxa* YC0136 (Liu *et al.*, 2020). Transcripts of auxin biosynthesis and auxin responsive IAA were upregulated which is in accordance with our qRT-PCR results obtained in our previous study (Sharma *et al.*, 2022). Surprisingly, transcripts associated with another class of auxin-responsive genes i.e., SAUR proteins were downregulated in inoculated roots. Similar studies reported that the expression of SAUR proteins was also downregulated in rice roots inoculated with *A. brasilense* and *H. seropedicae* (Brusamarello-Santos *et al.*, 2012, Wiggins *et al.*, 2022). A decrease in expression levels of transcript encoding ACO was observed which suggests the decreased amount of ethylene in inoculated roots. Wheat roots colonized with *Azosprillium brasilense* also reduced the expression of ACO encoding ESTs (Camilios-Neto *et al.*, 2014b). Downregulation of ACO leads to less ethylene production which is beneficial for roots as it prevents root growth by affecting cell elongation (Růžička *et al.*, 2007). Another key phytohormone is Abscisic acid (ABA) which regulates various biotic and abiotic stress responses in plants. Protein phosphatase 2C (PP2C), a negative regulator of ABA signalling (Hirayama and Shinozaki, 2007), was found to be

upregulated by 8.35-fold in inoculated roots while ABA receptor PYR/PYL, a positive regulator of ABA signalling (Ma *et al.*, 2009), was also upregulated (1.74-fold increase) but the expression was less as compared to PP2C (this study). Increased PP2C:PYR ratio lead to desensitization of ABA in *Arabidopsis thaliana* and hence less production of ABA (Santiago *et al.*, 2009). Plant growth and the endogenous concentration of ABA are negatively correlated (Pilet and Saugy, 1987). Moreover, transcripts involved in brassinosteroid (BR) biosynthesis, the sixth type of plant phytohormone, were found to be upregulated in inoculated *B.distachyon* roots. BR mutants which lack BRs production in *A.thaliana* inoculated with PGPR *Caulobacter* strain did not increase root biomass indicating that BR biosynthesis and signalling are necessary for the PGPR effect (Luo *et al.*, 2019).

5.5.1.2 Transcription Factors

It is well-documented that, transcription factors (TFs) play an important role in stress tolerance, root growth and development (Montiel *et al.*, 2004, Joshi *et al.*, 2016). In this study, we identified various TFs that are differentially expressed during B26 interaction **(Table 5.3).** The most abundant TFs of upregulated transcripts found in this study belonged to NAC family. TFs NAC, WRKY, MYB, basic leucine zipper (bZIP), and heat shock proteins involved in plant defense mechanism and abiotic stress tolerance (Nuruzzaman *et al.*, 2013, Guo *et al.*, 2017), were upregulated when B26 colonized *B.distachyon* roots in our study **(Table 5.3)**. In other studies, PGPR *Paenibacillus polymyxa* strain YC0136 induced the expression of TFs involved in abiotic stress tolerance of tobacco (Liu *et al.*, 2020). The expression of TFs bZIP, NAC and MYB were modulated in *A.thaliana* inoculated with *Pseudomonas putida* MTCC5279 (Srivastava *et al.*, 2012). When the rice cultivar was exposed to salt stress in presence of *Bacillus amyloliquefaciens* strain SN13, NAC TF was 5-fold upregulated resulting in stress mitigation (Tiwari *et al.*, 2021).

However, in our study, plants are not exposed to any type of abiotic stress yet NAC TFs were upregulated this might indicate that strain B26 is priming the plants for stressful situations by strengthening their resistance. TFs belonging to WRKY and NAC families have been found to enhance resistance in tobacco also (Abbas *et al.*, 2020). AUX/IAA TFs permit transcription of various auxin-related genes in plants. Similar results were observed in *A.thaliana* inoculated with *Burkholderia phytofirmans* PsJN where AUX/IAA was also upregulated in inoculated plants (Poupin *et al.*, 2013).

5.5.1.3 Ion transporters

Interaction between plant and rhizobacteria imparts a huge impact on the plant mineral nutrition (Pii *et al.*, 2015). Our list of differentially expressed genes contained transcripts associated with ion transport **(Supplementary Table 5.4).** It included high-affinity nitrate, glutamate, ammonium, sulfate, inorganic phosphate, sugars, and aquaporin transporters. Nitrate transporters are essential in transporting nitrate, peptides, amino acids, and hormones (Fan *et al.*, 2017). Nitrate transporters were upregulated when wheat and rice roots were inoculated with *Azospirillum brasilense* (Camilios-Neto *et al.*, 2014b, Thomas *et al.*, 2019). Ammonium ion (NH^{4+}) is also an important and preferred source of nitrogen as the energy requirements for assimilation are low (Raven *et al.*, 1992). We observed that ammonium transporter (BdiBd21-3.3G0604000) was upregulated in inoculated roots. Similar results were observed when *A.thaliana* roots were inoculated with consortia of *Bacillus* (Calvo *et al.*, 2019). There is a positive correlation between the transcript abundance of these transporter genes and nitrogen uptake which ultimately lead to enhanced plant growth (Calvo *et al.*, 2019). Sugar transporter proteins (STPs) are H+/sugar symporters located on plasma membranes (Yan, 2013, Deng *et al.*, 2019) and are affected during PGPR interactions. Six STPs were upregulated while one STP was downregulated in current study. The upregulation of

sugar transporter is common during symbiosis and plant-pathogen interaction to gain sugar from host plants (Desrut *et al.*, 2021). When rice roots were inoculated with *Azospirillum brasilense* and separately with *Herbaspirillum seropedicae*, a sugar transporter gene was upregulated (Wiggins *et al.*, 2022). Contrary, all sugar transporter genes in *A.thaliana* were repressed by PGPR strain *Pseudomonas simiae* WCS417r (Desrut *et al.*, 2021). This differential expression of STPs is not very well studied for PGPR-plant interaction. Changes in plant sugar transport may help establish and maintain PGPR-plant interaction by giving PGPR access to a controlled pool of sugar as a source of carbon (Hennion *et al.*, 2019).

5.5.1.4 Defense signalling and stress responsiveness

Plants recognize PGPR as a friend by downregulating the expression of various defense signalling genes as an initial response to colonization by PGPR (Desbrosses *et al.*, 2009).Our outcomes appear to support this theory as well , we observed the downregulation of transcripts associated with defense signalling in inoculated roots e.g., chitinases and thionin. Suppression of plant defense mechanisms helped strain B26 to make a beneficial interaction with *B.distachyon* roots leading to plant growth promotion. Transcripts of chitinases and thionin were downregulated in rice roots inoculated with *A. brasilense* (Thomas *et al.*, 2019). Surprisingly, an increased expression of lytic enzyme β-1,3-glucanases in inoculated roots indicates the role of B26 as a biocontrol agent which enhance resistance against fungal pathogens (Kim *et al.*, 2015a). Moreover, PGPRs protect the host plant from environmental stresses by the production or regulation of compounds like β-1,3-glucanases (Jha *et al.*, 2022). Leucine-rich repeat (LRR) receptors mediate responses to hormones and provide resistance to pathogens. In our study, LRR proteins were differentially expressed in inoculated roots. Most of them were upregulated with few exceptions. Rice plants inoculated with PGPR strain *B. amyloliquefaciens* FZB24 showed an up-regulated

expression pattern in LRR receptor genes (Xie *et al.*, 2019). Moreover, reduced expression of transcript encoding Glutathione S-transferase (GST) was detected. GST plays a ubiquitous role in plants including growth development and stress responsiveness (Gullner *et al.*, 2018). Similarly, *Bacillus subtilis* strain JS reduced the expression of GST in tobacco after inoculation (Kim *et al.*, 2015b). In fact, increased expression of GST is a sign of a plant's reaction to stress (Edwards *et al.*, 2000). Our plants were not challenged by any kind of stress so the observed reduction in expression of GST justifies the fact that plant is treating B26 as a non-pathogenic bacterium. However, PGPR in plants activates induced systemic resistance (ISR) which is a condition of enhanced defensive ability (Pieterse *et al.*, 2014). ISR utilizes pathways controlled by ethylene and jasmonate (Van der Ent *et al.*, 2009). Surprisingly, we observed reduced transcripts of jasmonic acid (JA) biosynthesis in inoculated roots. *B.distachyon* (Yang *et al.*, 2021) and *A.thaliana* (Pieterse *et al.*, 2000) roots colonized by PGPR-induced ISR but this induction was also not accompanied by an increase in JA and ethylene levels. These results support the alternative theory of ISR induction which is based on an enhanced sensitivity to JA and ethylene instead of increasing their biosynthesis (Pieterse *et al.*, 2014). These observations further confirm the priming ability of B26 to combat stressful situations.

5.5.1.5 Secondary Metabolites

Plants secrete a variety of secondary metabolites which help them in alleviating biotic and abiotic stresses. An enormous variety of secondary metabolites are produced by phenylpropanoid metabolism that significantly affects the interaction of plants with the pathogen (Mhlongo *et al.*, 2020) However, metabolites of the phenylpropanoid pathway act as strong indicators of PGPR priming (Mhlongo *et al.*, 2020). A major step in core phenyl propanoid pathway is the conversion of p-coumaric acid to p-coumaroyl-coA which is catalyzed by 4-coumarate-CoA ligase (4CL).

Transcripts of 4CL were upregulated in our results **(Supplementary Table 5.4)**. Overexpression of 4CL in transgenic tobacco enhanced lignin and flavonoids which led to the mechanical strengthening of plants (Dauwe *et al.*, 2007, Li *et al.*, 2020). Expression of 4CL was also upregulated when tobacco roots were inoculated with *Paenibacillus polymyxa* YC0136 (Liu *et al.*, 2020). The lignin branch of phenylpropanoid pathway is important for lignin production and accumulation which helps in providing mechanical strength to plants (Dauwe *et al.*, 2007, Chun *et al.*, 2019). Transcripts of cinnamyl alcohol dehydrogenase (CAD) and ferulic acid-5-hydroxylase (F5H) key enzymes involved in lignin biosynthesis, were upregulated and which might increase the lignin content in inoculated *B.distachyon* roots. Tobacco roots inoculated with *Paenibacillus polymyxa* YC0136 had more lignin accumulation due to the upregulation of CAD encoding transcript (Liu *et al.*, 2020). Moreover, these lignifying enzymes make cell wall stronger to resist biotic and abiotic stress (Liu *et al.*, 2018, Chun *et al.*, 2019).We hypothesize that upregulation of these transcripts could lead to the thickening of cell wall in inoculated *B.distachyon* roots. Our microscopy results confirmed this hypothesis. We observed the increased thickness of xylem secondary cell wall in inoculated roots as compared to control roots. Touldiene blue stained cross sections revealed that xylem is lignified since it showed bluish green color **(Figure 5.6 a,b)** (O'Brien *et al.*, 1964, Mitra and Loqué, 2014).

Previously, we studied the role of organic acids as chemo-attractants for the recruitment of B26 (Sharma *et al.*, 2020). The plant root exudates including organic acids, amino acids, sugars, vitamins, hormones, fatty acids, phenols and flavonoids are released from plants in the process of rhizodeposition (Villarino *et al.*, 2021). Flavonoids have been proven as a chemo-attractant for various beneficial microbes (Zuanazzi *et al.*, 1998, Dong and Song, 2020, Korenblum *et al.*, 2022). From our differential gene expression studies, we observed an upregulation of flavonoid

biosynthesis transcripts which would have possibly helped in attraction of strain B26. *Geum aleppicum* inoculated with a PGPR, *Pseudarthrobacter* sp. NIBRBAC000502770, increased plant growth and the amount of flavonoid (Ham *et al.*, 2022).

Figure 5.7 represents the overall consequences of B26 interaction with Bd21-3 roots. B26 helped in the improvement of root growth by increasing nutrient and ion uptake. Plant hormone homeostasis by B26 might also lead to improved root growth and induction of ISR as depicted by our transcriptomic results. In our dataset, we found upregulation of transcription factors and secondary metabolites in inoculated roots, which led to stress tolerance, mechanical strengthening and priming **(Figure 5.7)**.

We also observed an upregulation of flavonoid biosynthesis transcripts in inoculated roots. *Bacillus subtilis* induced the accumulation of flavonoids in tobacco which led to resistance against pathogen *Agrobacterium tumefaciens* (Nazari *et al.*, 2017). Moreover, flavonoid accumulation contributes to successful plant-PGPR colonization (Yu *et al.*, 2020). Flavonoids are one of the major secondary metabolites released from root exudates (Vives-Peris *et al.*, 2020).

In our previous results, we only investigated the effect of organic acids from *B.distachyon* root exudates on bacterial chemotaxis. Numerous reports suggest the important role of flavonoids in plant-PGPR interaction (Wang *et al.*, 2022). An increase in flavonoid biosynthesis transcripts might lead to increased flavonoid accumulation which in turn helped in the successful root colonization of B26.

We had previously used B26 for studying the plant-PGPR association and our results confirmed the positive effect of B26 on growth of *B.distachyon* accession Bd21-3 (Sharma *et al.*, 2022). In this study, we used RNA sequencing and identified the differentially expressed transcripts of

B.distachyon during its association with B26. Our transcriptome findings conclude that modulation of the hormone signalling pathway and increase in nutrient uptake could be the mechanisms by which B26 promotes plant growth observed in our previous findings (Sharma *et al.*, 2022). Additionally, B26 treatment altered the expression of numerous stress-related transcription factors, which are crucial for the expression of stress-responsive genes. This reflects the priming ability of B26 to combat various biotic and abiotic stresses. The robust dataset generated in this study improves our knowledge of plant-PGPR interaction and can serve as a model resource for poorly characterized plant and bacterial species. Our findings serve as a road map for future translational applications of PGPR in the field of sustainable agriculture.

5.6 Acknowledgements

We greatly acknowledge Dr Youssef Chebli (Multiscale Imaging Facility Manager, Macdonald Campus) for assistance with sample preparation and imaging for microscopy. We greatly acknowledge the financial support, through a Discovery grant (RGPIN-2016-04805) to Dr Suha Jabaji, which was provided by the Natural Sciences and Engineering Research Council of Canada. We thank Dr Jean Benoit Charron for providing wild-type *Brachypodium distachyon* seeds which were originally sourced from Dr David F. Garvin, USDA. We also thank Compute Canada for allowing us to use their high performance computing resources.

5.7 Author Contributions

Conception and design of the study: Meha Sharma (MS) and Suha Jabaji (SJ). Acquisition of data for the study: MS and SJ. Analysis of data for the work: MS. Interpretation of data for the work: MS and SJ. Manuscript revision and approval: MS and SJ.

5.8 Conflict of Interest Statement

The authors declare that the research was conducted in the absence of any commercial or financial relationships that could be construed as a potential conflict of interest

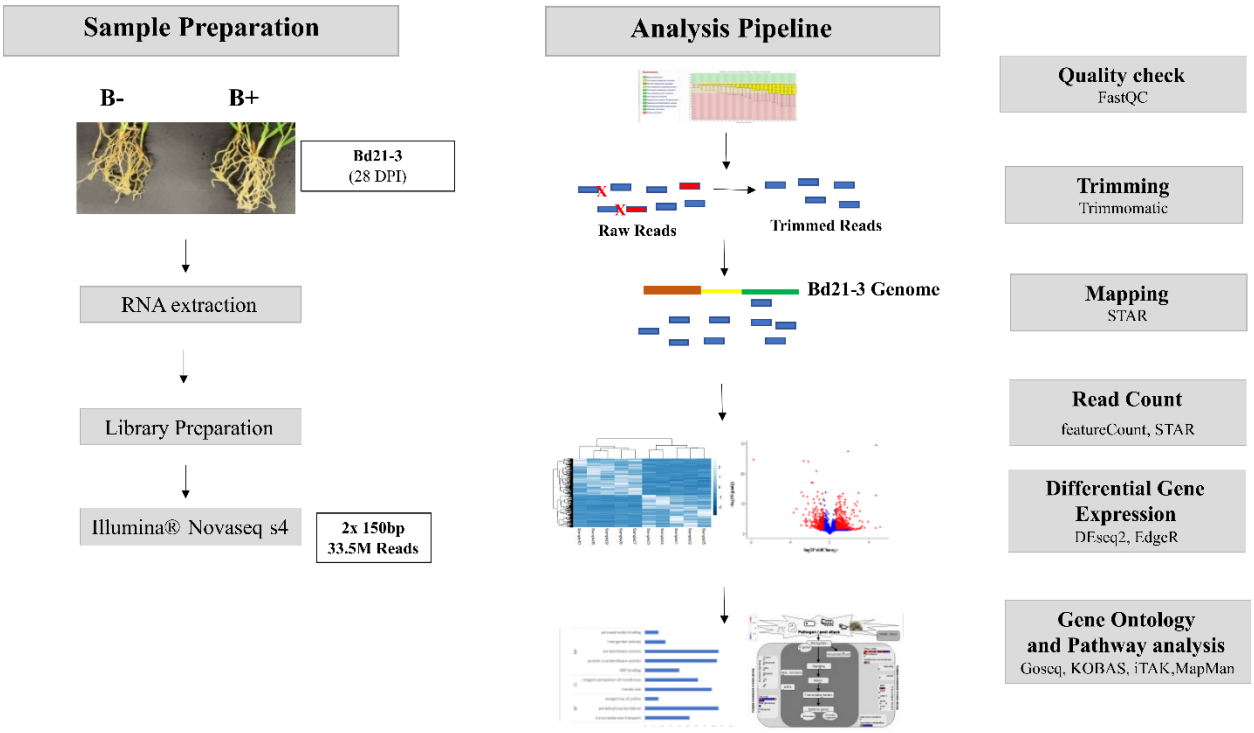

Figure 5.1 Pipeline used for bioinformatics analysis. Dpi: Days post inoculation, B- : Control roots, B+: Inoculated roots.

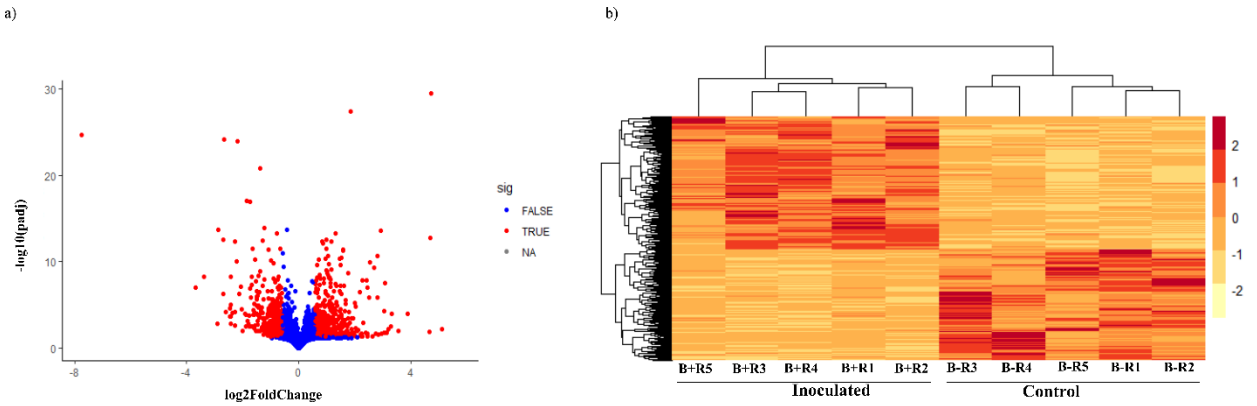

Figure 5.2 a) Volcano plot of all the expressed genes in RNA sequencing data. The mean log2fold change is plotted against -log10 adjust p-value for all the expressed genes. Red dots represent true significant (|log2(fold change)| > 1.5, False discovery rate < 0.05) Differentially Expressed Genes(DEGs) and blue dots represent false DEGs. b) Heatmap of 783 significant DEGs in inoculated and control roots.

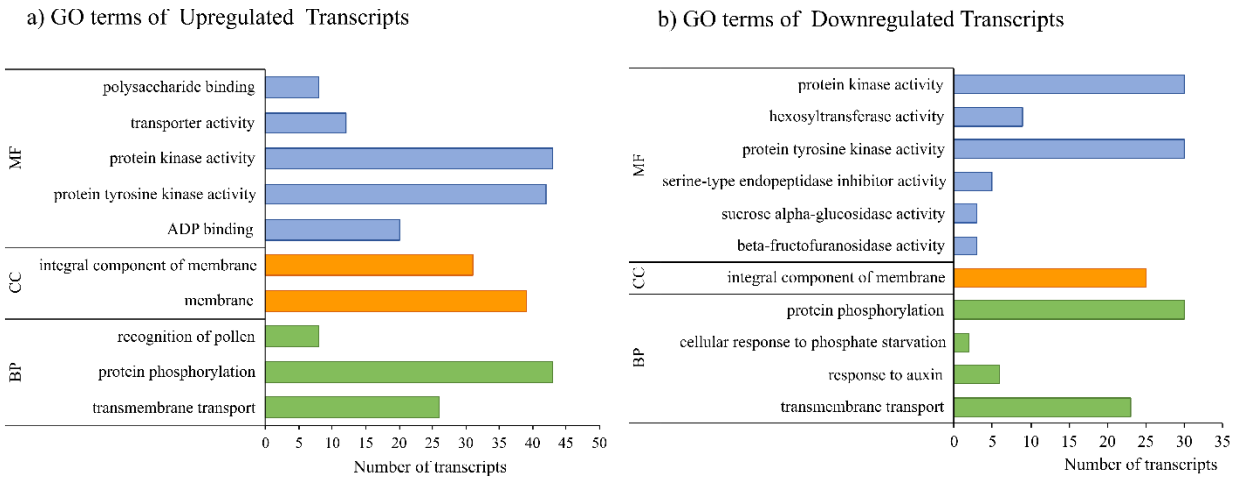

Figure 5.3 Gene Ontology (GO) categorization of significant a) Upregulated b) Downregulated transcripts. MF: Molecular Function, CC: Cellular Component, BP: Biological Process. Bars represent the number of Differentially Expressed Genes in that category.

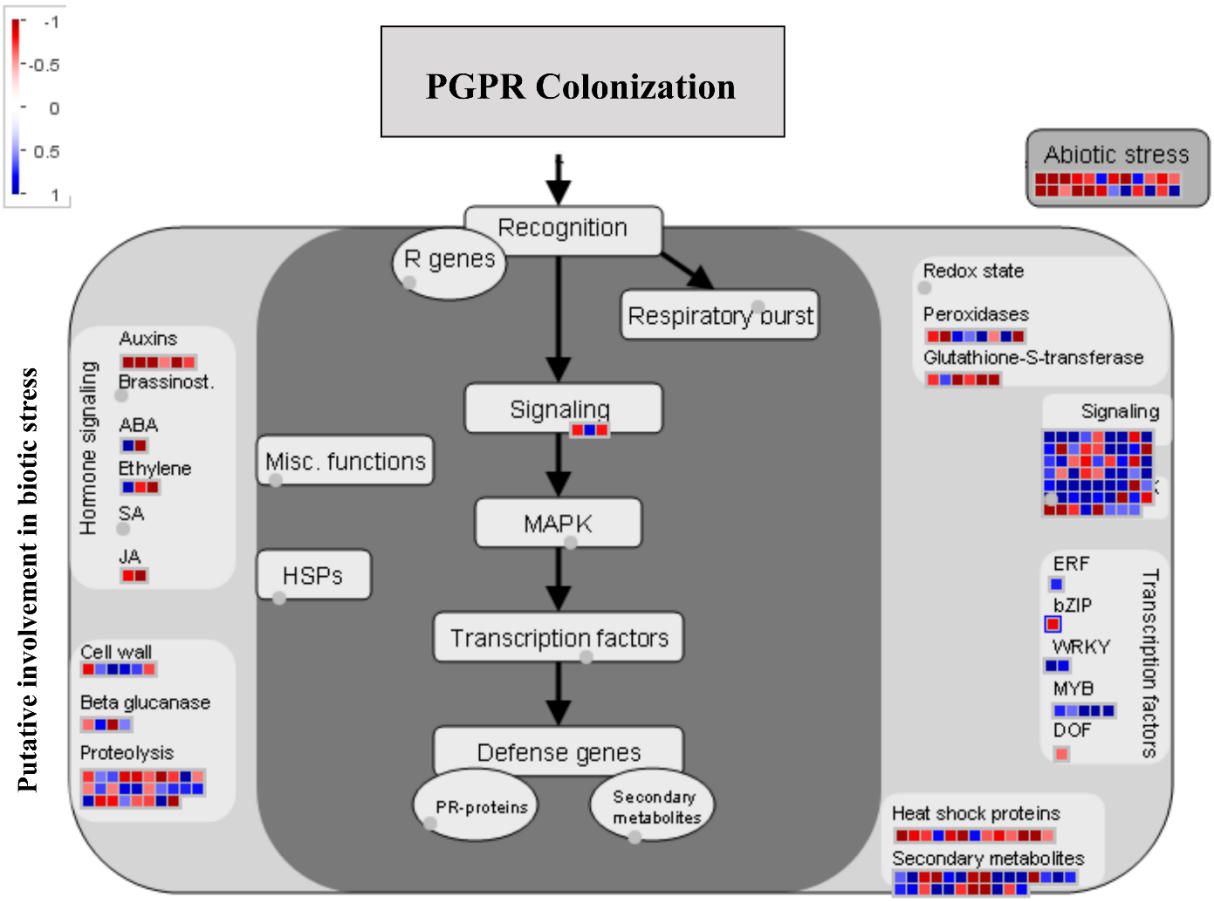

Figure 5.4 Biotic stress pathway analyses of Differentially Expressed Genes (DEGs) in inoculated *B.distachyon* roots using MAPMAN software. Blue boxes represent upregulated genes and red boxes represent downregulated genes. The pathway frame is from the MAPMAN software database.

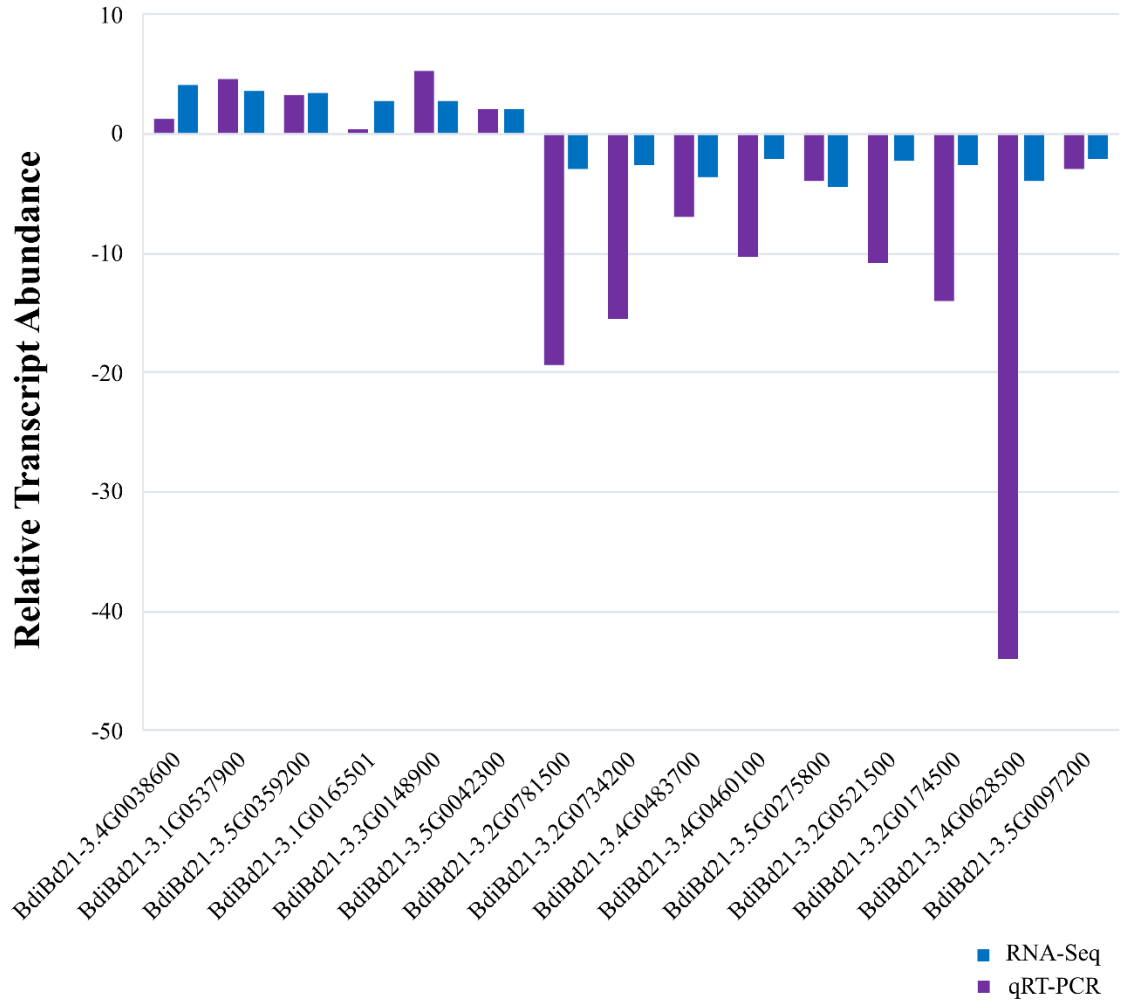

Figure 5.5 qRT-PCR validation of randomly selected Differentially Expressed Genes (DEGs) identified by RNA sequencing.

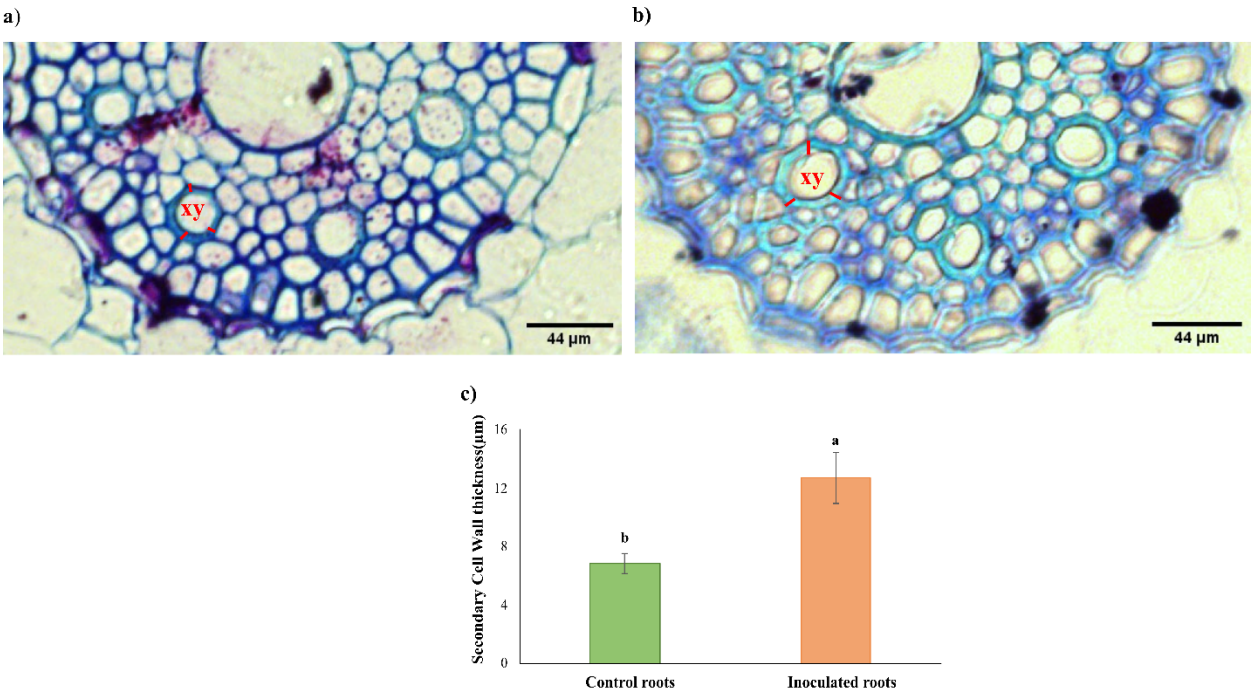

Figure 5.6 Light microscopy images of toluidine blue stained B.distachyon root sections a) Control b) Inoculated. Xylem secondary cell wall thickness was measured at three points highlighted with red lines in FIJI software. c) Bar graphs represent the xylem secondary cell wall thickness (µm) in control and inoculated roots. Different letters (a,b) indicate significant differences among means of control and inoculated roots. Error bars represent the standard errors of mean of replicates. Bars = 44 µm, xy = Xylem.

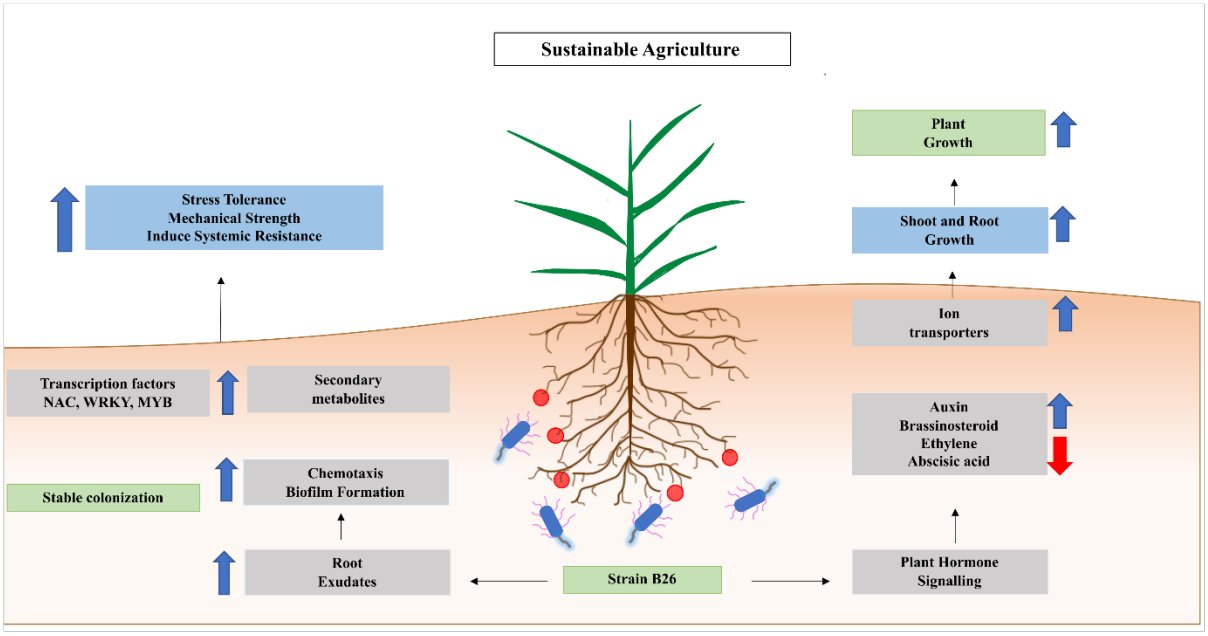

Figure 5. 7 Proposed model for the effect of strain B26 colonization on *B.distachyon* roots. Blue arrows represent the upregulation and red arrows represent the downregulation of genes or pathways in inoculated roots.

Table 5.1 Significantly over-represented Gene Ontology (GO) terms following enrichment analysis on up-and down-regulated genes

Upregulated differentially expressed transcripts					
GO term ID	**Term**	**DEGs in category**	**Expressed genes in category**	**Ontology**	**False Discovery Rate**
GO:0043531	ADP binding	20	272	MF	0.000945
GO:0016020	membrane	39	955	CC	0.001003
GO:0055085	transmembrane transport	26	475	BP	0.001003
GO:0004713	protein tyrosine kinase activity	42	1052	MF	0.003366
GO:0004672	protein kinase activity	43	1109	MF	0.003366
GO:0006468	protein phosphorylation	43	1114	BP	0.003366
GO:0048544	recognition of pollen	8	62	BP	0.005962
GO:0016021	integral component of membrane	31	783	CC	0.005962
GO:0005215	transporter activity	12	178	MF	0.018987
GO:0030247	polysaccharide binding	8	83	MF	0.032495
Downregulated differentially expressed transcripts					
GO term ID	**Term**	**DEGs in category**	**Expressed genes in category**	**Ontology**	**False Discovery Rate**
GO:0055085	transmembrane transport	23	472	BP	0.000293
GO:0004564	beta-fructofuranosidase activity	3	3	MF	0.001652
GO:0004575	sucrose alpha-glucosidase activity	3	3	MF	0.001652
GO:0009733	response to auxin	6	44	BP	0.006082
GO:0004867	serine-type endopeptidase inhibitor activity	5	27	MF	0.006082
GO:0016021	integral component of membrane	25	777	CC	0.016442
GO:0004713	protein tyrosine kinase activity	30	1040	MF	0.027082
GO:0016036	cellular response to phosphate starvation	2	2	BP	0.038213
GO:0016758	hexosyltransferase activity	9	150	MF	0.042059
GO:0004672	protein kinase activity	30	1096	MF	0.044769
GO:0006468	protein phosphorylation	30	1101	BP	0.044769

Table 5.2 List of statistically KEGG enriched pathways in upregulated and downregulated transcripts

Upregulated differentially expressed transcripts						
#Term	**Database**	**ID**	**Input number**	**Background number**	**P-Value**	**Corrected P-Value**
Brassinosteroid biosynthesis	KEGG PATHWAY	bdi00905	6	12	3.20E-09	3.52E-07
Biosynthesis of secondary metabolites	KEGG PATHWAY	bdi01110	50	1149	4.07E-06	0.000149
Metabolic pathways	KEGG PATHWAY	bdi01100	34	2189	8.30E-05	0.00083
Cysteine and methionine metabolism	KEGG PATHWAY	bdi00270	6	102	0.000186	0.001461
Glycolysis / Gluconeogenesis	KEGG PATHWAY	bdi00010	6	127	0.000569	0.003478
Phenylpropanoid biosynthesis	KEGG PATHWAY	bdi00940	7	222	0.001978	0.009889
Carbon metabolism	KEGG PATHWAY	bdi01200	7	242	0.003153	0.014451
Fatty acid elongation	KEGG PATHWAY	bdi00062	3	45	0.005907	0.024065
Starch and sucrose metabolism	KEGG PATHWAY	bdi00500	5	148	0.006531	0.024272
Fatty acid degradation	KEGG PATHWAY	bdi00071	3	48	0.006994	0.024818
Tyrosine metabolism	KEGG PATHWAY	bdi00350	3	49	0.007381	0.025373
Selenocompound metabolism	KEGG PATHWAY	bdi00450	2	16	0.0082	0.027053
Biosynthesis of amino acids	KEGG PATHWAY	bdi01230	6	222	0.008362	0.027053
Terpenoid backbone biosynthesis	KEGG PATHWAY	bdi00900	3	54	0.009504	0.029041
Plant hormone signal transduction	KEGG PATHWAY	bdi04075	6	230	0.009807	0.029157
alpha-Linolenic acid metabolism	KEGG PATHWAY	bdi00592	7	45	1.73E-06	0.000225
Flavonoid biosynthesis	KEGG PATHWAY	bdi00941	4	47	0.002497	0.048702
Downregulated differentially expressed transcripts						
#Term	**Database**	**ID**	**Input number**	**Background number**	**P-Value**	**Corrected P-Value**
Steroid biosynthesis	KEGG PATHWAY	bdi00100	7	40	7.13E-06	0.000323
Metabolic pathways	KEGG PATHWAY	bdi01100	60	2189	2.11E-05	0.000662
Glutathione metabolism	KEGG PATHWAY	bdi00480	9	107	7.86E-05	0.001687
Plant hormone signal transduction	KEGG PATHWAY	bdi04075	12	230	0.000399	0.006274
Biosynthesis of secondary metabolites	KEGG PATHWAY	bdi01110	32	1149	0.001499	0.018625
Starch and sucrose metabolism	KEGG PATHWAY	bdi00500	8	148	0.002931	0.031439

Table 5.3 Transcription factors (TFs) and Transcription regulators (TRs) identified among DEGs

Family	No of upregulated transcripts	No. of downregulated transcripts	Type
AP2/ERF-AP2	1	0	TF
AP2/ERF-ERF	0	1	TF
B3	1	0	TF
bHLH	1	0	TF
bZIP	3	1	TF
C2H2	1	0	TF
C2C2-CO-like	0	1	TF
C2C2-Dof	0	1	TF
EIL	0	1	TF
GARP-G2-like	1	4	TF
GRAS	2	2	TF
HB-BELL	2	0	TF
HB-HD-ZIP	0	1	TF
HB-KNOX	1	0	TF
HB-other	1	0	TF
HSF	0	1	TF
LOB	1	2	TF
MADS-M-type	3	0	TF
MYB	5	0	TF
MYB-related	2	0	TF
NAC	10	1	TF
SRS	1	2	TF
WRKY	3	0	TF
AUX/IAA	5	0	TR
Others	2	2	TR
SNF2	0	1	TR

Chapter 6. GENERAL DISCUSSION

Roots are the most vital and significant components of a plant that enable the plant to firmly anchor. The stronger the root system, the healthier will be the plant. The region of the soil in vicinity of roots is a hotspot for communication between plant roots and soil microflora which is called the rhizosphere. The term rhizosphere was first coined and defined by Lorenz Hiltner as the soil compartment influenced by the roots of growing plants (Hiltner, 1904). The crosstalk between roots and microbes led to signal exchange between prokaryotes and eukaryotes. Plant roots release organic compounds in the form of root exudates that facilitate the dialogue between plant and microbes. Root exudates act as a chemoattractant or chemorepellent for microbes in the rhizosphere and helps in recruitment of beneficial microbes (Dennis *et al.*, 2010, Ulbrich *et al.*, 2022). PGPRs promote positive plant-microbe interactions by increasing plant growth and stress resilience. Our lab has previously proved that *Bacillus velezensis* strain B26, a PGPR, successfully colonized *Brachypodium distachyon* roots and accelerated plant growth (Gagné-Bourque *et al.*, 2015). The aim of this thesis was to investigate the molecular mechanisms behind the interaction of *B.distachyon* and *B.velezensis*.

In chapter 3 (Sharma *et al.*, 2020) the role of root exudates and individual organic acids of *B.distachyon* was investigated in the recruitment of *B.velezensis*. Root exudates of *B.distachyon* is primarily composed of amino acids, sugars and organic acids (Kawasaki *et al.*, 2016). The Organic Acids (OAs) from tricarboxylic Acid (TCA) cycle, released by roots play an important role in the recruitment of PGPR. To collect root exudates, we generated a semi-hydroponics system for growing plants. Root exudates were collected from control and inoculated roots. We quantified the organic acids from roots and root exudates from both control and inoculated samples. Results of GC-MS analysis of root exudates indicated the maximum production of fumarate and succinate

followed by malate, citrate and isocitrate while roots were found rich in malate and citrate irrespective of treatment or control **(Figure 3.3)**. Interestingly, our observation was in accordance with a previously published report which states that *Brachypodium* root exudates are rich in malate, citrate, succinate, fumarate and oxalate (Kawasaki *et al.*, 2016). For successfull root colonization, chemotaxis and biofilm formation are the two most crucial activities performed by PGPR (Zhang *et al.*, 2014, Vora *et al.*, 2021). We tested the ability of various OAs and root exudates of *Brachypodium* to attract B26. Root exudates stimulated a very strong chemotactic response on B26 **(Figure 3.1a)**. We observed that all OAs, except oxalic acid, were capable to induce chemotaxis response in drop assay. Similar chemotactic responses were observed in *B. amyloliquefaciens* T-5, where malic acid, citric acid, succinic acid and fumaric acid promoted the recruitment of bacteria towards tomato roots(Tan *et al.*, 2013). Relative chemotactic ratio (RCR) was highest when B26 was grown in a medium containing malic acid. Numerous studies have reported malic acid as the best chemoattractant(Yuan *et al.*, 2015, Rekha *et al.*, 2018a, Jin *et al.*, 2019). The composition of root exudates resulting in chemotaxis shows that malic and citric acids act as chemoattractants for strain B26 and played an important role in root colonization. Malate and citrate from root exudates in tomato plants (Oku *et al.*, 2014), maize (Pineros *et al.*, 2002) and *Arabidopsis*(Badri and Vivanco, 2009) have been proven as chemoattractants for PGPRs.

After getting attached to the surface of roots bacteria aggregate in groups and begin the colonization process. This aggregation could be in sessile and motile forms. Bacteria swarm when it is mobile and move across the surface while in sessile form bacteria produce biofilm (Kearns, 2010). B26 could swarm which was affected by the presence of OAs. We have found that malic acid increases the swarming ability of B26. Biofilm in *Bacillus* is composed of extracellular of exopolysaccharide and highly hydrophobic (EPS)(Branda *et al.*, 2001). We detected a large

amount of EPS production by B26 and around 69% of hydrophobicity **(Table 3.4)**. BslA protein provides this hydrophobicity to the bacterial aggregation which protects the biofilm structure (Kalamara *et al.*, 2021). We also investigated the induction of biofilm in response to various OAs and root exudates. Our results demonstrated that *Brachypodium* root exudates and exogenously added organic acids significantly promoted B26 biofilm formation. Malic and fumaric acid increased the biofilm formation after 24 hours of growth, while after 48 hours of growth citric and oxalic acid seemed to increase the biofilm formation. In cucumber, citric acid induced biofilm formation by *Bacillus amyloliquefaciens* (Zhang *et al.*, 2014). Induction of biofilm formation in response to root exudates has been noted previously in *Bacillus velezensis* Strain S3-1 to maize root exudates (Jin *et al.*, 2019), *Bacillus velezensis* FZB42 to tomato root exudates (Al-Ali *et al.*, 2018), *B. subtilis* to *Arabidopsis* and tomato root exudates (Rudrappa *et al.*, 2008, Chen *et al.*, 2012) and *Bacillus amyloliquefaciens* NJN-6 to banana root exudates (Yuan *et al.*, 2015). Biofilm in *Bacillus* is composed of an extracellular of exopolysaccharide (EPS)(Branda *et al.*, 2001). A large amount of EPS production was quantified by B26.

We also checked the effect of various OAs on the transcription level of genes encoding the extracellular matrix of the biofilm, *eps A,B,D; yqxM* and hydrophobin component *bslA.* We found that succinic acid elevated the transcription of exopolysaccharide formation genes (*epsA* and *epsB*). Transcription of *epsB* gene was also increased by fumaric acid and malic acid **(Figure 3.5)**. While, *yqxM* and *bslA* were induced by citric and succinic acids. In various reports, malic acid was found to induce biofilm formation in *Bacillus subtilis* NCIB3610 by KinD-Spo0A pathway (Chen *et al.*, 2012); *Bacillus subtilis* FB17 increasing transcription of *yqxM* gene (Rudrappa *et al.*, 2008) while Fumaric acid was found to significantly elevate the expression of *epsD* and *yqXM* genes in *Bacillus amyloliquefaciens* NJN-6 (Yuan *et al.*, 2015). To identify the detailed structure of biofilm

formed, scanning electron microscopy (SEM) was utilized. SEM micrographs showed the presence of mesh-like matrix in inoculated roots of *B.distachyon* (**Figure 3.2**). Similar matrixes were formed by *B.subtilis* EA-CB0575 in tomato and banana roots(Posada *et al.*, 2018).

In chapter 3, we further analysed how strain B26 inoculation affected the transcription of organic acid genes involved in the TCA cycle in *B. distachyon* roots. Overall, an increase in the transcription level of OA genes was observed in inoculated roots as compared to the control. As anticipated, B26 significantly induced the transcript abundance of *Malate dehydrogenase* and *Citrate Synthase*. To further confirm the role of B26 on TCA cycle genes, we used *icdh* mutants. But our results were not conclusive as we did not observe any significant difference in transcript abundance of *ICDH* gene in mutant and wild type. Overall, B26 improved the root exudation composition of *B.distachyon* accession Bd21-3 which in turn helped in chemotaxis and biofilm formation by B26.

Apart from the biofilm, successful plant-PGPR colonization depends on various biotic (plant genotype, developmental stage, pathogens) and abiotic factors (soil richness, environmental conditions, water availability) (Hafeez *et al.*, 1998, Swarnalakshmi *et al.*, 2020). *Brachypodium* accessions manifest variations in phenotypic traits such as plant height, growth habit, flowering time, seed weight and cell wall composition (Tyler *et al.*, 2014). This led us to hypothesize that different accessions of *B.distachyon* may behave differently in the response to *Bacillus velezensis* strain B26.

In chapter 4, we selected four *B.distachyon* accessions based on flowering types. Early rapid flowering accessions Bd21, Bd21-3; Intermediate rapid flowering Bd30-1 and delayed flowering accessions Bd18-1 were used. These genotypes reacted differentially for each growth parameter observed. A positive response was demonstrated by genotypes Bd21 and Bd21-3, where

flowering induction was ramped up in response to B26 **(Figure 4.1c)**. Conversely, Bd30-1 did not respond to inoculation but surprisingly sustained B26 populations in both roots and shoots **(Table 4.2)**. Among winter wheat genotypes RonL and OK06318, genotype responded better to ACC deaminase bacterial inoculation (Salem *et al.*, 2018). Similar results were observed when 40 different *B.distachyon* accessions responded differentially to co-inoculation with two diazotrophic bacteria, *H. seropedicae* and *A. brasilense* (Do Amaral *et al.*, 2016). *B. distachyon* genotypes demonstrated significant and varied responses to infection by pathogenic insects and fungi (Sandoya and de Oliveira Buanafina, 2014). Wild type *Arabidopsis thaliana* showed reduced growth in response to *Pseudomonas fluorescence* (Haney *et al.*, 2015).

Our phenotypic data also suggested an increase in flowering in inoculated Bd21-3. Intriguingly, PGPR colonization resulted in more flowers and seed production in tobacco with no negative impact on plant health (Kumar et al., 2016). *Bacillus cereus* KI-2 induced early flowering in garden strawberries ("Hoko-wase") while no difference in flowering was observed in the other varieties of strawberry (KUROKURA *et al.*, 2017). This led us to investigate the molecular mechanisms underlying this increase. Flowering in *B. distachyon* controlled by three major genes viz., *VERNALIZATION1* (*VRN1*), *VRN2*, and *FLOWERING LOCUS T* (*FT*) (Higgins *et al.*, 2010). A differential expression pattern of selected flowering genes was observed in inoculated *B.distachyon* genotypes. Flowering promoter *FT1*, *FT2* and *VRN1* were upregulated in inoculated Bd21-3 but *VRN2* was downregulated upon inoculation. Bd21, an early flowering accession, also showed reduced *VRN2* expression in the absence of vernalization (Bettgenhaeuser et al., 2017). While *VRN2* was highly upregulated in Bd30-1, accession which did not respond to flowering **(Figure 4.2)**. In wheat and barley *VRN2* negatively control flowering(Yan *et al.*, 2004) however there is still ample amount of ambiguity around the role of *VRN2* in *B.distachyon* (Bettgenhaeuser

et al., 2017). An increase in expression of flowering genes *LEAFY* and *AP1* was observed in *Arabidopsis* inoculated with PGPR *Burkholderia phytofirmans* PsJN (Poupin *et al.*, 2013). We tested overexpressing flowering transgenic lines *UBI:FT1* and *UBI:VRN1* for their ability to respond to B26 inoculation. Upon inoculation, an increase in number of awns and root weight was observed in these overexpressing flowering transgenic lines. An increase in root volume was also observed in inoculated roots of wild type Bd21-3 and transgenic lines *UBI:FT1* and *UBI:VRN1*. Increase in root weight and root volume in the transgenic lines gave an indication to explore the role of roots in signalling and flower development. It has been hypothesised that the beginning of flowering may be a time when roots coordinate growth throughout the entire plant (Bouché *et al.*, 2016). This motivated us to investigate flowering genes in roots of control and inoculated wild type Bd21-3 and transgenic lines *UBI:FT1* and *UBI:VRN1*. As anticipated a tremendous increase in the transcripts of *FT1* was observed in roots of inoculated *UBI:FT1***(Figure 4.6).** A very few studies have reported the role of roots in flower development. Bouché *et al.,* (2016) found flowering time genes in *Arabidopsis* roots and during induction of flowering around 595 genes were differentially expressed in roots genes. Roots of *Camelina sativa* inoculated with *Pesudomonas migulae* 8R6 showed a decrease in expression of *Brother of Flowering Locus T* (a floral repressor) under salt stress (Heydarian *et al.*, 2018). An unknown root-derived signal was found to be involved in the control of flowering in *Sinapis alba* (Bernier *et al.*, 1993, Havelange *et al.*, 2000).

Additionally, it is well known that hormonal signalling plays a significant part in plant growth and development. PGPRs have affected the multiple plant hormones in various crops (Joo *et al.*, 2004, Kang *et al.*, 2009, Sgroy *et al.*, 2009). PGPR has the ability to influence plant growth through metabolism of phytohormones in the rhizosphere (Dodd *et al.*, 2010). We measured the

endogenous levels of phytohormones in control and inoculated roots of Bd21-3, *UBI:FT1* and *UBI:VRN1*. Gibberellins (GAs) were the most prevalent phytohormone found regardless of the treatment. While the levels of IAA and GA_7 in inoculated Bd21-3 were lower than the control, but surprisingly the transcripts of IAA were upregulated. Similar results were observed in *Arabidopsis* inoculated with *Burkholderia phytofirmans* PsJN which helped in growth promotion partially via degrading IAA whereas the expression level of auxin receptors was higher in inoculated plants (Zúñiga *et al.*, 2013). Hence, in addition to synthesising auxin, PGPR can also degrade it in order to alter the auxin concentration in the host plants. Another interesting observation was decrease in transcripts of GA biosynthesis gene while increase in transcript of DELLA protein, a negative regulator of GA synthesis. By exerting direct feedback DELLA proteins regulate the expression of the genes responsible for GA biosynthesis and GA receptors, assisting in the establishment of GA homeostasis(Zentella *et al.*, 2007).

In chapter 5, Transcriptome analysis of Bd21-3 inoculated roots revealed the transcripts associated with phytohormones were differentially expressed. Transcripts of auxin biosynthesis and auxin responsive IAA were upregulated which is in accordance with our qRT-PCR results obtained in chapter 4. Tobacco roots inoculated with *Paenibacillus polymyxa* YC0136 induced the expression of plant phytohormone genes (Liu *et al.*, 2020). Transcripts of SAUR proteins, auxin responsive genes, were downregulated in inoculated roots. Similar results were reported when rice roots inoculated with *A. brasilense* and *H. seropedicae* reduced the expression of SAUR proteins (Brusamarello-Santos *et al.*, 2012, Wiggins *et al.*, 2022). We also observed downregulation of transcript encoding 1-aminocyclopropane-1-carboxylate oxidase (ACO) which indicates less production of ethylene in inoculated roots. Less ethylene production is beneficial for mitigating stress and advantageous for roots because it reduces cell elongation, which inhibits root growth

(Růžička *et al.*, 2007, Qin and Huang, 2018, Fortt *et al.*, 2022). Another key phytohormone is Abscisic acid (ABA) which regulates various biotic and abiotic stress responses in plants. However, plant growth and the endogenous concentration of ABA are negatively correlated under non-stressed conditions (Pilet and Saugy, 1987, Xiong and Zhu, 2003). In our results, a negative regulator of ABA was upregulated and a positive regulator was downregulated which suggests the desensitization of ABA hence less production of ABA in inoculated roots (Santiago *et al.*, 2009). The relationship between plants and rhizobacteria has a significant impact on the nutrition of plants in terms of mineral acquisition (Pii *et al.*, 2015, Tabassum *et al.*, 2017).

The whole transcriptome of *B.distachyon* was altered when B26 interacted. We found differentially expressed transcripts associated with high-affinity nitrate, glutamate, ammonium, sulphate, inorganic phosphate, and sugars. An increase in nitrate and ammonium transporter was observed in inoculated roots. Both nitrate and ammonium transporter genes were also upregulated in *Arabidopsis* roots inoculated with consortia of *Bacillus* (Calvo *et al.*, 2019). There is a positive correlation between the transcript abundance of these transporter genes and nitrogen uptake which ultimately led to enhanced plant growth (Calvo *et al.*, 2019). Sugar transporter proteins (STPs) were also affected during PGPR interaction. The upregulation of sugar transporter is common during symbiosis and plant-pathogen interaction to gain sugar from host plants (Desrut *et al.*, 2021). However, in our study, six STPs were overrepresented and one STP was underrepresented. All STPs in *Arabidopsis* were downregulated by *Pseudomonas simiae* WCS417r (Desrut *et al.*, 2021). While a sugar transporter gene was upregulated in rice roots inoculated with *Azospirillum brasilense* and separately with *Herbaspirillum seropedicae* (Wiggins *et al.*, 2022). This differential expression of STPs is not very well studied for PGPR-plant interaction. Changes in plant sugar transport may help establish and maintain PGPR-plant interaction by giving PGPR access to a

controlled pool of sugar as a source of carbon (Hennion *et al.*, 2019).Various evidence depict the role of transcription factors (TFs) in early stress responsiveness, root growth and development (Montiel *et al.*, 2004, Joshi *et al.*, 2016). TFs NAC, WRKY, MYB, bZIP, and heat shock proteins were found to be upregulated in inoculated roots. *Paenibacillus polymyxa* strain YC0136 induced the expression of TFs WRKY and MYB in tobacco which are associated with abiotic stress(Liu *et al.*, 2020). The expression of TFs bZIP, NAC and MYB were modulated in *Arabidopsis* inoculated with *Pseudomonas putida* MTCC5279 (Srivastava *et al.*, 2012). No stress was applied to the plants in this study despite NAC TF being upregulated could mean that strain B26 is preparing the plants for stressful situations by strengthening their resistance. Plant recognize PGPR as a friend by downregulating the expression of various defense signalling genes as an initial response to colonization by PGPR(Desbrosses *et al.*, 2009). Our outcomes appear to support this theory as well, defense signalling genes encoding chitinases and thionin were downregulated in inoculated roots. Rice roots inoculated with *Herbaspirillum seropedicae and Azospirillum brasilense* also had reduced expression of chitinases and thionin (Wiggins et al., 2022). However, an increase in expression of lytic enzyme β-1,3-glucanases in inoculated root indicates the role of B26 as biocontrol agent which enhance resistance against fungal pathogens (Kim *et al.*, 2015a).

Moreover, reduced expression of transcript encoding Glutathione S-transferase (GST) was detected. GST play a ubiquitous role in plants including growth development and stress responsiveness (Gullner *et al.*, 2018). Similarly, *Bacillus subtilis* strain JS reduced the expression of GST in tobacco after inoculation (Kim *et al.*, 2015b). In fact, increased expression of GST is a sign of a plant's reaction to stress(Edwards *et al.*, 2000). Our plants were not challenged by any kind of stress so the observed reduction in expression of GST justifies the fact that plant is treating B26 as a non-pathogenic bacterium. However, PGPR in plants activates induced systemic

resistance (ISR) which is a condition of enhanced defensive ability(Pieterse *et al.*, 2014). ISR utilises pathways controlled by ethylene and jasmonate (Van der Ent *et al.*, 2009). Surprisingly, we observed reduced transcripts of jasmonic acid (JA) biosynthesis in inoculated roots. *Brachypodium* (Yang *et al.*, 2021) and *Arabidopsis* (Pieterse *et al.*, 2000) roots colonized by PGPR induced ISR but this induction was also not accompanied by an increase in JA and ethylene levels. These results support the alternative theory of ISR induction which is based on an enhanced sensitivity to JA and ethylene instead of increasing their biosynthesis (Pieterse *et al.*, 2014). These observations further confirm the priming ability of B26 to combat stressful situations. Plants secrete a variety of secondary metabolites which help them in alleviating biotic and abiotic stresses. An enormous variety of secondary metabolites are produced by phenylpropanoid metabolism that significantly affects the interaction of plants with the pathogen (Mhlongo *et al.*, 2020) However, metabolites of the phenylpropanoid pathway act as strong indicators of PGPR priming(Mhlongo *et al.*, 2020). 4 coumarate CoA ligase (4CL) a key enzyme in core phenyl propanoid pathway, was upregulated in inoculated roots. Overexpression of 4CL in transgenic tobacco enhanced lignin and flavonoids which led to a mechanical strengthening of plants (Dauwe *et al.*, 2007, Li *et al.*, 2020). PGPR *Paenibacillus polymyxa* YC0136 upregulated the expression of 4CL in tobacco roots (Liu *et al.*, 2020). We also observed the upregulation of transcripts encoding cinnamyl alcohol dehydrogenase (CAD), caffeic acid O-methyltransferase (COMT) and Ferulic acid-5-hydroxylase (F5H) which catalyses reactions of lignin branch in phenylpropanoid pathway (Yao *et al.*, 2021). These enzymes produce metabolites that lignify cell wall and make it stronger to resist biotic and abiotic stress(Liu *et al.*, 2018, Chun *et al.*, 2019).

In chapter 3, we studied the role of organic acids as chemo-attractants for the recruitment of B26. The plant roots exudates including organic acids, amino acids, sugars, vitamins, hormones,

fatty acids, phenols and flavonoids are released from plants in the process of rhizodeposition (Villarino *et al.*, 2021). Flavonoids have been proven as a chemoattractant for various beneficial microbes (Zuanazzi *et al.*, 1998, Dong and Song, 2020, Korenblum *et al.*, 2022). From our differential gene expression studies, we observed an upregulation of flavonoid biosynthesis transcripts which would have possibly helped in attraction of B26. *Geum aleppicum* inoculated with a PGPR, *Pseudarthrobacter* sp. NIBRBAC000502770, increased plant growth and amount of flavonoid (Ham *et al.*, 2022).

Chapter 7. CONCLUSION AND FURTURE DIRECTIONS

7.1 GENERAL CONCLUSION

The work presented in this thesis highlights the molecular mechanisms behind plant-PGPR interaction. These results help to unveil the mechanisms associated with bio-stimulant and biocontrol ability of B26.

In Chapter 3(Sharma *et al*., 2020), we focused on how root exudates and their by-products, such as succinic, citric, malic and fumaric acids, intermediates of the TCA cycle, affect B26. We conclude that chemotaxis, swarming and biofilm formation abilities are impacted by the presence of root exudates and organic acids. We propose that the upregulation of biofilm-associated genes by root exudates and organic acids is the cause of biofilm induction. In turn, strain B26 impacted the endogenous levels of organic acids of the TCA cycle. Irrespective of treatment, roots had higher levels of malate and citrate as compared to other organic acid. However, B26 had little to no effect on the endogenous levels of organic acids in inoculated roots, except for an increase in fumarate. While the inoculation significantly increased the endogenous levels of all organic acids in the root exudates which affirms that B26 improved the composition of root exudates. An additional factor supporting this improvement is the increased transcription of organic acid intermediates of TCA cycle in inoculated roots. The impact of PGPR on plant TCA cycle genes is being described for the first time in this study. These results improved our knowledge of the molecular mechanisms underlying the recruitment of PGPR by plants through root exudates.

B26 affected the phenological growth stages of different genotypes of *B. distachyon* but this response was not similar for all the genotypes. Flowering increased in response to colonisation in Bd21-3 due to the upregulation of transcripts encoding flowering in *Brachypodium*. Increased root

weight and root volume of Bd21-3 upon inoculation suggest the role of B26 in altering the root architecture. Our results also confirmed the role of B26 in modulating plant hormone homeostasis. Our findings provide new information about the role of *B. velezensis* in the expression of flowering genes and plant genotype determines whether a PGPR benefits the host or not.

B26 strongly impacted the transcriptome of *B.distachyon*. Our transcriptome findings indicate that modulation of the hormone signalling pathway and increase in nutrient uptake could be the mechanisms by which B26 promotes plant growth observed in chapter 4 (Sharma *et al.*, 2022). Additionally, B26 treatment altered the expression of numerous stress-related transcription factors (TFs), which are crucial for the expression of stress-responsive genes. This reflects the priming ability of B26 to combat various biotic and abiotic stresses. The robust and reliable data generated in this study provides us with a wealth of useful knowledge about the in-depth understanding of plant-PGPR interaction. This further improves our knowledge of rhizosphere biology. Our findings serve as a road map for future translational applications of PGPR in the field of sustainable agriculture.

7.2 FUTURE DIRECTIONS

The research described in this thesis can be used as a model resource to study the interaction among bacterial and plant species that have not been well characterized and studied. Following future studies will provide significant insights into plant-PGPR interaction:

- Root exudates are important for colonization and biofilm formation. Although we have confirmed that PGPR inoculation improves root exudates, our current understanding of root exudates is limited to only organic acids. Other significant compounds secreted by

roots also need to be identified. To determine the precise concentration changes in exudates upon inoculation, a quantitative analysis of root exudates will be helpful.

- Plant-PGPR communication initiate when root exudates are detected by chemoreceptors of a PGPR. Thus, systemic identification of these chemoreceptors and their corresponding ligands will further enhance our understanding of chemical intercommunication between plants and PGPR. In-depth genome analysis of B26 would be helpful to predict chemoreceptors.
- We recorded various phenological characteristics of different control and inoculated *B.distachyon* genotypes grown under controlled environmental conditions. The efficacy of B26 as a bioinoculant should also be investigated under field conditions. To test the suitability of strain B26 for use in farming practices, field experiments in various climates and locations are advised.
- Root mass was measured by CT-scanning plants grown in semi-hydroponics system. Although inert glass beads used in semi-hydroponic systems were sufficient to grow plants, they were not the ideal material for CT scanning. Growing plants in the soil will allow to examine changes in root architecture in greater detail.
- Phytohormone analysis in present study could only detect auxin, gibberellins and abscisic acid. The current protocol used in UPLC- multiple-reaction monitoring (MRM) mass spectrometry failed to detect cytokinin and ethylene. Improved protocols for the detection of cytokinin, ethylene and other important hormones jasmonic acid, salicylic acid and brassinosteroid should be identified.

- Studies on the transcriptome could be improved by taking samples on different days of post-inoculation. This will allow to find differential and temporal effect of inoculation and help to identify the best time of inoculation on a molecular basis.
- We were unable to find B26 transcriptomic reads in the inoculated Bd21-3 transcriptome. More improved protocols and in-depth sequencing techniques should be applied to simultaneously capture reads from both partners.
- Studying the effect of root exudates on the transcriptome of strain B26 would help to understand the mutualistic interactions between PGPR and plants. Transcriptomics along with metabolomics would help to identify chemicals and their expression during PGPR-plant communication.

7. APPENDIX

7.1 Supplementary Figures

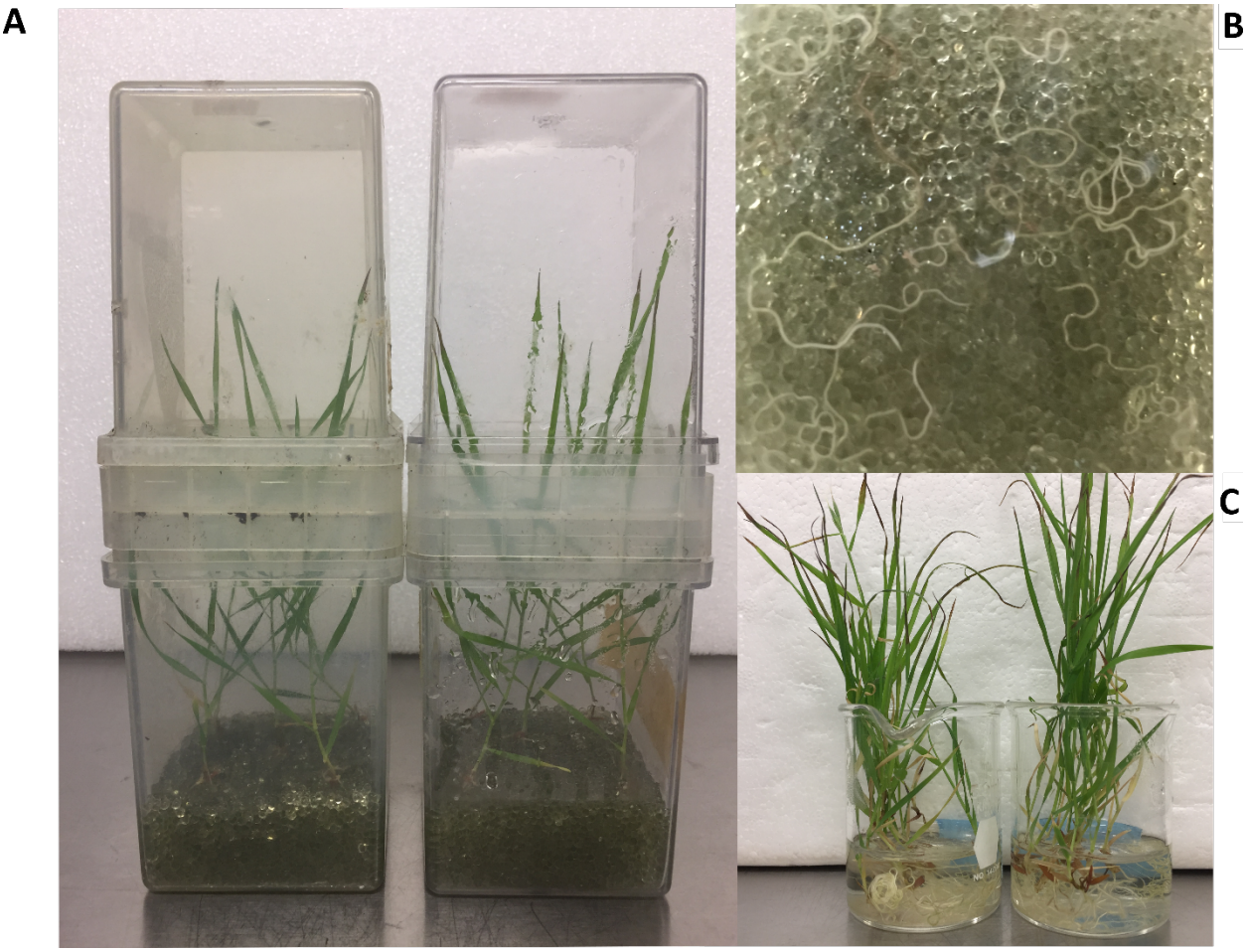

Supplementary Figure 3.1 (A) Semi-Hydroponics system in Magenta GA-7 tissue culture boxes for growing Bd21-3 under sterile conditions in glass beads saturated with 1/4th Hoagland's solution. (B) Growth of roots in magenta boxes. (C) Root exudate collection system.

.

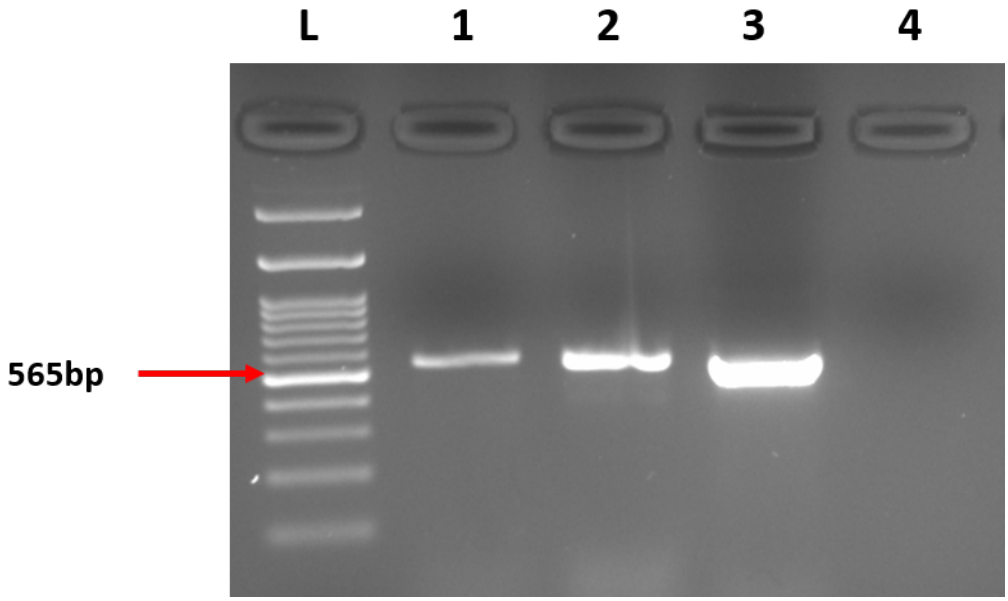

Supplementary Figure 3.2 PCR amplified products on 1% Agarose gel using specific B26 primers. L, 3Kb ladder; lane1, amplified DNA of Bd21-3 from inoculated *Brachypodium* roots before exudate collection. lane 2, amplified DNA product of Bd21-3 from inoculated *Brachypodium* roots after exudate collection. Lane 3; amplified DNA from culture of B26. Lane 4: negative control.

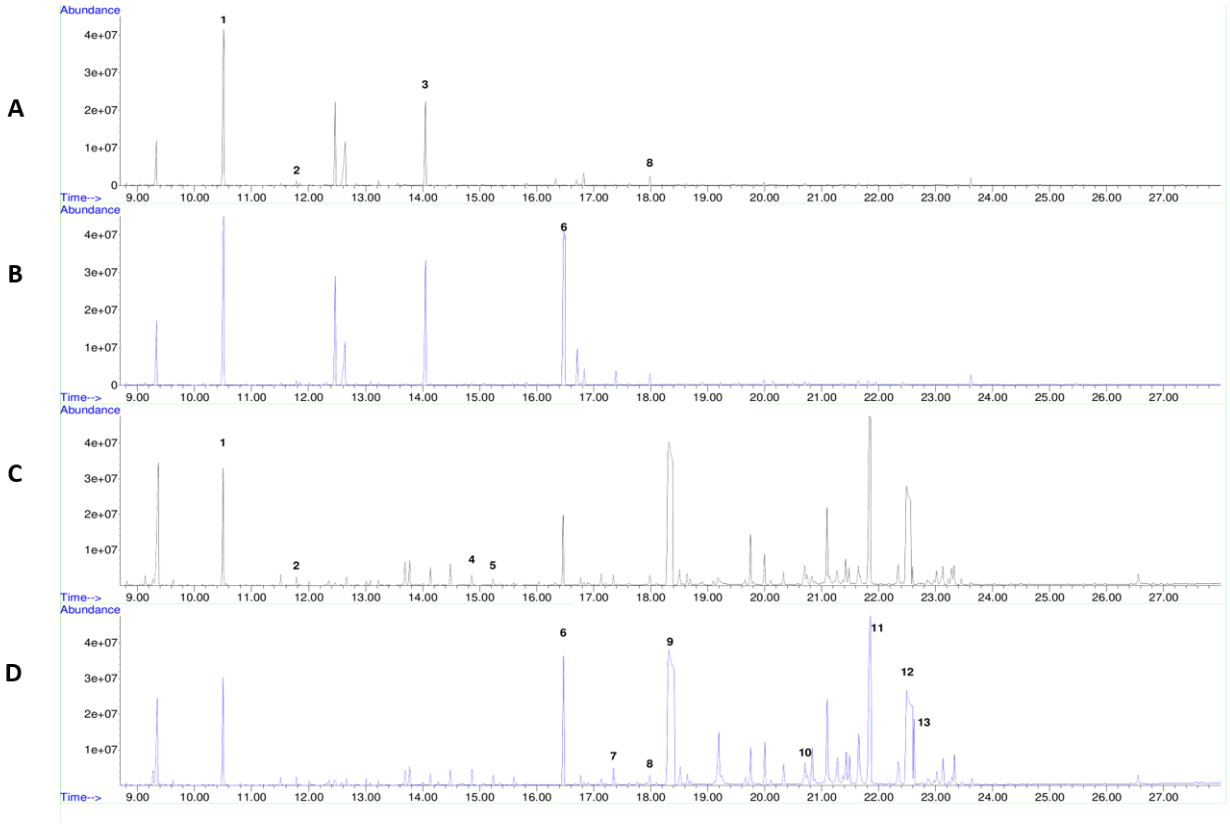

Supplementary Figure 3.3 Gas Chromatograms acquired in Scan mode for Bd21-3 samples: (A) Root Extracts Control (B) Root Extract Inoculated (C) Roots Control (D) Roots Inoculated 1 - Carbonate (always present, even in blanks) 2 - Lactic acid, 3 – Boric, 4- Succinic, 5 – Fumaric, 6- Phosphoric, 7 - 2-ketoglutaric, 8 - Myristic-d27 (Internal standard), 9 – Malic, 10 – Aconitic, 11- Dopamine, 12 –Citric, 13 – Isocitric.

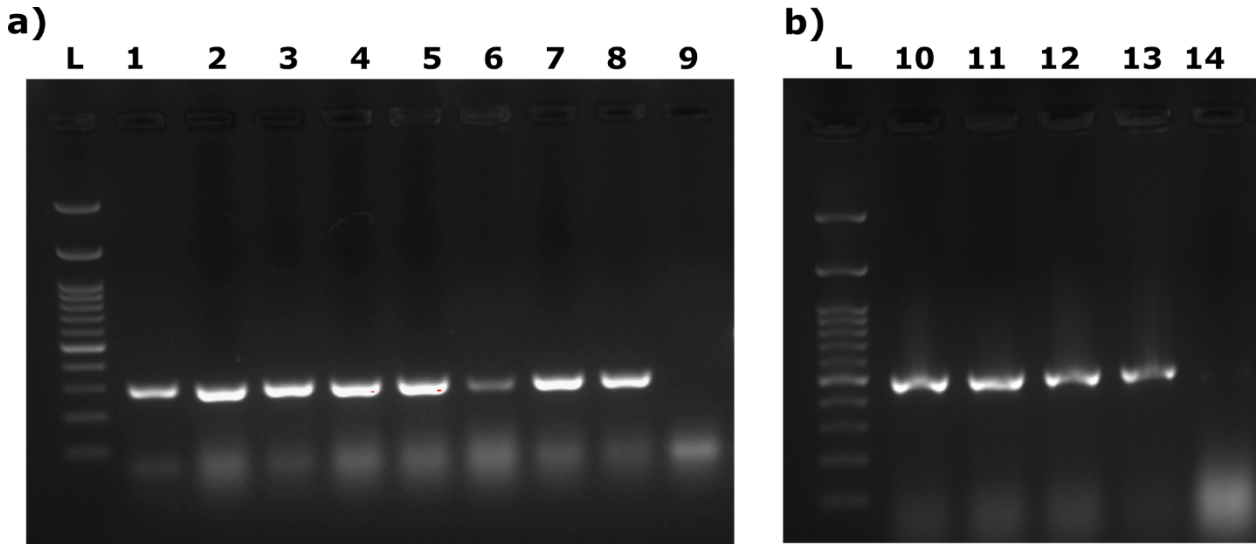

Supplementary Figure 4.1 Genotyping of flowering transgenic line a) UBI:VRN1 and b) UBI:FT1 using AcV5-R tag and gene-specific forward primer. L=100bp DNA ladder, Lane 1-8: Amplification of UBI:VRN1 DNA; Lane 10-13: Amplification of UBI:FT1 DNA; Lane 9 and 14: Bd21-3 DNA. Gel picture is complete only empty wells were cropped.

7.2 Supplementary Tables

Supplementary Table 4.1 *Brachypodium distachyon* genotypes used in this study

PI accession	Geographic origin	Growth Habitat	Vernalization Requirement	Flowering Class
Bd21	Iraq	Spring	2-3 weeks	Extremely Rapid Flowering
Bd21-3	Iraq	Spring	2-3 weeks	Rapid Flowering
Bd30-1	Spain	Spring	2-3 weeks	Intermediate Rapid Flowering
Bd18-1	Turkey	Winter	4-5 weeks	Delayed Flowering

Supplementary Table 4.2 Growth Response of *B. distachyon* accessions lines in response to *B.velezensis* strain B26 inoculation

			Growth Parameters[$]					
Time Point	**Accessions**	**Treatment**	**Plant Height(cm)**	**No. of leaves**	**No. of Tillers**	**No. of awns**	**Root Weight (g)**	**Shoot Weight (g)**
14dpi[&]		B+	11.85±1.00[a]	14.50±2.46[a]	3.60±0.29[a]	3.00±0.54[a]	0.41±0.10[a]	0.98±0.11[a]
	Bd21	B-	11.60±1.75[a]	14.60±3.48[a]	5.40±1.12[a]	1.20±0.20[b]	0.27±0.08[a]	0.28±0.07[b]
		%increase†	2.15%	-0.68%	-33.33%	**150%***	51.85%	**250%***
		B+	17.35±0.64[a]	19.00±2.51[a]	4.60±0.60[a]	2.40±0.74[a]	0.68±0.13[a]	1.48±0.11[b]
	Bd21-3	B-	16.00±1.44[a]	21.30±3.68[a]	4.90±1.05[a]	1.40±0.40[a]	0.65±0.13[a]	0.78±0.11[a]
		%increase	8.09%	-2.30%	-6.31%	71%	4.61%	**89.71%***
		B+	15.23±0.56[a]	18.00±1.43[b]	4.60±0.29[a]	0	1.53±0.30[a]	3.63±0.72[a]
	Bd18-1	B-	11.35±1.40[b]	10.10±2.17[a]	3.20±0.68[a]	0	0.73±0.14[a]	2.24±0.44[a]
		%increase	**34.18%***	**78.21%***	43.75%	NA	109.58%	62.05%
		B+	14.80±2.40[a]	9.45±0.73[a]	2.40±0.48[a]	3.50±0.97[a]	0.11±0.02[a]	0.34±0.10[a]
	Bd30	B-	12.25±0.79[a]	9.20±0.51[a]	2.80±0.20[a]	1.90±0.10[a]	0.13±0.02[a]	0.27±0.01[a]
		%increase	20.81%	2.71%	-14.28%	84.21%	-15.38%	25.92%
28dpi	**Bd21**	B+	12.37±1.34[a]	29.80±4.45[a]	4.30±0.94[a]	3.80±0.73 [a]	0.85±0.12[a]	1.62±0.18[a]
		B-	11.90±1.80[a]	21.60±3.82[a]	4.40±0.69[a]	1.40±0.40[b]	0.62±0.18[a]	0.86±0.34[a]
		%increase†	3.97%	37.96%	-2.22%	**171%***	37.09%	88.37%
		B+	20.70±1.00[a]	41.50±3.88[a]	7.10±0.55[a]	4.20±0.80[a]	1.36±0.21[a]	3.72±0.56[a]
	Bd21-3	B-	13.35±1.72[b]	19.60±4.77[a]	4.90±1.06[b]	1.80±0.20[b]	0.62±0.13[b]	1.93±0.42[b]
		%increase	**55.05%***	**111.73%***	**44.89%***	**133%***	**119.35%***	**92.74%***
		B+	18.25±1.11[a]	30.30±5.00[a]	6.20±1.04[a]	0	1.00±0.18[a]	0.65±0.07[a]
	Bd18-1	B-	16.05±2.53[a]	25.50±4.83[a]	5.90±1.10[a]	0	1.06±0.05[a]	0.62±0.06[a]
		%increase	13.70%	18.82%	5.08%	NA	-5.66%	4.83%
		B+	14.95±0.82[a]	7.80±1.03[a]	2.30±0.48[a]	3.70±0.64[a]	0.17±0.03[a]	0.65±0.07[a]
	Bd30-1	B-	13.25±0.68[a]	8.40±1.40[a]	2.00±0.20[a]	3.50±0.67[a]	0.24±0.03[a]	0.62±0.06[a]
		%increase	12.83%	-7.14%	15.00%	5.71%	-29.16%	3.22%

&, days post-inoculation

$, Growth parameters represent the average of 5 pots per treatment or 10 plants ± standard error

†, percentage increase relative to the control treatments

*, statistically significant values within a row between control and treatment at $p < 0.05$ according to Independent Student t-test

NA, Not Applicable

Supplementary Table 4.3 *Brachypodium* growth parameters of transgenic lines and wild type inoculated with strain B26

			Growth Parameters[$]						
	Accessions	**Treatment**	**Plant Height(cm)**	**No. of leaves**	**No. of Tillers**	**No. of awns**	**Root weight (g)**	**Shoot Weight (g)**	**Awn weight(g)**
14dpi[&]	**Bd21-3**	B-	16.77 ± 0.84a	9.47 ± 0.80a	2.33 ± 0.18a	1.27 ± 0.65a	0.19 ± 0.04a	0.66 ± 0.10a	0.05 ± 0.03a
		B+	19.27 ± 0.85a	10.27 ± 0.48a	2.60 ± 0.19a	2.33 ± 1.08a	0.20 ± 0.05a	0.78 ± 0.09a	0.07 ± 0.03a
		%increase†	**14.91**	**8.45**	**11.43**	**84.21**	**2.39**	**18.88**	**36.19**
	UBI:FT1	B-	18.07 ± 0.21a	7.47 ± 0.49a	2.27 ± 0.16a	3.00 ± 0.41a	0.11 ± 0.02b	0.826 ± 0.06a	0.19 ± 0.03a
		B+	18.30 ± 1.06a	7.00 ± 1.13a	2.20 ± 0.13a	3.27 ± 0.29a	0.18 ± 0.03a	0.834 ± 0.14a	0.20 ± 0.01a
		%increase	**1.29**	**-6.25**	**-2.94**	**8.89**	**57.89***	**0.97**	**3.31**
	UBI:VRN1	B-	17.10 ± 0.12a	11.47 ± 0.23a	3.80 ± 0.29a		0.33 ± 0.02a	1.40 ± 0.07a	NA
		B+	17.23 ± 0.15a	12.13 ± 0.23a	4.07 ± 0.07a		0.38 ± 0.05a	1.42 ± 0.05a	NA
		%increase	**0.78**	**5.81**	**7.02**	**NA**	**15.15**	**1.29**	**NA**
28dpi	**Bd21-3**	B-	25.20 ± 1.10b	13.47 ± 1.06a	2.40 ± 0.16a	4.53 ± 0.47b	0.12 ± 0.01b	1.15 ± 0.09a	0.51 ± 0.04b
		B+	29.40 ± 0.69a	9.93 ± 1.34a	2.07 ± 0.27a	6.07 ± 0.42a	0.78 ± 0.09a	1.64 ± 0.24a	0.72 ± 0.07a
		%increase†	**16.66***	**-26.24**	**-13.89**	**34***	**551.67***	**42.96**	**42.52***
	UBI:FT1	B-	21.77 ± 0.39a	7.73 ± 0.24a	2.13 ± 0.08a	4.73 ± 0.46 a	0.18 ± 0.06b	0.66 ± 0.21b	0.66 ± 0.09a
		B+	23.73 ± 0.85a	8.87 ± 1.07a	2.33 ± 0.21a	4.87 ± 0.54a	0.42 ± 0.08a	1.78 ± 0.12a	0.82 ± 0.10a
		%increase	**9.04**	**14.66**	**9.37**	**2.89**	**132.38***	**161.97***	**25.73**
	UBI:VRN1	B-	23.70 ± 0.40b	23.33 ± 1.22a	4.60 ± 0.24a		2.00 ± 0.25a	3.84 ± 0.14a	NA
		B+	25.32 ± 0.55a	22.73 ± 0.71a	4.00 ± 0.00b		1.97 ± 0.31a	2.44 ± 0.37b	NA
		%increase	**6.83***	**-2.57**	**-13.04***	**NA**	**-1.70**	**-36.52***	**NA**
42dpi	**Bd21-3**	B-	28.00 ± 1.69a	9.08 ± 0.98a	2.07 ± 0.07a	7.92 ± 1.06a	0.25 ± 0.15b	1.77 ± 0.05a	0.81 ± 0.03 a
		B+	28.42 ± 0.60a	10.83 ± 1.55a	2.25 ± 0.25a	8.33 ± 0.49a	0.65 ± 0.15a	2.18 ± 0.51a	1.00 ± 0.10a
		%increase†	**1.49**	**19.31**	**8.87**	**5.18**	**160***	**23.35**	**23.46**
	UBI:FT1	B-	23.00 ± 0.93a	8.75 ±1.40a	2.08 ± 0.08a	7.17 ± 0.29a	1.04 ± 0.21b	2.67 ± 0.40a	0.99 ± 0.08a
		B+	22.33 ± 0.89a	6.75 ± 0.55a	2.67 ± 0.47a	9.33 ± 1.16a	2.86 ± 0.35a	3.22 ± 0.23a	1.13 ± 0.15a
		%increase	**-2.90**	**-22.86**	**28.00**	**30.23**	**175.88***	**20.60**	**14.14**
42dpi	***UBI:VRN1***	B-	27.17 ± 0.74a	25.83 ± 1.37a	5.08 ±0.21a	12.00 ± 3.84a	1.93 ± 0.45b	3.15 ± 0.65a	0.64 ± 0.12a

	B+	27.67 ± 3.11a	25.88 ± 4.21a	4.33 ± 0.19a	10.17 ± 1.43a	2.75 ± 0.83a	3.27 ± 0.60a	0.67 ± 0.23a
	%increase	**1.84**	**0.16**	**-14.75**	**-15.28**	**42.46***	**3.73**	**-4.48**

&, days post inoculation

$, Growth parameters represent the average of 5 pots per treatment or 10 plants ± standard error

†, percentage increase relative to the control treatments

*, statistically significant values within a row between control and treatment at $p < 0.05$ according to Independent Student t-test

NA, Not Applicable

Supplementary Table 5.1 List of primers used for validation

Transcript_id/Primer	Annotation from Phytozome	Sequence (5'-3')	Source
Bd21-3.4G0038600-F	disease resistance protein RPM1 (RPM1, RPS3)	CCCTCTCTGCTCATTCTCATTC	This study
Bd21-3.4G0038600-R		GGGACAAGTCCAAGAGCTATAC	
Bd21-3.1G0537900-F	Peroxidase / Lactoperoxidase	TGCGTACGGAGATGATCAAG	
Bd21-3.1G0537900-R		GAAGCAGTCGTGGAAGAAGA	
Bd21-3.5G0359200-F	Leucine rich repeat N-terminal domain (LRRNT_2)	CGGTTTATGAGGTAGCCAAGAT	
Bd21-3.5G0359200-R		TGGTTGTTGGTCCCAGTTATT	
Bd21-3.1G0165501-F	Salt stress response/antifungal (Stress-antifung)	CGATTGCAACCGCAGATAATG	
Bd21-3.1G0165501-R		CCGCCTTCTCCAAGCTTATT	
Bd21-3.3G0148900-F	Wall-associated receptor kinase galacturonan-binding (GUB_WAK_bind)	CGACAACTGGATGAGGTTCTAC	
Bd21-3.3G0148900-R		GGAAGCTGTAGTTTCCCTTCTC	
Bd21-3.5G0042300-F	ALPHA/BETA HYDROLASE FOLD-CONTAINING PROTEIN	GTAGGAAGAAGGCCACACATAG	
Bd21-3.5G0042300-R		GCAATGTCCTCGTCAAACAAC	
Bd21-3.2G0781500-F	Shikimate O-hydroxycinnamoyltransferase	GCCATCCAGGTGACATTCTT	
Bd21-3.2G0781500-R		TCCTCACCGTCCTTGGATAA	
Bd21-3.2G0734200-F	Polygalacturonase / Pectinase	TCAAGGTCAGCGATGTGAAG	
Bd21-3.2G0734200-R		CACCATGGGACTCTGGTTATAC	
Bd21-3.4G0483700-F	Wall-associated receptor kinase galacturonan-binding (GUB_WAK_bind)	AGAGGAGGTGTTCGGGTAT	
Bd21-3.4G0483700-R		TGCTTCTCCTCCCTGATCT	
Bd21-3.4G0460100-F	SAUR family protein (SAUR)	GCCAACATGGAAAGGCTTATG	
Bd21-3.4G0460100-R		AGGGTGGTCAGGATTGATTTC	
Bd21-3.5G0275800-F	Cation transport protein (TrkH)	CCTGATCCCAGATGCAAAGA	
Bd21-3.5G0275800-R		CGAGGAACATCACCACGATAA	
Bd21-3.2G0521500-F	ALPHA/BETA HYDROLASE FOLD-CONTAINING PROTEIN	TGCCCGGAGGAGGATTAT	
Bd21-3.2G0521500-R		CCACGTACACCTTGCTCAC	
Bd21-3.2G0174500-F	GLUTATHIONE S-TRANSFERASE (GST)	AGAAGGTGCTCGACGTTTAC	
Bd21-3.2G0174500-R		CAGCAAGTGAAGGCGAAATG	
Bd21-3.4G0628500-F	P-HYDROXYBENZOIC ACID EFFLUX PUMP SUBUNIT	GAGAAGAGCGTGGCTTACAT	
Bd21-3.4G0628500-R		CTTCCTCTTCCTCAGCAGTAAC	

Bd21-3.5G0097200-F	OSMOTIC STRESS POTASSIUM TRANSPORTER	CTCTTCTCAGTCCAGCGTTTC
Bd21-3.5G0097200-R		CGAGGTTGTACATCCCAATACC

Supplementary Table 5.2 Summary of sequencing and mapping of RNA Sequencing Reads

Control Bd21-3 Roots					
	B-_R1*	**B-_R2**	**B-_R3**	**B-_R4**	**B-_R5**
Total Number of Reads	65977343	71097239	60750848	56374139	69218050
After Trimming	40582057	46540973	39444442	37749890	45303997
Mapped Reads to Plant Genome	31477666 (77.57%)	35037791 (75.28%)	30199077 (76.56%)	29128386 (77.16%)	34020501 (75.09%)
Inoculated Bd21-3 Roots					
	B+_R1	**B+_R2**	**B+_R3**	**B+_R4**	**B+_R5**
Total Number of Reads	41418637	56528001	44171236	51426726	60836063
After Trimming	26793818	38637892	28913797	33899049	39620761
Mapped Reads to Plant Genome	21018387 (78.44%)	30772159 (79.64%)	22135717 (76.56%)	25384432 (74.88%)	29687450 (74.93%)

***R1-R5: Biological replicates 1 to 5**

Supplementary Table 5.3 Output of DESeq2 with significant Differentially Expressed Genes (DEGs)

Transcript_name	log2FoldChange	pvalue	padj	Annotation_from_Phytozome
BdiBd21-3.3G0065200	-0.90531	2.41E-13	1.53E-10	4 hydroxyphenylpyruvate dioxygenase / p hydroxyphenylpyruvate oxidase
BdiBd21-3.3G0079800	-0.72116	0.002047	0.036357213	CHAPERONE PROTEIN CLPB4, MITOCHONDRIAL
BdiBd21-3.2G0631200	0.933298	0.000256	0.008051481	Glutamate carboxypeptidase II / Pteroylpoly gamma glutamate carboxypeptidase
BdiBd21-3.2G0449700	-2.46453	2.41E-06	0.000205323	OXIDOREDUCTASE, 2OG FE II OXYGENASE FAMILY PROTEIN // 1 AMINOCYCLOPROPANE 1 CARBOXYLATE OXIDASE 5
BdiBd21-3.2G0461800	1.354915	0.002501	0.042156078	Transferase family
BdiBd21-3.3G0074600	0.732482	0.000348	0.010042968	4 coumarate CoA ligase / 4 coumaryl CoA synthetase // Trans feruloyl CoA synthase / Trans feruloyl CoA synthetase
BdiBd21-3.2G0675700	-0.58794	0.000291	0.008818565	ASPARTYL PROTEASE DDI RELATED
BdiBd21-3.1G0785100	-2.67471	1.15E-28	7.31E-25	CBL INTERACTING SERINE/THREONINE PROTEIN KINASE 23
BdiBd21-3.2G0331300	-1.03392	0.000248	0.007866197	GLUTATHIONE S TRANSFERASE, GST, SUPERFAMILY, GST DOMAIN CONTAINING
BdiBd21-3.2G0336700	-1.52936	5.31E-11	1.85E-08	INOSINE URIDINE PREFERRING NUCLEOSIDE HYDROLASE FAMILY PROTEIN
BdiBd21-3.1G0897900	0.758269	1.58E-10	4.96E-08	Non specific protein tyrosine kinase / Cytoplasmic protein tyrosine kinase // Non specific serine/threonine protein kinase / Threonine specific protein kinase
BdiBd21-3.2G0237700	-0.69022	4.32E-05	0.002081049	Polygalacturonase / Pectinase
BdiBd21-3.2G0500200	-0.87899	0.000301	0.009037152	PROBABLE MEMBRANE PROTEIN DUF221 RELATED
BdiBd21-3.1G0815300	-1.83229	1.30E-05	0.000817304	SPX DOMAIN CONTAINING PROTEIN 3
BdiBd21-3.1G0571400	-0.73268	0.002049	0.036357213	Ubiquitinyl hydrolase 1 / Ubiquitin thiolesterase
BdiBd21-3.2G0521700	-2.87371	9.35E-18	2.16E-14	VACUOLAR CATION/PROTON EXCHANGER 1 RELATED
BdiBd21-3.3G0268200	0.704026	1.69E-05	0.001004573	2 HYDROXYACID DEHYDROGENASE RELATED
BdiBd21-3.5G0080500	0.757519	2.15E-05	0.00119974	ALCOHOL DEHYDROGENASE RELATED
BdiBd21-3.2G0521500	-2.19515	1.94E-28	9.86E-25	ALPHA/BETA HYDROLASE FOLD CONTAINING PROTEIN
BdiBd21-3.5G0007700	-0.7507	3.30E-11	1.25E-08	AMIDASE

BdiBd21-3.2G0725400	1.128423	3.19E-07	3.98E-05	AMINO ACID TRANSPORTER
BdiBd21-3.3G0002300	1.051819	7.96E-12	3.82E-09	AMINO ACID TRANSPORTER // TRANSMEMBRANE AMINO ACID TRANSPORTER RELATED
BdiBd21-3.2G0719800	0.586298	1.12E-10	3.62E-08	Aspartate transaminase / Transaminase A // Aspartate prephenate aminotransferase / Prephenate transaminase // Glutamate prephenate aminotransferase / Prephenate transaminase
BdiBd21-3.2G0660600	-0.6472	2.76E-15	2.83E-12	ASPARTYL PROTEASE FAMILY PROTEIN
BdiBd21-3.1G0784000	1.03787	2.65E-14	2.25E-11	BADF TYPE ATPASE DOMAIN CONTAINING PROTEIN
BdiBd21-3.3G0030500	-0.63744	3.51E-05	0.001774315	BAX INHIBITOR RELATED // BAX INHIBITOR 1
BdiBd21-3.4G0286700	2.255651	0.000907	0.020384628	Benzyl alcohol O benzoyltransferase
BdiBd21-3.2G0246100	0.816867	0.000423	0.011548555	BETA 1,3 GLUCANASE
BdiBd21-3.3G0145300	0.784665	6.75E-05	0.002885599	CALCINEURIN B LIKE PROTEIN 4
BdiBd21-3.2G0187900	1.173832	1.49E-12	8.24E-10	CCT MOTIF FAMILY PROTEIN
BdiBd21-3.1G0844650	-0.76022	0.000203	0.006711009	CGI 141 RELATED/LIPASE CONTAINING PROTEIN
BdiBd21-3.3G0344300	-1.69774	7.18E-09	1.40E-06	CHITINASE
BdiBd21-3.1G0165000	-0.95173	0.000555	0.014117286	CYSTEINE RICH SECRETORY PROTEIN RELATED
BdiBd21-3.5G0055300	1.86368	0.001149	0.023990405	Cytochrome P450
BdiBd21-3.1G0203700	0.756291	5.23E-07	5.84E-05	Cytochrome P450 CYP2 subfamily
BdiBd21-3.4G0372600	1.822187	0.001004	0.021821939	Cytochrome P450 CYP4/CYP19/CYP26 subfamilies
BdiBd21-3.5G0246300	-1.04211	0.000117	0.004424749	Cytochrome P450 CYP4/CYP19/CYP26 subfamilies
BdiBd21-3.2G0565400	-1.28244	7.83E-07	8.10E-05	CYTOCHROME P450 FAMILY MEMBER
BdiBd21-3.3G0258700	0.837312	0.001223	0.024950278	DIENELACTONE HYDROLASE
BdiBd21-3.3G0026200	-0.70492	0.00243	0.041359768	EF HAND CALCIUM BINDING DOMAIN CONTAINING PROTEIN
BdiBd21-3.2G0651101	-1.48924	1.02E-06	0.000101506	EF HAND CALCIUM BINDING DOMAIN CONTAINING PROTEIN // CALCIUM BINDING PROTEIN CML41 RELATED

BdiBd21-3.2G0128900	0.64333	3.91E-06	0.000306496	ELECTRON TRANSFER FLAVOPROTEIN UBIQUINONE OXIDOREDUCTASE
BdiBd21-3.4G0416800	0.907893	0.000149	0.00529723	ENDO 1,4 BETA GLUCANASE
BdiBd21-3.1G0007900	-2.36512	7.34E-07	7.72E-05	ethylene-responsive transcription factor 1 (ERF1)
BdiBd21-3.3G0071800	-0.68435	1.41E-06	0.000130885	EXPRESSED PROTEIN
BdiBd21-3.3G0543400	-1.15302	0.000919	0.020535141	F box domain
BdiBd21-3.3G0728700	-0.61031	0.00011	0.004195492	F BOX PROTEIN PP2 B13 RELATED
BdiBd21-3.3G0146400	-2.11657	2.31E-09	4.98E-07	GENOMIC DNA, CHROMOSOME 3, TAC CLONE:K13N2 RELATED
BdiBd21-3.2G0278000	0.580411	0.000817	0.018891786	Glucan endo 1,3 beta D glucosidase / Laminarinase
BdiBd21-3.2G0252000	-0.62923	0.001927	0.034963175	GLUCOSYL/GLUCURONOSYL TRANSFERASES
BdiBd21-3.2G0627400	-1.39758	3.40E-06	0.000273348	GLUCOSYL/GLUCURONOSYL TRANSFERASES
BdiBd21-3.3G0103300	-0.9274	4.10E-05	0.002002973	GLUCOSYL/GLUCURONOSYL TRANSFERASES
BdiBd21-3.1G0053400	1.698452	0.000516	0.013487645	GLUTATHIONE S TRANSFERASE
BdiBd21-3.2G0450600	0.699195	0.000493	0.013080238	GLUTATHIONE S TRANSFERASE, GST, SUPERFAMILY, GST DOMAIN CONTAINING
BdiBd21-3.2G0779900	-0.98923	2.37E-05	0.001292007	GLUTATHIONE S TRANSFERASE, GST, SUPERFAMILY, GST DOMAIN CONTAINING
BdiBd21-3.2G0457100	-0.69365	0.000123	0.004586969	GLYCOSYLTRANSFERASE
BdiBd21-3.3G0280400	-1.20481	0.00085	0.019457416	GLYCOSYLTRANSFERASE
BdiBd21-3.1G0163800	0.906187	3.69E-05	0.001844405	GLYCOSYLTRANSFERASE FAMILY PROTEIN 47
BdiBd21-3.5G0248800	0.734857	7.67E-12	3.76E-09	HISTONE H1/H5
BdiBd21-3.1G0131000	0.651505	6.52E-08	1.03E-05	HOMEOBOX PROTEIN TRANSCRIPTION FACTORS
BdiBd21-3.1G0773000	0.583875	0.000118	0.004449906	HOMEOBOX PROTEIN TRANSCRIPTION FACTORS
BdiBd21-3.3G0342500	0.647242	0.000932	0.020789851	HOMEOBOX PROTEIN TRANSCRIPTION FACTORS // BEL1 LIKE HOMEODOMAIN PROTEIN 6 RELATED
BdiBd21-3.1G0291700	-1.45017	0.000419	0.011456837	hydroxyphenylacetaldehyde oxime monooxygenase

BdiBd21-3.1G0702500	0.747733	0.000801	0.018657217	INHIBITOR OF APOPTOSIS
BdiBd21-3.4G0433000	1.359786	9.62E-06	0.000644382	IONOTROPIC GLUTAMATE RECEPTOR
BdiBd21-3.3G0317000	-0.73125	0.000855	0.019518151	Isoflavone 7 O beta glucoside 6" O malonyltransferase / Flavone/flavonol 7 O beta D glucoside malonyltransferase
BdiBd21-3.1G0938900	1.308495	1.28E-10	4.06E-08	KETOACYL COA SYNTHASE 5 RELATED
BdiBd21-3.2G0725200	-1.14631	3.29E-06	0.000264839	LEUCINE RICH RECEPTOR LIKE PROTEIN KINASE
BdiBd21-3.1G0581400	1.385123	7.34E-08	1.12E-05	LEUCINE RICH REPEAT CONTAINING PROTEIN
BdiBd21-3.1G0716400	1.803571	0.001031	0.022263987	LEUCINE RICH REPEAT CONTAINING PROTEIN
BdiBd21-3.2G0494800	1.041931	1.98E-05	0.001140306	LEUCINE RICH REPEAT CONTAINING PROTEIN
BdiBd21-3.3G0048700	1.203913	0.001258	0.02548366	LEUCINE RICH REPEAT CONTAINING PROTEIN
BdiBd21-3.4G0466800	0.604941	1.58E-05	0.000953184	LEUCINE RICH REPEAT CONTAINING PROTEIN
BdiBd21-3.5G0041200	1.103593	3.13E-05	0.001626566	LEUCINE RICH REPEAT CONTAINING PROTEIN
BdiBd21-3.2G0593801	1.175282	0.002814	0.045504	LUNG SEVEN TRANSMEMBRANE RECEPTOR
BdiBd21-3.3G0796100	-0.81831	0.000767	0.018066413	METALLO BETA LACTAMASE FAMILY PROTEIN
BdiBd21-3.5G0081400	-1.09542	7.39E-05	0.003097689	MULTIDRUG RESISTANCE PROTEIN
BdiBd21-3.1G0210000	1.176558	4.56E-07	5.25E-05	MULTIDRUG RESISTANCE PROTEIN // MATE EFFLUX FAMILY PROTEIN
BdiBd21-3.1G0568300	-0.76604	1.22E-07	1.73E-05	Myb like DNA binding domain
BdiBd21-3.2G0803300	0.61633	0.001297	0.026110591	MYB LIKE DNA BINDING PROTEIN MYB
BdiBd21-3.4G0476100	0.918628	7.51E-07	7.83E-05	NAC DOMAIN CONTAINING PROTEIN 38
BdiBd21-3.1G0514600	0.698973	3.45E-05	0.001758429	NAC DOMAIN CONTAINING PROTEIN 75 RELATED
BdiBd21-3.2G0732900	-0.83448	1.31E-06	0.000123426	NAD(P)H dehydrogenase (quinone) / Vitamin-K reductase // NADH:ubiquinone reductase (H(+)-translocating) / Ubiquinone reductase
BdiBd21-3.2G0711900	0.915244	1.81E-08	3.24E-06	NADPH OXIDASE // RESPIRATORY BURST OXIDASE HOMOLOG PROTEIN A RELATED
BdiBd21-3.1G0398600	1.628398	1.84E-10	5.65E-08	No apical meristem

BdiBd21-3.5G0201600	-2.42458	2.89E-06	0.000236979	No apical meristem
BdiBd21-3.5G0288200	1.051481	0.000429	0.011682441	No apical meristem
BdiBd21-3.4G0221200	-0.94997	5.43E-05	0.00245568	Non specific serine/threonine protein kinase / Threonine specific protein kinase
BdiBd21-3.2G0720200	0.947241	1.98E-09	4.35E-07	OLIGOPEPTIDE TRANSPORTER RELATED
BdiBd21-3.3G0370200	1.100103	1.82E-11	7.58E-09	OLIGOPEPTIDE TRANSPORTER RELATED // PROTEIN NRT1/ PTR FAMILY 5.2 RELATED
BdiBd21-3.1G0137800	-1.24463	0.000203	0.006711009	O-METHYLTRANSFERASE
BdiBd21-3.3G0567800	4.726509	1.28E-34	3.25E-30	OXIDOREDUCTASE, 2OG FE II OXYGENASE FAMILY PROTEIN // 1 AMINOCYCLOPROPANE 1 CARBOXYLATE OXIDASE RELATED
BdiBd21-3.1G0537900	2.762235	0.001135	0.023838883	Peroxidase / Lactoperoxidase
BdiBd21-3.2G0176200	2.855369	0.001392	0.027549167	Peroxidase / Lactoperoxidase
BdiBd21-3.2G0587100	-0.66048	2.57E-06	0.000216555	Persulfide dioxygenase / Sulfur oxygenase
BdiBd21-3.2G0043000	0.648855	1.53E-05	0.00093095	PHOSPHATIDYLINOSITOL N ACETYLGLUCOSAMINYLTRANSFERASE SUBUNIT P DOWN SYNDROME CRITICAL REGION PROTEIN 5 RELATED // PROTEIN TRM32
BdiBd21-3.3G0123800	-0.91845	1.23E-08	2.26E-06	PHOSPHOENOLPYRUVATE CARBOXYLASE
BdiBd21-3.2G0613800	0.671107	2.09E-05	0.001178095	PHOSPHOLIPASE A1 IIDELTA
BdiBd21-3.1G0859100	-0.63669	0.000211	0.006906857	PHOSPHOLIPID TRANSPORTING ATPASE 1
BdiBd21-3.5G0252700	-0.73325	0.000513	0.013457276	PPR repeat
BdiBd21-3.3G0082800	-1.43643	1.99E-06	0.000173943	Premnaspirodiene oxygenase / Hyoscymus muticus premnaspirodiene oxygenase
BdiBd21-3.1G0571200	1.572382	4.05E-15	3.97E-12	Protein kinase domain
BdiBd21-3.1G0774200	0.895322	0.000135	0.004957369	Protein kinase domain
BdiBd21-3.1G0775100	0.875537	0.000378	0.010684268	Protein kinase domain
BdiBd21-3.1G0775450	1.088213	5.05E-06	0.000375366	Protein kinase domain
BdiBd21-3.3G0059300	1.773943	5.33E-06	0.000390649	Protein kinase domain Pkinase) // Wall associated receptor kinase galacturonan binding

BdiBd21-3.1G0897800	0.885975	2.81E-05	0.001492882	PROTEIN PHOSPHATASE 2C
BdiBd21-3.1G0169700	-0.75926	5.15E-05	0.002355381	PROTEIN RELATED
BdiBd21-3.2G0496300	3.072191	8.10E-11	2.71E-08	Protein tyrosine kinase (Pkinase_Tyr) // Carbohydrate binding protein of the ER)
BdiBd21-3.3G0202750	1.258346	3.96E-05	0.001955401	REVERSE TRANSCRIPTASES
BdiBd21-3.4G0361700	1.64556	7.41E-06	0.000519226	RING FINGER DOMAIN CONTAINING // RING H2 FINGER PROTEIN ATL45 RELATED
BdiBd21-3.1G0963800	0.960843	0.002563	0.042824217	RNA BINDING PROTEIN PUMILIO RELATED
BdiBd21-3.3G0124300	-0.7187	1.22E-11	5.52E-09	RNA recognition motif
BdiBd21-3.2G0179701	1.346767	0.000199	0.006663278	S locus glycoprotein domain
BdiBd21-3.2G0561100	-2.41026	1.31E-11	5.75E-09	S TYPE ANION CHANNEL SLAH2 RELATED
BdiBd21-3.1G0334700	-0.75094	1.05E-05	0.000686379	Salt stress response/antifungal
BdiBd21-3.2G0172100	-0.68924	0.00022	0.007108234	Salt stress response/antifungal
BdiBd21-3.1G0863700	-0.99808	1.12E-13	7.72E-11	SERINE/THREONINE KINASE
BdiBd21-3.1G1023500	-1.17006	0.00039	0.010911205	SERINE/THREONINE PROTEIN KINASE // CBL INTERACTING SERINE/THREONINE PROTEIN KINASE 9
BdiBd21-3.1G0304200	-0.65671	0.001552	0.029861756	SERINE/THREONINE PROTEIN KINASE WNK11 RELATED
BdiBd21-3.3G0666700	-0.99884	0.000973	0.021389294	SWI/SNF RELATED MATRIX ASSOCIATED ACTIN DEPENDENT REGULATOR OF CHROMATIN SUBFAMILY RELATED // WD 40 REPEAT CONTAINING PROTEIN
BdiBd21-3.2G0706800	-1.14248	0.000591	0.014899044	Transferase family
BdiBd21-3.1G0857800	1.68476	1.43E-08	2.59E-06	TRANSMEMBRANE EMP24 DOMAIN CONTAINING PROTEIN
BdiBd21-3.1G0410000	1.039186	0.001655	0.031293588	Very long chain 3 oxoacyl CoA synthase / Very long chain beta ketoacyl CoA synthase
BdiBd21-3.2G0271500	-1.43749	9.90E-12	4.67E-09	VOLTAGE AND LIGAND GATED POTASSIUM CHANNEL
BdiBd21-3.1G0868100	1.018654	2.99E-05	0.001561765	ZINC FINGER FYVE DOMAIN CONTAINING PROTEIN
BdiBd21-3.3G0548600	-0.65111	8.98E-06	0.000607769	ZINC FINGER PROTEIN CONSTANS LIKE 14 RELATED

BdiBd21-3.3G0214600	2.972484	0.000919	0.020535141	beta-bisabolene synthase // (S)-beta-macrocarpene synthase
BdiBd21-3.2G0733300	2.679843	8.36E-13	4.73E-10	//PF00954//PF01453//PF08276 Protein kinase domain
BdiBd21-3.2G0687700	-1.19641	5.14E-06	0.000378915	0//PTHR22950:SF323 AMINO ACID TRANSPORTER
BdiBd21-3.2G0701800	-0.75921	0.000111	0.00423117	0:SF204 REGULATOR OF CHROMOSOME CONDENSATION REPEAT CONTAINING PROTEIN
BdiBd21-3.2G0087400	-0.85937	0.000421	0.011498091	-
BdiBd21-3.1G0729500	1.882695	0.000181	0.006220601	1 deoxy D xylulose 5 phosphate synthase / DXP synthase
BdiBd21-3.4G0004200	-0.6063	0.00047	0.012578877	1,4 dihydroxy 2 naphthoyl CoA hydrolase
BdiBd21-3.1G0079000	-1.39978	1.62E-09	3.74E-07	12 oxophytodienoic acid reductase
BdiBd21-3.2G0422400	-1.45324	4.26E-05	0.00206735	2//PTHR33102:SF12 FAMILY NOT NAMED // DVL10
BdiBd21-3.3G0475000	-0.59252	3.49E-07	4.27E-05	3 methylcrotonyl CoA carboxylase beta subunit
BdiBd21-3.1G0425100	-0.74198	3.46E-06	0.00027683	(6-4)DNA photolyase / DNA photolyase // Deoxyribodipyrimidine photo-lyase / Photoreactivating enzyme
BdiBd21-3.1G0644150	-1.24875	5.01E-05	0.002322101	3//PTHR24223:SF192 FAMILY NOT NAMED // ABC TRANSPORTER C FAMILY MEMBER 10
BdiBd21-3.3G0263300	1.533049	2.52E-09	5.38E-07	4 coumarate CoA ligase / 4 coumaryl CoA synthetase
BdiBd21-3.4G0045400	0.747465	0.000782	0.018307997	4' methoxyisoflavone 2' hydroxylase / Isoflavone 2' monooxygenase
BdiBd21-3.4G0333500	-1.04901	0.001071	0.022931951	4,4 dimethyl 9beta,19 cyclopropylsterol 4alpha methyl oxidase
BdiBd21-3.1G0176900	1.130342	2.68E-11	1.03E-08	5 methyltetrahydropteroyltriglutamate homocysteine S methyltransferase / Tetrahydropteroylglutamate homocysteine transmethylase
BdiBd21-3.2G0735850	0.65049	1.79E-05	0.001053383	5//PTHR23155:SF537 LEUCINE RICH REPEAT CONTAINING PROTEIN
BdiBd21-3.2G0753300	0.601918	1.45E-07	1.99E-05	5//PTHR33385:SF4 FAMILY NOT NAMED // PROTEIN XRI1
BdiBd21-3.2G0775700	1.057983	3.81E-05	0.00189616	5:SF32 F16F4.7 PROTEIN RELATED
BdiBd21-3.2G0456500	1.089141	0.001845	0.033909815	UDP GLYCOSYLTRANSFERASE 90A1 RELATED
BdiBd21-3.5G0254400	0.908841	2.19E-11	8.98E-09	L TYPE LECTIN DOMAIN CONTAINING RECEPTOR KINASE S.5 RELATED
BdiBd21-3.2G0685800	0.94778	1.69E-05	0.001004835	9 Ring finger domain

BdiBd21-3.1G0916900	0.741129	0.001525	0.029475526	PTHR31029:SF4 - F5O11.6
BdiBd21-3.2G0704400	0.832474	0.000216	0.007012281	9:SF9 LACCASE 7 RELATED
BdiBd21-3.2G0791200	-0.97378	0.003078	0.048336738	ABA/WDS induced protein
BdiBd21-3.2G0414100	0.82486	0.000143	0.005131714	ABC TRANSPORTER C FAMILY MEMBER 8
BdiBd21-3.2G0688900	0.800324	5.76E-05	0.00255319	abscisic acid receptor PYR/PYL family
BdiBd21-3.4G0050000	-0.60011	2.02E-06	0.000175243	ACID PHOSPHATASE RELATED
BdiBd21-3.4G0132200	-0.64327	0.001999	0.035816292	ACIDIC ENDOCHITINASE
BdiBd21-3.1G0282800	0.727194	8.18E-06	0.000562648	Acylglycerol lipase / Monoacylglycerol lipase // Triacylglycerol lipase / Triglyceride lipase
BdiBd21-3.2G0390900	1.306759	2.69E-17	4.99E-14	ADENINE/GUANINE PERMEASE AZG1
BdiBd21-3.3G0321400	-1.78998	2.54E-05	0.001377382	Agmatine N
BdiBd21-3.5G0073600	-0.71235	1.17E-06	0.000113444	ALCOHOL DEHYDROGENASE RELATED
BdiBd21-3.5G0276800	1.459378	6.55E-14	4.95E-11	Alcohol O acetyltransferase / AATASE
BdiBd21-3.3G0639132	-0.60611	0.001595	0.030490986	ALDO/KETO REDUCTASE
BdiBd21-3.5G0138400	0.682389	0.000645	0.015926016	Allene oxide cyclase
BdiBd21-3.4G0148400	-1.06806	0.000304	0.009091848	ALPHA/BETA HYDROLASE FOLD CONTAINING PROTEIN
BdiBd21-3.3G0342900	0.62092	0.002052	0.036357213	AMINO ACID TRANSPORTER
BdiBd21-3.2G0709300	0.845824	1.49E-06	0.000136361	AMINO ACID TRANSPORTER // GABA TRANSPORTER 1
BdiBd21-3.3G0604000	0.976415	0.000615	0.015412737	AMMONIUM TRANSPORTER
BdiBd21-3.3G0490300	2.442665	3.67E-10	1.00E-07	ANCIENT UBIQUITOUS PROTEIN
BdiBd21-3.5G0043700	0.86207	0.000769	0.018104665	Ankyrin repeats
BdiBd21-3.4G0430200	0.758439	0.000519	0.013549999	AP2 like factor, ANT lineage
BdiBd21-3.2G0400800	0.715091	0.000188	0.006391132	AQUAPORIN TRANSPORTER

BdiBd21-3.4G0509700	0.66472	0.001822	0.033557512	AQUAPORIN TRANSPORTER
BdiBd21-3.5G0207900	-0.63451	6.34E-05	0.002762796	AQUAPORIN TRANSPORTER
BdiBd21-3.1G0380500	-0.6765	0.001388	0.027503363	AQUAPORIN TRANSPORTER // AQUAPORIN PIP2 4 RELATED
BdiBd21-3.3G0196500	-0.6963	0.000593	0.014935606	Aromatic L amino acid decarboxylase / Tryptophan decarboxylase
BdiBd21-3.1G0882800	-0.75367	1.53E-05	0.000930968	ASPARAGINE SYNTHETASE
BdiBd21-3.2G0025900	-1.29369	2.46E-16	3.48E-13	ASPARTYL PROTEASES
BdiBd21-3.2G0263900	-0.88078	2.93E-06	0.000239815	ASPARTYL PROTEASES
BdiBd21-3.3G0709200	0.932802	3.53E-06	0.000281317	ASPARTYL PROTEASES
BdiBd21-3.2G0341600	-0.89207	0.00109	0.023154063	ASPARTYL PROTEASES // EUKARYOTIC ASPARTYL PROTEASE FAMILY PROTEIN
BdiBd21-3.3G0737500	0.824442	2.85E-05	0.001506668	AT HOOK MOTIF NUCLEAR LOCALIZED PROTEIN 19 RELATED
BdiBd21-3.1G0516300	0.584344	9.37E-05	0.003707381	ATP BINDING CASSETTE TRANSPORTER
BdiBd21-3.2G0133100	0.920293	3.36E-05	0.001718955	ATP BINDING CASSETTE TRANSPORTER
BdiBd21-3.5G0173600	1.951867	4.14E-06	0.00032216	ATP binding cassette, subfamily B
BdiBd21-3.1G0247200	2.214634	0.001417	0.027978361	ATP dependent RNA helicase DDX47/RRP3
BdiBd21-3.3G0435400	0.628057	0.002962	0.047033084	Auxin canalisation
BdiBd21-3.2G0254800	0.781257	0.000262	0.008200212	auxin responsive protein IAA
BdiBd21-3.1G0419300	-0.64343	0.000353	0.010122725	B box zinc finger
BdiBd21-3.3G0221700	1.206904	0.000513	0.013457276	B3 DNA binding domain
BdiBd21-3.1G0161200	-0.93589	0.001317	0.026411159	BAG domain
BdiBd21-3.3G0132400	-0.65965	6.25E-07	6.80E-05	BAG FAMILY MOLECULAR CHAPERONE REGULATOR 6
BdiBd21-3.3G0464500	-0.60728	1.65E-09	3.76E-07	BAND 7 PROTEIN RELATED
BdiBd21-3.1G0694500	-2.69422	2.70E-09	5.68E-07	Beta fructofuranosidase

BdiBd21-3.5G0221300	-0.93603	0.000249	0.007901855	beta fructofuranosidase
BdiBd21-3.2G0737400	0.631006	6.61E-10	1.68E-07	beta glucosidase
BdiBd21-3.1G0045900	-1.26765	0.000179	0.006194178	Bowman Birk serine protease inhibitor family
BdiBd21-3.1G0049800	-0.81978	0.001731	0.0322974	C2H2 type zinc finger
BdiBd21-3.2G0697000	-1.23898	3.98E-05	0.001959432	C2H2 type zinc finger
BdiBd21-3.1G0002200	1.116362	1.31E-07	1.83E-05	Ca2+-independent phospholipase A2
BdiBd21-3.3G0305000	-0.85315	0.002869	0.046122298	Calmodulin binding protein like
BdiBd21-3.2G0155900	-0.60258	3.35E-08	5.61E-06	cAMP regulated phosphoprotein/endosulfine conserved region
BdiBd21-3.1G0871100	0.756538	0.002301	0.039676683	CAMP RESPONSE ELEMENT BINDING PROTEIN RELATED
BdiBd21-3.4G0509400	0.728127	0.000757	0.017895529	CAMP RESPONSE ELEMENT BINDING PROTEIN RELATED
BdiBd21-3.4G0054001	2.820264	7.12E-09	1.39E-06	Carbohydrate binding protein of the ER
BdiBd21-3.1G0759800	0.731103	7.80E-09	1.50E-06	CARBOXYLESTERASE 15 RELATED
BdiBd21-3.4G0601500	-0.85657	0.000983	0.021524988	Carboxynorspermidine synthase / Carboxyspermidine dehydrogenase
BdiBd21-3.5G0275900	-7.76351	2.20E-29	1.86E-25	Cation transport protein
BdiBd21-3.4G0017400	-0.72318	0.001167	0.024147608	CATION/H(+) ANTIPORTER 19
BdiBd21-3.3G0264400	-0.9924	1.03E-05	0.000680405	CCT motif
BdiBd21-3.4G0335301	-1.18198	4.25E-05	0.002063645	CELL DIVISION PROTEIN KINASE
BdiBd21-3.4G0485400	0.631706	3.86E-11	1.43E-08	CENTAURIN/ARF // ADP RIBOSYLATION FACTOR GTPASE ACTIVATING PROTEIN AGD3
BdiBd21-3.5G0361500	-1.73082	5.20E-10	1.38E-07	CHAPERONIN
BdiBd21-3.1G0060700	-0.60838	0.000108	0.004138816	CHAPERONIN LIKE RBCX PROTEIN
BdiBd21-3.3G0344500	-1.04505	0.000765	0.018046016	CHITINASE
BdiBd21-3.3G0281000	-0.60151	3.64E-05	0.001833353	CHLORIDE CHANNEL

BdiBd21-3.2G0245900	0.735177	0.000612	0.015349397	Choline kinase
BdiBd21-3.3G0084500	0.869884	1.61E-05	0.000968267	CINNAMYL ALCOHOL DEHYDROGENASE 4 RELATED
BdiBd21-3.1G0100900	-1.08043	4.41E-15	4.16E-12	COLD REGULATED 413 PLASMA MEMBRANE PROTEIN 1 RELATED
BdiBd21-3.1G0972800	0.680469	0.002411	0.041093804	COLD REGULATED PROTEIN 27
BdiBd21-3.2G0116000	0.781184	4.72E-06	0.000356621	COPPER TRANSPORT PROTEIN ATOX1 RELATED
BdiBd21-3.3G0355700	-0.62268	0.001881	0.034328985	COPPER TRANSPORT PROTEIN ATOX1 RELATED
BdiBd21-3.2G0079600	-0.88823	3.09E-08	5.29E-06	Cotton fibre expressed protein
BdiBd21-3.4G0016700	1.135632	0.000825	0.01899321	Cotton fibre expressed protein
BdiBd21-3.4G0509000	1.79006	0.001345	0.026865319	Cotton fibre expressed protein
BdiBd21-3.3G0714300	-1.25322	4.53E-06	0.000345863	COUMAROYL COA:ANTHOCYANIDIN 3 O GLUCOSIDE 6" O COUMAROYLTRANSFERASE 1 RELATED
BdiBd21-3.3G0254300	2.921826	1.10E-17	2.33E-14	Cupin
BdiBd21-3.3G0203000	1.71371	0.00034	0.009913642	Cupin domain
BdiBd21-3.3G0203200	1.151075	0.001142	0.023887292	Cupin domain
BdiBd21-3.3G0235300	3.335991	9.93E-07	9.99E-05	Cupin domain
BdiBd21-3.5G0287200	-0.76095	0.001774	0.032915392	Cupin domain
BdiBd21-3.4G0114900	0.85962	0.001336	0.026738762	cyclin D3, plant
BdiBd21-3.3G0043500	-1.58851	4.66E-08	7.60E-06	CYCLOARTENOL SYNTHASE
BdiBd21-3.2G0490600	-1.56626	7.45E-07	7.80E-05	Cys rich Gliadin N terminal
BdiBd21-3.1G0665101	1.812649	2.29E-05	0.001262973	CYSTEINE RICH REPEAT SECRETORY PROTEIN
BdiBd21-3.5G0262800	1.142708	0.001035	0.02232018	CYSTEINE TYPE PEPTIDASE
BdiBd21-3.2G0614500	-0.59322	7.10E-07	7.50E-05	Cytidine deaminase / Cytosine nucleoside deaminase
BdiBd21-3.5G0244800	-1.09322	0.000353	0.010122725	Cytochrome P450 CYP4/CYP19/CYP26 subfamilies

BdiBd21-3.2G0061200	0.825321	0.002709	0.044470175	CYTOCHROME P450 FAMILY MEMBER
BdiBd21-3.4G0614200	0.638123	1.49E-05	0.000911611	CYTOCHROME P450 FAMILY MEMBER
BdiBd21-3.1G0034300	2.030336	0.002369	0.04046279	cytochrome P450, family 26, subfamily A
BdiBd21-3.3G0497100	0.759592	0.000394	0.010974394	cytokinin dehydrogenase
BdiBd21-3.3G0250100	0.926092	6.60E-06	0.000468106	D arabinono 1,4 lactone oxidase / D arabinono gamma lactone oxidase // L gulonolactone oxidase / L gulono gamma lactone oxidase
BdiBd21-3.5G0201500	-0.64112	2.89E-08	5.03E-06	dCTP diphosphatase / Deoxycytidine triphosphatase
BdiBd21-3.1G0823800	-0.69749	3.00E-09	6.20E-07	DENTIN SIALOPHOSPHOPROTEIN LIKE PROTEIN
BdiBd21-3.2G0159000	-0.62969	4.57E-06	0.000347846	Dihydrolipoyllysine residue
BdiBd21-3.5G0052200	1.450662	0.000999	0.021784745	DIMETHYLANILINE MONOOXYGENASE
BdiBd21-3.4G0038600	3.140999	0.000774	0.018177057	disease resistance protein RPM1
BdiBd21-3.1G0414000	0.80696	0.00089	0.020092625	DNA 3 methyladenine glycosylase I / DNA 3 methyladenine glycosidase I
BdiBd21-3.3G0409600	-1.07959	0.001298	0.026110591	DNA directed RNA polymerase subunit beta
BdiBd21-3.1G0074600	-1.04188	0.001154	0.024063508	DNA directed RNA polymerase subunit beta'
BdiBd21-3.2G0345600	0.80317	0.000105	0.004050886	DnaJ domain
BdiBd21-3.3G0493900	0.797825	0.001043	0.022441683	DnaJ domain
BdiBd21-3.3G0560400	-1.04607	3.99E-05	0.001960743	DnaJ domain
BdiBd21-3.2G0218100	-0.83425	8.19E-05	0.003358252	DNAJ HOMOLOG SUBFAMILY C MEMBER
BdiBd21-3.5G0345400	-0.62629	0.000516	0.013487645	Dof domain, zinc finger
BdiBd21-3.3G0697800	-0.72413	0.000753	0.017878907	dolichyldiphosphatase
BdiBd21-3.1G0473200	1.113629	1.46E-05	0.000900365	Domain of unknown function
BdiBd21-3.2G0200500	-0.88424	2.26E-11	9.10E-09	Domain of unknown function
BdiBd21-3.2G0294500	-0.6435	0.002107	0.036959401	Domain of unknown function

BdiBd21-3.4G0540800	1.174441	0.00082	0.018922131	Domain of unknown function
BdiBd21-3.5G0166700	0.781852	0.000169	0.00590687	Domain of unknown function
BdiBd21-3.2G0336300	0.879949	5.02E-05	0.002322101	EamA like transporter family
BdiBd21-3.4G0431500	-1.11669	1.08E-09	2.65E-07	EamA like transporter family
BdiBd21-3.4G0623400	-1.92373	1.14E-06	0.000111444	EF hand (EF-hand_5) // EF-hand domain pair (EF-hand_8)
BdiBd21-3.3G0051600	0.702703	0.001432	0.028233986	ENDO 1,4 BETA GLUCANASE
BdiBd21-3.5G0279900	0.807158	8.55E-05	0.003452238	ent-kaurene synthase (E4.2.3.19)
BdiBd21-3.3G0620300	-2.45244	2.04E-07	2.72E-05	ethylene insensitive protein 3
BdiBd21-3.1G0353600	0.672581	0.000169	0.00590687	EXORDIUM LIKE 7
BdiBd21-3.5G0098900	-0.65577	0.00019	0.006465863	EXOSTOSIN HEPARAN SULFATE GLYCOSYLTRANSFERASE RELATED
BdiBd21-3.2G0727500	-0.79814	2.33E-08	4.12E-06	F box and leucine rich repeat protein 1
BdiBd21-3.5G0173400	-1.10286	2.63E-06	0.000221172	F BOX AND WD40 DOMAIN PROTEIN // F21J9.19
BdiBd21-3.1G1034500	-0.66048	4.59E-06	0.000347846	F box domain
BdiBd21-3.3G0233300	0.633203	0.000282	0.008599216	F box domain
BdiBd21-3.4G0017200	-0.6991	0.002408	0.041093804	F box domain
BdiBd21-3.3G0202500	0.733705	0.000381	0.010746916	F box like
BdiBd21-3.1G1036000	3.103804	0.000739	0.017712577	ferulate 5 hydroxylase
BdiBd21-3.3G0401900	1.577343	5.36E-15	4.87E-12	ferulate 5 hydroxylase
BdiBd21-3.5G0074300	-0.84382	7.42E-11	2.52E-08	FK506 binding protein 4/5
BdiBd21-3.1G1044300	0.839498	8.95E-05	0.00358092	FLAVIN CONTAINING MONOOXYGENASE FMO GS OX LIKE 1 RELATED
BdiBd21-3.3G0300600	1.105368	0.000185	0.006319991	Flavin reductase
BdiBd21-3.4G0238700	0.818502	0.00114	0.023858697	flavonoid 3' monooxygenase

BdiBd21-3.2G0650400	0.775991	3.01E-05	0.001571134	Formamidase / Formamide amidohydrolase
BdiBd21-3.4G0200000	0.747552	0.000878	0.019896153	Galactolipase
BdiBd21-3.3G0454251	0.874629	3.15E-08	5.34E-06	GAMMA IRRADIATION AND MITOMYCIN C INDUCED 1
BdiBd21-3.1G0300500	1.059921	4.53E-05	0.002152721	GDSL ESTERASE/LIPASE CPRD49
BdiBd21-3.4G0102600	-1.11615	0.00212	0.03715533	GEM LIKE PROTEIN 5
BdiBd21-3.3G0596100	-0.99223	0.002156	0.037679077	Glucan endo 1,3 beta D glucosidase / Laminarinase
BdiBd21-3.5G0113500	-0.62234	6.13E-05	0.002679543	Glucan endo 1,3 beta D glucosidase / Laminarinase
BdiBd21-3.1G0357600	-0.8369	9.47E-05	0.003741225	GLUCOSYL/GLUCURONOSYL TRANSFERASES
BdiBd21-3.1G0711100	0.902566	1.42E-05	0.000879252	GLUCOSYL/GLUCURONOSYL TRANSFERASES
BdiBd21-3.2G0627900	0.620241	0.001213	0.024797166	GLUCOSYL/GLUCURONOSYL TRANSFERASES
BdiBd21-3.3G0214000	-0.79874	0.000129	0.004775627	GLUCOSYL/GLUCURONOSYL TRANSFERASES
BdiBd21-3.5G0045800	-0.81944	1.99E-06	0.000173943	GLUCOSYL/GLUCURONOSYL TRANSFERASES
BdiBd21-3.5G0045900	-0.81036	0.000278	0.008520937	GLUCOSYL/GLUCURONOSYL TRANSFERASES
BdiBd21-3.1G0660150	1.722579	0.001452	0.028492338	GLUTATHIONE S TRANSFERASE, GST, SUPERFAMILY, GST DOMAIN CONTAINING
BdiBd21-3.1G0888800	-0.69374	4.73E-07	5.40E-05	GLUTATHIONE S TRANSFERASE, GST, SUPERFAMILY, GST DOMAIN CONTAINING
BdiBd21-3.2G0174500	-2.42253	6.15E-08	9.85E-06	GLUTATHIONE S TRANSFERASE, GST, SUPERFAMILY, GST DOMAIN CONTAINING
BdiBd21-3.2G0601500	-0.73243	5.74E-10	1.50E-07	GLUTATHIONE S TRANSFERASE, GST, SUPERFAMILY, GST DOMAIN CONTAINING
BdiBd21-3.3G0415200	-0.72747	1.96E-06	0.000173538	GLUTATHIONE S TRANSFERASE, GST, SUPERFAMILY, GST DOMAIN CONTAINING
BdiBd21-3.3G0223600	-0.97148	1.21E-08	2.26E-06	Glycerol 3 phosphate transporting ATPase
BdiBd21-3.5G0234800	-1.68428	1.26E-11	5.64E-09	Glycerol 3 phosphate transporting ATPase
BdiBd21-3.1G0251800	0.639487	3.65E-05	0.001838023	GLYCOSYL HYDROLASE
BdiBd21-3.3G0527400	-1.22047	8.47E-06	0.00057818	GLYCOSYL HYDROLASE

BdiBd21-3.2G0764000	-0.68054	0.001019	0.022094052	GLYCOSYL HYDROLASE // BETA GLUCOSIDASE 1 RELATED
BdiBd21-3.4G0127400	-0.6241	1.07E-08	2.01E-06	GRAS domain family
BdiBd21-3.4G0580900	0.852364	0.003216	0.049669123	GRAS domain family
BdiBd21-3.3G0444800	0.617751	7.09E-10	1.79E-07	GTP BINDING PROTEIN RELATED // P LOOP CONTAINING NUCLEOSIDE TRIPHOSPHATE HYDROLASES SUPERFAMILY PROTEIN
BdiBd21-3.1G0855600	-0.80294	0.002692	0.044343575	HAD superfamily, subfamily IIIB
BdiBd21-3.2G0688300	-0.99891	1.89E-05	0.001101062	Haem binding uptake, Tiki superfamily, ChaN
BdiBd21-3.1G0896800	-1.2365	2.59E-11	1.01E-08	heat shock 70kDa protein 1/8
BdiBd21-3.5G0024800	-2.61832	6.07E-07	6.66E-05	HEAT SHOCK PROTEIN 90 // HEAT SHOCK PROTEIN 90 1
BdiBd21-3.3G0345400	-1.50289	9.05E-08	1.33E-05	HEAT SHOCK TRANSCRIPTION FACTOR
BdiBd21-3.4G0498400	-1.38925	2.79E-12	1.45E-09	HEAT SHOCK TRANSCRIPTION FACTOR
BdiBd21-3.4G0449500	-0.86341	0.000478	0.012730587	HEAT SHOCK TRANSCRIPTION FACTOR // HEAT STRESS TRANSCRIPTION FACTOR B 1
BdiBd21-3.3G0632700	0.752904	0.001573	0.030198264	High affinity nitrate transporter accessory
BdiBd21-3.2G0597300	0.989942	0.000532	0.01373192	histone chaperone ASF1
BdiBd21-3.1G0070300	0.668762	3.73E-13	2.26E-10	histone H1/5
BdiBd21-3.1G0663000	0.666684	1.44E-07	1.99E-05	histone H3
BdiBd21-3.3G0471300	-0.89854	4.89E-07	5.55E-05	Homeobox domain
BdiBd21-3.1G0306500	1.106067	1.90E-08	3.38E-06	homeobox leucine zipper protein
BdiBd21-3.1G0938800	1.06737	0.00055	0.014015711	Homocysteine S methyltransferase
BdiBd21-3.5G0222100	-0.63692	8.88E-05	0.003559239	HSP70 HSP90 ORGANIZING PROTEIN 1 RELATED
BdiBd21-3.1G0650400	-0.66755	0.001075	0.022947722	HYDROLASE LIKE PROTEIN
BdiBd21-3.1G0416000	-1.28943	4.28E-06	0.000331419	HYDROPHOBIC PROTEIN RCI2 LOW TEMPERATURE AND SALT RESPONSIVE PROTEIN LTI6 RELATED
BdiBd21-3.2G0463500	-1.3494	4.13E-07	4.87E-05	HYDROPHOBIC PROTEIN RCI2 LOW TEMPERATURE AND SALT RESPONSIVE PROTEIN LTI6 RELATED // HYDROPHOBIC PROTEIN RCI2A

BdiBd21-3.3G0630000	-0.67476	5.60E-05	0.002513982	Hypoxia induced protein conserved region
BdiBd21-3.1G0083000	1.34531	1.68E-05	0.000998548	Indole 3 acetaldehyde oxidase / Indoleacetaldehyde oxidase
BdiBd21-3.1G0071600	0.80942	0.000277	0.008505303	Indole 3 glycerol phosphate lyase/ TSA // Tryptophan synthase / Tryptophan synthetase
BdiBd21-3.3G0591500	-0.67146	1.66E-05	0.000996615	INHIBITOR OF APOPTOSIS
BdiBd21-3.2G0435300	2.467948	0.002655	0.043852674	inorganic pyrophosphatase
BdiBd21-3.3G0569400	-0.73368	3.26E-10	9.11E-08	inositol 1,3,4 trisphosphate 5/6 kinase / inositol tetrakisphosphate 1 kinase
BdiBd21-3.3G0475900	0.878148	4.07E-05	0.001990223	INOSITOL 5 PHOSPHATASE
BdiBd21-3.1G0043100	0.712552	9.28E-05	0.003691383	interleukin 1 receptor associated kinase 1
BdiBd21-3.2G0084700	-0.63337	0.000151	0.005342143	interleukin 1 receptor associated kinase 4
BdiBd21-3.1G0420600	0.832222	4.37E-05	0.002103721	IONOTROPIC GLUTAMATE RECEPTOR // GLUTAMATE RECEPTOR 2.5 RELATED
BdiBd21-3.4G0433100	1.263465	7.21E-05	0.003032407	IONOTROPIC GLUTAMATE RECEPTOR // GLUTAMATE RECEPTOR 2.5 RELATED
BdiBd21-3.2G0531400	1.251793	0.000459	0.012320528	IONOTROPIC GLUTAMATE RECEPTOR // GLUTAMATE RECEPTOR IIA RELATED
BdiBd21-3.3G0211900	1.040104	0.001172	0.024172364	Isoamylase / Debranching enzyme
BdiBd21-3.1G0109200	-0.95771	4.29E-08	7.04E-06	Isoflavone 2' hydroxylase / Isoflavone 2' monooxygenase
BdiBd21-3.2G0484300	-0.95712	1.85E-07	2.48E-05	Isovaleryl CoA dehydrogenase
BdiBd21-3.3G0610800	-0.7202	0.000818	0.018899093	KDEL LYS ASP GLU LEU CONTAINING RELATED
BdiBd21-3.3G0723700	2.132538	0.000269	0.008347205	Kelch motif
BdiBd21-3.3G0556400	-0.7101	5.17E-05	0.002362264	L iditol 2 dehydrogenase / Sorbitol dehydrogenase
BdiBd21-3.3G0223900	-1.01616	0.002539	0.042575779	large subunit ribosomal protein L16
BdiBd21-3.3G0254001	-1.17561	0.000824	0.01898371	large subunit ribosomal protein L2
BdiBd21-3.1G0345500	-1.58132	0.000143	0.005130286	large subunit ribosomal protein L32
BdiBd21-3.2G0121600	-0.99445	0.000163	0.00573399	Late embryogenesis abundant protein

BdiBd21-3.3G0530900	-0.61989	0.00024	0.00765046	Legume lectin domain
BdiBd21-3.1G0500901	1.147023	0.001516	0.029324128	Leucine Rich Repeat
BdiBd21-3.2G0624300	1.2786	0.000113	0.00429255	Leucine Rich Repeat
BdiBd21-3.2G0632400	-0.85221	0.000742	0.017727739	Leucine Rich Repeat
BdiBd21-3.2G0678000	0.831946	3.69E-16	4.70E-13	Leucine Rich Repeat
BdiBd21-3.5G0183200	0.796915	0.000525	0.013635603	Leucine Rich Repeat
BdiBd21-3.1G0293100	0.773094	8.55E-08	1.29E-05	LEUCINE RICH REPEAT CONTAINING PROTEIN
BdiBd21-3.1G0464600	0.704683	1.67E-05	0.000996848	LEUCINE RICH REPEAT CONTAINING PROTEIN
BdiBd21-3.2G0496500	0.653133	1.69E-09	3.77E-07	LEUCINE RICH REPEAT CONTAINING PROTEIN
BdiBd21-3.2G0773700	0.93838	3.68E-05	0.001844405	LEUCINE RICH REPEAT CONTAINING PROTEIN
BdiBd21-3.2G0773800	1.537837	1.89E-05	0.001101062	LEUCINE RICH REPEAT CONTAINING PROTEIN
BdiBd21-3.3G0200700	1.157179	3.94E-16	4.77E-13	LEUCINE RICH REPEAT CONTAINING PROTEIN
BdiBd21-3.4G0089900	1.461348	1.12E-09	2.69E-07	LEUCINE RICH REPEAT CONTAINING PROTEIN
BdiBd21-3.4G0135600	0.995235	1.61E-16	2.56E-13	LEUCINE RICH REPEAT CONTAINING PROTEIN
BdiBd21-3.4G0135700	1.127947	9.95E-11	3.24E-08	LEUCINE RICH REPEAT CONTAINING PROTEIN
BdiBd21-3.4G0139532	-0.86381	0.001939	0.035131031	LEUCINE RICH REPEAT CONTAINING PROTEIN
BdiBd21-3.4G0141600	0.737005	0.000188	0.006391132	LEUCINE RICH REPEAT CONTAINING PROTEIN
BdiBd21-3.4G0144600	1.048287	4.52E-09	9.27E-07	LEUCINE RICH REPEAT CONTAINING PROTEIN
BdiBd21-3.4G0196300	1.442043	0.000105	0.004051966	LEUCINE RICH REPEAT CONTAINING PROTEIN
BdiBd21-3.4G0197600	2.315633	2.06E-05	0.001167798	LEUCINE RICH REPEAT CONTAINING PROTEIN
BdiBd21-3.4G0595401	0.624114	0.001168	0.024147608	LEUCINE RICH REPEAT CONTAINING PROTEIN
BdiBd21-3.4G0613000	0.621599	4.82E-10	1.29E-07	LEUCINE RICH REPEAT CONTAINING PROTEIN

BdiBd21-3.5G0012000	0.797226	5.86E-07	6.45E-05	LEUCINE RICH REPEAT CONTAINING PROTEIN
BdiBd21-3.5G0057000	0.725737	7.18E-14	5.22E-11	LEUCINE RICH REPEAT CONTAINING PROTEIN
BdiBd21-3.4G0182350	-1.76351	7.18E-05	0.003028586	LEUCINE RICH REPEAT CONTAINING PROTEIN
BdiBd21-3.4G0532900	0.65134	4.49E-06	0.000344519	LEUCINE RICH REPEAT CONTAINING PROTEIN
BdiBd21-3.5G0359100	-1.52132	0.000436	0.011868311	Leucine rich repeat N terminal domain
BdiBd21-3.5G0359200	3.068662	4.44E-07	5.14E-05	Leucine rich repeat N terminal domain
BdiBd21-3.1G0126600	-0.83089	0.000718	0.017264257	LIPOXYGENASE
BdiBd21-3.3G0651600	0.855908	0.0013	0.026129378	LONG CHAIN ALCOHOL OXIDASE FAO1 RELATED
BdiBd21-3.5G0204300	-0.75347	3.01E-08	5.22E-06	Low specificity L threonine aldolase
BdiBd21-3.2G0288400	-0.77021	0.002813	0.045504	LURP one related
BdiBd21-3.2G0765000	-0.73971	0.001925	0.034943846	LURP one related
BdiBd21-3.2G0803401	1.970194	0.000724	0.017376227	MADS BOX PROTEIN
BdiBd21-3.4G0422900	0.675543	0.000306	0.009145087	MADS BOX PROTEIN
BdiBd21-3.3G0565300	-2.21196	1.24E-13	8.30E-11	MALE STERILITY PROTEIN 2 RELATED
BdiBd21-3.2G0171900	-0.89106	4.91E-07	5.55E-05	MEKK and related serine/threonine protein kinases // Serine/threonine protein kinase
BdiBd21-3.1G0084000	-1.2383	6.84E-05	0.002903229	MEMBER OF 'GDXG' FAMILY OF LIPOLYTIC ENZYMES
BdiBd21-3.1G0758900	1.095661	9.85E-06	0.00065667	MEMBER OF 'GDXG' FAMILY OF LIPOLYTIC ENZYMES
BdiBd21-3.1G0760600	-1.04045	2.22E-05	0.001233232	MEMBER OF 'GDXG' FAMILY OF LIPOLYTIC ENZYMES
BdiBd21-3.3G0304200	0.867818	2.68E-05	0.00143814	MEMBER OF 'GDXG' FAMILY OF LIPOLYTIC ENZYMES
BdiBd21-3.4G0299400	0.882082	0.000135	0.004945521	MEMBER OF 'GDXG' FAMILY OF LIPOLYTIC ENZYMES
BdiBd21-3.2G0154500	-0.8519	0.000442	0.011982299	MEMBRANE ASSOCIATED RING FINGER
BdiBd21-3.2G0407500	0.755573	0.002627	0.04355052	MEMBRANE ASSOCIATED RING FINGER

BdiBd21-3.2G0042400	0.757765	0.001862	0.034092795	Metallothionein
BdiBd21-3.1G0054500	0.60827	0.000122	0.004565759	Methylenetetrahydrofolate reductase
BdiBd21-3.2G0156800	-0.61676	0.000151	0.005350719	METHYLTRANSFERASE
BdiBd21-3.3G0683100	0.601044	0.000794	0.018543014	METHYLTRANSFERASE
BdiBd21-3.3G0015300	2.435368	3.88E-11	1.43E-08	MFS transporter, NNP family, nitrate/nitrite transporter
BdiBd21-3.5G0033500	-2.2799	6.24E-07	6.80E-05	MFS transporter, PHS family, inorganic phosphate transporter
BdiBd21-3.1G1020700	0.879107	0.00015	0.005342143	mlo protein
BdiBd21-3.3G0611900	-0.77824	0.001709	0.031960142	mlo protein
BdiBd21-3.3G0522500	-0.83785	4.08E-07	4.83E-05	molecular chaperone HtpG
BdiBd21-3.3G0780000	-0.70377	0.002678	0.044169722	MULTI COPPER OXIDASE
BdiBd21-3.1G0799700	0.908331	8.48E-11	2.80E-08	MULTIDRUG RESISTANCE PROTEIN
BdiBd21-3.1G0892400	-0.66446	5.05E-06	0.000375366	MULTIDRUG RESISTANCE PROTEIN
BdiBd21-3.3G0738200	3.215285	0.0002	0.006674959	MULTIDRUG RESISTANCE PROTEIN // MATE EFFLUX FAMILY PROTEIN
BdiBd21-3.1G0103400	-1.16954	0.000449	0.01211493	MYB FAMILY TRANSCRIPTION FACTOR
BdiBd21-3.1G0530200	0.668668	1.50E-11	6.49E-09	Myb like DNA binding domain
BdiBd21-3.3G0692600	1.295049	9.44E-07	9.57E-05	MYB LIKE DNA BINDING PROTEIN MYB
BdiBd21-3.4G0318100	0.997011	2.76E-09	5.75E-07	MYB LIKE DNA BINDING PROTEIN MYB
BdiBd21-3.4G0504000	0.75263	0.003008	0.04746365	MYB LIKE DNA BINDING PROTEIN MYB // MYB DOMAIN PROTEIN 42
BdiBd21-3.5G0196200	1.308681	0.000259	0.008141753	MYB LIKE DNA BINDING PROTEIN MYB // MYB DOMAIN PROTEIN 79
BdiBd21-3.2G0633000	0.595202	1.39E-09	3.24E-07	N acetylated alpha linked acidic dipeptidase [EC:3.4.17.21]
BdiBd21-3.1G0099800	-0.74029	0.00086	0.019596893	NA
BdiBd21-3.1G0152800	1.133624	0.001883	0.034332229	NA

BdiBd21-3.1G0178300	0.659754	0.000416	0.011435505	NA
BdiBd21-3.1G0209150	1.27682	6.69E-05	0.002866106	NA
BdiBd21-3.1G0232500	-1.38221	1.06E-06	0.000105322	NA
BdiBd21-3.1G0309850	0.796384	0.001465	0.028661177	NA
BdiBd21-3.1G0310200	1.2678	1.16E-09	2.75E-07	NA
BdiBd21-3.1G0315150	0.586433	0.000188	0.006391132	NA
BdiBd21-3.1G0343500	1.005894	0.000266	0.00831718	NA
BdiBd21-3.1G0355100	1.151408	3.56E-06	0.00028247	NA
BdiBd21-3.1G0392400	0.828723	0.000227	0.007297209	NA
BdiBd21-3.1G0477800	0.700166	0.00036	0.010276264	NA
BdiBd21-3.1G0493600	1.488137	4.41E-13	2.61E-10	NA
BdiBd21-3.1G0530300	1.331586	1.09E-06	0.000107953	NA
BdiBd21-3.1G0535200	-0.94892	0.002649	0.043780296	NA
BdiBd21-3.1G0609000	2.269914	0.002828	0.045640727	NA
BdiBd21-3.1G0624000	-0.64199	0.000224	0.007203277	NA
BdiBd21-3.1G0624350	-0.86114	8.38E-05	0.003419409	NA
BdiBd21-3.1G0642450	0.61658	0.000141	0.005099505	NA
BdiBd21-3.1G0706700	-0.8207	2.29E-07	2.99E-05	NA
BdiBd21-3.1G0759400	1.361439	0.000798	0.018623162	NA
BdiBd21-3.1G0777000	2.39237	0.000682	0.01666777	NA
BdiBd21-3.1G0849000	0.902671	0.001544	0.02976608	NA
BdiBd21-3.1G0930600	1.109532	9.86E-06	0.00065667	NA

BdiBd21-3.1G0933350	0.768949	0.001444	0.028382525	NA
BdiBd21-3.1G0966100	2.260165	0.003243	0.049932911	NA
BdiBd21-3.1G0992300	2.826698	2.79E-14	2.29E-11	NA
BdiBd21-3.1G0994500	0.597484	0.002284	0.039495558	NA
BdiBd21-3.1G1001600	-2.26893	4.77E-05	0.002247436	NA
BdiBd21-3.2G0026200	-1.06249	1.08E-08	2.01E-06	NA
BdiBd21-3.2G0095000	-0.6161	0.001784	0.033044207	NA
BdiBd21-3.2G0198900	3.303177	7.54E-05	0.003135236	NA
BdiBd21-3.2G0234700	0.619992	0.001156	0.024068508	NA
BdiBd21-3.2G0238201	-1.37	0.00037	0.010465602	NA
BdiBd21-3.2G0238801	-1.25481	2.58E-05	0.001392658	NA
BdiBd21-3.2G0264900	0.703388	1.26E-05	0.000795157	NA
BdiBd21-3.2G0279033	-0.63998	3.81E-06	0.000300269	NA
BdiBd21-3.2G0279100	-0.62769	0.000294	0.008886854	NA
BdiBd21-3.2G0303500	0.665305	0.00027	0.008360287	NA
BdiBd21-3.2G0309100	-0.92185	5.52E-07	6.11E-05	NA
BdiBd21-3.2G0325900	-1.50988	9.31E-08	1.36E-05	NA
BdiBd21-3.2G0326000	-1.09798	1.11E-06	0.000108665	NA
BdiBd21-3.2G0376200	-0.58907	0.000148	0.005273019	NA
BdiBd21-3.2G0408200	-0.97321	0.002488	0.042017856	NA
BdiBd21-3.2G0422350	-0.87121	8.73E-06	0.000592497	NA
BdiBd21-3.2G0438700	0.878994	0.000213	0.006955995	NA

BdiBd21-3.2G0467400	0.599435	0.001065	0.022851882	NA
BdiBd21-3.2G0519400	0.893581	0.001395	0.027591482	NA
BdiBd21-3.2G0532500	-0.77802	4.39E-05	0.002108549	NA
BdiBd21-3.2G0554000	2.033095	1.02E-07	1.47E-05	NA
BdiBd21-3.2G0572300	-1.31177	1.53E-07	2.08E-05	NA
BdiBd21-3.2G0596100	1.750352	0.000375	0.010604606	NA
BdiBd21-3.2G0742500	0.727088	0.001258	0.02548366	NA
BdiBd21-3.3G0030000	-2.89654	2.88E-05	0.001515312	NA
BdiBd21-3.3G0034500	0.678455	0.002726	0.044610428	NA
BdiBd21-3.3G0036000	-0.77194	0.000171	0.005952631	NA
BdiBd21-3.3G0049000	1.576451	8.26E-05	0.003379253	NA
BdiBd21-3.3G0126700	1.136791	0.001283	0.025889803	NA
BdiBd21-3.3G0140700	1.369456	0.00108	0.023002848	NA
BdiBd21-3.3G0172200	0.677743	0.001162	0.024147608	NA
BdiBd21-3.3G0211700	1.100647	0.000634	0.015736406	NA
BdiBd21-3.3G0212050	1.566803	1.52E-05	0.000930281	NA
BdiBd21-3.3G0239200	-0.77638	0.00108	0.023002848	NA
BdiBd21-3.3G0267200	0.668176	0.002745	0.044833328	NA
BdiBd21-3.3G0388200	-2.04465	2.30E-07	2.99E-05	NA
BdiBd21-3.3G0405900	-0.91014	0.002255	0.039140987	NA
BdiBd21-3.3G0418100	-0.66675	0.002448	0.04159402	NA
BdiBd21-3.3G0454150	0.858841	0.002585	0.043133255	NA

BdiBd21-3.3G0465500	-0.76984	0.000751	0.017861429	NA
BdiBd21-3.3G0471800	-0.96953	0.00027	0.008352774	NA
BdiBd21-3.3G0503066	1.193925	0.001184	0.024379569	NA
BdiBd21-3.3G0552100	-0.95718	0.000697	0.016851946	NA
BdiBd21-3.3G0569900	0.662737	9.67E-05	0.003798344	NA
BdiBd21-3.3G0596600	-1.2694	0.001566	0.03008823	NA
BdiBd21-3.3G0611400	-0.95507	7.15E-05	0.00302125	NA
BdiBd21-3.3G0703100	-0.61389	0.001168	0.024147608	NA
BdiBd21-3.3G0753900	-1.61193	3.83E-07	4.62E-05	NA
BdiBd21-3.3G0773100	0.602415	0.000124	0.004596153	NA
BdiBd21-3.3G0788000	1.34151	0.002827	0.045640727	NA
BdiBd21-3.3G0791200	-0.58829	1.33E-05	0.000830892	NA
BdiBd21-3.3G0796600	-1.03363	0.001137	0.023849575	NA
BdiBd21-3.3G0797400	-0.65286	0.001695	0.03175273	NA
BdiBd21-3.4G0046901	0.963597	6.62E-14	4.95E-11	NA
BdiBd21-3.4G0071300	1.059286	7.02E-08	1.09E-05	NA
BdiBd21-3.4G0105001	0.718321	0.001031	0.022263987	NA
BdiBd21-3.4G0114475	4.667103	0.000457	0.012283315	NA
BdiBd21-3.4G0133201	1.516223	0.001093	0.023174143	NA
BdiBd21-3.4G0145900	-0.64255	3.61E-10	9.99E-08	NA
BdiBd21-3.4G0152150	0.596839	0.00214	0.037477425	NA
BdiBd21-3.4G0179500	1.320694	0.001797	0.033200612	NA

BdiBd21-3.4G0233400	-0.86479	0.001354	0.027001817	NA
BdiBd21-3.4G0321900	0.836469	0.000866	0.019669525	NA
BdiBd21-3.4G0342100	-0.68615	0.000197	0.006618507	NA
BdiBd21-3.4G0344100	0.698388	0.001037	0.022342434	NA
BdiBd21-3.4G0347266	-0.61573	0.002411	0.041093804	NA
BdiBd21-3.4G0389200	0.739818	0.001575	0.030210146	NA
BdiBd21-3.4G0398100	1.539378	3.21E-06	0.000258988	NA
BdiBd21-3.4G0400750	1.469817	4.03E-07	4.81E-05	NA
BdiBd21-3.4G0427300	-0.86665	3.27E-07	4.02E-05	NA
BdiBd21-3.4G0434300	-0.73	0.000869	0.019701328	NA
BdiBd21-3.4G0441150	-1.0232	1.44E-06	0.000132915	NA
BdiBd21-3.4G0459000	0.668977	0.000679	0.016649829	NA
BdiBd21-3.4G0467700	-1.08778	0.000267	0.00831718	NA
BdiBd21-3.4G0493100	-0.76822	0.000195	0.006586411	NA
BdiBd21-3.4G0574600	-0.66507	0.001733	0.032307739	NA
BdiBd21-3.4G0599000	0.684921	5.88E-05	0.002597764	NA
BdiBd21-3.4G0603100	1.787381	6.61E-07	7.10E-05	NA
BdiBd21-3.4G0603200	0.789438	0.000199	0.006663278	NA
BdiBd21-3.4G0603300	1.509207	2.78E-07	3.55E-05	NA
BdiBd21-3.4G0603900	1.338425	2.64E-08	4.64E-06	NA
BdiBd21-3.5G0092600	0.839901	0.001769	0.032845893	NA
BdiBd21-3.5G0170900	2.456399	0.001125	0.023692644	NA

BdiBd21-3.5G0217300	1.684169	5.15E-08	8.29E-06	NA
BdiBd21-3.5G0232600	-0.58549	0.002803	0.045418743	NA
BdiBd21-3.5G0234900	-2.40898	2.99E-05	0.001561765	NA
BdiBd21-3.5G0326100	1.508185	2.16E-10	6.54E-08	NA
BdiBd21-3.1G0176300	1.500742	6.68E-05	0.002866106	NA+/CA2+ K+ INDEPENDENT EXCHANGER // CATION/CALCIUM EXCHANGER 1
BdiBd21-3.3G0782000	2.188294	1.63E-09	3.74E-07	NAC DOMAIN CONTAINING PROTEIN 94 RELATED
BdiBd21-3.1G0932200	-0.78453	2.44E-06	0.000206847	NAD(+) ADP-ribosyltransferase / Poly(ADP-ribose)polymerase
BdiBd21-3.3G0350300	-0.72172	0.000192	0.006502067	NAD(P)H-quinone oxidoreductase subunit H (ndhH)
BdiBd21-3.3G0541300	-0.84075	0.001494	0.029016802	NAD DEPENDENT EPIMERASE/DEHYDRATASE
BdiBd21-3.5G0092200	-0.59419	0.000471	0.012616271	NADH DEHYDROGENASE // NAD
BdiBd21-3.4G0327800	-0.66599	4.42E-07	5.14E-05	NADH KINASE POS5, MITOCHONDRIAL
BdiBd21-3.2G0503700	0.585489	2.52E-07	3.25E-05	NB ARC domain
BdiBd21-3.1G0223500	-0.76315	0.00121	0.024752969	Nicotianamine synthase
BdiBd21-3.4G0024100	0.792176	2.29E-11	9.10E-09	No apical meristem
BdiBd21-3.1G0419400	1.142235	3.21E-08	5.41E-06	Non specific protein tyrosine kinase / Cytoplasmic protein tyrosine kinase
BdiBd21-3.1G0934200	0.699563	6.64E-07	7.11E-05	Non specific serine/threonine protein kinase / Threonine specific protein kinase
BdiBd21-3.2G0340500	1.523248	4.55E-14	3.62E-11	Non specific serine/threonine protein kinase / Threonine specific protein kinase
BdiBd21-3.3G0738000	0.807305	0.000411	0.011333438	Non specific serine/threonine protein kinase / Threonine specific protein kinase
BdiBd21-3.4G0151500	1.654643	3.96E-07	4.75E-05	Non specific serine/threonine protein kinase / Threonine specific protein kinase
BdiBd21-3.4G0412300	0.779271	0.000274	0.00842982	Non specific serine/threonine protein kinase / Threonine specific protein kinase
BdiBd21-3.4G0558700	0.984483	2.67E-15	2.83E-12	Non specific serine/threonine protein kinase / Threonine specific protein kinase
BdiBd21-3.4G0622600	0.694915	6.00E-10	1.54E-07	Non specific serine/threonine protein kinase / Threonine specific protein kinase

BdiBd21-3.5G0325100	0.956685	0.002601	0.043231886	Non specific serine/threonine protein kinase / Threonine specific protein kinase
BdiBd21-3.3G0725000	-1.24566	1.31E-08	2.39E-06	Non specific serine/threonine protein kinase / Threonine specific protein kinase // Phosphoenolpyruvate carboxykinase
BdiBd21-3.3G0292300	1.744367	0.001002	0.021795093	NORGANIC PHOSPHATE TRANSPORTER 1 4
BdiBd21-3.3G0680400	0.591153	0.000109	0.004177981	nucleobase:cation symporter 1, NCS1 family
BdiBd21-3.2G0755700	1.237304	5.08E-06	0.000376084	Nucleotide diphospho sugar transferase
BdiBd21-3.1G0639400	0.758912	8.00E-06	0.000552005	O METHYLTRANSFERASE RELATED
BdiBd21-3.1G0274000	-0.78772	0.002365	0.040420122	OLIGOPEPTIDE TRANSPORTER RELATED
BdiBd21-3.3G0432100	-1.66922	7.09E-05	0.003003063	OLIGOPEPTIDE TRANSPORTER RELATED
BdiBd21-3.3G0705900	2.042943	0.000131	0.004819121	OLIGOPEPTIDE TRANSPORTER RELATED
BdiBd21-3.4G0292300	0.764979	0.002344	0.040157005	OLIGOPEPTIDE TRANSPORTER RELATED
BdiBd21-3.5G0184300	0.919448	9.02E-08	1.33E-05	OLIGOPEPTIDE TRANSPORTER RELATED
BdiBd21-3.5G0184400	0.861753	7.17E-16	8.30E-13	OLIGOPEPTIDE TRANSPORTER RELATED
BdiBd21-3.5G0266800	-1.0827	0.001276	0.025782352	OLIGOPEPTIDE TRANSPORTER RELATED
BdiBd21-3.2G0375600	0.779733	5.65E-05	0.002516543	OLIGOPEPTIDE TRANSPORTER RELATED // PROTEIN NRT1/ PTR FAMILY 2.1 RELATED
BdiBd21-3.1G0505500	0.798676	0.001103	0.023317071	OLIGOPEPTIDE TRANSPORTER RELATED // PROTEIN NRT1/ PTR FAMILY 4.5 RELATED
BdiBd21-3.3G0226900	-1.56451	7.91E-14	5.60E-11	OLIGOPEPTIDE TRANSPORTER RELATED // PROTEIN NRT1/ PTR FAMILY 6.3
BdiBd21-3.3G0790000	-0.76469	0.000349	0.010042968	OMA1 HOMOLOG, ZINC METALLOPEPTIDASE // METALLOENDOPEPTIDASE OMA1, MITOCHONDRIAL
BdiBd21-3.3G0666200	-1.1668	2.72E-05	0.00145365	OPT oligopeptide transporter protein
BdiBd21-3.3G0666300	-0.92645	0.00022	0.007113611	OPT oligopeptide transporter protein
BdiBd21-3.4G0512200	-1.28951	2.40E-10	6.94E-08	Ornithine decarboxylase / L ornithine carboxy lyase
BdiBd21-3.1G0243200	-1.23598	4.88E-18	1.38E-14	OSMOTIC STRESS POTASSIUM TRANSPORTER
BdiBd21-3.3G0499100	-0.65724	0.001056	0.022682316	OSMOTIC STRESS POTASSIUM TRANSPORTER

BdiBd21-3.5G0097200	-2.0775	2.72E-10	7.68E-08	OSMOTIC STRESS POTASSIUM TRANSPORTER
BdiBd21-3.4G0413100	-0.64204	1.84E-06	0.000164022	OSMOTIC STRESS POTASSIUM TRANSPORTER // POTASSIUM TRANSPORTER 12 RELATED
BdiBd21-3.1G0158800	-0.72938	0.000944	0.02098272	Oxalate oxidase
BdiBd21-3.1G0158900	-1.66745	1.67E-10	5.18E-08	Oxalate oxidase
BdiBd21-3.1G0630900	0.946404	0.001076	0.022957407	OXIDOREDUCTASE, 2OG FE II OXYGENASE FAMILY PROTEIN
BdiBd21-3.1G0491400	1.064004	0.000122	0.004565759	OXIDOREDUCTASE, 2OG FE II OXYGENASE FAMILY PROTEIN
BdiBd21-3.1G0491500	1.233823	0.000156	0.005527332	OXIDOREDUCTASE, 2OG FE II OXYGENASE FAMILY PROTEIN
BdiBd21-3.1G0631600	-0.77625	9.55E-05	0.003761027	OXIDOREDUCTASE, 2OG FE II OXYGENASE FAMILY PROTEIN
BdiBd21-3.2G0514100	1.201602	6.49E-09	1.29E-06	OXIDOREDUCTASE, 2OG FE II OXYGENASE FAMILY PROTEIN
BdiBd21-3.4G0628500	-3.68862	4.05E-10	1.10E-07	P HYDROXYBENZOIC ACID EFFLUX PUMP SUBUNIT RELATED
BdiBd21-3.2G0772700	1.010857	2.32E-12	1.23E-09	PAX TRANSCRIPTION ACTIVATION DOMAIN INTERACTING PROTEIN
BdiBd21-3.2G0635300	-0.88866	1.21E-06	0.000116735	PDDEXK like family of unknown function
BdiBd21-3.2G0750100	-1.10472	0.000174	0.006028959	PDDEXK like family of unknown function
BdiBd21-3.4G0502500	-0.98416	0.002557	0.042751345	Peptidase Do / Protease Do
BdiBd21-3.2G0201100	-1.01079	9.57E-08	1.39E-05	Peptidase of plants and bacteria
BdiBd21-3.1G0553900	0.684265	7.53E-06	0.000522947	PEPTIDASE S41 FAMILY PROTEIN
BdiBd21-3.3G0577300	-0.72027	3.81E-07	4.62E-05	PEPTIDYL PROLYL CIS TRANS ISOMERASE // PEPTIDYL PROLYL CIS TRANS ISOMERASE FKBP65
BdiBd21-3.1G0107700	0.613049	0.00055	0.014015711	Peroxidase
BdiBd21-3.1G0233000	0.864441	6.75E-08	1.06E-05	Peroxidase / Lactoperoxidase
BdiBd21-3.1G0521700	-2.00936	0.000403	0.011166009	Peroxidase / Lactoperoxidase
BdiBd21-3.4G0387000	-0.58081	0.003062	0.04816919	Peroxidase / Lactoperoxidase
BdiBd21-3.5G0356800	-1.0486	4.78E-05	0.002247436	Peroxidase / Lactoperoxidase

BdiBd21-3.5G0363500	-0.77549	0.001767	0.032831064	PEROXIDASE 47
BdiBd21-3.5G0041300	0.990874	2.85E-06	0.000235337	Phloroisovalerophenone synthase / Valerophenone synthase
BdiBd21-3.1G0912100	1.142639	0.000911	0.020433431	phosphoenolpyruvate carboxykinase
BdiBd21-3.3G0337300	-0.6474	1.84E-05	0.00108111	PHOSPHOFRUCTOKINASE
BdiBd21-3.1G0857000	0.760704	0.002993	0.047371284	Phosphoglycerate mutase
BdiBd21-3.1G0684600	-1.65869	2.78E-15	2.83E-12	Phosphopyruvate hydratase / Enolase
BdiBd21-3.1G0917100	-0.5927	4.16E-05	0.002026621	Phosphopyruvate hydratase / Enolase
BdiBd21-3.5G0257700	-1.55413	5.05E-05	0.002324278	Plant invertase/pectin methylesterase inhibitor
BdiBd21-3.3G0178100	1.187125	0.00022	0.007121357	Plant protein of unknown function
BdiBd21-3.1G1043500	-1.5781	1.40E-06	0.000130772	Plant thionin
BdiBd21-3.1G0020100	0.644746	0.001941	0.035131031	Plastocyanin like domain
BdiBd21-3.4G0344700	0.941759	6.27E-06	0.000450813	POLYOL TRANSPORTER 3 RELATED
BdiBd21-3.2G0500600	-1.02391	1.01E-05	0.000668737	Potato inhibitor I family
BdiBd21-3.2G0753200	0.629199	0.000272	0.008383694	Predicted E3 ubiquitin ligase
BdiBd21-3.3G0558900	5.106944	0.000214	0.006978907	Predicted K+/H+ antiporter
BdiBd21-3.4G0611500	0.988343	0.002062	0.036459578	Predicted K+/H+ antiporter
BdiBd21-3.1G0266100	-0.70929	7.40E-05	0.003097689	Predicted splicing regulator, contains RRM, SWAP and RPR domains
BdiBd21-3.1G0306100	-1.48513	1.11E-09	2.69E-07	Predicted transporter
BdiBd21-3.1G0325400	-0.59603	0.000122	0.004565759	Predicted transporter
BdiBd21-3.3G0619700	0.981282	1.98E-12	1.07E-09	Predicted transporter
BdiBd21-3.4G0178600	0.621078	1.24E-07	1.76E-05	Predicted transporter
BdiBd21-3.5G0151000	0.867622	9.74E-05	0.003820337	Predicted transporter

BdiBd21-3.3G0423200	0.688767	4.31E-05	0.00207998	Predicted transporter ADD1
BdiBd21-3.1G0660300	0.699986	5.43E-06	0.000396156	Predicted transporter/transmembrane protein
BdiBd21-3.5G0247600	1.057122	1.98E-06	0.000173943	Predicted transporter/transmembrane protein
BdiBd21-3.1G0090500	0.996364	9.79E-05	0.003830289	Premnaspirodiene oxygenase / Hyoscymus muticus premnaspirodiene oxygenase
BdiBd21-3.2G0220100	-1.00403	0.000952	0.021073378	PRONE Plant specific Rop nucleotide exchanger
BdiBd21-3.3G0136600	1.343504	5.01E-08	8.12E-06	PROPROTEIN CONVERTASE SUBTILISIN/KEXIN
BdiBd21-3.3G0744700	-0.72919	0.000369	0.010465602	protease IV [EC:3.4.21.]
BdiBd21-3.4G0596900	-0.76471	2.75E-17	4.99E-14	PROTEIN ACS 13, ISOFORM C
BdiBd21-3.3G0650600	0.980385	8.73E-06	0.000592497	PROTEIN CER1 LIKE 1 RELATED
BdiBd21-3.1G0425800	1.951099	0.001336	0.026738762	Protein kinase domain
BdiBd21-3.1G0775600	2.545654	1.70E-13	1.11E-10	Protein kinase domain
BdiBd21-3.1G0776901	3.901925	1.07E-06	0.000105761	Protein kinase domain
BdiBd21-3.3G0135600	0.968384	1.00E-09	2.50E-07	Protein kinase domain
BdiBd21-3.3G0457000	1.328151	3.20E-07	3.98E-05	Protein kinase domain
BdiBd21-3.3G0740800	-0.71704	0.000342	0.009941124	Protein kinase domain
BdiBd21-3.4G0018600	0.622801	4.23E-06	0.000327978	Protein kinase domain
BdiBd21-3.4G0342200	-0.69614	1.99E-05	0.001141324	Protein kinase domain
BdiBd21-3.4G0344200	-0.75372	1.19E-06	0.000114682	Protein kinase domain
BdiBd21-3.4G0344300	-0.82945	3.96E-05	0.001955401	Protein kinase domain
BdiBd21-3.4G0563200	-0.72484	1.51E-06	0.000137395	Protein kinase domain
BdiBd21-3.5G0039800	1.741415	7.69E-05	0.003187626	Protein kinase domain
BdiBd21-3.5G0042300	1.777337	3.97E-05	0.001957013	Protein kinase domain

BdiBd21-3.5G0121900	1.621432	0.000805	0.018727026	Protein kinase domain
BdiBd21-3.5G0302900	1.493172	1.68E-09	3.77E-07	Protein kinase domain
BdiBd21-3.2G0383200	0.58958	4.85E-05	0.002263202	PROTEIN LIGHT DEPENDENT SHORT HYPOCOTYLS 6
BdiBd21-3.4G0004700	-0.96179	0.000964	0.021254534	PROTEIN NRT1/ PTR FAMILY 2.10 RELATED
BdiBd21-3.1G0380800	-1.47808	1.05E-05	0.000686379	Protein of unknown function
BdiBd21-3.1G0909700	1.434679	2.70E-06	0.000224933	Protein of unknown function
BdiBd21-3.2G0142400	1.252394	1.17E-05	0.000751502	Protein of unknown function
BdiBd21-3.2G0320600	1.86677	2.98E-32	3.80E-28	Protein of unknown function
BdiBd21-3.2G0754300	0.998535	0.002052	0.036357213	Protein of unknown function
BdiBd21-3.3G0375200	0.604282	3.05E-07	3.84E-05	Protein of unknown function
BdiBd21-3.3G0725600	-0.98073	0.000511	0.013428129	Protein of unknown function
BdiBd21-3.4G0553800	-0.58051	0.002325	0.039924117	Protein of unknown function
BdiBd21-3.5G0129100	0.596449	1.35E-05	0.000839625	Protein of unknown function
BdiBd21-3.5G0308700	0.729551	0.000296	0.008922019	Protein of unknown function
BdiBd21-3.1G0197800	-1.24789	0.000347	0.01003377	Protein of unknown function DUF260
BdiBd21-3.1G0298900	-1.00982	0.000201	0.00668963	Protein of unknown function DUF260
BdiBd21-3.1G0885000	2.270017	3.96E-11	1.44E-08	Protein of unknown function DUF260
BdiBd21-3.2G0131300	1.452233	4.96E-05	0.0023099	Protein of unknown function, DUF594
BdiBd21-3.4G0073300	-0.95091	1.70E-06	0.000152531	Protein of unknown function, DUF594
BdiBd21-3.4G0225800	0.864556	4.39E-06	0.000338453	Protein of unknown function, DUF594
BdiBd21-3.3G0461100	-0.93891	2.77E-06	0.00022991	Protein of unknown function, DUF599
BdiBd21-3.1G0549300	0.802865	3.35E-05	0.001712907	Protein of unknown function, DUF617

BdiBd21-3.3G0574400	1.238673	3.89E-06	0.000305322	PROTEIN PHOSPHATASE 2C
BdiBd21-3.5G0004900	3.062389	0.000815	0.018871766	PROTEIN PHOSPHATASE 2C
BdiBd21-3.5G0157500	1.238814	0.000431	0.011728542	PROTEIN PLANT CADMIUM RESISTANCE 11 RELATED
BdiBd21-3.2G0496700	1.252392	1.69E-07	2.28E-05	Protein tyrosine kinase
BdiBd21-3.3G0148900	2.525033	7.02E-09	1.38E-06	Protein tyrosine kinase
BdiBd21-3.4G0053700	1.555798	9.98E-05	0.003875959	Protein tyrosine kinase
BdiBd21-3.4G0458800	0.936906	0.000476	0.012691073	Protein tyrosine kinase
BdiBd21-3.5G0048300	1.170713	0.000629	0.015629498	Protein tyrosine kinase
BdiBd21-3.5G0050100	-1.04748	2.14E-06	0.000184091	Protein tyrosine kinase
BdiBd21-3.3G0758800	-0.73635	0.001806	0.033326687	Protochlorophyllide reductase / Protochlorophyllide oxidoreductase
BdiBd21-3.4G0566400	-0.64149	0.000849	0.019446363	PSBP DOMAIN CONTAINING PROTEIN 4, CHLOROPLASTIC
BdiBd21-3.2G0660300	-0.8936	7.93E-08	1.21E-05	PURPLE ACID PHOSPHATASE 10
BdiBd21-3.1G0262600	0.672973	3.14E-06	0.000254243	Pyruvate dehydrogenase
BdiBd21-3.1G0832600	-0.67922	1.29E-06	0.000123241	Pyruvate dehydrogenase
BdiBd21-3.3G0484500	-0.96042	1.17E-09	2.75E-07	Quinate O hydroxycinnamoyltransferase / Hydroxycinnamoyl coenzyme A quinate transferase
BdiBd21-3.1G0704600	0.913488	0.001944	0.035164923	RAB GDP DISSOCIATION INHIBITOR
BdiBd21-3.3G0665000	0.630847	0.000143	0.005131714	Ras suppressor protein
BdiBd21-3.5G0274200	0.744338	0.000418	0.011456837	Ras suppressor protein
BdiBd21-3.4G0626200	0.783749	5.95E-06	0.000429953	RBR FAMILY RING FINGER AND IBR DOMAIN CONTAINING // C3H4 TYPE ZINC FINGER PROTEIN RELATED
BdiBd21-3.3G0112500	-0.68239	2.27E-10	6.65E-08	Receptor protein tyrosine kinase / Receptor protein tyrosine kinase // Non specific protein tyrosine kinase / Cytoplasmic protein tyrosine kinase // Non specific serine/threonine protein kinase / Threonine specific protein kinase
BdiBd21-3.3G0587600	-1.4667	4.82E-09	9.82E-07	RELATED TO MULTIFUNCTIONAL CYCLIN DEPENDENT KINASE RELATED

BdiBd21-3.1G0262800	2.624891	0.002555	0.042747243	REPLICATION FACTOR A 1, RFA1
BdiBd21-3.5G0144800	0.657242	0.002054	0.036357213	RESPONSE REGULATOR OF TWO COMPONENT SYSTEM
BdiBd21-3.1G0274500	-0.6478	8.03E-08	1.22E-05	Ribonuclease
BdiBd21-3.2G0519200	0.637496	0.001203	0.024645331	RIBONUCLEASE P SUBUNIT P38 // EMB|CAB82814.1
BdiBd21-3.1G0522600	0.935431	0.003148	0.049034876	RING FINGER DOMAIN CONTAINING
BdiBd21-3.1G0528100	0.948465	0.000417	0.01145668	RING FINGER DOMAIN CONTAINING
BdiBd21-3.3G0442400	-0.59459	2.00E-06	0.000173943	RING FINGER DOMAIN CONTAINING
BdiBd21-3.5G0112100	-0.65968	5.29E-05	0.002402906	Root cap
BdiBd21-3.1G0278100	0.81026	5.06E-06	0.000375366	S-(hydroxymethyl)glutathione dehydrogenase / alcohol dehydrogenase (frmA)
BdiBd21-3.2G0162100	0.691785	6.01E-05	0.002640447	S adenosylmethionine synthetase
BdiBd21-3.2G0162200	0.610445	5.00E-06	0.000374487	S adenosylmethionine synthetase
BdiBd21-3.3G0206600	0.773498	4.42E-05	0.00211474	S locus glycoprotein domain
BdiBd21-3.3G0577200	2.007887	3.89E-08	6.47E-06	S locus glycoprotein domain
BdiBd21-3.4G0519000	-0.90865	6.08E-05	0.002666383	S locus glycoprotein domain
BdiBd21-3.4G0592600	1.212945	2.40E-05	0.001305999	S locus glycoprotein domain
BdiBd21-3.1G0165501	1.880403	0.002798	0.045411705	Salt stress response/antifungal
BdiBd21-3.1G0252300	-0.65214	0.000334	0.009786493	Salt stress response/antifungal
BdiBd21-3.1G0334000	0.710666	5.74E-05	0.002549343	Salt stress response/antifungal
BdiBd21-3.1G0334866	-0.82536	1.36E-07	1.90E-05	Salt stress response/antifungal
BdiBd21-3.1G0334932	-0.60272	9.36E-07	9.53E-05	Salt stress response/antifungal
BdiBd21-3.1G0336600	0.599974	0.000454	0.012207662	Salt stress response/antifungal
BdiBd21-3.2G0469700	-1.50543	1.31E-08	2.39E-06	Salt stress response/antifungal

BdiBd21-3.5G0055800	0.721415	0.001249	0.025350668	Salt stress response/antifungal
BdiBd21-3.1G0434200	-1.4826	5.97E-09	1.20E-06	SAUR family protein
BdiBd21-3.1G0434300	-1.01409	9.76E-07	9.86E-05	SAUR family protein
BdiBd21-3.3G0586000	-0.5857	0.002962	0.047033084	SAUR family protein
BdiBd21-3.4G0483700	-3.38811	1.12E-11	5.18E-09	SAUR family protein
BdiBd21-3.5G0286800	-0.70831	1.30E-06	0.000123385	SAUR family protein
BdiBd21-3.1G0462500	-1.37142	3.65E-25	1.55E-21	SAUR family protein
BdiBd21-3.2G0569700	-1.32921	9.11E-05	0.003635815	Scopoletin glucosyltransferase
BdiBd21-3.1G0207300	1.498177	0.00027	0.008352774	SECRETORY CARRIER ASSOCIATED MEMBRANE PROTEIN SCAMP
BdiBd21-3.3G0301700	0.727297	0.000185	0.006319991	SERINE PROTEASE FAMILY S10 SERINE CARBOXYPEPTIDASE
BdiBd21-3.4G0313900	1.39389	7.33E-06	0.000515533	SERINE PROTEASE FAMILY S10 SERINE CARBOXYPEPTIDASE
BdiBd21-3.2G0081600	-1.08102	2.16E-07	2.86E-05	SERINE THREONINE PROTEIN KINASE
BdiBd21-3.4G0442600	2.098108	0.000334	0.009792592	SERINE THREONINE PROTEIN KINASE
BdiBd21-3.4G0513500	-0.82525	9.04E-08	1.33E-05	SERINE THREONINE PROTEIN KINASE
BdiBd21-3.1G0278400	-0.73872	8.62E-09	1.65E-06	SERINE/THREONINE KINASE // SERINE/THREONINE PROTEIN KINASE SRK2C
BdiBd21-3.3G0485200	-1.06283	3.05E-07	3.84E-05	SERINE/THREONINE PROTEIN KINASE
BdiBd21-3.4G0616600	-1.43845	8.84E-08	1.32E-05	SERINE/THREONINE PROTEIN KINASE
BdiBd21-3.1G0548900	0.798366	1.22E-05	0.000772127	Serine/threonine protein kinase // Serine/threonine protein kinase
BdiBd21-3.1G0369400	-1.0774	1.85E-05	0.00108244	SERINE/THREONINE PROTEIN KINASE KINX RELATED
BdiBd21-3.2G0315400	-1.88525	1.31E-06	0.000123385	SERINE/THREONINE PROTEIN KINASE RIO
BdiBd21-3.2G0768400	0.727505	6.48E-06	0.000463048	SERINE/THREONINE PROTEIN KINASE RIO
BdiBd21-3.4G0616000	-2.28822	3.04E-16	4.07E-13	SERINE/THREONINE PROTEIN KINASE WNK4 RELATED

BdiBd21-3.5G0189100	1.070667	2.87E-13	1.78E-10	shikimate O hydroxycinnamoyltransferase
BdiBd21-3.4G0297500	-1.06569	0.000192	0.006503359	Sinapoylglucose choline O sinapoyltransferase / Sinapine synthase
BdiBd21-3.2G0338101	-1.44463	1.66E-07	2.24E-05	SMALL EDRK RICH FACTOR 1
BdiBd21-3.1G0903600	-1.07995	0.00011	0.004195492	SMALL HEAT SHOCK PROTEIN HSP20 FAMILY
BdiBd21-3.3G0772900	-0.86886	0.001979	0.035551947	SMALL HEAT SHOCK PROTEIN HSP20 FAMILY // 23.5 KDA HEAT SHOCK PROTEIN, MITOCHONDRIAL RELATED
BdiBd21-3.4G0003000	1.132104	2.54E-10	7.25E-08	SNARE PROTEINS
BdiBd21-3.3G0524900	-1.05789	5.62E-05	0.00251615	solute carrier family 13
BdiBd21-3.3G0359800	1.214021	2.03E-05	0.001156526	SOLUTE CARRIER FAMILY 13 MEMBER
BdiBd21-3.1G0281100	-1.61467	1.63E-06	0.000146809	SPX DOMAIN CONTAINING PROTEIN 3
BdiBd21-3.3G0370600	1.06952	0.00064	0.01585286	STEROL DESATURASE
BdiBd21-3.1G0782600	0.658824	0.000349	0.010042968	STEROL REGULATORY ELEMENT BINDING PROTEIN
BdiBd21-3.3G0009900	-2.6909	2.08E-16	3.11E-13	Sucrose:sucrose fructosyltransferase / Sucrose:sucrose 1 fructosyltransferase // Beta fructofuranosidase / Saccharase
BdiBd21-3.1G0960000	0.75292	5.03E-05	0.002322101	Sugar (and other) transporter (Sugar tr)
BdiBd21-3.1G0960100	0.66947	0.00029	0.008789845	Sugar (and other) transporter (Sugar_tr)
BdiBd21-3.3G0800200	-0.76119	0.00018	0.006194178	Sugar (and other) transporter (Sugar_tr) // Major Facilitator Superfamily (MFS_1)
BdiBd21-3.4G0425900	0.710855	1.76E-06	0.000157354	SUGAR TRANSPORT PROTEIN 7
BdiBd21-3.4G0409200	0.809432	2.29E-06	0.000195423	Sugar transporter/spinster transmembrane protein
BdiBd21-3.5G0317700	1.026411	4.18E-12	2.13E-09	SULFATE TRANSPORTER
BdiBd21-3.2G0618100	-0.90883	0.000259	0.008132126	SULFATE TRANSPORTER 3.5 RELATED
BdiBd21-3.3G0672700	1.75565	4.56E-12	2.27E-09	SULFOTRANSFERASE SULT
BdiBd21-3.4G0523100	0.813544	6.77E-05	0.002885599	SULFOTRANSFERASE SULT
BdiBd21-3.3G0688100	0.999118	5.63E-05	0.00251615	SWI/SNF COMPLEX RELATED // PROTEIN REVEILLE 7 LIKE

BdiBd21-3.2G0707700	1.531928	1.42E-06	0.000131705	Tetratricopeptide repeat
BdiBd21-3.4G0044000	1.117045	0.000271	0.008367373	Thiosulfate sulfurtransferase / Thiosulfate thiotransferase
BdiBd21-3.1G0511200	1.094851	1.39E-05	0.0008621	Thromboxane A synthase / Thromboxane synthetase
BdiBd21-3.4G0549200	-0.80165	0.00074	0.017712577	TLC domain
BdiBd21-3.3G0100500	-0.8344	0.002474	0.041911963	transcription factor HY5
BdiBd21-3.5G0306800	-1.11727	0.000892	0.020099641	Transferase family
BdiBd21-3.4G0552500	-1.08389	0.000137	0.005005703	Transferred entry
BdiBd21-3.2G0631100	0.936295	2.13E-05	0.001192744	Transferrin receptor like dimerisation domain
BdiBd21-3.1G0324400	-1.74427	3.96E-21	1.26E-17	TRANSPORTER B0361.11 RELATED
BdiBd21-3.1G0361100	0.953269	0.003098	0.048479472	TREHALOSE 6 PHOSPHATE SYNTHASE
BdiBd21-3.4G0121800	-1.26848	0.000116	0.004400496	TRYPTOPHAN BIOSYNTHESIS PROTEIN
BdiBd21-3.3G0745101	0.877736	7.80E-05	0.003210196	U BOX DOMAIN CONTAINING PROTEIN 42 RELATED
BdiBd21-3.5G0270000	-0.81757	0.000621	0.015533996	UBIQUINOL OXIDASE 1A, MITOCHONDRIAL RELATED
BdiBd21-3.3G0447900	-0.78685	2.63E-05	0.00141335	ubiquitin carboxyl terminal hydrolase 36/42 [EC:3.4.19.12]
BdiBd21-3.3G0376800	0.902754	6.35E-07	6.84E-05	Ubiquitinyl hydrolase 1 / Ubiquitin thiolesterase
BdiBd21-3.1G0287200	1.074629	1.59E-11	6.73E-09	UDP arabinopyranose mutase
BdiBd21-3.2G0164900	0.646528	0.002188	0.038107975	UDP GLYCOSYLTRANSFERASE 75B1 RELATED
BdiBd21-3.1G0067500	1.194026	6.80E-08	1.06E-05	UNCHARACTERIZED NODULIN LIKE PROTEIN
BdiBd21-3.1G0010400	-0.80908	0.002911	0.046507382	uncharacterized protein
BdiBd21-3.4G0522900	-1.06656	0.000779	0.018263467	uncharacterized protein
BdiBd21-3.4G0556400	1.282661	0.000275	0.008449727	uncharacterized protein
BdiBd21-3.4G0092100	-1.88856	7.66E-05	0.003180225	Ureide permease

BdiBd21-3.1G0826000	4.687323	9.62E-17	1.63E-13	Very long chain 3 oxoacyl CoA synthase / Very long chain beta ketoacyl CoA synthase
BdiBd21-3.1G0290600	3.557623	0.000352	0.010099883	Vestitone reductase
BdiBd21-3.2G0575500	-1.75946	2.05E-06	0.000177286	VOLTAGE AND LIGAND GATED POTASSIUM CHANNEL
BdiBd21-3.2G0643300	1.901107	4.80E-06	0.000361396	VOLTAGE AND LIGAND GATED POTASSIUM CHANNEL
BdiBd21-3.3G0654000	1.136621	0.000335	0.00979283	VOLTAGE AND LIGAND GATED POTASSIUM CHANNEL
BdiBd21-3.2G0114400	-1.026	0.000999	0.021784745	Voltage dependent anion channel
BdiBd21-3.1G0084200	0.82637	0.000202	0.006711009	VQ motif
BdiBd21-3.1G0225700	0.928801	4.79E-05	0.002247436	VQ motif
BdiBd21-3.5G0259800	0.866095	2.34E-05	0.001284283	WDSAM1 PROTEIN
BdiBd21-3.2G0214400	0.856542	0.001859	0.034059519	WRKY DNA binding domain
BdiBd21-3.2G0684600	1.662623	3.84E-05	0.001910999	WRKY DNA binding domain
BdiBd21-3.4G0461900	0.634934	3.46E-05	0.001759395	X BOX TRANSCRIPTION FACTOR RELATED
BdiBd21-3.1G0495700	-1.20288	3.80E-05	0.001894032	XENOTROPIC AND POLYTROPIC RETROVIRUS RECEPTOR 1 RELATED // SPX DOMAIN CONTAINING PROTEIN 1 RELATED
BdiBd21-3.4G0605700	1.355353	2.18E-10	6.54E-08	ZINC FINGER DHHC DOMAIN CONTAINING PROTEIN
BdiBd21-3.1G0695500	0.917255	1.14E-07	1.64E-05	ZINC FINGER FYVE DOMAIN CONTAINING PROTEIN
BdiBd21-3.2G0623600	-1.86019	2.47E-21	8.98E-18	ZINC FINGER FYVE DOMAIN CONTAINING PROTEIN
BdiBd21-3.4G0406900	0.592902	4.69E-05	0.002217635	zinc finger of the FCS type, C2 C2
BdiBd21-3.5G0257200	-0.58139	8.52E-05	0.00344886	zinc finger of the FCS type, C2 C2
BdiBd21-3.1G0838060	1.231816	7.59E-07	7.89E-05	Zinc knuckle

Supplementary Table 5.4 Subset of DEGs results according to their roles

Phytohormone signalling				
Transcript_name	**log2FoldChange**	**pvalue**	**padj**	**Annotation_from_Phytozome**
BdiBd21-3.1G0434200	-1.482603551	5.97E-09	1.20E-06	SAUR family protein
BdiBd21-3.1G0434300	-1.014090585	9.76E-07	9.86E-05	SAUR family protein
BdiBd21-3.3G0586000	-0.585703775	0.00296197	0.047033084	SAUR family protein
BdiBd21-3.4G0483700	-3.388108326	1.12E-11	5.18E-09	SAUR family protein
BdiBd21-3.5G0286800	-0.708312505	1.30E-06	0.000123385	SAUR family protein
BdiBd21-3.1G0462500	-1.371424406	3.65E-25	1.55E-21	SAUR family protein
BdiBd21-3.2G0254800	0.781256794	0.000261956	0.008200212	auxin responsive protein IAA
BdiBd21-3.1G0083000	1.345310465	1.68E-05	0.000998548	Indole 3 acetaldehyde oxidase / Indoleacetaldehyde oxidase
BdiBd21-3.1G0071600	0.809420444	0.000277383	0.008505303	Indole 3 glycerol phosphate lyase/ TSA // Tryptophan synthase / Tryptophan synthetase
BdiBd21-3.2G0449700	-2.464528586	2.41E-06	0.000205323	1 AMINOCYCLOPROPANE 1 CARBOXYLATE OXIDASE 5
BdiBd21-3.2G0688900	0.800323607	5.76E-05	0.00255319	abscisic acid receptor PYR/PYL family
BdiBd21-3.5G0004900	3.062388916	0.000814934	0.018871766	PROTEIN PHOSPHATASE 2C
BdiBd21-3.2G0061200	0.825320587	0.002709333	0.044470175	CYTOCHROME P450 FAMILY MEMBER
Transcription factors				
BdiBd21-3.1G0103400	-1.169536996	0.000448895	0.01211493	MYB FAMILY TRANSCRIPTION FACTOR
BdiBd21-3.3G0692600	1.295048505	9.44E-07	9.57E-05	MYB LIKE DNA BINDING PROTEIN MYB
BdiBd21-3.4G0318100	0.997011275	2.76E-09	5.75E-07	MYB LIKE DNA BINDING PROTEIN MYB
BdiBd21-3.4G0504000	0.752630105	0.003008207	0.04746365	MYB LIKE DNA BINDING PROTEIN MYB // MYB DOMAIN PROTEIN 42
BdiBd21-3.5G0196200	1.308680693	0.000259491	0.008141753	MYB LIKE DNA BINDING PROTEIN MYB // MYB DOMAIN PROTEIN 79
BdiBd21-3.2G0214400	0.856542393	0.001858887	0.034059519	WRKY DNA binding domain
BdiBd21-3.2G0684600	1.662622521	3.84E-05	0.001910999	WRKY DNA binding domain
BdiBd21-3.3G0345400	-1.502891903	9.05E-08	1.33E-05	HEAT SHOCK TRANSCRIPTION FACTOR
BdiBd21-3.4G0498400	-1.389251312	2.79E-12	1.45E-09	HEAT SHOCK TRANSCRIPTION FACTOR
BdiBd21-3.4G0449500	-0.863414177	0.00047821	0.012730587	HEAT SHOCK TRANSCRIPTION FACTOR // HEAT STRESS TRANSCRIPTION FACTOR B 1
BdiBd21-3.1G0007900	-2.365123192	7.34E-07	7.72E-05	ethylene-responsive transcription factor 1 (ERF1)
BdiBd21-3.1G0131000	0.651504844	6.52E-08	1.03E-05	HOMEOBOX PROTEIN TRANSCRIPTION FACTORS
BdiBd21-3.1G0773000	0.58387463	0.000118023	0.004449906	HOMEOBOX PROTEIN TRANSCRIPTION FACTORS

BdiBd21-3.3G0342500	0.647241858	0.000932071	0.020789851	HOMEOBOX PROTEIN TRANSCRIPTION FACTORS // BEL1 LIKE HOMEODOMAIN PROTEIN 6 RELATED
BdiBd21-3.4G0476100	0.918627786	7.51E-07	7.83E-05	NAC DOMAIN CONTAINING PROTEIN 38
BdiBd21-3.1G0514600	0.698972986	3.45E-05	0.001758429	NAC DOMAIN CONTAINING PROTEIN 75 RELATED
BdiBd21-3.3G0782000	2.188294111	1.63E-09	3.74E-07	NAC DOMAIN CONTAINING PROTEIN 94 RELATED
Plant pathogen interaction				
BdiBd21-3.1G0500901	1.147022849	0.001516328	0.029324128	Leucine Rich Repeat
BdiBd21-3.2G0624300	1.278600091	0.000112838	0.00429255	Leucine Rich Repeat
BdiBd21-3.2G0632400	-0.852206196	0.000741848	0.017727739	Leucine Rich Repeat
BdiBd21-3.2G0678000	0.831945592	3.69E-16	4.70E-13	Leucine Rich Repeat
BdiBd21-3.5G0183200	0.796915459	0.000525064	0.013635603	Leucine Rich Repeat
BdiBd21-3.1G0293100	0.773094476	8.55E-08	1.29E-05	LEUCINE RICH REPEAT CONTAINING PROTEIN
BdiBd21-3.1G0464600	0.704683358	1.67E-05	0.000996848	LEUCINE RICH REPEAT CONTAINING PROTEIN
BdiBd21-3.2G0496500	0.653133012	1.69E-09	3.77E-07	LEUCINE RICH REPEAT CONTAINING PROTEIN
BdiBd21-3.2G0773700	0.938379835	3.68E-05	0.001844405	LEUCINE RICH REPEAT CONTAINING PROTEIN
BdiBd21-3.2G0773800	1.537836675	1.89E-05	0.001101062	LEUCINE RICH REPEAT CONTAINING PROTEIN
BdiBd21-3.3G0200700	1.157178513	3.94E-16	4.77E-13	LEUCINE RICH REPEAT CONTAINING PROTEIN
BdiBd21-3.4G0089900	1.461348475	1.12E-09	2.69E-07	LEUCINE RICH REPEAT CONTAINING PROTEIN
BdiBd21-3.4G0135600	0.995235013	1.61E-16	2.56E-13	LEUCINE RICH REPEAT CONTAINING PROTEIN
BdiBd21-3.4G0135700	1.127946849	9.95E-11	3.24E-08	LEUCINE RICH REPEAT CONTAINING PROTEIN
BdiBd21-3.4G0139532	-0.863809609	0.001939455	0.035131031	LEUCINE RICH REPEAT CONTAINING PROTEIN
BdiBd21-3.4G0141600	0.737004974	0.000187653	0.006391132	LEUCINE RICH REPEAT CONTAINING PROTEIN
BdiBd21-3.4G0144600	1.048287411	4.52E-09	9.27E-07	LEUCINE RICH REPEAT CONTAINING PROTEIN
BdiBd21-3.4G0196300	1.442043189	0.00010508	0.004051966	LEUCINE RICH REPEAT CONTAINING PROTEIN
BdiBd21-3.4G0197600	2.315632658	2.06E-05	0.001167798	LEUCINE RICH REPEAT CONTAINING PROTEIN
BdiBd21-3.4G0595401	0.624113607	0.001168004	0.024147608	LEUCINE RICH REPEAT CONTAINING PROTEIN
BdiBd21-3.4G0613000	0.621599297	4.82E-10	1.29E-07	LEUCINE RICH REPEAT CONTAINING PROTEIN
BdiBd21-3.5G0012000	0.79722628	5.86E-07	6.45E-05	LEUCINE RICH REPEAT CONTAINING PROTEIN
BdiBd21-3.5G0057000	0.725736562	7.18E-14	5.22E-11	LEUCINE RICH REPEAT CONTAINING PROTEIN
BdiBd21-3.4G0182350	-1.763509321	7.18E-05	0.003028586	LEUCINE RICH REPEAT CONTAINING PROTEIN
BdiBd21-3.4G0532900	0.651340066	4.49E-06	0.000344519	LEUCINE RICH REPEAT CONTAINING PROTEIN
BdiBd21-3.5G0359100	-1.521321251	0.000436493	0.011868311	Leucine rich repeat N terminal domain
BdiBd21-3.5G0359200	3.068661777	4.44E-07	5.14E-05	Leucine rich repeat N terminal domain

BdiBd21-3.3G0344300	-1.697735101	7.18E-09	1.40E-06	CHITINASE
BdiBd21-3.3G0344500	-1.045051435	0.000765094	0.018046016	CHITINASE
BdiBd21-3.2G0246100	0.816866668	0.000423371	0.011548555	BETA 1,3 GLUCANASE
BdiBd21-3.1G1043500	-1.578102509	1.40E-06	0.000130772	Plant thionin
Stress tolerance				
BdiBd21-3.2G0331300	-1.033923201	0.000247577	0.007866197	GLUTATHIONE S TRANSFERASE, GST, SUPERFAMILY, GST DOMAIN CONTAINING
BdiBd21-3.1G0053400	1.698452121	0.000516187	0.013487645	GLUTATHIONE S TRANSFERASE
BdiBd21-3.2G0450600	0.699194673	0.000493475	0.013080238	GLUTATHIONE S TRANSFERASE, GST, SUPERFAMILY, GST DOMAIN CONTAINING
BdiBd21-3.2G0779900	-0.989225343	2.37E-05	0.001292007	GLUTATHIONE S TRANSFERASE, GST, SUPERFAMILY, GST DOMAIN CONTAINING
BdiBd21-3.1G0660150	1.722578528	0.001452046	0.028492338	GLUTATHIONE S TRANSFERASE, GST, SUPERFAMILY, GST DOMAIN CONTAINING
BdiBd21-3.1G0888800	-0.69374122	4.73E-07	5.40E-05	GLUTATHIONE S TRANSFERASE, GST, SUPERFAMILY, GST DOMAIN CONTAINING
BdiBd21-3.2G0174500	-2.422534788	6.15E-08	9.85E-06	GLUTATHIONE S TRANSFERASE, GST, SUPERFAMILY, GST DOMAIN CONTAINING
BdiBd21-3.2G0601500	-0.732430397	5.74E-10	1.50E-07	GLUTATHIONE S TRANSFERASE, GST, SUPERFAMILY, GST DOMAIN CONTAINING
BdiBd21-3.3G0415200	-0.727467761	1.96E-06	0.000173538	GLUTATHIONE S TRANSFERASE, GST, SUPERFAMILY, GST DOMAIN CONTAINING
Phenyl propanoid pathway				
BdiBd21-3.3G0074600	0.732481796	0.000348321	0.010042968	4 coumarate CoA ligase / 4 coumaryl CoA synthetase // Trans feruloyl CoA synthase / Trans feruloyl CoA synthetase
BdiBd21-3.2G0704400	0.832474077	0.000215741	0.007012281	LACCASE 7 RELATED
BdiBd21-3.1G0107700	0.613048938	0.000549918	0.014015711	Peroxidase
BdiBd21-3.1G0233000	0.864440638	6.75E-08	1.06E-05	Peroxidase / Lactoperoxidase
BdiBd21-3.3G0484500	-0.960416698	1.17E-09	2.75E-07	Quinate O hydroxycinnamoyltransferase / Hydroxycinnamoyl coenzyme A quinate transferase
BdiBd21-3.1G0639400	0.758912275	8.00E-06	0.000552005	O METHYLTRANSFERASE RELATED
BdiBd21-3.1G1036000	3.103803505	0.000739337	0.017712577	ferulate 5 hydroxylase
BdiBd21-3.3G0401900	1.577343074	5.36E-15	4.87E-12	ferulate 5 hydroxylase
BdiBd21-3.5G0189100	1.070666685	2.87E-13	1.78E-10	shikimate O hydroxycinnamoyltransferase
BdiBd21-3.3G0084500	0.869883942	1.61E-05	0.000968267	CINNAMYL ALCOHOL DEHYDROGENASE 4 RELATED

Flavonoid biosynthesis				
BdiBd21-3.2G0627900	0.620240962	0.001213064	0.024797166	GLUCOSYL/GLUCURONOSYL TRANSFERASES
BdiBd21-3.4G0238700	0.818502344	0.001139968	0.023858697	flavonoid 3' monooxygenase
BdiBd21-3.2G0164900	0.646528495	0.002187691	0.038107975	UDP GLYCOSYLTRANSFERASE 75B1 RELATED
Jasmonic acid biosynthesis				
BdiBd21-3.1G0126600	-0.830893505	0.000718383	0.017264257	LIPOXYGENASE
BdiBd21-3.5G0138400	0.682389209	0.00064455	0.015926016	Allene oxide cyclase
Signal transduction				
BdiBd21-3.4G0485400	0.631705908	3.86E-11	1.43E-08	CENTAURIN/ARF // ADP RIBOSYLATION FACTOR GTPASE ACTIVATING PROTEIN AGD3
BdiBd21-3.3G0444800	0.617751377	7.09E-10	1.79E-07	GTP BINDING PROTEIN RELATED // P LOOP CONTAINING NUCLEOSIDE TRIPHOSPHATE HYDROLASES SUPERFAMILY PROTEIN
BdiBd21-3.2G0449700	-2.464528586	2.41E-06	0.000205323	OXIDOREDUCTASE, 2OG FE II OXYGENASE FAMILY PROTEIN // 1 AMINOCYCLOPROPANE 1 CARBOXYLATE OXIDASE 5
BdiBd21-3.5G0144800	0.657242053	0.00205429	0.036357213	RESPONSE REGULATOR OF TWO COMPONENT SYSTEM
Ion Transport				
BdiBd21-3.3G0632700	0.752904311	0.001573395	0.030198264	High affinity nitrate transporter accessory
BdiBd21-3.3G0015300	2.435367856	3.88E-11	1.43E-08	MFS transporter, NNP family, nitrate/nitrite transporter
BdiBd21-3.2G0435300	2.467948103	0.002655284	0.043852674	inorganic pyrophosphatase
BdiBd21-3.5G0033500	-2.279903448	6.24E-07	6.80E-05	MFS transporter, PHS family, inorganic phosphate transporter
BdiBd21-3.5G0317700	1.02641053	4.18E-12	2.13E-09	SULFATE TRANSPORTER
BdiBd21-3.2G0618100	-0.908826608	0.000258822	0.008132126	SULFATE TRANSPORTER 3.5 RELATED
BdiBd21-3.3G0604000	0.976414573	0.000615298	0.015412737	AMMONIUM TRANSPORTER
BdiBd21-3.4G0433000	1.359786252	9.62E-06	0.000644382	IONOTROPIC GLUTAMATE RECEPTOR
BdiBd21-3.1G0420600	0.832221509	4.37E-05	0.002103721	IONOTROPIC GLUTAMATE RECEPTOR // GLUTAMATE RECEPTOR 2.5 RELATED
BdiBd21-3.4G0433100	1.26346543	7.21E-05	0.003032407	IONOTROPIC GLUTAMATE RECEPTOR // GLUTAMATE RECEPTOR 2.5 RELATED
BdiBd21-3.2G0531400	1.251792517	0.000458934	0.012320528	IONOTROPIC GLUTAMATE RECEPTOR // GLUTAMATE RECEPTOR IIA RELATED
BdiBd21-3.3G0292300	1.744367382	0.001001975	0.021795093	INORGANIC PHOSPHATE TRANSPORTER 1 4
BdiBd21-3.1G0176300	1.50074227	6.68E-05	0.002866106	NA+/CA2+ K+ INDEPENDENT EXCHANGER // CATION/CALCIUM EXCHANGER 1

BdiBd21-3.2G0719800	0.586298446	1.12E-10	3.62E-08	Aspartate transaminase / Transaminase A // Aspartate prephenate aminotransferase / Prephenate transaminase // Glutamate prephenate aminotransferase / Prephenate transaminase
BdiBd21-3.2G0400800	0.715091382	0.000187775	0.006391132	AQUAPORIN TRANSPORTER
BdiBd21-3.4G0509700	0.664720091	0.001822259	0.033557512	AQUAPORIN TRANSPORTER
BdiBd21-3.5G0207900	-0.634506832	6.34E-05	0.002762796	AQUAPORIN TRANSPORTER
BdiBd21-3.1G0380500	-0.67649925	0.001387596	0.027503363	AQUAPORIN TRANSPORTER // AQUAPORIN PIP2 4 RELATED
BdiBd21-3.1G0067500	0.248144778	6.80E-08	1.06E-05	UNCHARACTERIZED NODULIN LIKE PROTEIN
BdiBd21-3.4G0425900	0.710855373	1.76E-06	0.000157354	SUGAR TRANSPORT PROTEIN 7
BdiBd21-3.4G0409200	0.809431729	2.29E-06	0.000195423	Sugar transporter/spinster transmembrane protein
BdiBd21-3.1G0960000	0.752920267	5.03E-05	0.002322101	Sugar (and other) transporter (Sugar tr)
BdiBd21-3.1G0960100	0.669470335	0.000290117	0.008789845	Sugar (and other) transporter (Sugar tr)
BdiBd21-3.4G0425900	0.710855373	1.76E-06	0.000157354	SUGAR TRANSPORT PROTEIN 7
BdiBd21-3.4G0409200	0.809431729	2.29E-06	0.000195423	Sugar transporter/spinster transmembrane protein
BdiBd21-3.3G0800200	-0.761194485	0.266418347	0.00017963	Sugar (and other) transporter (Sugar tr) // Major Facilitator Superfamily (MFS 1)
Biosynthesis of secondary metabolites				
BdiBd21-3.1G0107700	0.613048938	0.000549918	0.014015711	Peroxidase
BdiBd21-3.1G0176900	1.130342321	2.68E-11	1.03E-08	5 methyltetrahydropteroyltriglutamate homocysteine S methyltransferase / Tetrahydropteroylglutamate homocysteine transmethylase
BdiBd21-3.1G0233000	0.864440638	6.75E-08	1.06E-05	Peroxidase / Lactoperoxidase
BdiBd21-3.1G0251800	0.639487362	3.65E-05	0.001838023	GLYCOSYL HYDROLASE
BdiBd21-3.1G0278100	0.810259847	5.06E-06	0.000375366	S-(hydroxymethyl)glutathione dehydrogenase / alcohol dehydrogenase (frmA)
BdiBd21-3.1G0410000	1.039185743	0.001655056	0.031293588	Very long chain 3 oxoacyl CoA synthase / Very long chain beta ketoacyl CoA synthase
BdiBd21-3.1G0537900	2.762235168	0.001135274	0.023838883	Peroxidase / Lactoperoxidase
BdiBd21-3.1G0639400	0.758912275	8.00E-06	0.000552005	O METHYLTRANSFERASE RELATED
BdiBd21-3.1G0729500	1.882694684	0.000181118	0.006220601	1 deoxy D xylulose 5 phosphate synthase / DXP synthase
BdiBd21-3.1G0826000	4.687322836	9.62E-17	1.63E-13	Very long chain 3 oxoacyl CoA synthase / Very long chain beta ketoacyl CoA synthase
BdiBd21-3.1G0857000	0.760703778	0.002993046	0.047371284	Phosphoglycerate mutase
BdiBd21-3.1G0912100	1.142639057	0.000911275	0.020433431	phosphoenolpyruvate carboxykinase
BdiBd21-3.1G0938800	1.067369736	0.000550165	0.014015711	Homocysteine S methyltransferase
BdiBd21-3.1G0938900	1.308494594	1.28E-10	4.06E-08	KETOACYL COA SYNTHASE 5 RELATED

BdiBd21-3.2G0128900	0.643329868	3.91E-06	0.000306496	ELECTRON TRANSFER FLAVOPROTEIN UBIQUINONE OXIDOREDUCTASE
BdiBd21-3.2G0162100	0.691785173	6.01E-05	0.002640447	S adenosylmethionine synthetase
BdiBd21-3.2G0162200	0.610444515	5.00E-06	0.000374487	S adenosylmethionine synthetase
BdiBd21-3.2G0176200	2.855368714	0.001392072	0.027549167	Peroxidase / Lactoperoxidase
BdiBd21-3.2G0627900	0.620240962	0.001213064	0.024797166	GLUCOSYL/GLUCURONOSYL TRANSFERASES
BdiBd21-3.2G0719800	0.586298446	1.12E-10	3.62E-08	Aspartate transaminase / Transaminase A // Aspartate prephenate aminotransferase / Prephenate transaminase // Glutamate prephenate aminotransferase / Prephenate transaminase
BdiBd21-3.2G0737400	0.63100566	6.61E-10	1.68E-07	beta glucosidase
BdiBd21-3.3G0074600	0.732481796	0.000348321	0.010042968	4 coumarate CoA ligase / 4 coumaryl CoA synthetase // Trans feruloyl CoA synthase / Trans feruloyl CoA synthetase
BdiBd21-3.3G0370600	1.069519973	0.000640343	0.01585286	STEROL DESATURASE
BdiBd21-3.3G0490300	2.442665499	3.67E-10	1.00E-07	ANCIENT UBIQUITOUS PROTEIN
BdiBd21-3.3G0650600	0.980385051	8.73E-06	0.000592497	PROTEIN CER1 LIKE 1 RELATED
BdiBd21-3.4G0238700	0.818502344	0.001139968	0.023858697	flavonoid 3' monooxygenase
BdiBd21-3.5G0080500	0.757518708	2.15E-05	0.00119974	ALCOHOL DEHYDROGENASE RELATED
BdiBd21-3.5G0138400	0.682389209	0.00064455	0.015926016	Allene oxide cyclase
BdiBd21-3.5G0189100	1.070666685	2.87E-13	1.78E-10	shikimate O hydroxycinnamoyltransferase
BdiBd21-3.5G0217300	1.684169008	5.15E-08	8.29E-06	NA
BdiBd21-3.5G0279900	0.807157601	8.55E-05	0.003452238	ent-kaurene synthase (E4.2.3.19)
BdiBd21-3.4G0416800	0.907892886	0.000148614	0.00529723	ENDO 1,4 BETA GLUCANASE
BdiBd21-3.3G0051600	0.702702994	0.001432223	0.028233986	ENDO 1,4 BETA GLUCANASE
Cellulose biosynthesis				
BdiBd21-3.4G0416800	0.907892886	0.000148614	0.00529723	ENDO 1,4 BETA GLUCANASE
BdiBd21-3.3G0051600	0.702702994	0.001432223	0.028233986	ENDO 1,4 BETA GLUCANASE
Starch and sucrose metabolism				
BdiBd21-3.1G0361100	0.953268829	0.003098206	0.048479472	TREHALOSE 6 PHOSPHATE SYNTHASE
BdiBd21-3.1G0251800	0.639487362	3.65E-05	0.001838023	GLYCOSYL HYDROLASE

8. REFERENCES

Abbas, H.M.K., Ahmad, A., Dong, W., Xiang, J., Iqbal, J., Ali, S., Akram, W. and Zhong, Y.-J. (2020) Heterologous WRKY and NAC transcription factors triggered resistance in Nicotiana benthamiana. *Journal of King Saud University-Science*, **32**, 3005-3013.

Abdullahi, S., Haris, H., Zarkasi, K.Z. and Amir, H.G. (2021) Complete genome sequence of plant growth-promoting and heavy metal-tolerant Enterobacter tabaci 4M9 (CCB-MBL 5004). *Journal of Basic Microbiology*, **61**, 293-304.

Adeleke, R., Nwangburuka, C. and Oboirien, B. (2017) Origins, roles and fate of organic acids in soils: A review. *South African Journal of Botany*, **108**, 393-406.

Adeyemo, O.S., Hyde, P.T. and Setter, T.L. (2019) Identification of FT family genes that respond to photoperiod, temperature and genotype in relation to flowering in cassava (Manihot esculenta, Crantz). *Plant reproduction*, **32**, 181-191.

Agake, S.-i., do Amaral, F.P., Yamada, T., Sekimoto, H., Stacey, G., Yokoyama, T. and Ohkama-Ohtsu, N. (2022) Plant Growth-promoting Effects of Viable and Dead Spores of Bacillus pumilus TUAT1 on Setaria viridis. *Microbes and environments*, **37**, ME21060.

Ahemad, M. and Khan, M.S. (2012) Effects of pesticides on plant growth promoting traits of Mesorhizobium strain MRC4. *Journal of the Saudi Society of Agricultural Sciences*, **11**, 63-71.

Ahmad, J.S. and Baker, R. (1987) Rhizosphere competence of Trichoderma harzianum. *Phytopathology*, **77**, 182-189.

Akinrinlola, R.J., Yuen, G.Y., Drijber, R.A. and Adesemoye, A.O. (2018) Evaluation of Bacillus strains for plant growth promotion and predictability of efficacy by in vitro physiological traits. *International journal of microbiology*, **2018**.

Al-Ali, A., Deravel, J., Krier, F., Béchet, M., Ongena, M. and Jacques, P. (2018) Biofilm formation is determinant in tomato rhizosphere colonization by Bacillus velezensis FZB42. *Environmental Science and Pollution Research*, **25**, 29910-29920.

Alaa, F.M. (2018) Effectiveness of exopolysaccharides and biofilm forming plant growth promoting rhizobacteria on salinity tolerance of faba bean (Vicia faba L.). *African Journal of Microbiology Research*, **12**, 399-404.

Allard-Massicotte, R., Tessier, L., LÚcuyer, F., Lakshmanan, V., Lucier, J.-F., Garneau, D., Caudwell, L., Vlamakis, H., Bais, H.P. and Beauregard, P.B. (2016) Bacillus subtilis early colonization of Arabidopsis thaliana roots involves multiple chemotaxis receptors. *MBio*, **7**, e01664-01616.

Amasino, R.M. and Michaels, S.D. (2010) The timing of flowering. *Plant Physiol.*, **154**, 516-520.

An, T., Cai, Y., Zhao, S., Zhou, J., Song, B., Bux, H. and Qi, X. (2016) Brachypodium distachyon T-DNA insertion lines: a model pathosystem to study nonhost resistance to wheat stripe rust. *Scientific reports*, **6**, 1-9.

Andrews, S. (2010) FastQC: a quality control tool for high throughput sequence data: Babraham Bioinformatics, Babraham Institute, Cambridge, United Kingdom.

Ansari, F., Jabeen, M. and Ahmad, I. (2021) Pseudomonas azotoformans FAP5, a novel biofilm-forming PGPR strain, alleviates drought stress in wheat plant. *International Journal of Environmental Science and Technology*, **18**, 3855-3870.

Araujo, W.L., NUNES-NESI, A., Nikoloski, Z., Sweetlove, L.J. and Fernie, A.R. (2012) Metabolic control and regulation of the tricarboxylic acid cycle in photosynthetic and heterotrophic plant tissues. *Plant, cell & environment*, **35**, 1-21.

Arshad, M. and Frankenberger Jr, W.T. (1997) Plant growth-regulating substances in the rhizosphere: microbial production and functions. *Advances in agronomy*, **62**, 45-151.

Asari, S., Tarkowská, D., Rolčík, J., Novák, O., Palmero, D.V., Bejai, S. and Meijer, J. (2017) Analysis of plant growth-promoting properties of Bacillus amyloliquefaciens UCMB5113 using Arabidopsis thaliana as host plant. *Planta*, **245**, 15-30.

Baddal, B., Muzzi, A., Censini, S., Calogero, R.A., Torricelli, G., Guidotti, S., Taddei, A.R., Covacci, A., Pizza, M. and Rappuoli, R. (2015) Dual RNA-seq of nontypeable Haemophilus influenzae and host cell transcriptomes reveals novel insights into host-pathogen cross talk. *MBio*, **6**, e01765-01715.

Badri, D.V. and Vivanco, J.M. (2009) Regulation and function of root exudates. *Plant, cell & environment*, **32**, 666-681.

Bais, H.P., Fall, R. and Vivanco, J.M. (2004) Biocontrol of Bacillus subtilis against infection of Arabidopsis roots by Pseudomonas syringae is facilitated by biofilm formation and surfactin production. *Plant physiology*, **134**, 307-319.

Bakker, P., Ran, L., Pieterse, C. and Van Loon, L. (2003) Understanding the involvement of rhizobacteria-mediated induction of systemic resistance in biocontrol of plant diseases. *Canadian Journal of Plant Pathology*, **25**, 5-9.

Bar-Ness, E., Chen, Y., Hadar, Y., Marschner, H. and Römheld, V. (1991) Siderophores of Pseudomonas putida as an iron source for dicot and monocot plants. In *Iron nutrition and interactions in plants*: Springer, pp. 271-281.

Bartolini, M., Cogliati, S., Vileta, D., Bauman, C., Rateni, L., Leñini, C., Argañaraz, F., Francisco, M., Villalba, J. and Steil, L. (2019) Regulation of biofilm aging and dispersal in Bacillus subtilis by the alternative sigma factor SigB. *Journal of bacteriology*, **201**, e00473-00418.

Batista, B.D., Dourado, M.N., Figueredo, E.F., Hortencio, R.O., Marques, J.P.R., Piotto, F.A., Bonatelli, M.L., Settles, M.L., Azevedo, J.L. and Quecine, M.C. (2021) The auxin-producing Bacillus thuringiensis RZ2MS9 promotes the growth and modifies the root architecture of tomato (Solanum lycopersicum cv. Micro-Tom). *Archives of Microbiology*, **203**, 3869-3882.

Be'er, A. and Harshey, R.M. (2011) Collective motion of surfactant-producing bacteria imparts superdiffusivity to their upper surface. *Biophysical journal*, **101**, 1017-1024.

Beattie, G.A. (2007) Plant-associated bacteria: survey, molecular phylogeny, genomics and recent advances. *Plant-associated bacteria*, 1-56.

Beauregard, P.B. (2015) Not just sweet talkers: How roots stimulate their colonization by beneficial bacteria. In *Advances in botanical research*: Elsevier, pp. 1-20.

Benizri, E., Baudoin, E. and Guckert, A. (2001) Root colonization by inoculated plant growth-promoting rhizobacteria. *Biocontrol science and technology*, **11**, 557-574.

Bernier, G., Havelange, A.e., Houssa, C., Petitjean, A. and Lejeune, P. (1993) Physiological signals that induce flowering. *The Plant Cell*, **5**, 1147.

Bettgenhaeuser, J., Corke, F.M., Opanowicz, M., Green, P., Hernández-Pinzón, I., Doonan, J.H. and Moscou, M.J. (2017) Natural variation in Brachypodium links vernalization and flowering time loci as major flowering determinants. *Plant Physiology*, **173**, 256-268.

Bevan, M.W., Garvin, D.F. and Vogel, J.P. (2010) Brachypodium distachyon genomics for sustainable food and fuel production. *Current Opinion in Biotechnology*, **21**, 211-217.

Bhattacharyya, C., Bakshi, U., Mallick, I., Mukherji, S., Bera, B. and Ghosh, A. (2017) Genome-guided insights into the plant growth promotion capabilities of the physiologically versatile Bacillus aryabhattai strain AB211. *Frontiers in microbiology*, **8**, 411.

Bhattacharyya, P.N. and Jha, D.K. (2012) Plant growth-promoting rhizobacteria (PGPR): emergence in agriculture. *World Journal of Microbiology and Biotechnology*, **28**, 1327-1350.

Bodenhausen, N., Bortfeld-Miller, M., Ackermann, M. and Vorholt, J.A. (2014) A synthetic community approach reveals plant genotypes affecting the phyllosphere microbiota. *PLoS Genet.*, **10**, e1004283.

Bogino, P.C., de las Mercedes Oliva, M., Sorroche, F.G. and Giordano, W. (2013) The role of bacterial biofilms and surface components in plant-bacterial associations. *International journal of molecular sciences*, **14**, 15838-15859.

Bolger, A.M., Lohse, M. and Usadel, B. (2014) Trimmomatic: a flexible trimmer for Illumina sequence data. *Bioinformatics*, **30**, 2114-2120.

Bouché, F., D'Aloia, M., Tocquin, P., Lobet, G., Detry, N. and Périlleux, C. (2016) Integrating roots into a whole plant network of flowering time genes in Arabidopsis thaliana. *Scientific reports*, **6**, 1-12.

Bragg, J.N., Wu, J., Gordon, S.P., Guttman, M.E., Thilmony, R., Lazo, G.R., Gu, Y.Q. and Vogel, J.P. (2012a) Generation and characterization of the Western Regional Research Center Brachypodium T-DNA insertional mutant collection.

Bragg, J.N., Wu, J., Gordon, S.P., Guttman, M.E., Thilmony, R., Lazo, G.R., Gu, Y.Q. and Vogel, J.P. (2012b) Generation and characterization of the Western Regional Research Center Brachypodium T-DNA insertional mutant collection. *PLoS One*, **7**, e41916.

Branda, S.S., Chu, F., Kearns, D.B., Losick, R. and Kolter, R. (2006) A major protein component of the Bacillus subtilis biofilm matrix. *Molecular microbiology*, **59**, 1229-1238.

Branda, S.S., González-Pastor, J.E., Ben-Yehuda, S., Losick, R. and Kolter, R. (2001) Fruiting body formation by Bacillus subtilis. *Proceedings of the National Academy of Sciences*, **98**, 11621-11626.

Branda, S.S., González-Pastor, J.E., Dervyn, E., Ehrlich, S.D., Losick, R. and Kolter, R. (2004) Genes involved in formation of structured multicellular communities by Bacillus subtilis. *Journal of bacteriology*, **186**, 3970-3979.

Bringel, F. and Couée, I. (2015) Pivotal roles of phyllosphere microorganisms at the interface between plant functioning and atmospheric trace gas dynamics. *Frontiers in microbiology*, **6**, 486.

Brkljacic, J., Grotewold, E., Scholl, R., Mockler, T., Garvin, D.F., Vain, P., Brutnell, T., Sibout, R., Bevan, M. and Budak, H. (2011) Brachypodium as a model for the grasses: today and the future. *Plant Physiology*, **157**, 3-13.

Brusamarello-Santos, L., Pacheco, F., Aljanabi, S., Monteiro, R., Cruz, L., Baura, V., Pedrosa, F., Souza, E. and Wassem, R. (2012) Differential gene expression of rice roots inoculated with the diazotroph Herbaspirillum seropedicae. *Plant and Soil*, **356**, 113-125.

Brusamarello-Santos, L.C.C., Alberton, D., Valdameri, G., Camilios-Neto, D., Covre, R., Lopes, K.d.P., Zibetti Tadra-Sfeir, M., Faoro, H., Adele Monteiro, R. and Barbosa-Silva, A. (2019) Modulation of defence and iron homeostasis genes in rice roots by the diazotrophic endophyte Herbaspirillum seropedicae. *Scientific reports*, **9**, 1-15.

Bu, D., Luo, H., Huo, P., Wang, Z., Zhang, S., He, Z., Wu, Y., Zhao, L., Liu, J. and Guo, J. (2021) KOBAS-i: intelligent prioritization and exploratory visualization of biological functions for gene enrichment analysis. *Nucleic acids research*, **49**, W317-W325.

Bukhat, S., Imran, A., Javaid, S., Shahid, M., Majeed, A. and Naqqash, T. (2020) Communication of plants with microbial world: Exploring the regulatory networks for PGPR mediated defense signaling. *Microbiological research*, **238**, 126486.

Bulgarelli, D., Garrido-Oter, R., Münch, P.C., Weiman, A., Dröge, J., Pan, Y., McHardy, A.C. and Schulze-Lefert, P. (2015) Structure and function of the bacterial root microbiota in wild and domesticated barley. *Cell host & microbe*, **17**, 392-403.

Bünning, E. (1989) *Ahead of His Time, Wilhelm Pfeffer: Early Advances in Plant Biology*: McGill-Queen's Press-MQUP.

Cairns, L.S., Hobley, L. and Stanley-Wall, N.R. (2014) Biofilm formation by B acillus subtilis: new insights into regulatory strategies and assembly mechanisms. *Molecular microbiology*, **93**, 587-598.

Calvo, P. (2013) Effect of Microbial Inoculation on Nitrogen Plant Uptake and Nitrogen Losses from Soil and Plant-Soil Systems: Doctoral Dissertation, Auburn University, Auburn, AL.

Calvo, P., Ormeño-Orrillo, E., Martínez-Romero, E. and Zúñiga, D. (2010) Characterization of Bacillus isolates of potato rhizosphere from andean soils of Peru and their potential PGPR characteristics. *Brazilian Journal of Microbiology*, **41**, 899-906.

Calvo, P., Zebelo, S., McNear, D., Kloepper, J. and Fadamiro, H. (2019) Plant growth-promoting rhizobacteria induce changes in Arabidopsis thaliana gene expression of nitrate and ammonium uptake genes. *Journal of Plant Interactions*, **14**, 224-231.

Camilios-Neto, D., Bonato, P., Wassem, R., Tadra-Sfeir, M.Z., Brusamarello-Santos, L.C., Valdameri, G., Donatti, L., Faoro, H., Weiss, V.A. and Chubatsu, L.S. (2014a) Dual RNA-seq transcriptional analysis of wheat roots colonized by Azospirillum brasilense reveals up-regulation of nutrient acquisition and cell cycle genes. *BMC genomics*, **15**, 378.

Camilios-Neto, D., Bonato, P., Wassem, R., Tadra-Sfeir, M.Z., Brusamarello-Santos, L.C., Valdameri, G., Donatti, L., Faoro, H., Weiss, V.A. and Chubatsu, L.S. (2014b) Dual RNA-seq transcriptional analysis of wheat roots colonized by Azospirillum brasilense reveals up-regulation of nutrient acquisition and cell cycle genes. *BMC genomics*, **15**, 1-13.

Canarini, A., Kaiser, C., Merchant, A., Richter, A. and Wanek, W. (2019) Root exudation of primary metabolites: mechanisms and their roles in plant responses to environmental stimuli. *Frontiers in Plant Science*, **10**, 157.

Cao, Y., Zhang, Z., Ling, N., Yuan, Y., Zheng, X., Shen, B. and Shen, Q. (2011) Bacillus subtilis SQR 9 can control Fusarium wilt in cucumber by colonizing plant roots. *Biology and fertility of soils*, **47**, 495-506.

Cartieaux, F., Contesto, C., Gallou, A., Desbrosses, G., Kopka, J., Taconnat, L., Renou, J.-P. and Touraine, B. (2008) Simultaneous interaction of Arabidopsis thaliana with Bradyrhizobium sp. strain ORS278 and Pseudomonas syringae pv. tomato DC3000 leads to complex transcriptome changes. *Molecular plant-microbe interactions*, **21**, 244-259.

Chandler, D., Davidson, G., Grant, W., Greaves, J. and Tatchell, G. (2008) Microbial biopesticides for integrated crop management: an assessment of environmental and regulatory sustainability. *Trends in Food Science & Technology*, **19**, 275-283.

Chang, W.-S., Van De Mortel, M., Nielsen, L., Nino de Guzman, G., Li, X. and Halverson, L.J. (2007) Alginate production by Pseudomonas putida creates a hydrated

microenvironment and contributes to biofilm architecture and stress tolerance under water-limiting conditions: Am Soc Microbiol.

Chaparro, J.M., Badri, D.V., Bakker, M.G., Sugiyama, A., Manter, D.K. and Vivanco, J.M. (2013) Root exudation of phytochemicals in Arabidopsis follows specific patterns that are developmentally programmed and correlate with soil microbial functions. *PloS one*, **8**, e55731.

Chaudhry, V., Sharma, S., Bansal, K. and Patil, P.B. (2017) Glimpse into the Genomes of Rice Endophytic Bacteria: Diversity and Distribution of Firmicutes. *Frontiers in microbiology*, **7**, 2115.

Chauhan, P.S., Lata, C., Tiwari, S., Chauhan, A.S., Mishra, S.K., Agrawal, L., Chakrabarty, D. and Nautiyal, C.S. (2019) Transcriptional alterations reveal Bacillus amyloliquefaciens-rice cooperation under salt stress. *Scientific reports*, **9**, 1-13.

Chen, Y., Cao, S., Chai, Y., Clardy, J., Kolter, R., Guo, J.h. and Losick, R. (2012) A Bacillus subtilis sensor kinase involved in triggering biofilm formation on the roots of tomato plants. *Molecular microbiology*, **85**, 418-430.

Chittem, K., Yajima, W.R., Goswami, R.S. and del Río Mendoza, L.E. (2020) Transcriptome analysis of the plant pathogen Sclerotinia sclerotiorum interaction with resistant and susceptible canola (Brassica napus) lines. *PLoS One*, **15**, e0229844.

Chun, H.J., Baek, D., Cho, H.M., Lee, S.H., Jin, B.J., Yun, D.-J., Hong, Y.-S. and Kim, M.C. (2019) Lignin biosynthesis genes play critical roles in the adaptation of Arabidopsis plants to high-salt stress. *Plant signaling & behavior*, **14**, 1625697.

Czaczyk, K. and Myszka, K. (2007) Biosynthesis of extracellular polymeric substances (EPS) and its role in microbial biofilm formation. *Polish Journal of Environmental Studies*, **16**.

Dauwe, R., Morreel, K., Goeminne, G., Gielen, B., Rohde, A., Van Beeumen, J., Ralph, J., Boudet, A.M., Kopka, J. and Rochange, S.F. (2007) Molecular phenotyping of lignin-modified tobacco reveals associated changes in cell-wall metabolism, primary metabolism, stress metabolism and photorespiration. *The Plant Journal*, **52**, 263-285.

Davey, M.E. and O'toole, G.A. (2000) Microbial biofilms: from ecology to molecular genetics. *Microbiology and molecular biology reviews*, **64**, 847-867.

de Weert, S., Vermeiren, H., Mulders, I.H., Kuiper, I., Hendrickx, N., Bloemberg, G.V., Vanderleyden, J., De Mot, R. and Lugtenberg, B.J. (2002) Flagella-driven chemotaxis towards exudate components is an important trait for tomato root colonization by Pseudomonas fluorescens. *Molecular Plant-Microbe Interactions*, **15**, 1173-1180.

De Zelicourt, A., Al-Yousif, M. and Hirt, H. (2013) Rhizosphere microbes as essential partners for plant stress tolerance. *Molecular plant*, **6**, 242-245.

Deng, X., An, B., Zhong, H., Yang, J., Kong, W. and Li, Y. (2019) A novel insight into functional divergence of the MST gene family in rice based on comprehensive expression patterns. *Genes*, **10**, 239.

Dennis, E.S. and Peacock, W.J. (2009) Vernalization in cereals. *J. Biol.*, **8**, 1-4.

Dennis, P.G., Miller, A.J. and Hirsch, P.R. (2010) Are root exudates more important than other sources of rhizodeposits in structuring rhizosphere bacterial communities? *FEMS microbiology ecology*, **72**, 313-327.

Derbyshire, P. and Byrne, M.E. (2013) MORE SPIKELETS1 is required for spikelet fate in the inflorescence of Brachypodium. *Plant physiology*, **161**, 1291-1302.

Desbrosses, G., Contesto, C., Varoquaux, F., Galland, M. and Touraine, B. (2009) PGPR-Arabidopsis interactions is a useful system to study signaling pathways involved in plant developmental control. *Plant Signaling & Behavior*, **4**, 319-321.

Desrut, A., Thibault, F., Mercado-Blanco, J., Coutos-Thévenot, P. and Vriet, C. (2021) Transcriptional regulation of plant sugar transporter genes by beneficial rhizobacteria. *Journal of Plant Interactions*, **16**, 443-451.

Distelfeld, A., Li, C. and Dubcovsky, J. (2009) Regulation of flowering in temperate cereals. *Curr. Opin. Plant Biol.*, **12**, 178-184.

Do Amaral, F.P., Pankievicz, V., Arisi, A.C.M., de Souza, E.M., Pedrosa, F. and Stacey, G. (2016) Differential growth responses of Brachypodium distachyon genotypes to inoculation with plant growth promoting rhizobacteria. *Plant molecular biology*, **90**, 689-697.

Dobbelaere, S., Vanderleyden, J. and Okon, Y. (2003) Plant growth-promoting effects of diazotrophs in the rhizosphere. *Critical reviews in plant sciences*, **22**, 107-149.

Dobin, A., Davis, C.A., Schlesinger, F., Drenkow, J., Zaleski, C., Jha, S., Batut, P., Chaisson, M. and Gingeras, T.R. (2013) STAR: ultrafast universal RNA-seq aligner. *Bioinformatics*, **29**, 15-21.

Dodd, I., Zinovkina, N., Safronova, V. and Belimov, A. (2010) Rhizobacterial mediation of plant hormone status. *Annals of Applied Biology*, **157**, 361-379.

Dong, W. and Song, Y. (2020) The significance of flavonoids in the process of biological nitrogen fixation. *International journal of molecular sciences*, **21**, 5926.

Draper, J., Mur, L.A., Jenkins, G., Ghosh-Biswas, G.C., Bablak, P., Hasterok, R. and Routledge, A.P. (2001) Brachypodium distachyon. A new model system for functional genomics in grasses. *Plant physiology*, **127**, 1539-1555.

Dubcovsky, J., Loukoianov, A., Fu, D., Valarik, M., Sanchez, A. and Yan, L. (2006) Effect of photoperiod on the regulation of wheat vernalization genes VRN1 and VRN2. *Plant Mol. Biol.*, **60**, 469-480.

Eastman, A.W., Weselowski, B., Nathoo, N. and Yuan, Z.-C. (2014) Complete genome sequence of Paenibacillus polymyxa CR1, a plant growth-promoting bacterium isolated from the corn rhizosphere exhibiting potential for biocontrol, biomass degradation, and biofuel production. *Genome Announcements*, **2**, e01218-01213.

Eaton, C.J., Cox, M.P. and Scott, B. (2011) What triggers grass endophytes to switch from mutualism to pathogenism? *Plant Science*, **180**, 190-195.

Edwards, R., Dixon, D.P. and Walbot, V. (2000) Plant glutathione S-transferases: enzymes with multiple functions in sickness and in health. *Trends in plant science*, **5**, 193-198.

Egamberdieva, D., Wirth, S.J., Alqarawi, A.A., Abd_Allah, E.F. and Hashem, A. (2017) Phytohormones and beneficial microbes: essential components for plants to balance stress and fitness. *Frontiers in microbiology*, **8**, 2104.

Eilers, K.G., Lauber, C.L., Knight, R. and Fierer, N. (2010) Shifts in bacterial community structure associated with inputs of low molecular weight carbon compounds to soil. *Soil Biology and Biochemistry*, **42**, 896-903.

Elhaissoufi, W., Khourchi, S., Ibnyasser, A., Ghoulam, C., Rchiad, Z., Zeroual, Y., Lyamlouli, K. and Bargaz, A. (2020) Phosphate solubilizing rhizobacteria could have a stronger influence on wheat root traits and aboveground physiology than rhizosphere P solubilization. *Frontiers in plant science*, **11**, 979.

Elsholz, A.K., Wacker, S.A. and Losick, R. (2014) Self-regulation of exopolysaccharide production in Bacillus subtilis by a tyrosine kinase. *Genes & development*, **28**, 1710-1720.

Errington, J. (2003) Regulation of endospore formation in Bacillus subtilis. *Nature Reviews Microbiology*, **1**, 117.

Fan, X., Naz, M., Fan, X., Xuan, W., Miller, A.J. and Xu, G. (2017) Plant nitrate transporters: from gene function to application. *Journal of Experimental Botany*, **68**, 2463-2475.

Feng, H., Zhang, N., Du, W., Zhang, H., Liu, Y., Fu, R., Shao, J., Zhang, G., Shen, Q. and Zhang, R. (2018) Identification of chemotaxis compounds in root exudates and their sensing chemoreceptors in plant-growth-promoting rhizobacteria Bacillus amyloliquefaciens SQR9. *Molecular Plant-Microbe Interactions*, **31**, 995-1005.

Fernando, W., Nakkeeran, S. and Zhang, Y. (2005) Biosynthesis of antibiotics by PGPR and its relation in biocontrol of plant diseases. In *PGPR: biocontrol and biofertilization*: Springer, pp. 67-109.

Fleischmann, R.D., Adams, M.D., White, O., Clayton, R.A., Kirkness, E.F., Kerlavage, A.R., Bult, C.J., Tomb, J.-F., Dougherty, B.A. and Merrick, J.M. (1995) Whole-genome random sequencing and assembly of Haemophilus influenzae Rd. *Science*, **269**, 496-512.

Flemming, H.-C. and Wingender, J. (2010) The biofilm matrix. *Nature reviews microbiology*, **8**, 623-633.

Fortt, J., González, M., Morales, P., Araya, N., Remonsellez, F., de la Peña, T.C., Ostria-Gallardo, E. and Stoll, A. (2022) Bacterial Modulation of the Plant Ethylene Signaling Pathway Improves Tolerance to Salt Stress in Lettuce (Lactuca sativa L.). *Frontiers in Sustainable Food Systems*, **6**.

Fu, X., Fu, N., Guo, S., Yan, Z., Xu, Y., Hu, H., Menzel, C., Chen, W., Li, Y. and Zeng, R. (2009) Estimating accuracy of RNA-Seq and microarrays with proteomics. *BMC genomics*, **10**, 161.

Fuqua, W.C., Winans, S.C. and Greenberg, E.P. (1994) Quorum sensing in bacteria: the LuxR-LuxI family of cell density-responsive transcriptional regulators. *Journal of bacteriology*, **176**, 269-275.

Gagné-Bourque, F., Bertrand, A., Claessens, A., Aliferis, K.A. and Jabaji, S. (2016) Alleviation of drought stress and metabolic changes in timothy (Phleum pratense L.) colonized with Bacillus subtilis B26. *Frontiers in Plant Science*, **7**, 584.

Gagne-Bourque, F., Mayer, B.F., Charron, J.-B., Vali, H., Bertrand, A. and Jabaji, S. (2015) Accelerated growth rate and increased drought stress resilience of the model grass Brachypodium distachyon colonized by Bacillus subtilis B26. *PLoS One*, **10**, e0130456.

Gagné-Bourque, F., Mayer, B.F., Charron, J.-B., Vali, H., Bertrand, A. and Jabaji, S. (2015) Accelerated growth rate and increased drought stress resilience of the model grass Brachypodium distachyon colonized by Bacillus subtilis B26. *PLoS One*, **10**, e0130456.

Gagne-Bourgue, F., Aliferis, K., Seguin, P., Rani, M., Samson, R. and Jabaji, S. (2013a) Isolation and characterization of indigenous endophytic bacteria associated with leaves of switchgrass (P anicum virgatum L.) cultivars. *Journal of Applied Microbiology*, **114**, 836-853.

Gagne-Bourgue, F., Aliferis, K., Seguin, P., Rani, M., Samson, R. and Jabaji, S. (2013b) Isolation and characterization of indigenous endophytic bacteria associated with leaves of switchgrass (Panicum virgatum L.) cultivars. *Journal of applied microbiology*, **114**, 836-853.

Gaiero, J.R., McCall, C.A., Thompson, K.A., Day, N.J., Best, A.S. and Dunfield, K.E. (2013) Inside the root microbiome: bacterial root endophytes and plant growth promotion. *American journal of botany*, **100**, 1738-1750.

Gamalero, E. and Glick, B.R. (2011) Mechanisms used by plant growth-promoting bacteria. In *Bacteria in agrobiology: plant nutrient management*: Springer, pp. 17-46.

Gamalero, E., Lingua, G., Berta, G. and Glick, B.R. (2009) Beneficial role of plant growth promoting bacteria and arbuscular mycorrhizal fungi on plant responses to heavy metal stress. *Canadian journal of microbiology*, **55**, 501-514.

García de Salamone, I.E., Hynes, R.K. and Nelson, L.M. (2001) Cytokinin production by plant growth promoting rhizobacteria and selected mutants. *Canadian Journal of microbiology*, **47**, 404-411.

Garvin, D.F., Gu, Y.Q., Hasterok, R., Hazen, S.P., Jenkins, G., Mockler, T.C., Mur, L.A. and Vogel, J.P. (2008) Development of genetic and genomic research resources for Brachypodium distachyon, a new model system for grass crop research. *Crop Sci.*, **48**, S-69-S-84.

Gaworzewska, E.T. and Carlile, M.J. (1982) Positive chemotaxis of Rhizobium leguminosarum and other bacteria towards root exudates from legumes and other plants. *Microbiology*, **128**, 1179-1188.

Glick, B.R., Holguin, G., Patten, C. and Penrose, D.M. (1999) *Biochemical and genetic mechanisms used by plant growth promoting bacteria*: World Scientific.

Glick, B.R., Penrose, D.M. and Li, J. (1998) A model for the lowering of plant ethylene concentrations by plant growth-promoting bacteria. *Journal of theoretical biology*, **190**, 63-68.

Goswami, M. and Suresh, D. (2020) Plant growth-promoting rhizobacteria—alleviators of abiotic stresses in soil: a review. *Pedosphere*, **30**, 40-61.

Gray, E. and Smith, D. (2005) Intracellular and extracellular PGPR: commonalities and distinctions in the plant–bacterium signaling processes. *Soil biology and biochemistry*, **37**, 395-412.

Greenup, A., Peacock, W.J., Dennis, E.S. and Trevaskis, B. (2009) The molecular biology of seasonal flowering-responses in Arabidopsis and the cereals. *Ann. Bot.*, **103**, 1165-1172.

Grover, M., Bodhankar, S., Sharma, A., Sharma, P., Singh, J. and Nain, L. (2021) PGPR mediated alterations in root traits: way toward sustainable crop production. *Frontiers in Sustainable Food Systems*, **4**, 618230.

Gullner, G., Komives, T., Király, L. and Schröder, P. (2018) Glutathione S-transferase enzymes in plant-pathogen interactions. *Frontiers in plant science*, **9**, 1836.

Guo, Y., Pang, C., Jia, X., Ma, Q., Dou, L., Zhao, F., Gu, L., Wei, H., Wang, H. and Fan, S. (2017) An NAM domain gene, GhNAC79, improves resistance to drought stress in upland cotton. *Frontiers in plant science*, **8**, 1657.

Hacquard, S., Kracher, B., Hiruma, K., Münch, P.C., Garrido-Oter, R., Thon, M.R., Weimann, A., Damm, U., Dallery, J.-F. and Hainaut, M. (2016) Survival trade-offs in plant roots during colonization by closely related beneficial and pathogenic fungi. *Nature communications*, **7**, 11362.

Hafeez, F., Ahmad, T., Asad, T., Malik, K., Shah, N. and Danso, S. (1998) Field evaluations of N 2 fixation by grain legumes in Pakistan.

Haichar, F.e.Z., Marol, C., Berge, O., Rangel-Castro, J.I., Prosser, J.I., Balesdent, J., Heulin, T. and Achouak, W. (2008) Plant host habitat and root exudates shape soil bacterial community structure. *The ISME journal*, **2**, 1221-1230.

Halverson, L.J. (2009) Role of alginate in bacterial biofilms. In *Alginates: Biology and applications*: Springer, pp. 135-151.

Ham, S.H., Yoon, A.R., Oh, H.E. and Park, Y.G. (2022) Plant Growth-Promoting Microorganism Pseudarthrobacter sp. NIBRBAC000502770 Enhances the Growth and Flavonoid Content of Geum aleppicum. *Microorganisms*, **10**, 1241.

Haney, C.H., Samuel, B.S., Bush, J. and Ausubel, F.M. (2015) Associations with rhizosphere bacteria can confer an adaptive advantage to plants. *Nature plants*, **1**, 1-9.

Hardoim, P.R., Van Overbeek, L.S., Berg, G., Pirttilä, A.M., Compant, S., Campisano, A., Döring, M. and Sessitsch, A. (2015) The hidden world within plants: ecological and evolutionary considerations for defining functioning of microbial endophytes. *Microbiology and Molecular Biology Reviews*, **79**, 293-320.

Hardoim, P.R., van Overbeek, L.S. and van Elsas, J.D. (2008) Properties of bacterial endophytes and their proposed role in plant growth. *Trends in microbiology*, **16**, 463-471.

Hashem, A., Tabassum, B. and Abd_Allah, E.F. (2019) Bacillus subtilis: A plant-growth promoting rhizobacterium that also impacts biotic stress. *Saudi journal of biological sciences*, **26**, 1291-1297.

Hasterok, R., Draper, J. and Jenkins, G. (2004) Laying the cytotaxonomic foundations of a new model grass, Brachypodium distachyon (L.) Beauv. *Chromosome Research*, **12**, 397-403.

Havelange, A., Lejeune, P. and Bernier, G. (2000) Sucrose/cytokinin interaction in Sinapis alba at floral induction: a shoot-to-root-to-shoot physiological loop. *Physiologia plantarum*, **109**, 343-350.

Hawes, M.C., Gunawardena, U., Miyasaka, S. and Zhao, X. (2000) The role of root border cells in plant defense. *Trends in plant science*, **5**, 128-133.

Hazelbauer, G.L. (2012) Bacterial chemotaxis: the early years of molecular studies. *Annual review of microbiology*, **66**, 285.

Hennion, N., Durand, M., Vriet, C., Doidy, J., Maurousset, L., Lemoine, R. and Pourtau, N. (2019) Sugars en route to the roots. Transport, metabolism and storage within plant roots and towards microorganisms of the rhizosphere. *Physiologia plantarum*, **165**, 44-57.

Heydarian, Z., Gruber, M., Glick, B.R. and Hegedus, D.D. (2018) Gene expression patterns in roots of Camelina sativa with enhanced salinity tolerance arising from inoculation of soil with plant growth promoting bacteria producing 1-aminocyclopropane-1-carboxylate deaminase or expression the corresponding acds gene. *Frontiers in microbiology*, **9**, 1297.

Higgins, J.A., Bailey, P.C. and Laurie, D.A. (2010) Comparative genomics of flowering time pathways using Brachypodium distachyon as a model for the temperate grasses. *PloS one*, **5**, e10065.

Hiltner, L. (1904) Uber nevere Erfahrungen und Probleme auf dem Gebiet der Boden Bakteriologie und unter besonderer Beurchsichtigung der Grundungung und Broche. *Arbeit. Deut. Landw. Ges. Berlin*, **98**, 59-78.

Hirayama, T. and Shinozaki, K. (2007) Perception and transduction of abscisic acid signals: keys to the function of the versatile plant hormone ABA. *Trends in plant science*, **12**, 343-351.

Hodge, A., Berta, G., Doussan, C., Merchan, F. and Crespi, M. (2009) Plant root growth, architecture and function. *Plant and soil*, **321**, 153-187.

Hoffman, B.M., Dean, D.R. and Seefeldt, L.C. (2009) Climbing nitrogenase: toward a mechanism of enzymatic nitrogen fixation. *Accounts of chemical research*, **42**, 609-619.

Hong, S.-Y., Seo, P.J., Yang, M.-S., Xiang, F. and Park, C.-M. (2008) Exploring valid reference genes for gene expression studies in Brachypodium distachyonby real-time PCR. *BMC plant biology*, **8**, 1-11.

Hong, S.Y., Park, J.H., Cho, S.H., Yang, M.S. and Park, C.M. (2011) Phenological growth stages of Brachypodium distachyon: codification and description. *Weed Res.*, **51**, 612-620.

Houry, A., Briandet, R., Aymerich, S. and Gohar, M. (2010) Involvement of motility and flagella in Bacillus cereus biofilm formation. *Microbiology*, **156**, 1009-1018.

Hsia, M.M., O'Malley, R., Cartwright, A., Nieu, R., Gordon, S.P., Kelly, S., Williams, T.G., Wood, D.F., Zhao, Y. and Bragg, J. (2017) Sequencing and functional validation of the JGI Brachypodium distachyon T-DNA collection. *The Plant Journal*, **91**, 361-370.

Initiative, I.B. (2010) Genome sequencing and analysis of the model grass Brachypodium distachyon. *Nature*, **463**, 763.

Jeukens, J., Kukavica-Ibrulj, I., Freschi, L., Jabaji, S. and Levesque, R.C. (2015a) Draft genome sequences of two lipopeptide-producing strains of Bacillus methylotrophicus. *Genome Announcements*, **3**, e01176-01115.

Jeukens, J., Kukavica-Ibrulj, I., Freschi, L., Jabaji, S. and Levesque, R.C. (2015b) Draft genome sequences of two lipopeptide-producing strains of Bacillus methylotrophicus. *Genome Announc.*, **3**, e01176-01115.

Jha, Y., Dehury, B., Kumar, S., Chaurasia, A., Singh, U.B., Yadav, M.K., Angadi, U., Ranjan, R., Tripathy, M. and Subramanian, R. (2022) Delineation of molecular interactions of plant growth promoting bacteria induced β-1, 3-glucanases and guanosine triphosphate ligand for antifungal response in rice: a molecular dynamics approach. *Molecular biology reports*, **49**, 2579-2589.

Jin, C.W., He, Y.F., Tang, C.X., Wu, P. and Zheng, S.J. (2006) Mechanisms of microbially enhanced Fe acquisition in red clover (Trifolium pratense L.). *Plant, cell & environment*, **29**, 888-897.

Jin, Y., Zhu, H., Luo, S., Yang, W., Zhang, L., Li, S., Jin, Q., Cao, Q., Sun, S. and Xiao, M. (2019) Role of maize root exudates in promotion of colonization of Bacillus velezensis strain S3-1 in rhizosphere soil and root tissue. *Current Microbiology*, **76**, 855-862.

Jones, D.L. (1998) Organic acids in the rhizosphere–a critical review. *Plant and soil*, **205**, 25-44.

Joo, G.-J., Kim, Y.-M., Lee, I.-J., Song, K.-S. and Rhee, I.-K. (2004) Growth promotion of red pepper plug seedlings and the production of gibberellins by Bacillus cereus, Bacillus macroides and Bacillus pumilus. *Biotechnology letters*, **26**, 487-491.

Joshi, R., Wani, S.H., Singh, B., Bohra, A., Dar, Z.A., Lone, A.A., Pareek, A. and Singla-Pareek, S.L. (2016) Transcription factors and plants response to drought stress: current understanding and future directions. *Frontiers in Plant Science*, **7**, 1029.

Kalam, H., Fontana, M.F. and Kumar, D. (2017) Alternate splicing of transcripts shape macrophage response to Mycobacterium tuberculosis infection. *PLoS pathogens*, **13**, e1006236.

Kalamara, M., Abbott, J.C., MacPhee, C.E. and Stanley-Wall, N.R. (2021) Biofilm hydrophobicity in environmental isolates of Bacillus subtilis. *bioRxiv*.

Kamilova, F., Kravchenko, L.V., Shaposhnikov, A.I., Makarova, N. and Lugtenberg, B. (2006) Effects of the tomato pathogen Fusarium oxysporum f. sp. radicis-lycopersici and of the biocontrol bacterium Pseudomonas fluorescens WCS365 on the composition of

organic acids and sugars in tomato root exudate. *Molecular plant-microbe interactions*, **19**, 1121-1126.

Kang, S.-M., Joo, G.-J., Hamayun, M., Na, C.-I., Shin, D.-H., Kim, H.Y., Hong, J.-K. and Lee, I.-J. (2009) Gibberellin production and phosphate solubilization by newly isolated strain of Acinetobacter calcoaceticus and its effect on plant growth. *Biotechnology letters*, **31**, 277-281.

Kang, S.-M., Radhakrishnan, R., Khan, A.L., Kim, M.-J., Park, J.-M., Kim, B.-R., Shin, D.-H. and Lee, I.-J. (2014) Gibberellin secreting rhizobacterium, Pseudomonas putida H-2-3 modulates the hormonal and stress physiology of soybean to improve the plant growth under saline and drought conditions. *Plant Physiology and Biochemistry*, **84**, 115-124.

Kashyap, B.K., Solanki, M.K., Pandey, A.K., Prabha, S., Kumar, P. and Kumari, B. (2019) Bacillus as plant growth promoting rhizobacteria (PGPR): a promising green agriculture technology. In *Plant health under biotic stress*: Springer, pp. 219-236.

Kaul, S., Sharma, T. and K Dhar, M. (2016a) "Omics" Tools for Better Understanding the Plant–Endophyte Interactions. *Frontiers in plant science*, **7**, 955.

Kaul, S., Sharma, T. and K. Dhar, M. (2016b) "Omics" tools for better understanding the plant–endophyte interactions. *Frontiers in plant science*, **7**, 955.

Kawahara, Y., Oono, Y., Kanamori, H., Matsumoto, T., Itoh, T. and Minami, E. (2012) Simultaneous RNA-seq analysis of a mixed transcriptome of rice and blast fungus interaction. *PloS one*, **7**, e49423.

Kawasaki, A., Donn, S., Ryan, P.R., Mathesius, U., Devilla, R., Jones, A. and Watt, M. (2016) Microbiome and exudates of the root and rhizosphere of Brachypodium distachyon, a model for wheat. *PloS one*, **11**, e0164533.

Kearns, D.B. (2010) A field guide to bacterial swarming motility. *Nature Reviews Microbiology*, **8**, 634-644.

Khanna, K., Jamwal, V.L., Sharma, A., Gandhi, S.G., Ohri, P., Bhardwaj, R., Al-Huqail, A.A., Siddiqui, M.H., Marraiki, N. and Ahmad, P. (2019) Evaluation of the role of rhizobacteria in controlling root-knot nematode infection in Lycopersicon esculentum plants by modulation in the secondary metabolite profiles. *AoB Plants*, **11**, plz069.

Kim, D.-H., Doyle, M.R., Sung, S. and Amasino, R.M. (2009) Vernalization: winter and the timing of flowering in plants. *Annual Review of Cell and Developmental*, **25**, 277-299.

Kim, J. and Rees, D.C. (1994) Nitrogenase and biological nitrogen fixation. *Biochemistry*, **33**, 389-397.

Kim, J.-S., Lee, J., Lee, C.-h., Woo, S.Y., Kang, H., Seo, S.-G. and Kim, S.-H. (2015a) Activation of pathogenesis-related genes by the rhizobacterium, Bacillus sp. JS, which induces systemic resistance in tobacco plants. *The plant pathology journal*, **31**, 195.

Kim, J.-S., Lee, J., Seo, S.-G., Lee, C., Woo, S.Y. and Kim, S.-H. (2015b) Gene expression profile affected by volatiles of new plant growth promoting rhizobacteria, Bacillus subtilis strain JS, in tobacco. *Genes & Genomics*, **37**, 387-397.

Kim, J.F., Jeong, H., Park, S.-Y., Kim, S.-B., Park, Y.K., Choi, S.-K., Ryu, C.-M., Hur, C.-G., Ghim, S.-Y. and Oh, T.K. (2010) Genome sequence of the polymyxin-producing plant-probiotic rhizobacterium Paenibacillus polymyxa E681. *Journal of bacteriology*, **192**, 6103-6104.

Kloepper, J., Gutierrez-Estrada, A. and McInroy, J. (2007) Photoperiod regulates elicitation of growth promotion but not induced resistance by plant growth-promoting rhizobacteria. *Canadian Journal of Microbiology*, **53**, 159-167.

Kloepper, J. and Schroth, M. (1981a) Plant growth-promoting rhizobacteria and plant growth under gnotobiotic conditions. *Phytopathology*, **71**, 642-644.

Kloepper, J. and Schroth, M. (1981b) Relationship of in vitro antibiosis of plant growth-promoting rhizobacteria to plant growth and the displacement of root microflora. *Phytopathology*, **71**, 1020-1024.

Knief, C. (2014) Analysis of plant microbe interactions in the era of next generation sequencing technologies. *Frontiers in plant science*, **5**, 216.

Kobayashi, K. and Iwano, M. (2012) BslA (YuaB) forms a hydrophobic layer on the surface of Bacillus subtilis biofilms. *Molecular microbiology*, **85**, 51-66.

Kong, W., Chen, N., Liu, T., Zhu, J., Wang, J., He, X. and Jin, Y. (2015) Large-scale transcriptome analysis of cucumber and Botrytis cinerea during infection. *PLoS One*, **10**, e0142221.

Kong, Z. and Liu, H. (2022) Modification of Rhizosphere Microbial Communities: A Possible Mechanism of Plant Growth Promoting Rhizobacteria Enhancing Plant Growth and Fitness. *Frontiers in Plant Science*, **13**.

Korenblum, E., Massalha, H. and Aharoni, A. (2022) Plant–microbe interactions in the rhizosphere via a circular metabolic economy. *The Plant Cell*, **34**, 3168-3182.

Kucey, R.M.N., Janzen, H. and Leggett, M. (1989) Microbially mediated increases in plant-available phosphorus. *Advances in agronomy*, **42**, 199-228.

Kudoyarova, G., Arkhipova, T., Korshunova, T., Bakaeva, M., Loginov, O. and Dodd, I.C. (2019) Phytohormone mediation of interactions between plants and non-symbiotic growth promoting bacteria under edaphic stresses. *Frontiers in plant science*, **10**, 1368.

Kunst, F., Ogasawara, N., Moszer, I., Albertini, A., Alloni, G., Azevedo, V., Bertero, M., Bessières, P., Bolotin, A. and Borchert, S. (1997) The complete genome sequence of the gram-positive bacterium Bacillus subtilis. *Nature*, **390**, 249-256.

KUROKURA, T., HIRAIDE, S., SHIMAMURA, Y. and YAMANE, K. (2017) PGPR improves yield of strawberry species under less-fertilized conditions. *Environmental Control in Biology*, **55**, 121-128.

Lambrecht, M., Okon, Y., Broek, A.V. and Vanderleyden, J. (2000) Indole-3-acetic acid: a reciprocal signalling molecule in bacteria–plant interactions. *Trends in microbiology*, **8**, 298-300.

Lareen, A., Burton, F. and Schäfer, P. (2016) Plant root-microbe communication in shaping root microbiomes. *Plant molecular biology*, **90**, 575-587.

Lemon, K., Earl, A., Vlamakis, H., Aguilar, C. and Kolter, R. (2008) Biofilm development with an emphasis on Bacillus subtilis. *Bacterial biofilms*, 1-16.

Li, S.-S., Chang, Y., Li, B. and Shao, S.-L. (2020) Functional analysis of 4-coumarate: CoA ligase from Dryopteris fragrans in transgenic tobacco enhances lignin and flavonoids. *Genetics and Molecular Biology*, **43**.

Li, T., Mann, R., Kaur, J., Spangenberg, G. and Sawbridge, T. (2021) Transcriptome Analyses of Barley Roots Inoculated with Novel Paenibacillus sp. and Erwinia gerundensis Strains Reveal Beneficial Early-Stage Plant–Bacteria Interactions. *Plants*, **10**, 1802.

Liao, Y., Smyth, G.K. and Shi, W. (2014) featureCounts: an efficient general purpose program for assigning sequence reads to genomic features. *Bioinformatics*, **30**, 923-930.

Ling, N., Raza, W., Ma, J., Huang, Q. and Shen, Q. (2011) Identification and role of organic acids in watermelon root exudates for recruiting Paenibacillus polymyxa SQR-21 in the rhizosphere. *European Journal of Soil Biology*, **47**, 374-379.

Liu, H., Wang, J., Sun, H., Han, X., Peng, Y., Liu, J., Liu, K., Ding, Y., Wang, C. and Du, B. (2020) Transcriptome profiles reveal the growth-promoting mechanisms of Paenibacillus polymyxa YC0136 on tobacco (Nicotiana tabacum L.). *Frontiers in Microbiology*, **11**, 584174.

Liu, Q., Luo, L. and Zheng, L. (2018) Lignins: biosynthesis and biological functions in plants. *International journal of molecular sciences*, **19**, 335.

Liu, Y., Chen, L., Wu, G., Feng, H., Zhang, G., Shen, Q. and Zhang, R. (2017) Identification of root-secreted compounds involved in the communication between cucumber, the beneficial Bacillus amyloliquefaciens, and the soil-borne pathogen Fusarium oxysporum. *Molecular Plant-Microbe Interactions*, **30**, 53-62.

Livak, K.J. and Schmittgen, T.D. (2001) Analysis of relative gene expression data using real-time quantitative PCR and the 2− ΔΔCT method. *methods*, **25**, 402-408.

Love, M.I., Huber, W. and Anders, S. (2014) Moderated estimation of fold change and dispersion for RNA-seq data with DESeq2. *Genome biology*, **15**, 1-21.

Lu, T., Ke, M., Lavoie, M., Jin, Y., Fan, X., Zhang, Z., Fu, Z., Sun, L., Gillings, M. and Peñuelas, J. (2018) Rhizosphere microorganisms can influence the timing of plant flowering. *Microbiome*, **6**, 1-12.

Lugtenberg, B. and Kamilova, F. (2009) Plant-growth-promoting rhizobacteria. *Annual review of microbiology*, **63**, 541-556.

Lugtenberg, B.J. and Bloemberg, G.V. (2002) Microbe–plant interactions: principles and mechanisms. *Antonie Van Leeuwenhoek*, **81**, 373-383.

Luo, D., Langendries, S., Mendez, S.G., De Ryck, J., Liu, D., Beirinckx, S., Willems, A., Russinova, E., Debode, J. and Goormachtig, S. (2019) Plant growth promotion driven by a novel Caulobacter strain. *Molecular Plant-Microbe Interactions*, **32**, 1162-1174.

Lv, B., Nitcher, R., Han, X., Wang, S., Ni, F., Li, K., Pearce, S., Wu, J., Dubcovsky, J. and Fu, D. (2014) Characterization of FLOWERING LOCUS T1 (FT1) gene in Brachypodium and wheat. *PLoS One*, **9**, e94171.

Ma, Y., Szostkiewicz, I., Korte, A., Moes, D., Yang, Y., Christmann, A. and Grill, E. (2009) Regulators of PP2C phosphatase activity function as abscisic acid sensors. *Science*, **324**, 1064-1068.

Mahoney, A.K., Yin, C. and Hulbert, S.H. (2017) Community structure, species variation, and potential functions of rhizosphere-associated bacteria of different winter wheat (Triticum aestivum) cultivars. *Frontiers in plant science*, **8**, 132.

Mariano, E.D., Jorge, R.A., Keltjens, W.G. and Menossi, M. (2005) Metabolism and root exudation of organic acid anions under aluminium stress. *Brazilian Journal of Plant Physiology*, **17**, 157-172.

Marsh, J.W., Humphrys, M.S. and Myers, G.S. (2017) A Laboratory Methodology for Dual RNA-Sequencing of Bacteria and their Host Cells In Vitro. *Frontiers in microbiology*, **8**, 1830.

Matteoli, F.P., Passarelli-Araujo, H., Reis, R.J.A., da Rocha, L.O., de Souza, E.M., Aravind, L., Olivares, F.L. and Venancio, T.M. (2018) Genome sequencing and assessment of plant growth-promoting properties of a Serratia marcescens strain isolated from vermicompost. *BMC genomics*, **19**, 1-19.

May, T.B. and Chakrabarty, A. (1994) Pseudomonas aeruginosa: genes and enzymes of alginate synthesis. *Trends in microbiology*, **2**, 151-157.

Mazumder, R., Phelps, T.J., Krieg, N.R. and Benoit, R.E. (1999) Determining chemotactic responses by two subsurface microaerophiles using a simplified capillary assay method. *Journal of microbiological methods*, **37**, 255-263.

Mehnaz, S. and Lazarovits, G. (2006) Inoculation effects of Pseudomonas putida, Gluconacetobacter azotocaptans, and Azospirillum lipoferum on corn plant growth under greenhouse conditions. *Microbial Ecology*, **51**, 326-335.

Mena-Violante, H.G. and Olalde-Portugal, V. (2007) Alteration of tomato fruit quality by root inoculation with plant growth-promoting rhizobacteria (PGPR): Bacillus subtilis BEB-13bs. *Scientia Horticulturae*, **113**, 103-106.

Metzker, M.L. (2010) Sequencing technologies—the next generation. *Nature reviews genetics*, **11**, 31-46.

Mhlongo, M.I., Piater, L.A., Steenkamp, P.A., Labuschagne, N. and Dubery, I.A. (2020) Metabolic profiling of PGPR-treated tomato plants reveal priming-related adaptations of secondary metabolites and aromatic amino acids. *Metabolites*, **10**, 210.

Mitra, P.P. and Loqué, D. (2014) Histochemical staining of Arabidopsis thaliana secondary cell wall elements. *JoVE (Journal of Visualized Experiments)*, e51381.

Montiel, G., Gantet, P., Jay-Allemand, C. and Breton, C. (2004) Transcription factor networks. Pathways to the knowledge of root development. *Plant Physiology*, **136**, 3478-3485.

Mutasa-Göttgens, E. and Hedden, P. (2009) Gibberellin as a factor in floral regulatory networks. *J. Exp. Bot.*, **60**, 1979-1989.

Nagórska, K., Ostrowski, A., Hinc, K., Holland, I. and Obuchowski, M. (2010) Importance ofeps genes fromBacillus subtilis in biofilm formation and swarming. *Journal of applied genetics*, **51**, 369-381.

Nana, E.M. and Alemneh, A.A. (2015) Rhizobia strain and legume genome interaction effects on nitrogen fixation and yield of grain legume: a review. *Molecular Soil Biology*, **6**.

Nazari, F., Safaie, N., Soltani, B.M., Shams-Bakhsh, M. and Sharifi, M. (2017) Bacillus subtilis affects miRNAs and flavanoids production in Agrobacterium-Tobacco interaction. *Plant Physiology and Biochemistry*, **118**, 98-106.

Neinhuis, C. and Edelmann, H. (1996) Methanol as a rapid fixative for the investigation of plant surfaces by SEM. *Journal of Microscopy*, **184**, 14-16.

Ngumbi, E. and Kloepper, J. (2016) Bacterial-mediated drought tolerance: current and future prospects. *Applied Soil Ecology*, **105**, 109-125.

Nieto, K. and Frankenberger Jr, W. (1989) Biosynthesis of cytokinins by Azotobacter chroococcum. *Soil Biology and Biochemistry*, **21**, 967-972.

Niyogi, K.K. and Fink, G.R. (1992) Two anthranilate synthase genes in Arabidopsis: defense-related regulation of the tryptophan pathway. *The Plant Cell*, **4**, 721-733.

Notaguchi, M. and Okamoto, S. (2015) Dynamics of long-distance signaling via plant vascular tissues. *Frontiers in Plant Science*, **6**, 161.

Nuruzzaman, M., Sharoni, A.M. and Kikuchi, S. (2013) Roles of NAC transcription factors in the regulation of biotic and abiotic stress responses in plants. *Frontiers in microbiology*, **4**, 248.

O'Brien, T., Feder, N. and McCully, M.E. (1964) Polychromatic staining of plant cell walls by toluidine blue O. *Protoplasma*, **59**, 368-373.

Oburger, E. and Schmidt, H. (2016) New methods to unravel rhizosphere processes. *Trends in plant science*, **21**, 243-255.

Oku, S., Komatsu, A., Nakashimada, Y., Tajima, T. and Kato, J. (2014) Identification of Pseudomonas fluorescens chemotaxis sensory proteins for malate, succinate, and fumarate, and their involvement in root colonization. *Microbes and environments*, **29**, 413-419.

Opanowicz, M., Vain, P., Draper, J., Parker, D. and Doonan, J.H. (2008) Brachypodium distachyon: making hay with a wild grass. *Trends in plant science*, **13**, 172-177.

Ormeño-Orrillo, E., Rogel, M.A., Chueire, L.M.O., Tiedje, J.M., Martínez-Romero, E. and Hungria, M. (2012) Genome sequences of Burkholderia sp. strains CCGE1002 and H160, isolated from legume nodules in Mexico and Brazil: Am Soc Microbiol.

Ortíz-Castro, R., Contreras-Cornejo, H.A., Macías-Rodríguez, L. and López-Bucio, J. (2009) The role of microbial signals in plant growth and development. *Plant signaling & behavior*, **4**, 701-712.

Păcurar, D.I., Thordal-Christensen, H., Nielsen, K.K. and Lenk, I. (2008) A high-throughput Agrobacterium-mediated transformation system for the grass model species Brachypodium distachyon L. *Transgenic research*, **17**, 965-975.

Park, Y.-G., Mun, B.-G., Kang, S.-M., Hussain, A., Shahzad, R., Seo, C.-W., Kim, A.-Y., Lee, S.-U., Oh, K.Y. and Lee, D.Y. (2017) Bacillus aryabhattai SRB02 tolerates oxidative and nitrosative stress and promotes the growth of soybean by modulating the production of phytohormones. *PLoS One*, **12**, e0173203.

Pascale, A., Proietti, S., Pantelides, I.S. and Stringlis, I.A. (2020) Modulation of the root microbiome by plant molecules: the basis for targeted disease suppression and plant growth promotion. *Frontiers in Plant Science*, **10**, 1741.

Patel, T. and Saraf, M. (2017) Biosynthesis of phytohormones from novel rhizobacterial isolates and their in vitro plant growth-promoting efficacy. *Journal of Plant Interactions*, **12**, 480-487.

Paulsen, I.T., Press, C.M., Ravel, J., Kobayashi, D.Y., Myers, G.S., Mavrodi, D.V., DeBoy, R.T., Seshadri, R., Ren, Q. and Madupu, R. (2005) Complete genome sequence of the plant commensal Pseudomonas fluorescens Pf-5. *Nature biotechnology*, **23**, 873-878.

Peiffer, J.A., Spor, A., Koren, O., Jin, Z., Tringe, S.G., Dangl, J.L., Buckler, E.S. and Ley, R.E. (2013) Diversity and heritability of the maize rhizosphere microbiome under field conditions. *Proceedings of the National Academy of Sciences*, **110**, 6548-6553.

Pieterse, C.M., Van Pelt, J.A., Ton, J., Parchmann, S., Mueller, M.J., Buchala, A.J., Métraux, J.-P. and Van Loon, L.C. (2000) Rhizobacteria-mediated induced systemic resistance (ISR) in Arabidopsis requires sensitivity to jasmonate and ethylene but is not accompanied by an increase in their production. *Physiological and molecular plant pathology*, **57**, 123-134.

Pieterse, C.M., Zamioudis, C., Berendsen, R.L., Weller, D.M., Van Wees, S.C. and Bakker, P.A. (2014) Induced systemic resistance by beneficial microbes. *Annual review of phytopathology*, **52**, 347-375.

Pii, Y., Mimmo, T., Tomasi, N., Terzano, R., Cesco, S. and Crecchio, C. (2015) Microbial interactions in the rhizosphere: beneficial influences of plant growth-promoting rhizobacteria on nutrient acquisition process. A review. *Biology and fertility of soils*, **51**, 403-415.

Pilet, P.-E. and Saugy, M. (1987) Effect on root growth of endogenous and applied IAA and ABA: a critical reexamination. *Plant Physiology*, **83**, 33-38.

Pillay, V. and Nowak, J. (1997) Inoculum density, temperature, and genotype effects on in vitro growth promotion and epiphytic and endophytic colonization of tomato (Lycopersicon

esculentum L.) seedlings inoculated with a pseudomonad bacterium. *Canadian Journal of Microbiology*, **43**, 354-361.

Pineros, M.A., Magalhaes, J.V., Carvalho Alves, V.M. and Kochian, L.V. (2002) The physiology and biophysics of an aluminum tolerance mechanism based on root citrate exudation in maize. *Plant Physiology*, **129**, 1194-1206.

Posada, L.F., Álvarez, J., Romero-Tabarez, M., de-Bashan, L. and Villegas-Escobar, V. (2018) Enhanced molecular visualization of root colonization and growth promotion by Bacillus subtilis EA-CB0575 in different growth systems. *Microbiological research*, **217**, 69-80.

Poupin, M.J., Timmermann, T., Vega, A., Zuñiga, A. and González, B. (2013) Effects of the plant growth-promoting bacterium Burkholderia phytofirmans PsJN throughout the life cycle of Arabidopsis thaliana. *PLoS One*, **8**, e69435.

Prithiviraj, B., Zhou, X., Souleimanov, A., Kahn, W. and Smith, D. (2003) A host-specific bacteria-to-plant signal molecule (Nod factor) enhances germination and early growth of diverse crop plants. *Planta*, **216**, 437-445.

Qin, H. and Huang, R. (2018) Auxin controlled by ethylene steers root development. *International Journal of Molecular Sciences*, **19**, 3656.

Rajkumar, M., Ae, N., Prasad, M.N.V. and Freitas, H. (2010) Potential of siderophore-producing bacteria for improving heavy metal phytoextraction. *Trends in biotechnology*, **28**, 142-149.

Ramey, B.E., Koutsoudis, M., von Bodman, S.B. and Fuqua, C. (2004) Biofilm formation in plant–microbe associations. *Current opinion in microbiology*, **7**, 602-609.

Raven, J.A., Wollenweber, B. and Handley, L.L. (1992) A comparison of ammonium and nitrate as nitrogen sources for photolithotrophs. *New Phytologist*, **121**, 19-32.

Ream, T.S., Woods, D.P., Schwartz, C.J., Sanabria, C.P., Mahoy, J.A., Walters, E.M., Kaeppler, H.F. and Amasino, R.M. (2014) Interaction of photoperiod and vernalization determines flowering time of Brachypodium distachyon. *Plant physiology*, **164**, 694-709.

Rekha, K., Baskar, B., Srinath, S. and Usha, B. (2018a) Plant-growth-promoting rhizobacteria Bacillus subtilis RR4 isolated from rice rhizosphere induces malic acid biosynthesis in rice roots. *Canadian journal of microbiology*, **64**, 20-27.

Rekha, K., Kumar, R.M., Ilango, K., Rex, A. and Usha, B. (2018b) Transcriptome profiling of rice roots in early response to Bacillus subtilis (RR4) colonization. *Botany*, **96**, 749-765.

Rieu, I., Ruiz-Rivero, O., Fernandez-Garcia, N., Griffiths, J., Powers, S.J., Gong, F., Linhartova, T., Eriksson, S., Nilsson, O. and Thomas, S.G. (2008) The gibberellin biosynthetic genes AtGA20ox1 and AtGA20ox2 act, partially redundantly, to promote growth and development throughout the Arabidopsis life cycle. *The Plant Journal*, **53**, 488-504.

Rudrappa, T., Czymmek, K.J., Paré, P.W. and Bais, H.P. (2008) Root-secreted malic acid recruits beneficial soil bacteria. *Plant physiology*, **148**, 1547-1556.

Růžička, K., Ljung, K., Vanneste, S., Podhorská, R., Beeckman, T., Friml, J.i. and Benková, E. (2007) Ethylene regulates root growth through effects on auxin biosynthesis and transport-dependent auxin distribution. *The Plant Cell*, **19**, 2197-2212.

Salazar, F., Ortiz, A. and Sansinenea, E. (2017) Characterisation of two novel bacteriocin-like substances produced by Bacillus amyloliquefaciens ELI149 with broad-spectrum antimicrobial activity. *Journal of global antimicrobial resistance*, **11**, 177-182.

Saleh, D., Sharma, M., Seguin, P. and Jabaji, S. (2020) Organic acids and root exudates of Brachypodium distachyon: effects on chemotaxis and biofilm formation of endophytic bacteria. *Canadian journal of microbiology*, **66**, 562-575.

Salem, G., Stromberger, M.E., Byrne, P.F., Manter, D.K., El-Feki, W. and Weir, T.L. (2018) Genotype-specific response of winter wheat (Triticum aestivum L.) to irrigation and inoculation with ACC deaminase bacteria. *Rhizosphere*, **8**, 1-7.

Samaras, A., Kamou, N., Tzelepis, G., Karamanoli, K., Menkissoglu-Spiroudi, U. and Karaoglanidis, G.S. (2022) Root Transcriptional and Metabolic Dynamics Induced by the Plant Growth Promoting Rhizobacterium (PGPR) Bacillus subtilis Mbi600 on Cucumber Plants. *Plants*, **11**, 1218.

Sandoya, G.V. and de Oliveira Buanafina, M.M. (2014) Differential responses of Brachypodium distachyon genotypes to insect and fungal pathogens. *Physiological and Molecular Plant Pathology*, **85**, 53-64.

Santiago, J., Rodrigues, A., Saez, A., Rubio, S., Antoni, R., Dupeux, F., Park, S.Y., Márquez, J.A., Cutler, S.R. and Rodriguez, P.L. (2009) Modulation of drought resistance by the abscisic acid receptor PYL5 through inhibition of clade A PP2Cs. *The Plant Journal*, **60**, 575-588.

Sasaki, K., Ikeda, S., Eda, S., Mitsui, H., Hanzawa, E., Kisara, C., Kazama, Y., Kushida, A., Shinano, T. and Minamisawa, K. (2010) Impact of plant genotype and nitrogen level on rice growth response to inoculation with Azospirillum sp. strain B510 under paddy field conditions. *Soil Science & Plant Nutrition*, **56**, 636-644.

Sasani, S., Hemming, M.N., Oliver, S.N., Greenup, A., Tavakkol-Afshari, R., Mahfoozi, S., Poustini, K., Sharifi, H.-R., Dennis, E.S. and Peacock, W.J. (2009) The influence of vernalization and daylength on expression of flowering-time genes in the shoot apex and leaves of barley (Hordeum vulgare). *J. Exp. Bot.*, **60**, 2169-2178.

Sasse, J., Kant, J., Cole, B.J., Klein, A.P., Arsova, B., Schlaepfer, P., Gao, J., Lewald, K., Zhalnina, K. and Kosina, S. (2019) Multilab EcoFAB study shows highly reproducible physiology and depletion of soil metabolites by a model grass. *New Phytologist*, **222**, 1149-1160.

Sasse, J., Martinoia, E. and Northen, T. (2018) Feed your friends: do plant exudates shape the root microbiome? *Trends in plant science*, **23**, 25-41.

Schindelin, J., Arganda-Carreras, I., Frise, E., Kaynig, V., Longair, M., Pietzsch, T., Preibisch, S., Rueden, C., Saalfeld, S. and Schmid, B. (2012) Fiji: an open-source platform for biological-image analysis. *Nature methods*, **9**, 676-682.

Schwartz, C.J., Doyle, M.R., Manzaneda, A.J., Rey, P.J., Mitchell-Olds, T. and Amasino, R.M. (2010) Natural variation of flowering time and vernalization responsiveness in Brachypodium distachyon. *Bioenergy Research*, **3**, 38-46.

Sgroy, V., Cassán, F., Masciarelli, O., Del Papa, M.F., Lagares, A. and Luna, V. (2009) Isolation and characterization of endophytic plant growth-promoting (PGPB) or stress homeostasis-regulating (PSHB) bacteria associated to the halophyte Prosopis strombulifera. *ApplIed microbiology and Biotechnology*, **85**, 371-381.

Shameer, S. and Prasad, T. (2018) Plant growth promoting rhizobacteria for sustainable agricultural practices with special reference to biotic and abiotic stresses. *Plant Growth Regulation*, **84**, 603-615.

Shanmugam, V. and Kanoujia, N. (2011) Biological management of vascular wilt of tomato caused by Fusarium oxysporum f. sp. lycospersici by plant growth-promoting rhizobacterial mixture. *Biological control*, **57**, 85-93.

Sharma, A., Johri, B., Sharma, A. and Glick, B. (2003) Plant growth-promoting bacterium Pseudomonas sp. strain GRP3 influences iron acquisition in mung bean (Vigna radiata L. Wilzeck). *Soil Biology and Biochemistry*, **35**, 887-894.

Sharma, M., Charron, J.-B., Rani, M. and Jabaji, S. (2022) Bacillus velezensis strain B26 modulates the inflorescence and root architecture of Brachypodium distachyon via hormone homeostasis. *Scientific reports*, **12**, 1-12.

Sharma, M., Saleh, D., Charron, J.-B. and Jabaji, S. (2020) A crosstalk between Brachypodium root exudates, organic acids, and Bacillus velezensis B26, a growth promoting bacterium. *Frontiers in Microbiology*, **11**, 575578.

Shi, H., Ye, T., Song, B., Qi, X. and Chan, Z. (2015) Comparative physiological and metabolomic responses of four Brachypodium distachyon varieties contrasting in drought stress resistance. *Acta Physiologiae Plantarum*, **37**, 1-12.

Shimada, S., Ogawa, T., Kitagawa, S., Suzuki, T., Ikari, C., Shitsukawa, N., Abe, T., Kawahigashi, H., Kikuchi, R. and Handa, H. (2009) A genetic network of flowering-time genes in wheat leaves, in which an APETALA1/FRUITFULL-like gene, VRN1, is upstream of FLOWERING LOCUS T. *The Plant Journal*, **58**, 668-681.

Shinjo, R., Tanaka, A., Sugiura, D., Suzuki, T., Uesaka, K., Takebayashi, Y., Kojima, M., Sakakibara, H., Takemoto, D. and Kondo, M. (2020) Comprehensive analysis of the mechanisms underlying enhanced growth and root N acquisition in rice by the endophytic diazotroph, Burkholderia vietnamiensis RS1. *Plant and Soil*, **450**, 537-555.

Silby, M.W., Cerdeño-Tárraga, A.M., Vernikos, G.S., Giddens, S.R., Jackson, R.W., Preston, G.M., Zhang, X.-X., Moon, C.D., Gehrig, S.M. and Godfrey, S.A. (2009) Genomic and genetic analyses of diversity and plant interactions of Pseudomonas fluorescens. *Genome biology*, **10**, 1-16.

Singh, R.P., Nalwaya, S. and Jha, P.N. (2017) The draft genome sequence of the plant growth promoting rhizospheric bacterium Enterobacter cloacae SBP-8. *Genomics Data*, **12**, 81-83.

Slavokhotova, A., Korostyleva, T., Shelenkov, A., Pukhalskiy, V., Korottseva, I., Slezina, M., Istomina, E. and Odintsova, T. (2021) Transcriptomic analysis of genes involved in plant defense response to the cucumber green mottle mosaic virus infection. *Life*, **11**, 1064.

Somers, E., Vanderleyden, J. and Srinivasan, M. (2004) Rhizosphere bacterial signalling: a love parade beneath our feet. *Critical reviews in microbiology*, **30**, 205-240.

Sood, G., Kaushal, R. and Sharma, M. (2020) Significance of inoculation with Bacillus subtilis to alleviate drought stress in wheat (Triticum aestivum L.). *Vegetos*, **33**, 782-792.

Srivastava, S., Chaudhry, V., Mishra, A., Chauhan, P.S., Rehman, A., Yadav, A., Tuteja, N. and Nautiyal, C.S. (2012) Gene expression profiling through microarray analysis in Arabidopsis thaliana colonized by Pseudomonas putida MTCC5279, a plant growth promoting rhizobacterium. *Plant signaling & behavior*, **7**, 235-245.

Stutz, E., Défago, G. and Kern, H. (1986) Naturally occurring fluorescent Pseudomonads involved in suppression. *Phytopathology*, **76**, 181-185.

Suchan, D.M., Bergsveinson, J., Manzon, L., Pierce, A., Kryachko, Y., Korber, D., Tan, Y., Tambalo, D.D., Khan, N.H. and Whiting, M. (2020) Transcriptomics reveal core activities of the plant growth-promoting bacterium Delftia acidovorans RAY209 during interaction with canola and soybean roots. *Microbial genomics*, **6**.

Sudhakar, P., Chattopadhyay, G., Gangwar, S. and Ghosh, J. (2000) Effect of foliar application of Azotobacter, Azospirillum and Beijerinckia on leaf yield and quality of mulberry (Morus alba). *The Journal of Agricultural Science*, **134**, 227-234.

Sukul, P., Kumar, J., Rani, A., Abdillahi, A.M., Rakesh, R.B. and Kumar, M.H. (2021) Functoning of plant growth promoting rhizobacteria (PGPR) and their mode of actions: an overview from chemistry point of view. *Plant Archives*, **21**, 628-634.

Sun, S., Wang, J., Zhu, L., Liao, D., Gu, M., Ren, L., Kapulnik, Y. and Xu, G. (2012) An active factor from tomato root exudates plays an important role in efficient establishment of mycorrhizal symbiosis.

Suryanarayanan, T.S. (2013) Endophyte research: going beyond isolation and metabolite documentation. *Fungal ecology*, **6**, 561-568.

Swain, M.R., Naskar, S.K. and Ray, R.C. (2007) Indole-3-acetic acid production and effect on sprouting of yam (Dioscorea rotundata L.) minisetts by Bacillus subtilis isolated from culturable cowdung microflora. *Polish Journal of Microbiology*, **56**, 103.

Swarnalakshmi, K., Yadav, V., Tyagi, D., Dhar, D.W., Kannepalli, A. and Kumar, S. (2020) Significance of plant growth promoting rhizobacteria in grain legumes: Growth promotion and crop production. *Plants*, **9**, 1596.

Tabassum, B., Khan, A., Tariq, M., Ramzan, M., Khan, M.S.I., Shahid, N. and Aaliya, K. (2017) Bottlenecks in commercialisation and future prospects of PGPR. *Applied Soil Ecology*, **121**, 102-117.

Tan, S., Yang, C., Mei, X., Shen, S., Raza, W., Shen, Q. and Xu, Y. (2013) The effect of organic acids from tomato root exudates on rhizosphere colonization of Bacillus amyloliquefaciens T-5. *Applied Soil Ecology*, **64**, 15-22.

Thimm, O., Bläsing, O., Gibon, Y., Nagel, A., Meyer, S., Krüger, P., Selbig, J., Müller, L.A., Rhee, S.Y. and Stitt, M. (2004) MAPMAN: a user-driven tool to display genomics data sets onto diagrams of metabolic pathways and other biological processes. *The Plant Journal*, **37**, 914-939.

Thole, V., Peraldi, A., Worland, B., Nicholson, P., Doonan, J.H. and Vain, P. (2012) T-DNA mutagenesis in Brachypodium distachyon. *J. Exp. Bot.*, **63**, 567-576.

Thomas, J., Kim, H.R., Rahmatallah, Y., Wiggins, G., Yang, Q., Singh, R., Glazko, G. and Mukherjee, A. (2019) RNA-seq reveals differentially expressed genes in rice (Oryza sativa) roots during interactions with plant-growth promoting bacteria, Azospirillum brasilense. *PLoS One*, **14**, e0217309.

Timmusk, S., Grantcharova, N. and Wagner, E.G.H. (2005) Paenibacillus polymyxa invades plant roots and forms biofilms. *Applied and environmental microbiology*, **71**, 7292-7300.

Timmusk, S., Nicander, B., Granhall, U. and Tillberg, E. (1999) Cytokinin production by Paenibacillus polymyxa. *Soil Biology and Biochemistry*, **31**, 1847-1852.

Tiwari, S., Gupta, S.C., Chauhan, P.S. and Lata, C. (2021) An OsNAM gene plays important role in root rhizobacteria interaction in transgenic Arabidopsis through abiotic stress and phytohormone crosstalk. *Plant Cell Reports*, **40**, 143-155.

Tiwari, S., Prasad, V. and Lata, C. (2019) Bacillus: plant growth promoting bacteria for sustainable agriculture and environment. In *New and future developments in microbial biotechnology and bioengineering*: Elsevier, pp. 43-55.

Tyler, L., Fangel, J.U., Fagerström, A.D., Steinwand, M.A., Raab, T.K., Willats, W.G. and Vogel, J.P. (2014) Selection and phenotypic characterization of a core collection of Brachypodium distachyon inbred lines. *BMC Plant Biology*, **14**, 1-15.

Ulbrich, T.C., Rivas-Ubach, A., Tiemann, L.K., Friesen, M.L. and Evans, S.E. (2022) Plant root exudates and rhizosphere bacterial communities shift with neighbor context. *Soil Biology and Biochemistry*, 108753.

Vacheron, J., Desbrosses, G., Bouffaud, M.-L., Touraine, B., Moënne-Loccoz, Y., Muller, D., Legendre, L., Wisniewski-Dyé, F. and Prigent-Combaret, C. (2013) Plant growth-promoting rhizobacteria and root system functioning. *Frontiers in plant science*, **4**, 356.

Vain, P., Worland, B., Thole, V., McKenzie, N., Alves, S.C., Opanowicz, M., Fish, L.J., Bevan, M.W. and Snape, J.W. (2008) Agrobacterium-mediated transformation of the temperate grass Brachypodium distachyon (genotype Bd21) for T-DNA insertional mutagenesis. *Plant biotechnology journal*, **6**, 236-245.

Valetti, L., Iriarte, L. and Fabra, A. (2018) Growth promotion of rapeseed (Brassica napus) associated with the inoculation of phosphate solubilizing bacteria. *Applied Soil Ecology*, **132**, 1-10.

Van de Broek, A., Lambrecht, M. and Vanderleyden, J. (1998) Bacterial chemotactic motility is important for the initiation of wheat root colonization by Azospirillum brasilense. *Microbiology*, **144**, 2599-2606.

Van der Ent, S., Van Wees, S.C. and Pieterse, C.M. (2009) Jasmonate signaling in plant interactions with resistance-inducing beneficial microbes. *Phytochemistry*, **70**, 1581-1588.

Van Loon, L. (2007) Plant responses to plant growth-promoting rhizobacteria. *New perspectives and approaches in plant growth-promoting Rhizobacteria research*, 243-254.

Van Loon, L., Bakker, P. and Pieterse, C. (1998) Systemic resistance induced by rhizosphere bacteria. *Annual review of phytopathology*, **36**, 453-483.

Van Peer, R., Niemann, G. and Schippers, B. (1991) Induced resistance and phytoalexin accumulation in biological control of Fusarium wilt of carnation by Pseudomonas sp. strain WCS 417 r. *Phytopathology*, **81**, 728-734.

Van Peer, R. and Schippers, B. (1992) Lipopolysaccharides of plant-growth promoting Pseudomonas sp. strain WCS417r induce resistance in carnation to Fusarium wilt. *Netherlands Journal of Plant Pathology*, **98**, 129-139.

Verhagen, B.W., Glazebrook, J., Zhu, T., Chang, H.-S., Van Loon, L. and Pieterse, C.M. (2004) The transcriptome of rhizobacteria-induced systemic resistance in Arabidopsis. *Molecular Plant-Microbe Interactions*, **17**, 895-908.

Vessey, J.K. (2003) Plant growth promoting rhizobacteria as biofertilizers. *Plant and soil*, **255**, 571-586.

Villarino, S.H., Pinto, P., Jackson, R.B. and Piñeiro, G. (2021) Plant rhizodeposition: A key factor for soil organic matter formation in stable fractions. *Science Advances*, **7**, eabd3176.

Vives-Peris, V., de Ollas, C., Gómez-Cadenas, A. and Pérez-Clemente, R.M. (2020) Root exudates: from plant to rhizosphere and beyond. *Plant cell reports*, **39**, 3-17.

Vogel, J.P., Garvin, D.F., Leong, O.M. and Hayden, D.M. (2006) Agrobacterium-mediated transformation and inbred line development in the model grass Brachypodium distachyon. *Plant Cell Tiss. Org. Cult.*, **84**, 199-211.

von Wirén, N., Khodr, H. and Hider, R.C. (2000) Hydroxylated phytosiderophore species possess an enhanced chelate stability and affinity for iron (III). *Plant Physiology*, **124**, 1149-1158.

Vora, S.M., Joshi, P., Belwalkar, M. and Archana, G. (2021) Root exudates influence chemotaxis and colonization of diverse plant growth promoting rhizobacteria in the pigeon pea–maize intercropping system. *Rhizosphere*, **18**, 100331.

Walukiewicz, H.E., Tohidifar, P., Ordal, G.W. and Rao, C.V. (2014) Interactions among the three adaptation systems of B acillus subtilis chemotaxis as revealed by an in vitro receptor-kinase assay. *Molecular microbiology*, **93**, 1104-1118.

Wang, G., Wang, L., Cui, Y., Yu, M., Dang, C., Wang, H., Jin, X., Yan, L., Wu, Q. and Li, D. (2017) RNA-seq analysis of Brachypodium distachyon responses to Barley stripe mosaic virus infection. *The Crop Journal*, **5**, 1-10.

Wang, L., Chen, M., Lam, P.-Y., Dini-Andreote, F., Dai, L. and Wei, Z. (2022) Multifaceted roles of flavonoids mediating plant-microbe interactions. *Microbiome*, **10**, 233.

Weller, D.M. (1988) Biological control of soilborne plant pathogens in the rhizosphere with bacteria. *Annual review of phytopathology*, **26**, 379-407.

Westermann, A.J., Gorski, S.A. and Vogel, J. (2012) Dual RNA-seq of pathogen and host. *Nature Reviews Microbiology*, **10**, 618.

Wiggins, G., Thomas, J., Rahmatallah, Y., Deen, C., Haynes, A., Degon, Z., Glazko, G. and Mukherjee, A. (2022) Common gene expression patterns are observed in rice roots during associations with plant growth-promoting bacteria, Herbaspirillum seropedicae and Azospirillum brasilense. *Scientific Reports*, **12**, 1-11.

Wipat, A. and Harwood, C.R. (1999) The Bacillus subtilis genome sequence: the molecular blueprint of a soil bacterium. *FEMS Microbiology Ecology*, **28**, 1-9.

Woodman, M.E. (2008) Direct PCR of intact bacteria (colony PCR). *Current protocols in microbiology*, **9**, A. 3D. 1-A. 3D. 6.

Woods, D., Dong, Y., Bouche, F., Bednarek, R., Rowe, M., Ream, T. and Amasino, R. (2019) A florigen paralog is required for short-day vernalization in a pooid grass. *Elife*, **8**, e42153.

Woods, D.P., McKeown, M.A., Dong, Y., Preston, J.C. and Amasino, R.M. (2016) Evolution of VRN2/Ghd7-like genes in vernalization-mediated repression of grass flowering. *Plant physiology*, **170**, 2124-2135.

Xie, Z., Nolan, T.M., Jiang, H. and Yin, Y. (2019) AP2/ERF transcription factor regulatory networks in hormone and abiotic stress responses in Arabidopsis. *Frontiers in plant science*, **10**, 228.

Xiong, L. and Zhu, J.-K. (2003) Regulation of abscisic acid biosynthesis. *Plant physiology*, **133**, 29-36.

Xu, Z., Shao, J., Li, B., Yan, X., Shen, Q. and Zhang, R. (2013) Contribution of bacillomycin D in Bacillus amyloliquefaciens SQR9 to antifungal activity and biofilm formation. *Applied and environmental microbiology*, **79**, 808-815.

Yan, L., Loukoianov, A., Blechl, A., Tranquilli, G., Ramakrishna, W., SanMiguel, P., Bennetzen, J.L., Echenique, V. and Dubcovsky, J. (2004) The wheat VRN2 gene is a flowering repressor down-regulated by vernalization. *Science*, **303**, 1640-1644.

Yan, N. (2013) Structural advances for the major facilitator superfamily (MFS) transporters. *Trends in biochemical sciences*, **38**, 151-159.

Yang, J., Kloepper, J.W. and Ryu, C.-M. (2009) Rhizosphere bacteria help plants tolerate abiotic stress. *Trends in plant science*, **14**, 1-4.

Yang, X., Hill, K.A., Austin, R.S. and Tian, L. (2021) Differential gene expression of Brachypodium distachyon roots colonized by Gluconacetobacter diazotrophicus and the role of BdCESA8 in the colonization. *Molecular Plant-Microbe Interactions*, **34**, 1143-1156.

Yao, T., Feng, K., Xie, M., Barros, J., Tschaplinski, T.J., Tuskan, G.A., Muchero, W. and Chen, J.-G. (2021) Phylogenetic occurrence of the phenylpropanoid pathway and lignin biosynthesis in plants. *Frontiers in Plant Science*, **12**.

Yasmin, F., Othman, R., Sijam, K. and Saad, M.S. (2007) Effect of PGPR inoculation on growth and yield of sweetpotato. *J. Biol. Sci*, **7**, 421-424.

Yin, C., Casa Vargas, J.M., Schlatter, D.C., Hagerty, C.H., Hulbert, S.H. and Paulitz, T.C. (2021) Rhizosphere community selection reveals bacteria associated with reduced root disease. *Microbiome*, **9**, 1-18.

Yoshida, H., Hirano, K., Sato, T., Mitsuda, N., Nomoto, M., Maeo, K., Koketsu, E., Mitani, R., Kawamura, M. and Ishiguro, S. (2014) DELLA protein functions as a transcriptional activator through the DNA binding of the indeterminate domain family proteins. *Proceedings of the National Academy of Sciences*, **111**, 7861-7866.

Young, M.D., Wakefield, M.J., Smyth, G.K. and Oshlack, A. (2010) Gene ontology analysis for RNA-seq: accounting for selection bias. *Genome biology*, **11**, 1-12.

Youssef, M. and Eissa, M. (2014) Biofertilizers and their role in management of plant parasitic nematodes. A review. *Journal of Biotechnology and Pharmaceutical Research*, **5**, 1-6.

Yu, X.Q., Yan, X., Zhang, M.Y., Zhang, L.Q. and He, Y.X. (2020) Flavonoids repress the production of antifungal 2, 4-DAPG but potentially facilitate root colonization of the rhizobacterium Pseudomonas fluorescens. *Environmental Microbiology*, **22**, 5073-5089.

Yuan, J., Wu, Y., Zhao, M., Wen, T., Huang, Q. and Shen, Q. (2018) Effect of phenolic acids from banana root exudates on root colonization and pathogen suppressive properties of Bacillus amyloliquefaciens NJN-6. *Biological Control*, **125**, 131-137.

Yuan, J., Zhang, N., Huang, Q., Raza, W., Li, R., Vivanco, J.M. and Shen, Q. (2015) Organic acids from root exudates of banana help root colonization of PGPR strain Bacillus amyloliquefaciens NJN-6. *Scientific reports*, **5**, 1-8.

Zahir, Z., Munir, A., Asghar, H., Shaharoona, B. and Arshad, M. (2008) Effectiveness of rhizobacteria containing ACC deaminase for growth promotion of peas (Pisum sativum) under drought conditions. *Journal of Microbiology and Biotechnology*, **18**, 958-963.

Zentella, R., Zhang, Z.-L., Park, M., Thomas, S.G., Endo, A., Murase, K., Fleet, C.M., Jikumaru, Y., Nambara, E. and Kamiya, Y. (2007) Global analysis of DELLA direct targets in early gibberellin signaling in Arabidopsis. *The Plant Cell*, **19**, 3037-3057.

Zhang, J., Wang, P., Tian, H., Tao, Z. and Guo, T. (2020) Transcriptome analysis of ice plant growth-promoting endophytic bacterium Halomonas sp. strain MC1 to identify the genes involved in salt tolerance. *Microorganisms*, **8**, 88.

Zhang, N., Wang, D., Liu, Y., Li, S., Shen, Q. and Zhang, R. (2014) Effects of different plant root exudates and their organic acid components on chemotaxis, biofilm formation and colonization by beneficial rhizosphere-associated bacterial strains. *Plant and soil*, **374**, 689-700.

Zhang, W., Sun, J., Ding, W., Lin, J., Tian, R., Lu, L., Liu, X., Shen, X. and Qian, P.-Y. (2015) Extracellular matrix-associated proteins form an integral and dynamic system during Pseudomonas aeruginosa biofilm development. *Frontiers in cellular and infection microbiology*, **5**, 40.

Zhang, W., Wang, Z., Dan, Z., Zhang, L., Xu, M., Yang, G., Chai, M., Li, Z., Xie, H. and Cong, L. (2022) Transcriptome Analysis of Fusarium Root-Rot-Resistant and-Susceptible Alfalfa (Medicago sativa L.) Plants during Plant–Pathogen Interactions. *Genes*, **13**, 788.

Zhang, Y. and Fernie, A.R. (2018) On the role of the tricarboxylic acid cycle in plant productivity. *Journal of integrative plant biology*, **60**, 1199-1216.

Zheng, Y., Jiao, C., Sun, H., Rosli, H.G., Pombo, M.A., Zhang, P., Banf, M., Dai, X., Martin, G.B. and Giovannoni, J.J. (2016) iTAK: a program for genome-wide prediction and classification of plant transcription factors, transcriptional regulators, and protein kinases. *Molecular plant*, **9**, 1667-1670.

Zhu, A., Ibrahim, J.G. and Love, M.I. (2019) Heavy-tailed prior distributions for sequence count data: removing the noise and preserving large differences. *Bioinformatics*, **35**, 2084-2092.

Zoueki, C.W., Tufenkji, N. and Ghoshal, S. (2010) A modified microbial adhesion to hydrocarbons assay to account for the presence of hydrocarbon droplets. *Journal of Colloid and Interface Science*, **344**, 492-496.

Zuanazzi, J.A.S., Clergeot, P.H., Quirion, J.-C., Husson, H.-P., Kondorosi, A. and Ratet, P. (1998) Production of Sinorhizobium meliloti nod gene activator and repressor flavonoids from Medicago sativa roots. *Molecular plant-microbe interactions*, **11**, 784-794.

Zúñiga, A., Poupin, M.J., Donoso, R., Ledger, T., Guiliani, N., Gutiérrez, R.A. and González, B. (2013) Quorum sensing and indole-3-acetic acid degradation play a role in colonization and plant growth promotion of Arabidopsis thaliana by Burkholderia phytofirmans PsJN. *Molecular Plant-Microbe Interactions*, **26**, 546-553.